

RADIOLOGY AND ONCOLOGY

vol.53 no.2
june 2019



NOVO

CABOMETYX®

(kabozantinib) tablete

60 mg | 40 mg | 20 mg

CABOMETYX® pomembno izboljša PFS, OS in ORR v drugi liniji zdravljenja napredovalega karcinoma ledvičnih celic¹

RAZŠIRITEV INDIKACIJE:

Sedaj tudi za zdravljenje napredovalega karcinoma ledvičnih celic (KLC) pri predhodno nezdravljenih odraslih bolnikih s srednje ugodnim ali slabim prognostičnim obetom.²

- ✓ PFS²
- ✓ OS²
- ✓ ORR²

ORR: objektivna stopnja odziva; OS: celokupno preživetje; PFS: preživetje brez napredovanja bolezni

Referenci:

1. Choueiri TK, Escudier B, Powles T, et al. Cabozantinib versus everolimus in advanced renal cell carcinoma (METEOR): final results from a randomised, open-label, phase 3 trial. *The Lancet Oncology*. 2016;17(7):917-27.
2. Povzetek glavnih značilnosti zdravila Cabometyx.

Skrajšan povzetek glavnih značilnosti zdravila

CABOMETYX 20 mg filmsko obložene tablete
CABOMETYX 40 mg filmsko obložene tablete
CABOMETYX 60 mg filmsko obložene tablete
(kabozantinib)

TERAPEVTSKE INDIKACIJE Zdravljenje napredovalega karcinoma ledvičnih celic (KLC) pri predhodno nezdravljenih odraslih bolnikih s srednje ugodnim ali slabim prognostičnim obetom ter pri odraslih bolnikih po predhodnem zdravljenju, usmerjenem v vaskularni endoteljski rastni faktor (VEGF). V monoterapiji zdravljenje hepatocelularnega karcinoma (HCC) pri odraslih bolnikih, ki so se predhodno že zdravili s sorafenibom. **ODMERJANJE IN NAČIN UPORABE** Pri bolnikih s KLC in HCC je poročen odmerek 60 mg enkrat na dan. Zdravljenje je treba nadaljevati tako dolgo, dokler bolnik več nima kliničnih koristi od terapije ali do pojava nesprejemljive toksičnosti. Pri sumu na neželene reakcije na zdravilo bo morda treba zdravljenje začasno prekiniti in/ali zmanjšati odmerke. Če je treba odmerke zmanjšati, se priporoča zmanjšanje na 40 mg na dan in nato na 20 mg na dan. Prekinitev odmerka se priporoča pri obravnavi toksičnosti 3. ali višje stopnje po CTCAE (*common terminology criteria for adverse events*) ali nevzdržni toksičnosti 2. stopnje. Zmanjšanje odmerka se priporoča za dogodke, ki bi lahko čez čas postali resni ali nevzdržni. V primeru pojavnosti neželenih učinkov 1. in 2. stopnje, ki jih bolnik prenaša in jih je možno enostavno obravnavati, prilagoditev odmerjanja običajno ni potrebna. Treba je uvesti podporno oskrbo. V primeru pojavnosti neželenih učinkov 2. stopnje, ki jih bolnik ne prenaša in jih ni mogoče obravnavati z zmanjšanjem odmerka ali podporno oskrbo, je treba zdravljenje prekiniti, dokler neželeni učinki ne izvenijo do ≤ 1. stopnje, uvesti podporno oskrbo in razmisli o ponovni uvedbi zdravljenja z zmanjšanim odmerkom. V primeru pojavnosti neželenih učinkov 3. stopnje je treba zdravljenje prekiniti, dokler neželeni učinki ne izvenijo do ≤ 1. stopnje, uvesti podporno oskrbo in ponovno uvesti zdravljenje z zmanjšanim odmerkom. V primeru pojavnosti neželenih učinkov 4. stopnje je treba zdravljenje prekiniti, uvesti ustrezno zdravniško oskrbo, in če neželeni učinki izvenijo do ≤ 1. stopnje, ponovno uvesti zdravljenje z zmanjšanim odmerkom. Če neželeni učinki ne izvenijo, je treba trajno prenehati z uporabo zdravila. Pri bolnikih z blago **okvaro jeter** odmerka ni treba prilagajati. Pri bolnikih z zmerno okvaro jeter (Child Pugh B) priporočil za odmerjanje ni možno podati. Pri teh bolnikih je priporočljivo skrbno spremljanje celokupne varnosti. Pri bolnikih s hudo okvaro jeter (Child Pugh C) uporaba kabozantiniba ni priporočljiva. **Način uporabe:** Tablete je treba pogoltniti cele in jih ni dovoljeno drobiti. Bolnikom je treba naročiti, naj vsaj 2 uri pred uporabo zdravila in 1 uro po tem nicesar ne jedo. **KONTRAINDIKACIJE** Preobčutljivost na učinkovino ali katero koli pomožno snov. **POSEBNA OPOZORILA IN PREVIDNOSTNI UKREPI** Večina dogodkov se pojavi zgodaj v teku zdravljenja, zato mora zdravnik bolnika v prvih 8 tednih zdravljenja skrbno spremljati, da oceni, ali je treba odmerke prilagoditi. Dogodki, ki se običajno pojavijo zgodaj, vključujejo hipokalcemijo, hipokalemijo, tromboticpenijo, hipertenzijo, sindrom palmarno-plantarne eritrodisezestije (PPES), proteinurijo in gastrointestinalne dogodke (bolečine v trebuhu, vnetje sluznice, zaprtje, driska, bruhanje). Pred uvedbo zdravljenja s kabozantinibom je priporočljivo izvesti preiskave delovanja jeter (ALT, AST in bilirubin), vrednosti skrbno spremljati med zdravljenjem in po potrebi prilagoditi odmerke. Bolnike je treba spremljati glede znakov in simptomov jetrne encelofalopatije. Bolnike, ki imajo vnetno bolezen zvezda (npr. Crohnovo bolezen, ulcerozni kolitis, peritonitis, divertikulitis ali apendicitis), ki imajo tumorsko infiltracijo prebavil ali so imeli pred posegom na prebavnih zapletih (zlasti v povezavi z zapoznelim ali nepopolnim celjenjem), je treba pred uvedbo zdravljenja skrbno oceniti, nato pa natančno spremljati za pojav simptomov perforacij in fistul, vključno z abscesi in sepsa. Trajna ali

▼ Za to zdravilo se izvaja dodatno spremljanje varnosti. Tako bodo hitreje na voljo nove informacije o njegovi varnosti. Zdravstvene delavce naprošamo, da poročajo o katerem koli domnevem neželenem učinku zdravila.

ponavljajoča se driska med zdravljenjem je lahko dejavnik tveganja za nastanek analne fistule. Uporaba kabozantiniba je treba pri bolnikih, pri katerih se pojavi gastrointestinalna perforacija ali fistula, ki je ni možno ustrezno obravnavati, prekiniti. Driska, navzea/bruhanje, zmanjšanje apetita in vnetje ustne sluznice/bolečina v ustni votlini so nekateri od najpogostejših poročanih neželenih učinkov na prebavila. Nemudoma je treba uvesti ustrezne medicinske ukrepe, vključno s podpornim zdravljenjem z antiemetiki, antiidiariki ali antacidi, da se prepreči dehidracija, neravnovesje elektrolitov in izguba telesne mase. Če pomembni neželeni učinki na prebavila vztrajajo ali se ponavljajo, je treba presoditi o prekinitvi odmerjanja, zmanjšanju odmerka ali trajni ukinitvi zdravljenja s kabozantinibom. Kabozantinib je treba uporabljati previdno pri bolnikih, pri katerih obstaja tveganje za pojav venske tromboembolije, vključno s pljučno embolijo, in arterijske tromboembolije ali imajo te dogodke v anamnezi. Z uporabo je treba prenehati pri bolnikih, pri katerih se razvije akutni miokardni infarkt ali drugi klinično pomembni znaki zapletov tromboembolije. Kabozantiniba se ne sme dajati bolnikom, ki hudo krvavijo, ali pri katerih obstaja tveganje za hudo krvavitev. Med zdravljenjem s kabozantinibom je treba spremljati vrednosti trombocitov in odmerke prilagoditi glede na resnost trombocitopenije. Zdravljenje s kabozantinibom je treba ustaviti vsaj 28 dni pred načrtovanim kirurškim posegom, vključno z zobozdravstvenim, če je mogoče. Kabozantinib je treba ukiniti pri bolnikih z zapleti s celjenjem rane, zaradi katerih je potrebna zdravniška pomoč. Pred uvedbo kabozantiniba je treba dobro obvladati krvni tlak. Med zdravljenjem je treba vse bolnike spremljati za pojav hipertenzije in jih po potrebi zdraviti s standardnimi antihipertenzivi. V primeru trdovratne hipertenzije, kljub uporabi antihipertenzivov, je treba odmerke kabozantiniba zmanjšati. Z uporabo je treba prenehati, če je hipertenzija resna ali trdovratna kljub zdravljenju z antihipertenzivi in zmanjšanimu odmerku kabozantiniba. V primeru hipertenzijske krize je treba zdravljenje prekiniti. Pri resni PPES je treba razmisliti o prekinitvi zdravljenja. Nadaljevanje zdravljenja naj se začne z nižjim odmerkom, ko se PPES umiri do 1. stopnje. V času zdravljenja je treba redno spremljati beljakovine v urinu. Pri bolnikih, pri katerih se razvije nefrotični sindrom, je treba z uporabo kabozantiniba prenehati. Pri uporabi kabozantiniba so opazili sindrom reverzibilne posteriorne levkoencefalopatije (RPLS), znan tudi kot sindrom posteriorne reverzibilne encelofalopatije (PRES). Na ta sindrom je treba pomisliti pri vseh bolnikih s številnimi prisotnimi simptomi, vključno s epileptičnimi napadi, glavobolom, motnjami vida, zmedenostjo ali spremenjenim mentalnim delovanjem. Pri bolnikih z RPLS je treba zdravljenje prekiniti. Kabozantinib je treba uporabljati previdno pri bolnikih s podaljšanjem intervala QT v anamnezi, pri bolnikih, ki jemljejo antiaritmike, in pri bolnikih z relevantno obstoječo boleznijo srca, bradikardijo ali elektrolitskimi motnjami. Uporaba kabozantiniba je bila povezana z večjo pojavnostjo elektrolitskih nepravilnosti (vključno s hipokalemijo, hipokalcemijo, hipomagnezjemijo, hipokalcemijo in hiponatremijo), zato je priporočljivo spremljati biokemijske parametre in po potrebi uvesti ustrezno nadomestno zdravljenje v skladu s standardno klinično prakso. Bolniki z redko dedno intoleranco za galaktozo, laponsko obliko zmanjšane aktivnosti laktaze ali malabsorpcijo glukoze/galaktoze ne smejo jemati tega zdravila. **Plodnost, nosečnost in dojenje.** Ženskam v rodni dobi je treba svetovati, da v času zdravljenja s kabozantinibom ne smejo zanositi. Zanositev morajo preprečiti tudi ženske partnerice moških bolnikov, ki uporabljajo kabozantinib. Med zdravljenjem in še vsaj 4 mesece po končanju terapije morajo tako bolniki in bolnice kot tudi njihovi partnerji uporabljati zanesljiv način kontracepcije. Kabozantiniba se ne sme uporabljati med nosečnostjo, razen če zdravljenje ni nujno potrebno zaradi kliničnega stanja ženske. Matere med zdravljenjem s kabozantinibom in še 4 mesece po končanju terapije ne smejo dojiti. Zdravljenje s kabozantinibom lahko predvaja tveganje za plodnost pri moških in ženskah. **INTERAKCIJE** Kabozantinib je substrat za CYP3A4. Pri sočasni uporabi močnih zaviralcev CYP3A4 (npr. ritonavirja, itrakonazola, eritromicina, klaritromicina, soka grenivke) je potrebna previdnost. Kronični sočasni uporabi močnih

induktorjev CYP3A4 (npr. fenitoina, karbamazepina, rifampicina, fenobarbitala ali pripravkov zeliščnega izvora iz šentjanževke) se je treba izogibati. Razmisliti je treba o sočasni uporabi alternativnih zdravil, ki CYP3A4 ne inducirajo in ne zavirajo ali pa inducirajo in zavirajo le neznatno. Pri sočasni uporabi zaviralcev MRP2 (npr. ciklosporin, efavirenz, emtricitabin) je potrebna previdnost, saj lahko povzročijo povečanje koncentracij kabozantiniba v plazmi. Učinka kabozantiniba na farmakokinetiko kontraceptivnih steroidov niso preučili, vendar pa se priporoča dodatna kontracepcijska metoda (pregradna metoda). Zaradi visoke stopnje vezave kabozantiniba na plazemske beljakovine je možna interakcija z varfarinom v obliki izpodrivanja s plazemskih beljakov, zato je treba spremljati vrednosti INR. Kabozantinib morda lahko poveča koncentracije sočasno uporabljenih substratov P-gp v plazmi. Osebe je treba opozoriti na uporabo substratov P-gp (npr. feksofenadina, aliskirena, ambrisentana, dabigatran teleskila, digoksina, kolhicina, maraviroka, posakonazola, ranolazina, saksaglipatina, sitagliptina, talinolola, tolvaptana) sočasno s kabozantinibom. **NEŽELENI UČINKI** Za popolno informacijo o neželenih učinkih, prosimo, preberite celoten povzetek glavnih značilnosti zdravila Cabometyx. Najpogostejši resni neželeni učinki zdravila v populaciji bolnikov s KLC so bili driska, hipertenzija, dehidracija, hiponatremija, navzea, zmanjšanje apetita, embolija, utrujenost, hipomagnezija in PPES. Najpogostejši neželeni učinki katere koli stopnje (ki so se pojavili pri vsaj 25 % bolnikov) v populaciji bolnikov s KLC so bili driska, hipertenzija, utrujenost, zvišanje vrednosti AST, zvišanje vrednosti ALT, navzea, zmanjšanje apetita, PPES, paragevzja, zmanjšanje števila trombocitov, stomatitis, anemija, bruhanje, zmanjšanje telesne mase, dispneja in konstipacija. Najpogostejši resni neželeni učinki zdravila v populaciji bolnikov s HCC so bili jetrna encelofalopatija, PPES, astenija in driska. Najpogostejši neželeni učinki katere koli stopnje (ki so se pojavili pri vsaj 25 % bolnikov) v populaciji bolnikov s HCC so bili driska, PPES, utrujenost, zmanjšanje apetita, hipertenzija in navzea. Zelo pogosti (≥ 1/10): anemija, hipotroidizem, zmanjšan apetit, hipomagnezija, hipokalcemija, paragevzja, glavobol, omotica, hipertenzija, krvavitve, dispneja, kašelj, driska, navzea, bruhanje, stomatitis, konstipacija, bolečine v trebuhu, dispneja, bolečina v zgornjem predelu trebuha, PPES, izpuščaji, bolečine v okončinah, utrujenost, vnetje sluznice, astenija, periferni edem, zmanjšanje telesne mase, zvišanje vrednosti ALT v serumu, zvišanje vrednosti AST. *Pogosti* (≥ 1/100, < 1/10): absces, tromboticpenija, nevropatija, dehidracija, hipalbuminemija, hipofosfatemija, hiponatremija, hipokalcemija, hipokalcemija, hiperbilirubinemija, hiperglikemija, hipoglikemija, periferna senzorična nevropatija, tinitus, venska tromboza, arterijska tromboza, pljučna embolija, gastrointestinalna perforacija, fistula, gastroezofagealna refluksna bolezen, hemoroidi, bolečina v ustni votlini, suha usta, jetrna encelofalopatija, pruritus, alopecija, suha koža, akneliformni dermatitis, sprememba barve las oz. dlak, mišični krči, artralgijski, proteinurija, zvišanje vrednosti ALP v krvi, GGt, kreatinina v krvi, amilaze, lipaze, holesterola v krvi, zmanjšanje števila belih krvnih celic. *Občasni* (≥ 1/1000, < 1/100): limfopenija, konvulzije, pankreatitis, glosodija, holistični hepatitis, osteonekroza čeljusti, zvišanje vrednosti trigliceridov v krvi, zapleti z ranami. *Neznana pogostost (ni mogoče oceniti iz razpoložljivih podatkov):* možganska kap, miokardni infarkt. **Vesta ovojinine in vsebina:** Plastenka vsebuje 30 filmsko obloženih tablet. **Režim izdaje:** Ro/Spc **Imetnik dovoljenja za promet z zdravilom:** Iosens Pharma, 65 quai Georges Gorse, 92100 Boulogne-Billancourt, Francija. **Pred predpisovanjem, prosimo, preberite celoten povzetek glavnih značilnosti zdravila!** CAB-121118

 **PharmaSwiss**
Choose More Life

Odgovoren za trženje v Sloveniji:
PharmaSwiss d.o.o., Brodišče 32, 1236 Trzin
telefon: +386 1 236 47 00, faks: +386 1 283 38 10

 **IPSEN**
Innovation for patient care

SAMO ZA STROKOVNO JAVNOST
CABO219-01, februar 2019



Publisher

Association of Radiology and Oncology

Affiliated with

Slovenian Medical Association – Slovenian Association of Radiology, Nuclear Medicine Society,

Slovenian Society for Radiotherapy and Oncology, and Slovenian Cancer Society

Croatian Medical Association – Croatian Society of Radiology

Societas Radiologorum Hungarorum

Friuli-Venezia Giulia regional groups of S.I.R.M.

Italian Society of Medical Radiology

Aims and scope

Radiology and Oncology is a journal devoted to publication of original contributions in diagnostic and interventional radiology, computerized tomography, ultrasound, magnetic resonance, nuclear medicine, radiotherapy, clinical and experimental oncology, radiobiology, radiophysics and radiation protection.

Editor-in-Chief

Gregor Serša, Institute of Oncology Ljubljana, Department of Experimental Oncology, Ljubljana, Slovenia (Subject Area: Experimental Oncology)

Executive Editor

Viljem Kovač, Institute of Oncology Ljubljana, Department of Radiation Oncology, Ljubljana, Slovenia (Subject Areas: Clinical Oncology, Radiotherapy)

Editorial Board

Subject Areas:
Radiology and Nuclear Medicine

Sotirios Bisdas, National Hospital for Neurology and Neurosurgery, Department of Neuroradiology, London, UK

Karl H. Bohuslavizki, Nuklearmedizin Spitalerhof, Hamburg, Germany

Boris Brkljačić, University Hospital "Dubrava", Department of Diagnostic and Interventional Radiology, Zagreb, Croatia

Maria Gódehy, National Institute of Oncology, Budapest, Hungary

Gordana Ivanac, University Hospital Dubrava, Department of Diagnostic and Interventional Radiology, Zagreb, Croatia

Damir Miletić, Clinical Hospital Centre Rijeka, Department of Radiology, Rijeka, Croatia

Katarina Šurlan Popovič, University Medical Center Ljubljana, Clinical Institute of Radiology, Ljubljana, Slovenia

Jernej Vidmar, University Medical Center Ljubljana, Clinical Institute of Radiology, Ljubljana, Slovenia

Advisory Committee

Tullio Giraldi, University of Trieste, Faculty of Medicine and Psychology, Department of Life Sciences, Trieste, Italy

Vassil Hadjidekov, Medical University, Department of Diagnostic Imaging, Sofia, Bulgaria

Marko Hočevar, Institute of Oncology Ljubljana, Department of Surgical Oncology, Ljubljana, Slovenia

Miklós Kásler, National Institute of Oncology, Budapest, Hungary

Deputy Editors

Andrej Cör, University of Primorska, Faculty of Health Science, Izola, Slovenia (Subject Areas: Clinical Oncology, Experimental Oncology)

Maja Čemažar, Institute of Oncology Ljubljana, Department of Experimental Oncology, Ljubljana, Slovenia (Subject Area: Experimental Oncology)

Igor Kocijančič, University Medical Center Ljubljana, Institute of Radiology, Ljubljana, Slovenia (Subject Areas: Radiology, Nuclear Medicine)

Subject Areas:
Clinical Oncology and Radiotherapy

Luca Campana, Veneto Institute of Oncology (IOV-IRCCS), Padova, Italy

Christian Dittrich, Kaiser Franz Josef - Spital, Vienna, Austria

Dirk Rades, University of Lubeck, Department of Radiation Oncology, Lubeck, Germany

Luka Milas, UT M. D. Anderson Cancer Center, Houston, USA

Csaba Polgar, National Institute of Oncology, Budapest, Hungary

Mirjana Rajer, University Clinic of Pulmonary and Allergic Diseases Golnik, Golnik, Slovenia

Luis Souhami, McGill University, Montreal, Canada

Borut Štabuc, University Medical Center Ljubljana, Division of Internal Medicine, Department of Gastroenterology, Ljubljana, Slovenia

Andrea Veronesi, Centro di Riferimento Oncologico- Aviano, Division of Medical Oncology, Aviano, Italy

Branko Zakotnik, Institute of Oncology Ljubljana, Department of Medical Oncology, Ljubljana, Slovenia

Serena Bonin, University of Trieste, Department of Medical Sciences, Cattinara Hospital, Surgical Pathology Blg, Molecular Biology Lab, Trieste, Italy

Maja Osmak, Ruder Bošković Institute, Department of Molecular Biology, Zagreb, Croatia

Dušan Pavčnik, Dotter Interventional Institute, Oregon Health Science University, Oregon, Portland, USA

Stojan Plesničar, Institute of Oncology Ljubljana, Department of Radiation Oncology, Ljubljana, Slovenia

Tomaž Benulič, Institute of Oncology Ljubljana, Department of Radiation Oncology, Ljubljana, Slovenia

Karmen Stanič, Institute of Oncology Ljubljana, Department of Radiation Oncology, Ljubljana, Slovenia (Subject Areas: Radiotherapy; Clinical Oncology)

Primož Strojjan, Institute of Oncology Ljubljana, Department of Radiation Oncology, Ljubljana, Slovenia (Subject Areas: Radiotherapy, Clinical Oncology)

Subject Area:
Experimental Oncology

Metka Filipič, National Institute of Biology, Department of Genetic Toxicology and Cancer Biology, Ljubljana, Slovenia

Janko Kos, University of Ljubljana, Faculty of Pharmacy, Ljubljana, Slovenia

Tamara Lah Turnšek, National Institute of Biology, Ljubljana, Slovenia

Damijan Miklavčič, University of Ljubljana, Faculty of Electrical Engineering, Ljubljana, Slovenia

Geoffrey J. Pilkington, University of Portsmouth, Institute of Biomedical and Biomolecular Sciences, School of Pharmacy and Biomedical Sciences, Portsmouth, UK

Justin Teissié, CNRS, IPBS, Toulouse, France
Gillian M. Tozer, University of Sheffield, Academic Unit of Surgical Oncology, Royal Hallamshire Hospital, Sheffield, UK

Subject Area: Radiophysics

Robert Jeraj, University of Wisconsin, Carbone Cancer Center, Madison, Wisconsin, USA

Håkan Nyström, Skandionkliniken, Uppsala, Sweden

Ervin B. Podgoršak, McGill University, Medical Physics Unit, Montreal, Canada

Matthew Podgorsak, Roswell Park Cancer Institute, Departments of Biophysics and Radiation Medicine, Buffalo, NY, USA

Editorial office

Radiology and Oncology

Zaloška cesta 2

P. O. Box 2217

SI-1000 Ljubljana

Slovenia

Phone: +386 1 5879 369

Phone/Fax: +386 1 5879 434

E-mail: gsera@onko-i.si

Copyright © Radiology and Oncology. All rights reserved.

Reader for English

Vida Kološa

Secretary

Mira Klemenčič

Zvezdana Vukmirović

Design

Monika Fink-Serša, Samo Rován, Ivana Ljubanović

Layout

Matjaž Lužar

Printed by

Tiskarna Ozimek, Slovenia

Published quarterly in 400 copies

Beneficiary name: DRUŠTVO RADIOLOGIJE IN ONKOLOGIJE

Zaloška cesta 2

1000 Ljubljana

Slovenia

Beneficiary bank account number: SI56 02010-0090006751

IBAN: SI56 0201 0009 0006 751

Our bank name: Nova Ljubljanska banka, d.d.,

Ljubljana, Trg republike 2,

1520 Ljubljana; Slovenia

SWIFT: LJBAS12X

Subscription fee for institutions EUR 100, individuals EUR 50

The publication of this journal is subsidized by the Slovenian Research Agency.

Indexed and abstracted by:

- Baidu Scholar
- Case
- Chemical Abstracts Service (CAS) - CAplus
- Chemical Abstracts Service (CAS) - SciFinder
- CNKI Scholar (China National Knowledge Infrastructure)
- CNPIEC - cnpLINKer
- Dimensions
- DOAJ (Directory of Open Access Journals)
- EBSCO (relevant databases)
- EBSCO Discovery Service
- Embase
- Genamics JournalSeek
- Google Scholar
- Japan Science and Technology Agency (JST)
- J-Gate
- Journal Citation Reports/Science Edition
- JournalGuide
- JournalTOCs
- KESLI-NDSL (Korean National Discovery for Science Leaders)
- Medline
- Meta
- Microsoft Academic
- Naviga (Softweco)
- Primo Central (ExLibris)
- ProQuest (relevant databases)
- Publons
- PubMed
- PubMed Central
- PubsHub
- QOAM (Quality Open Access Market)
- ReadCube
- Reaxys
- SCImago (SJR)
- SCOPUS
- Sherpa/RoMEO
- Summon (Serials Solutions/ProQuest)
- TDNet
- Ulrich's Periodicals Directory/ulrichsweb
- WanFang Data
- Web of Science - Current Contents/Clinical Medicine
- Web of Science - Science Citation Index Expanded
- WorldCat (OCLC)

This journal is printed on acid-free paper

On the web: ISSN 1581-3207

<https://content.sciendo.com/raon>

<http://www.radioloncol.com>

contents

review

- 131 **The biology and clinical potential of circulating tumor cells**
Taja Lozar, Klara Gersak, Maja Cemazar, Cvetka Grasic Kuhar, Tanja Jesenko
- 148 **Cisplatin and beyond: molecular mechanisms of action and drug resistance development in cancer chemotherapy**
Tomaz Makovec
- 159 **Multiparametric MRI - local staging of prostate cancer and beyond**
Iztok Caglic, Viljem Kovac, Tristan Barrett

radiology

- 171 **Evaluation of MRI accuracy after primary systemic therapy in breast cancer patients considering tumor biology: optimizing the surgical planning**
Alberto Bouzón, Ángela Iglesias, Benigno Acea, Cristina Mosquera, Paz Santiago, Joaquín Mosquera
- 178 **Diagnostic accuracy of haemophilia early arthropathy detection with ultrasound (HEAD-US): a comparative magnetic resonance imaging (MRI) study**
Domen Plut, Barbara Faganel Kotnik, Irena Preloznik Zupan, Damjana Kljucevsek, Gaj Vidma, Ziga Snoj, Carlo Martinoli, Vladka Salapura
- 187 **Efficacy and durability of radiopaque gelified ethanol in management of herniated discs**
Dimitrij Kuhelj, Anita Dobrovec, Igor Jozef Kocijancic

experimental oncology

- 194 **The use of high-frequency short bipolar pulses in cisplatin electrochemotherapy in vitro**
Maria Scuderi, Matej Rebersek, Damijan Miklavcic, Janja Dermol-Cerne

clinical oncology

- 206 **The influence of genetic variability of DNA repair mechanisms on the risk of malignant mesothelioma**
Kristina Levpuscek, Katja Goricar, Viljem Kovac, Vita Dolzan, Alenka Franko
- 213 **Radiological and clinical patterns of myeloid sarcoma**
Hans-Jonas Meyer, Maximilian Beimler, Gudrun Borte, Wolfram Pönisch, Alexey Surov

- 219 **A new instrument for predicting survival of patients with cerebral metastases from breast cancer developed in a homogeneously treated cohort**
Stefan Janssen, Heinke C. Hansen, Liesa Dziggel, Steven E. Schild, Dirk Rades
- 225 **Swallowing disorders after treatment for head and neck cancer**
Martina Pezdirec, Primož Strojani, Irena Hocevar Boltezar
- 231 **Health-related quality of life in Slovenian patients with colorectal cancer: a single tertiary care center study**
Jan Grosek, Jerica Novak, Katja Kitek, Alta Bajric, Ana Majdic, Jurij Ales Kosir, Aleš Tomazic
- 238 **Long term survival in 200 patients with advanced stage of colorectal carcinoma and diabetes mellitus - a single institution experience**
Nikola Besic, Milena Kerin Povsic
- 245 **Impact of perioperative treatment on survival of resectable gastric cancer patients after D2 lymphadenectomy: a single European centre propensity score matching analysis.**
Tomaz Jagric, Bojan Ilijavec, Vaneja Velenik, Janja Ocvirk, Stojan Potrc
- 256 **Impact of body-mass factors on setup displacement during pelvic irradiation in patients with lower abdominal cancer**
Wei-Chieh Wu, Yi-Ru Chang, Yo-Liang Lai, An-Cheng Shiau, Ji-An Liang, Chun-Ru Chien, Yu-Cheng Kuo, Shang-Wen Chen

I *slovenian abstracts*

The biology and clinical potential of circulating tumor cells

Taja Lozar¹, Klara Gersak^{1,2,3}, Maja Cemazar^{2,4}, Cvetka Grasic Kuhar², Tanja Jesenko²

¹ Faculty of Medicine, University of Ljubljana, Ljubljana, Slovenia

² Institute of Oncology Ljubljana, Ljubljana, Slovenia

³ General Hospital Izola, Izola, Slovenia

⁴ Faculty of Health Sciences, University of Primorska, Izola, Slovenia

Radiol Oncol 2019; 53(2): 131-147.

Received 23 March 2019

Accepted 3 May 2019

Correspondence to: Tanja Jesenko, Ph.D., Institute of Oncology Ljubljana, Department of Experimental Oncology, Zaloška 2, SI-1000 Ljubljana, Slovenia. Phone: +386 1 5879 545; E-mail: tjesenko@onko-i.si

Disclosure: No potential conflicts of interest were disclosed.

Background. Tumor cells can shed from the tumor, enter the circulation and travel to distant organs, where they can seed metastases. These cells are called circulating tumor cells (CTCs). The ability of CTCs to populate distant tissues and organs has led us to believe they are the primary cause of cancer metastasis. The biological properties and interaction of CTCs with other cell types during intravasation, circulation in the bloodstream, extravasation and colonization are multifaceted and include changes of CTC phenotypes that are regulated by many signaling molecules, including cytokines and chemokines. Considering a sample is readily accessible by a simple blood draw, monitoring CTC levels in the blood has exceptional implications in oncology field. A method called the liquid biopsy allows the extraction of not only CTC, but also CTC products, such as cell free DNA (cfDNA), cell free RNA (cfRNA), microRNA (miRNA) and exosomes.

Conclusions. The clinical utility of CTCs and their products is increasing with advances in liquid biopsy technology. Clinical applications of liquid biopsy to detect CTCs and their products are numerous and could be used for screening of the presence of the cancer in the general population, as well as for prognostic and predictive biomarkers in cancer patients. With the development of better CTC isolation technologies and clinical testing in large prospective trials, increasing clinical utility of CTCs can be expected. The understanding of their biology and interactions with other cell types, particularly with those of the immune system and the rise of immunotherapy also hold great promise for novel therapeutic possibilities.

Key words: circulating tumor cells; CTC; metastasis; liquid biopsy; cancer; disseminated tumor cells.

Introduction

The pathologist Thomas Ashworth first described tumor cells found in the circulation of a deceased patient in 1869. By comparing these cells to cells extracted from the patient's various malignant masses he considered a mutual origin of cancer in the patient.¹ We now know tumor cells can shed from the tumor and enter the circulation and travel to distant organs, where they can seed metastases. These cells are called circulating tumor cells (CTCs). CTCs can also enter the bone marrow and stay in a dormant state for different length of time.

These cells are called disseminated tumor cells (DTCs).² The ability of CTCs to populate distant tissues and organs has led us to believe they are the primary cause of cancer metastasis. Considering a sample is readily accessible by a simple blood draw, monitoring CTC levels in the blood has exceptional implications for the treatment of cancer patients. However, due to small numbers and short half-life of CTCs in the blood, the detection and identification remains a big diagnostic challenge. Additionally, CTCs experience constant genotypic and phenotypic changes, which make their identification even more challenging. Understanding

CTC biology, tumor heterogeneity and metastatic spread on the one hand and improvement of detection methods and evaluation of prognostic and predictive value of CTCs on the other hand are one of the main objectives of cancer research as demonstrated by the enormous amounts of published literature in the recent years.

CTC biology

CTCs represent an intermediate step of the metastatic cascade. A tumor cell first leaves the primary or metastatic tumor site, invades into a blood or lymphatic vessel and circulates in the bloodstream before successfully forming a new tumor at a distant organ site. As determined in rat tumor model, millions of tumor cells break out of the primary tumor each day.³ However, the clearance of CTCs from the blood is fast as only a few of them can survive in the bloodstream due to a combination of physical stress (shear forces), anoikis (a form of cell death that occurs in anchorage-dependent cells when they detach from the surrounding extracellular matrix), immune surveillance and the lack of growth factors. The number of CTCs in the bloodstream is extremely small (1 to 10 cells per 10 ml of blood). They can be found in the form of individual cells or cell clusters.⁴ Aceto *et al.* have demonstrated that breast cancer CTC clusters arise from oligoclonal tumor cell groupings held together through plakoglobin-dependent intercellular adhesions and not from intravascular aggregation of tumor cells.⁵ Similar polyclonal collective dissemination of keratin 14-expressing tumor cell clusters was observed in breast cancer mouse tumor model.⁶ It has also been demonstrated that cell clusters have 23 to 50-fold increased metastatic potential compared to individual CTCs, which could be mediated through increased viability of cancer cells within a cluster.⁵ CTC clusters can extravasate faster, therefore they have a shorter half-life in the circulation as individual CTCs (6–10 min for clusters vs. 25–30 min for single cells) that also aids in their survival and outgrowth.⁵ Due to emerging evidence on the importance of CTC clusters in metastatic cascade, molecular mechanisms of cell cluster formation and migration are being investigated. The study of Giampieri *et al.* demonstrated that transforming growth factor beta (TGF β) signaling is involved in determination of the motile state of breast cancer cells.⁷ Two distinct modes of motility were observed: collective and as single cells. TGF β 1 switched cells from collective to single cell

motility through a transcriptional program involving a Smad family co-mediator protein (Smad4), epidermal growth factor receptor (EGFR), neural precursor cell expressed developmentally down-regulated protein 9 (Nedd9), myosin phosphatase Rho-interacting protein (M-RIP) and Ras homolog gene family, member C (RhoC). When TGF β signaling was blocked, only collective migration was observed.⁷ These findings are important in the scope of targeted therapy, as signaling pathways that contribute to the formation and migration of CTC clusters could be targeted.

Epithelial-mesenchymal plasticity of CTCs

In the early stages of the metastatic cascade, epithelial cells lose their apical-basal orientation, cell-to-cell junctions and cell-to-matrix interactions, gaining the ability to separate from the primary tumor in the process of epithelial-mesenchymal transition (EMT), which is a fundamental physiological phenomenon that occurs during embryogenesis and wound healing.⁸ Factors that trigger EMT can be extracellular factors such as TGF β , epidermal growth factor (EGF), hepatocyte growth factor (HGF), insulin-like growth factor (IGF), fibroblast growth factor (FGF), Notch and homologous wingless (wg) and Int-1 (Wnt) protein family and others, as well as mechanical factors such as extracellular matrix density.^{9,10} These extracellular factors usually activate the transcription factors Twist family BHLH transcription factor 1 (TWIST1), Zinc finger protein SNAI1 (SNAIL), Zinc finger e-box binding homeobox 1 (ZEB1), Zinc finger e-box-binding homeobox 2 (ZEB2) (SIP1) and others.¹¹ During EMT, the cell loses its epithelial markers (such as E-cadherin, epithelial cell adhesion molecule (EpCAM), cytokeratins and others) and obtains mesenchymal markers (such as vimentin and N-cadherin). The newly obtained mesenchymal phenotype allows the cells to migrate and invade through the basement membrane into the blood vessels. After intravasation, cells circulate in the bloodstream as CTCs, until they exit the vessel at a distant site to seed micro metastases. In order to successfully seed and form a secondary tumor, the cells must regain their epithelial phenotype, hence they undergo a reverse process of EMT - mesenchymal-epithelial transition (MET).¹² EMT and MET thus enable tumor cells of epithelial origin to disseminate and colonize distant organs. Therefore, CTCs show high level of epithelial-mesenchymal plastic-

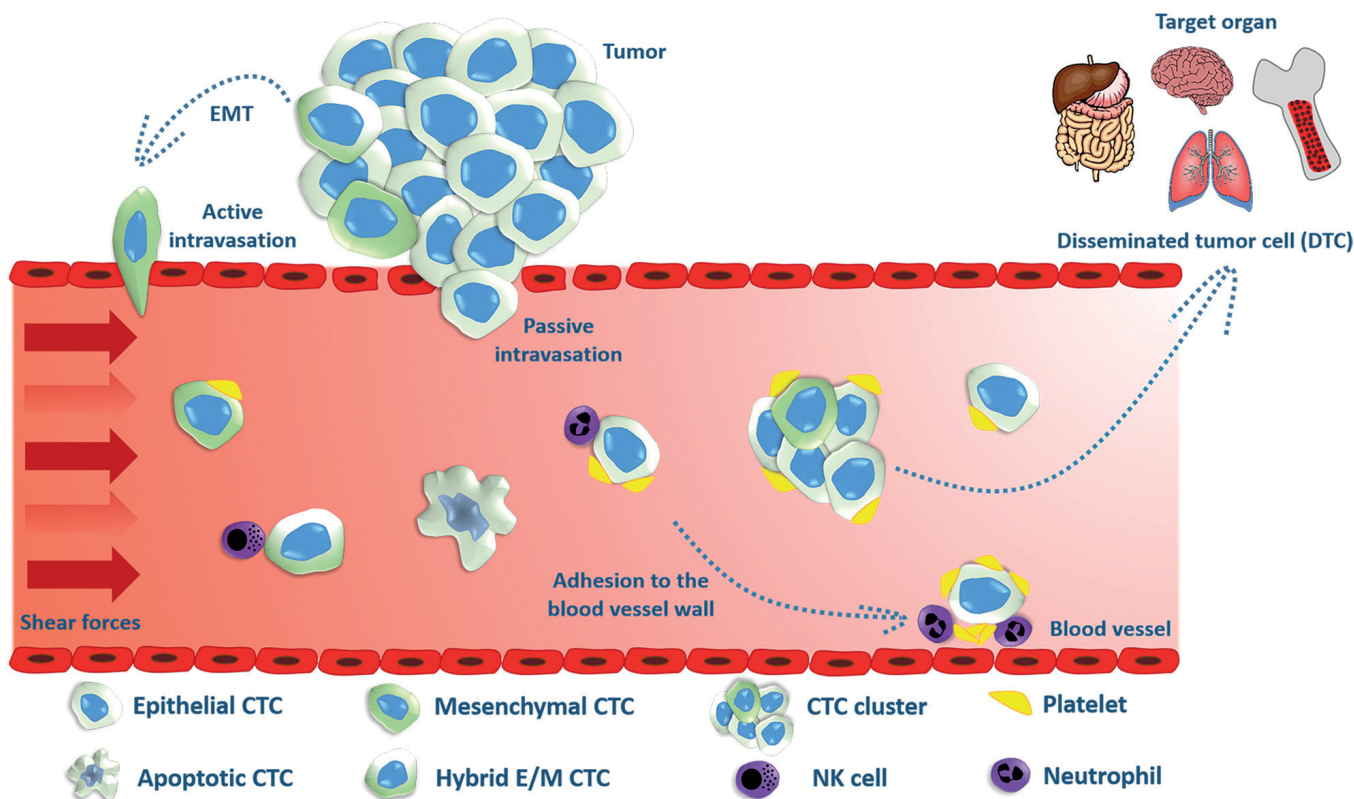


FIGURE 1. Circulating tumor cells (CTCs) can enter the blood vessel via active intravasation involving epithelial-mesenchymal transition (EMT) or by passive shedding due to compromised tumor vasculature. CTCs can exist in different phenotypes- epithelial, mesenchymal or both- hybrid epithelial/ mesenchymal phenotype (hybrid E/M). CTCs can be found in the form of individual cells or cell clusters; the latter show increased metastatic potential compared to individual CTCs. Platelet-CTC interaction in the blood vessel acts as a shield against the shear stress of blood flow, immune attack and also enables the adhesion to the blood vessel wall and extravasation. After the arrest of CTCs in the bone marrow or distant organ, they can extravasate and remain in the target tissue in the form of disseminated tumor cell (DTC).

ity and can be isolated from peripheral blood in different phenotypes-epithelial, mesenchymal or both- hybrid epithelial/mesenchymal phenotype (hybrid E/M), also referred to as partial, intermediate or incomplete EMT phenotype (Figure 1).¹³⁻¹⁵ Cells in hybrid E/M phenotype have mixed epithelial (*e.g.*, adhesion) and mesenchymal (*e.g.*, migration and invasion) properties that enable collective migration and invasion in the form of cell clusters. Therefore, hybrid E/M cell clusters seem to have the highest metastatic potential of all CTC variants.⁵ Furthermore, they also exhibit stemness; *i.e.* tumor-initiating properties.^{16,17}

CTCs in the circulation

Tumor cells can enter the circulation through a blood or lymphatic vessel, depending on a number of factors including their accessibility, physical restrictions and active mechanisms for attracting

cells to specific types of vasculature.¹⁸ Lymphatic intravasation is also a pathway by which tumor cells can enter the blood vessels, since lymph vessels eventually drain into the blood in the major thoracic duct.¹⁸ However, there is little evidence that lymphatic vessels do indeed enable further passage of significant numbers of cancer cells to the bloodstream, which indicates lymph vessel deposits are probably simply dead ends for cancer cells and may reveal the extent of parallel, concomitant dissemination from the primary tumor.¹⁹ On the other hand, direct hematogenous transport is likely the main route of distant metastatic colonization. Along the way, lymphatic fluid is filtered through a series of lymph nodes, which are often the first sites of metastasis. Intravasation into a blood vessel can be an active or passive event, which depends on the tumor type, tumor micro-environment and blood vessel integrity. Active intravasation includes the invasion of tumor cells or cell clusters with increased migratory potential ac-

quired through EMT into the blood vessel, whereas individual cells or cell clusters can also be shed passively into the blood stream due to compromised tumor vasculature (Figure 1).²⁰ Once in the circulation, CTCs are exposed to the shear stress of blood flow, which together with anoikis and immune surveillance may be enough to destroy a large proportion of CTCs entering into the bloodstream.²¹ It has also been demonstrated that CTCs in the blood stream have a short half-life; in patients with localized prostate cancer who had detectable CTCs, most of them no longer have evident CTCs at 24 hours following surgical resection of the primary tumor.²² However, some of the CTCs are capable of surviving the journey through circulation and forming distant metastasis. There is increasing evidence that interaction of CTCs with other blood components is crucial for their survival and metastatic potential. The most studied is indeed the interaction of CTCs with platelets.²³ Platelet-CTC interactions may occur soon after the entry of CTCs into the circulation. One of the first interactions is the formation of platelet-rich thrombi around tumor cells, which is triggered by the platelet tissue factor (factor III/CD142) expressed by the tumor cells.²⁴ This interaction acts as a shield against the shear stress of blood flow, immune attack and also enables the adhesion to the blood vessel wall and extravasation (Figure 1).²⁴⁻²⁶ It has been demonstrated that activated platelets can transfer the major histocompatibility complex (MHC) to CTCs, which enables the CTCs to mimic host cells and escape from immune surveillance.²⁷ Furthermore, platelets can prevent tumor cell recognition and lysis by natural killer cells (NK cells).²⁸ It has also been demonstrated that platelets can promote EMT of tumor cells within the circulation via the release of TGF β , also enhancing metastatic potential of CTCs.²⁹ CTCs may also interact with various types of leucocytes; neutrophils, monocytes and macrophages, which could promote CTC survival and promote the interaction of CTCs with endothelial cells and extravasation.¹⁹

Interaction of CTCs with immune cells in the bloodstream

In tumor progression, tumors eventually go through the immunoediting process, which enables the tumor to establish an immunosuppressive microenvironment and escape from the immune surveillance.³⁰ In the escape phase, tumor

cells evade immune recognition through different mechanisms, including immune suppression mediated by immunosuppressive cells (regulatory T cells - Tregs) and myeloid-derived suppressor cells (MDSCs), reduction of immune recognition by down-regulation of antigen processing machinery affecting the major histocompatibility complex (MHC) I pathway, release of immune suppressive mediators (cytokines such as TGF β , vascular endothelial growth factor [VEGF] and expression of immunoregulatory molecules such as indoleamine-pyrrole 2,3-dioxygenase [IDO], programmed cell death protein 1 [PD-1] / programmed death ligand 1 [PD-L1], T cell Ig domain and mucin domain 3 [Tim-3] / galectin-9, lymphocyte-activation gene 3 [LAG-3]).^{30,31} Once the tumor cell leaves the immunosuppressive microenvironment of the primary tumor and enters the bloodstream, it interacts with several different types of immune cells, which can destroy the CTC in the bloodstream before its extravasation at distant site. On the other hand, interaction of tumor cells with immune cells can also promote tumor progression with the generation of hospitable microenvironment for metastatic growth^{32,33} or by maintaining CTC viability in the bloodstream and facilitating extravasation.^{23,34} Therefore, immune cells can hinder or favor the dissemination of CTCs.

CTCs interact with the components of the innate immune system in different ways. Natural killer cells (NK cells) in the bloodstream can intercept CTCs and destroy them before extravasation, thus preventing metastasis (Figure 1). Preclinical studies have shown that hosts with high NK cell activity (adult mice) are very resistant to metastasis compared to hosts with low NK cell activity (young mice)³⁵ and that direct perforin-dependent killing by NK cells is more effective than indirect killing with apoptosis-inducing factors.³⁶ It has also been demonstrated in metastatic breast, colorectal, and prostate cancer patients that NK cell cytotoxic activity was decreased in patients with a relatively high number of CTCs in peripheral blood compared to patients with a relatively low number of CTCs.³⁷ Therefore, the increase of NK cell cytotoxic activity should be considered in future research as a treatment option in patients with relatively high numbers of CTCs.

There is increasing evidence that CTCs in the bloodstream can also associate with neutrophils. It has recently been demonstrated that CTCs in breast cancer patients were frequently associated with neutrophils and that this association drives cell cycle progression within the bloodstream

and expands the metastatic potential of CTCs.³⁴ Neutrophils seem to mediate adhesion of cancer cells and facilitate their extravasation (Figure 1), as demonstrated by several *in vivo* studies showing CTC interaction with endothelium-bound neutrophils in the vascular network and their promotion of adhesive and migratory activity through different molecular targets.³⁸⁻⁴¹

Two subpopulations, classical and non-classical monocytes are also found in the circulation. Whereas classical monocytes can extravasate and differentiate into macrophages with protumor and prometastatic functions, non-classical monocytes display a protective role against metastasis. They accumulate in the capillaries in response to chemokines and clear cellular debris.⁴² A preclinical study on mouse tumor models has demonstrated that after tumor cells injection, non-classical monocytes were recruited to premetastatic lung capillaries in response to chemokine CX3CL1, where they engulfed tumor material and secreted CCL3, CCL4 and CCL5, leading to the activation of NK cells.⁴³

CTCs also interact with the adaptive arm of the immune system. However, our current knowledge concerning the function of lymphocytes in immune surveillance of CTCs is very limited. It was shown that in patients with metastatic breast cancer low circulating lymphocyte levels and high CTC levels were found to be independent predictive factors of poor diagnosis, progression-free survival and overall survival.⁴⁴ Similarly, low percentage of lymphocytes were found in patients with inflammatory breast cancer and advanced non-small-cell lung cancer (NSCLC), which could contribute to immune evasion.^{45,46} Several studies in patients with different types of cancer have also shown that CTCs frequently express PD-L1, one of the mechanisms responsible for CTC escape from immune surveillance.⁴⁷⁻⁴⁹ Further studies are needed in this field, however, monitoring of PD-L1 expression in CTCs could be used in the future as a prognostic biomarker or/and as predictive biomarker for checkpoint inhibitor-based immunotherapy.⁵⁰⁻⁵²

Extravasation and colonization of distant tissues

In contrast to the short half-life of CTCs in the blood, the metastatic process takes months and years.⁵³ Cancer cells spread throughout the body and leave the circulation at potential secondary tumor sites in a process called extravasation. Extravasation requires tumor cells to traverse the

endothelial wall in the process of transendothelial migration.⁵⁴ The ability of CTCs to extravasate can be influenced by several factors, such as monocytes, which may differentiate into metastasis-associated macrophages, or platelets which release ATP and increase the permeability of the capillary walls.^{55,56} Extravasation of CTCs takes place in small capillaries with a diameter similar to that of the CTC. In this manner, the CTCs are trapped in the vessel. The first step of extravasation thus appears to be the stopping and physical restriction of a CTC in the vessel and subsequent attachment to the endothelium.⁵⁷ Adhesion to the endothelium requires the expression of ligands and receptors on cancer cells and endothelial cells, such as selectins, integrins, cadherins, antigen CD44 and immunoglobulin superfamily receptors. The cancer cells or cancer cell-related leukocytes release cytokines that promote E-selectin expression on the endothelial cell surface.⁵⁴ A CTC then binds to an E-selectin molecule on the endothelium.⁵⁸ Different tumor types exhibit different metastatic patterns, a phenomenon termed tissue tropism.⁵³ These patterns are largely dependent on the vasculature of the secondary organ and the chemokines and their receptors expressed between the target endothelium and the cancer cells.^{54,59} In addition to E-selectin expression on endothelial cell surface, chemokines also play an important role in CTC and endothelial interaction. Chemokines are released by the target tissue to attract tumor cells. The role of the chemokine C-X-C motif 12 ligand (CXCL12), also called stromal-derived factor-1 α (SDF-1 α), has been extensively investigated. The ligand is produced by stromal cells.⁶⁰ It then binds to its receptors C-X-C motif chemokine receptor 4 (CXCR 4) and C-X-C motif chemokine receptor 7 (CXCR 7) on cancer cells. *In vitro* stimulation by the CXCL12 increased interactions of pancreatic and prostate cancer cells with the endothelium and the subsequent trans-endothelial migration.⁶¹

The attachment of a cancer cell to the E-selectin molecule is followed by interactions via integrins, CD44 antigen and mucin 1 (MUC1), contributing to a more stable attachment to the endothelial cell. This is followed by transendothelial migration, which can take place paracellularly or transcellularly. *In vitro*, most cells use the paracellular route⁵⁴, in which the opening of tight endothelial cell-junctions is initiated by factors released by either the tumor or the immune cells, such as TGF β and VEGF^{62,63}, however, it is not known which the preferred route is *in vivo*. The subsequent crossing of the tumor cell through the basal lamina is

the final step in the process of extravasation. If not eliminated, the newly extravasated cells can then enter a state of dormancy or proliferate in this new microenvironment to form metastases. The vast majority of tumor cells undergo cell death after extravasation.⁵⁴

Similarly to primary tumors, newly formed micrometastases depend on stromal support to survive.⁶⁴ The transition of tumor cells from dormant state to proliferation can be provoked by changes in the tumor microenvironment, such as angiogenesis.⁵⁷ Another factor might be the induction of inflammation, as described by the De Cock *et al.*⁶⁵ In 2017, a Chinese study similarly reported that CTC-mediated systemic inflammation and neutrophil recruitment to pre-metastatic tissues is the mechanism of metastatic colonization by the CTCs.⁶⁶ This was demonstrated *in vitro* using an anti-inflammatory cytokine interleukin 37 (IL-37) to deplete neutrophils, suppress inflammatory response and thus the promoting effect of CTCs on tumor metastasis.⁶⁶ The mechanism is based on the assumption of functional plasticity of neutrophils in the tumor microenvironment. Depending on environmental factors, neutrophils can switch between anti-tumor and pro-tumor phenotypes.⁶⁷ IL-37 was able to suppress CTC-induced conversion of neutrophil function to pro-tumor phenotype. These findings suggest anti-inflammatory therapy could be used when higher CTC count is detected.⁶⁶

In addition, the support of the extracellular matrix (ECM) may also aid in metastatic colonization. Specific ECM components associated with colonization of the lung in breast cancer have been identified.^{68,69} Hypoxia and fibrosis have also been linked to metastasis.^{19,70} Interestingly, suitable microenvironment may start to develop prior to extravasation of tumor cells as a result of systemic effects of the primary tumor.¹⁹ An observation by Costa-Silva *et al.* describes exosomes derived from tumor cells carrying DNA, mRNA, miRNA and proteins which prime the liver for metastasis of pancreatic ductal adenocarcinoma.⁷¹ These particles have become the focus of recent studies and may cause a broad spectrum of actions, such as immunosuppression and/or induction of angiogenesis, inflammation, extracellular remodeling, and metabolic reprogramming.

Apart from the above described factors, the survival of a cancer cell in this microenvironment is also dependent on its genetic profile. Some of the genes associated with increased survival of cancer cells in various secondary tissues have been identified. A study by Zhang *et al.* identified a popula-

tion of breast cancer cells that do not express the EpCAM cell surface antigen, but do express human epidermal growth factor receptor 2 (HER2), EGFR, heparanase (HSPE) and Notch 1, and selectively metastasize to the brain.⁷² Genes that mediate metastases to the lung and bone have also been identified.^{73,74}

Liquid biopsy and CTC detection

Distant metastases are the main cause of cancer-related mortality. Following primary tumor removal, DTC and micrometastases can remain dormant for long periods of time before causing disease relapse and are thus termed minimal residual disease (MRD).⁷⁵ DTCs cannot be detected by radiologic imaging. However, they can be studied by performing biopsies of their reservoirs. The bone marrow is considered to be the primary indicator of MRD and poor outcome.⁷⁶ It can be accessed by an iliac crest biopsy. Because bone marrow biopsy is a highly invasive procedure, current research is focusing on clinical utility of CTCs in the blood.⁷⁷ A method called the liquid biopsy allows the extraction and testing of blood for tumor cell presence, and is able to detect CTC, cell free DNA (cfDNA), cell free RNA (cfRNA), microRNA (miRNA) and exosomes.

Detection of CTCs in a blood sample is challenging as these cells are present in very small numbers and are surrounded by billions of other blood cells (1 CTC per 10^7 of leukocytes per ml of blood).⁷⁸ Highly sensitive and specific analytical methods are required, which can be achieved by using capture, enrichment and detection procedures.⁷⁹ Most isolation devices combine capture and enrichment procedures and may also include detection and enumeration technology. Capture procedures aim to overcome the low specificity of a regular blood draw by increasing its yield. The GILUPI nanodetector[®] detects and captures CTC in the blood *in vivo*. The detector is located on a steel wire and is covered by chimeric anti-EpCAM antibodies. The device is inserted through a standard venous cannula into a peripheral vein for 30 minutes. During this time, the 2 cm functional area of the detector will come into contact with up to 1.5 litres of blood, enabling contact with a significantly larger amount of CTCs than during a regular blood draw. After removal, CTCs can be identified via immunocytochemical staining and counted. This protocol has been tested in patients with breast cancer and non-

small cell lung cancer (NSCLC) with no adverse effects.⁸⁰

Enrichment procedures aim to increase the percentage of CTCs in the sample. They are based on various properties of CTCs that distinguish them from the surrounding normal hematopoietic cells. These properties are either physical (size, density, electric charge, deformability) or biological (cell-surface protein expression and viability). Physical properties of the CTCs are the functional basis of membrane filters (size), microfluidic systems (deformability), density gradient centrifugation (density), and dielectrophoresis (electric charge). Biological properties are exploited by the immunobead assays, which use antibodies against tumor or non-tumor associated antigens, and microdevices.⁸¹ Isolation of CTCs based on their physical properties has certain advantages. They do not rely on biomarker expression, thus the isolated cells are viable, intact and can be used for further *in vitro* characterization and experiments. Enrichment time is short, and the cost of the procedure is low because ligands for CTC capture are not required. On the other hand, the limitation of these technologies is their low specificity, which requires downstream procedures for purity analyses.⁷⁹ Among these physical methods, size-based isolation of CTCs takes advantage of their increased size (12–25 μm) compared to leukocytes (5–20 μm).⁸² Size-based isolation of CTCs includes membrane microfilters and size-based microfluidic CTC sorting devices.⁸³ Isolation by size of epithelial tumor cells (ISET) technology uses polycarbonate microfilters of 8 μm diameter pores for CTC enrichment.⁸⁴ The CTC sorting system Parsortix© is designed as a channel with stepped obstacles that progressively decrease as the cells in suspension flow through it. Both size and deformability contribute to successful CTC isolation. 10- μm was set as cut-off size for cancer cells isolation. The main advantage of the device is high capture purity and isolation of viable cancer cells.⁸⁵ Density gradient centrifugation for separation of different cell types was observed by S.H. Seal in 1959.⁸⁶ From top to bottom, centrifugation yields the following layers: erythrocytes, granulocytes, density gradient, buffy coat with mononuclear cells and CTCs, and plasma. AccuCyte© is an advanced density-gradient separation technology combining a separation tube and a collector device, which allows buffy coat collection into a small volume. The collected layer can be applied to a microscopic slide without cell lysis or wash steps with possible loss of CTC.⁸⁷ Another recently validated technology is a microfluidic chip that

is able to focus and capture CTCs with high cell yield and without the need for further purification. In the course of the validation study, single CTCs, CTC clusters and tumor microemboli (observed as multicellular tumour aggregates of CTC and white blood cells) were identified in patients with head and neck cancer.⁸⁸

Biological property that is the most widely used for enrichment of CTCs is based on positive immunoselection. Specific cell-surface antigen expression in CTCs from epithelial carcinomas versus leukocytes allows for positive selection of CTCs. Specific antibodies are added to a blood sample to mark tumor cell-specific cell-surface markers, most commonly the EpCAM, which is a transmembrane glycoprotein expressed by the majority of tumors of epithelial origin. Other positive selection antibodies include anti HER2 and anti EGFR. On the other hand, a negative immunoselection of leukocytes based on their biological characteristics can also lead to enrichment of CTCs. The most commonly used negative selection target is the leukocyte antigen CD45.^{81,89} The enrichment step should be followed by tumor cell detection and verification. In most methods, this step includes immunofluorescence staining and high-resolution imaging. A certain amount of leukocytes is still present in the enriched fraction and single-cell level identification is required. Most of the established CTC assays use cytokeratin (CK), CD45 and nuclear dye 4,6-diamidino-2-phenylindole (DAPI) staining. Fluorescence microscopy should identify stained CTCs as CK positive, CD45 negative and DAPI positive.⁸¹ An alternative to immunocytochemical staining are real-time polymerase chain reaction (RT-PCR) assays based on the detection of mRNA expression.^{90,91} CellSearch© is an established immunomagnetic CTC isolation assay, which uses magnetic beads covered with anti-EpCAM antibodies for positive selection. CTC separation and magnetic bead washing is followed by secondary selection based on morphology, CK staining and CD45 antigen expression. The CellSearch© is the only CTC isolation assay to have been approved by the Food and Drug Administration (FDA) as a prognostic tool in the management of breast cancer, prostate cancer and colorectal cancer patients.⁹²

An important concern is the fact that most CTC isolation technologies are based on epithelial cell-surface marker detection, because mesenchymal markers are expressed in white blood cells. In this way, a potentially crucial CTC population which expresses mesenchymal markers and is related to a more aggressive disease course could be over-

looked.⁹³ Detection protocols should be improved in order to optimize selection based on a combination of EMT and cancer cell markers.

Clinical applications

Clinical oncology has always faced limitations due to disease heterogeneity. The diagnostics of a tumor biopsy sample is deficient in case of gross tumor heterogeneity and the therapy prescribed might not be the most suitable option for the patient. Different tumor subpopulations, including distant metastases, can express various molecular targets, resulting in poor response to therapy and contributing to the development of drug resistance. These challenges could be solved by regular monitoring of CTCs and their products in the circulation by performing a liquid biopsy, thus allowing disease course surveillance, detect emerging drug resistance, recognition of new molecular targets and defining disease status in real time. CTCs contribute greatly to the metastatic process and are as such a promising target for early cancer detection, prognosis-oriented testing as well as personalized cancer therapy (Figure 2). The following text summarizes the aspects of CTC utility in clinical medicine.

Screening

Studies that investigate screening usually start by comparing patients with cancer with controls

(healthy individuals or patients with benign diseases). Subsequent cohort studies are cumbersome and require large study populations and extended follow-up times. Focusing on screening of patients with high risk of developing cancer is a good strategy to speed up the clinical validation process.⁹⁴

In 2004, a milestone study showed circulating epithelial cells to be extremely rare in healthy women, never reaching more than 2 cells per 7.5 ml of blood.⁹⁵ However, higher circulating epithelial cell levels were observed in patients with benign inflammatory bowel disease, such as diverticulosis and Crohn's disease, and in patients with elevated prostate specific antigen (PSA) values.^{96,97} The utility of CTCs for screening is therefore limited by its low sensitivity and specificity. But there are studies in selected populations where CTC screening might be applicable. In patients with chronic obstructive pulmonary disease (COPD), a major risk factor for lung cancer, CTCs were detected 1–4 years earlier than radiologic signs of malignancy could be found on a computed tomography scan.⁹⁸ Interestingly, CTCs detected in patients with COPD had a heterogeneous expression of epithelial and mesenchymal markers. These preliminary findings need to be validated in larger cohorts, and sources that may lead to unspecific findings in non-cancer patients, such as the release of epithelial cells into the blood of patients with inflammatory bowel diseases, need to be identified. On the other hand, CTC values over 25 cells per 7.5 ml of blood could be used to distinguish lung carcinoma from benign lesions in patients with suspicious radiological findings, as demonstrated by a study using size-based isolation on ScreenCell Cyto filtration device and subsequent immunohistochemistry.⁹⁹

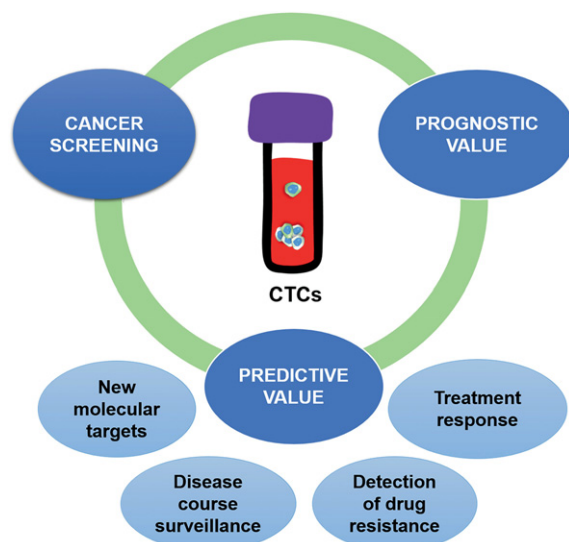


FIGURE 2. Clinical applications of CTCs.

Prognostic value

Numerous studies have thus far demonstrated the prognostic significance of CTC in patients with various types of solid tumors, most notably breast cancer. Interestingly, the 2010 TNM classification of malignant tumors already included a new stage called cM 0 (i +), with "i + " referring to isolated tumor cells detection in blood, bone marrow, and lymph nodes.¹⁰⁰ In clinical practice however, this classification stage is rarely used, most notably due to low CTC counts in M 0 patients, which has raised doubts about their utility as a reliable marker.⁹⁴ Nevertheless, there is increasing evidence that the determination of CTC counts before or after initial surgery in M0 patients is a reliable indicator of an unfavorable prognosis.⁹⁴

Patients with detectable CTCs are known to have shorter overall survival (OS) and progression free survival (PFS).¹⁰¹⁻¹⁰⁷ CTCs can also help evaluate MRD and select patients who are more at risk for relapse.^{108,109} Patients with high CTC levels during chemotherapy have significantly shorter survival. Metastatic patients with high baseline CTC counts that decrease after one cycle of chemotherapy have better prognosis.^{104,106,110-112}

Additional prognostic information can be obtained from morphological properties of CTCs. Patients with apoptotic CTCs or CTC clusters in blood samples after systemic therapy initiation had worse prognosis in terms of PFS and OS than patients with CTCs without these properties, indicating morphological characterization of CTCs could be an important prognostic marker during therapy in patients with ≥ 5 CTC per 7.5 ml blood.¹¹³

Predictive value

CTCs are a heterogeneous group of cells subjected to dynamic changes. The population of CTCs is rapidly being replaced by new circulating cells from different cell reservoirs, be it primary tumor or metastatic sites, thus mirroring the changes in systemic disease in real time. The main objectives of studies assessing the clinical applications of CTCs are: their possible role as a surrogate tumor sample for liquid biopsy; changes in CTC counts and properties during therapy as an indicator of response to therapy, and targeting CTC- and metastasis-related features.⁸⁹

CTCs as surrogate material for biopsy can help determine the risk of relapse and guide adjuvant therapy. Despite the fact, that many localized cancers can be cured by surgery only, some patients still experience late relapse. This is hypothesized to be the result of the presence of MRD of different carcinomas, which has no sensitive and specific enough biomarker. A study in colon cancer patients demonstrated that 72.5% of CTC-positive patients experienced relapse after surgery compared to 12% of patients with no detected CTCs. Using CTC presence in the bloodstream, patients with MRD could be identified and given adjuvant chemotherapy.^{114,115} An intriguing study from 2018 investigated the benefit of radiotherapy in early stage breast cancer patients who underwent breast conserving surgery based on their CTC status. They found longer overall survival in patients with detectable CTCs that received radiotherapy. Radiotherapy did not influence overall survival in patients with no detectable CTCs. This is the

first identified predictive factor for the therapeutic benefit of radiotherapy.¹¹⁶ Liquid biopsy can also be used to monitor patients during therapy as a surrogate marker for response to therapy, as confirmed by studies in prostate and breast cancer patients.¹¹⁷⁻¹¹⁹ CTC levels can also be used to monitor response to anti-tumor vaccines and immunotherapy.^{120,121} Molecular targets expressed by CTCs are not necessarily the same than those expressed by the primary tumor and could be used to guide targeted therapy. Evaluation of HER2, estrogen receptor (ER) and progesteron receptor (PR) status on CTCs in breast cancer patients has been extensively studied, but no standardized method or consensus on positivity criteria has been provided.¹²²

In current clinical practice, the expression of these markers on primary tumor tissue/based on primary tumor biopsy is used to guide treatment and prognosis, which is why a CTC-guided approach would have great clinical utility.¹²³ Agreement of ER and PR expression on CTCs and the corresponding primary tumor ranges from 40 to 70%.^{122,124-127} A study of HER2 expression on CTCs in early breast cancer patients also showed frequent discordance between the HER2 expression of CTCs and that of the primary tumor.¹²⁸ Administration of trastuzumab was able to eliminate chemotherapy-resistant CK19 mRNA-positive CTCs and prolong disease-free survival (DFS) compared to observation in a breast cancer population with HER2 negative primary tumors and detectable CK19 mRNA-positive CTCs before and after adjuvant therapy, of who 89% had HER2-positive CTCs.¹²⁹

A recent study found PD-L1 is evaluable in CTCs of patients with NSCLC and head and neck cancer, while it is predictive of poorer outcomes only in head and neck cancer.¹³⁰ Another recent study reported PD-L1 expression only in CTCs in contrast to primary tumor tissue samples.⁵²

On the other hand, androgen receptor variant 7 (AR-V7) expression on CTCs in metastatic castration resistant prostate cancer patients was identified as a biomarker for superior clinical outcomes on taxane therapy, indicating it may serve as a treatment selection (predictive) biomarker.¹³¹ Other studied biomarkers include EGFR and CD133, which is a potential chemoresistance marker.^{132,133} Further multicenter clinical trials are needed to define the role of expression of different targets on CTCs for patient selection.

In 2013, patient-derived CTC cultures were first established¹³⁴, though implementation of the procedure into regular clinical practice has proven to be difficult due to the low efficiency of available

detection methods as well as prolonged periods needed to establish cell lines.¹³⁵ CTC-based patient-derived xenografts represent an innovation in cancer research with the potential to guide therapy or pre-clinical drug testing and biomarker identification. CTCs are isolated from the patient's blood and injected into immunocompromised animals. Subsequently generated xenografts can be used for functional testing or as a bioptic sample for molecular characterization. This experimental model has been successfully tested in prostate cancer, small cell lung cancer and breast cancer patients and represents another important step towards personalized medicine.¹³⁶⁻¹³⁹

Clinical applications in specific cancer types

In **breast cancer**, the presence of 5 or more CTCs per 7.5 ml of blood has been associated with a reduction in progression free survival, overall survival^{95,140-142}, as well as with higher disease progression and mortality of metastatic breast cancer patients.¹⁴³⁻¹⁴⁷ Moreover, in metastatic breast cancer patients, evidence suggests that CTC detection can be an earlier indicator of disease change compared to radiologic changes.¹⁴⁸ Nevertheless, in metastatic breast cancer patients, detection of CTCs appears to be metastatic site dependent, with a positive correlation with brain metastases and an inverse correlation with bone metastases.¹⁴⁹ In spite of the prognostic value of CTC detection, switching to an alternate chemotherapy has not shown to prolong survival time.¹⁵⁰ Underestimation of CTC count is probably the result of epithelial cell marker loss after EMT, which is believed to be paramount for cell dissemination and chemotherapy resistance.¹⁵¹⁻¹⁵³ In HER2-positive patients treated with HER2-targeting therapy, detected levels of CTCs seem to have no prognostic value.¹⁵⁴ In triple-negative metastatic breast cancer patients on the other hand, the CTCs levels have been reported to carry a significant negative prognostic value.^{127,155}

In non-metastatic breast cancer, clinical utility of CTC detection remains a topic of discussion, as the detected values and their incidence are lower than in metastatic breast cancer cases.¹⁵⁶ Still, a pooled analyses showed strong evidence in favor of the independent prognostic value of CTC detection in estimating disease-free, overall, breast cancer-specific, and distant disease-free survival.¹⁰⁵ Moreover, in non-metastatic breast cancer, positive CTC results before treatment were related to

lymph node metastasis, and were shown to have a significant prognostic impact on disease-free and overall survival.¹⁵⁷ The fact that the detected presence of CTCs does not correlate with any established clinico-pathologic parameters demonstrates the value of additional independent information provided by the method.¹⁵⁸⁻¹⁶² CTC detection also shows promise in neoadjuvant therapy and provides a rapid way to assess the therapeutic efficacy.¹⁵⁶ CTC detection before neoadjuvant setting carry an independent prognostic value for a reduced disease-free and overall survival¹⁶³, while not being associated with pathologic complete response^{164,165}, again demonstrating the method's independent prognostic value.¹⁵⁶ Current research is focused also on investigating possible therapeutic targets on CTCs.¹⁵⁶

Multiple large phase II and III trials have established the prognostic value of CTC in advanced **prostate cancer**, most notably metastatic castration-resistant prostate cancer.^{112,166-170} The value of ≥ 5 CTCs per 7.5 ml of blood demonstrates a cutoff point with a significantly altered overall survival in metastatic castration-resistant prostate cancer patients.^{112,168-170} Measured prior to, during and following cytotoxic therapy in castration-resistant prostate cancer, CTC detection has been shown to be the strongest independent predictor of overall survival.^{112,166} A conversion from unfavorable to favorable CTC baseline concentrations (or vice versa) during chemotherapy, reflects disease outcome.^{112,168} The method of CTC detection has even been shown superior to PSA measurements, both in the rapidity of detectable change as well as reliability, and has consequently been approved by the Food and Drug Administration for prostate cancer therapy monitoring in 2008.¹¹² In addition, it is recommended that therapy should not be changed based on PSA values alone.¹⁷¹ Fixed cutoff values simplify therapeutic decision-making. Nevertheless, strong evidence exists in favor of the assumption that patient survival is independent of a specific CTC concentration threshold.^{166,172} Also, treatment should be continued regardless of the cutoff value of ≥ 5 CTCs per 7.5 ml of blood, as long as CTC levels remain stable or decrease under therapy. Similarly, an increase in CTC concentrations may indicate primary treatment resistance and warrant therapy switch.¹⁵⁶ In estimation of treatment effectiveness, CTC detection coupled with lactate dehydrogenase measurements has been shown superior to baseline serum lactate dehydrogenase measurements alone.¹⁶⁶ While CTC isolation has been extensively studied in castration

resistant prostate cancer, relevance in other disease stages such as hormone sensitive or early prostate cancer are still scarce.¹⁵⁶ Patients in these disease stages present with infrequent and low CTC counts (1–2 on average) show no correlation with other established clinicopathologic parameters (Gleason grade, PSA, TNM staging).^{97,173–175} In hormone sensitive metastatic prostate cancer, cutoff values of ≥ 5 CTCs per 7.5 ml of blood^{176,177} have been shown to anticipate lower hormone deprivation responsiveness and shortened transition times to castration-resistant prostate cancer, associated with shorter progression free survival and overall survival.¹⁷⁸ This could indicate the aggressiveness of the disease and resultantly warrant closer monitoring and earlier treatment switches.¹⁵⁶

In **non-metastatic urinary carcinoma** of the bladder, detection of CTCs correlates positively with worse progression free survival, overall survival, cancer-specific survival¹⁷⁹ as well as recurrence-free survival¹⁸⁰, and is an independent prognostic factor for early systemic disease¹⁸⁰, both in cases of pure and variant urinary carcinoma of the bladder.¹⁸¹ Moreover, a comparison between CTC and primary tumor HER2 status showed dissimilarities in 23% of cases, pointing out a possible benefit of HER2-targeting therapy in selected patients.¹⁸⁰

Presently, the presence of CTCs in patients with seminoma and non-seminoma **testicular germ cell tumors** is not well established¹⁵⁶, and has been associated with the tumor stage, elevated serum levels of alpha-fetoprotein and beta-human chorionic gonadotropin.¹⁸²

In spite of frequent EpCAM negativity of **renal cell cancer**¹⁸³, one study detected CTCs in 16% of subjects with metastatic renal cell carcinoma.¹⁸⁴

The incidence of CTCs in metastatic **colorectal cancer** has been shown to be higher than in non-metastatic disease, and correlates well with both progression free survival and overall survival, thus demonstrating the prognostic utility of the method.¹⁸⁵ In newly diagnosed non-metastatic colorectal cancer, a higher presence of CTCs before surgery shows a good correlation with shorter relapse-free survival and cancer specific survival.¹⁸⁵

Higher CTC levels following therapy in **gastric and esophageal cancer** are associated with worse prognosis.¹⁵⁶

In **pancreatic cancer**, the presence of CTCs at baseline is an independent prognostic factor for overall survival¹⁰⁷, with higher detection rates in metastatic disease compared to non-metastatic disease.¹⁵⁶ Moreover, CTC detection in the portal vein has been associated with higher rates of liver

metastases after surgery in contrast to detection in peripheral blood.¹⁸⁶ Compared to other types of carcinoma, pancreatic cancer CTC detection rates are thought to be lower due to CTC sequestration by the liver, decreased vascularity in aggressive tumors and the inability to detect CTCs following EMT.¹⁸⁷

As in other tumor types, CTCs in **cholangiocarcinoma** were detected and correlated with shorter overall survival.¹⁸⁸

CTC concentration is approximately ten times higher in **small cell lung cancer** compared to that in **NSCLC**.¹⁵⁶ CTC detection of ≥ 50 CTCs per 7.5 ml of blood in small cell lung cancer patients prior to chemotherapy is associated with a shorter progression free survival and overall survival.¹⁰⁴ Similar is true for the incidence of metastases to other organs, especially liver.¹⁸⁹ CTC enumeration has also been used to discriminate between localized (median 6 CTCs/7.5 ml of blood) and extensive (median 63 CTCs/7.5 ml of blood) disease at baseline.¹⁹⁰ CTC ≥ 5 per 7.5 ml of blood is an independent negative prognostic factor in NSCLC.^{104,156,190}

Decreasing values of detected CTCs in patients undergoing chemotherapy could carry a predictive value for therapy response in cancer of **unknown primary origin**.¹⁹¹

Several studies investigating the viability of CTC based disease detection and monitoring in **gynecologic, head and neck, neuroendocrine tumors and melanomas**, have shown poor clinical outcomes in cases of CTC detection.¹⁵⁶

Conclusions

The management of a cancer patient is based on radiological evidence and histopathological properties of the primary tumor. Cancer is a constantly evolving disease prone to selection pressure caused by therapy. By relying on the biopsy of the tumor, our insight into the patient's disease is both space- and time-limited, resulting in insufficient information for proper patient management. The concept of a liquid biopsy enables real-time disease control while being both more accessible and less invasive for the patient. The number of CTCs in the blood is a strong prognostic factor and can be used for monitoring response to therapy. In addition, detection of specific molecular targets on CTCs can improve and guide novel treatment approaches. Isolated CTCs can be used to analyze DNA, RNA or proteins produced by the tumor cell. Furthermore, they can be used to produce patient-derived xen-

ografts for functional testing. On the other hand, CTC detection faces its limitations because of the rarity of these cells compared to the background of billions of normal blood cells. Highly sensitive and specific methods are required for successful isolation and detection. With the development of better CTC isolation technologies and clinical testing in large prospective trials, increasing clinical utility of CTCs can be expected. The understanding of their biology and interactions with the immune system and the rise of immunotherapy also hold great promise for novel therapeutic possibilities.

Acknowledgement

The authors acknowledge the financial support from the state budget by the Slovenian Research Agency (program no. P3-0003, P3-0321 and project no. Z3-8204).

References

- Ashworth T. A case of cancer in which cells similar to those in the tumours were seen in the blood after death. *Aust Med J* 1869; **14**: 146-7.
- Riethdorf S, Pantel K. Disseminated tumor cells in bone marrow and circulating tumor cells in blood of breast cancer patients: current state of detection and characterization. *Pathobiology* 2008; **75**: 140-8. doi: 10.1159/000123852
- Butler TP, Gullino PM. Quantitation of cell shedding into efferent blood of mammary adenocarcinoma. *Cancer Res* 1975; **35**: 512-6. PMID: 1090362
- Fabisiewicz A, Grzybowska E. CTC clusters in cancer progression and metastasis. *Med Oncol* 2017; **34**: 12. doi: 10.1007/s12032-016-0875-0
- Aceto N, Bardia A, Miyamoto DT, Donaldson MC, Wittner BS, Spencer JA, et al. Circulating tumor cell clusters are oligoclonal precursors of breast cancer metastasis. *Cell* 2014; **158**: 1110-22. doi: 10.1016/j.cell.2014.07.013
- Cheung KJ, Padmanaban V, Silvestri V, Schipper K, Cohen JD, Fairchild AN, et al. Polyclonal breast cancer metastases arise from collective dissemination of keratin 14-expressing tumor cell clusters. *Proc Natl Acad Sci* 2016; **113**: E854-63. doi: 10.1073/pnas.1508541113
- Giampieri S, Manning C, Hooper S, Jones L, Hill CS, Sahai E. Localized and reversible TGF β signalling switches breast cancer cells from cohesive to single cell motility. *Nat Cell Biol* 2009; **11**: 1287-96. doi: 10.1038/ncb1973
- Kalluri R, Weinberg RA. The basics of epithelial-mesenchymal transition. *J Clin Invest* 2009; **119**: 1420-8. doi: 10.1172/JCI39104
- Thiery JP, Sleeman JP. Complex networks orchestrate epithelial-mesenchymal transitions. *Nat Rev Mol Cell Biol* 2006; **7**: 131-42. doi: 10.1038/nrm1835
- Kumar S, Das A, Sen S. Extracellular matrix density promotes EMT by weakening cell-cell adhesions. *Mol Biosyst* 2014; **10**: 838-50. doi: 10.1039/c3mb70431a
- Craene B De, Bex G. Regulatory networks defining EMT during cancer initiation and progression. *Nat Rev Cancer* 2013; **13**: 97-110. doi: 10.1038/nrc3447
- Yao D, Dai C, Peng S. Mechanism of the mesenchymal-epithelial transition and its relationship with metastatic tumor formation. *Mol Cancer Res* 2011; **9**: 1608-20. doi: 10.1158/1541-7786.MCR-10-0568
- Jolly MK, Boareto M, Huang B, Jia D, Lu M, Ben-Jacob E, et al. Implications of the hybrid epithelial/mesenchymal phenotype in metastasis. *Front Oncol* 2015; **5**: 155. doi: 10.3389/fonc.2015.00155
- Lecharpentier A, Vielh P, Perez-Moreno P, Planchard D, Soria JC, Farace F. Detection of circulating tumour cells with a hybrid (epithelial/mesenchymal) phenotype in patients with metastatic non-small cell lung cancer. *Br J Cancer* 2011; **105**: 1338-41. doi: 10.1038/bjc.2011.405
- Armstrong AJ, Marengo MS, Oltean S, Kemeny G, Bittling RL, Turnbull JD, et al. Circulating tumor cells from patients with advanced prostate and breast cancer display both epithelial and mesenchymal markers. *Mol Cancer Res* 2011; **9**: 997-1007. doi: 10.1158/1541-7786.MCR-10-0490
- Grosse-Wilde A, Fouquier d'Hérouël A, McIntosh E, Ertaylan G, Skupin A, Kuestner RE, et al. Stemness of the hybrid epithelial/mesenchymal atate in breast cancer and its association with poor survival. *PLoS One* 2015; **10**: e0126522. doi: 10.1371/journal.pone.0126522
- Jolly MK, Mani SA, Levine H. Hybrid epithelial/mesenchymal phenotype(s): the "fittest" for metastasis? *Biochim Biophys Acta* 2018; **870**: 151-7. doi: 10.1016/j.bbcan.2018.07.001
- Wong SY, Hynes RO. Lymphatic or hematogenous dissemination: how does a metastatic tumor cell decide? *Cell Cycle* 2006; **5**: 812-7. doi: 10.4161/cc.5.8.2646
- Lambert AW, Pattabiraman DR, Weinberg RA. Emerging biological principles of metastasis. *Cell* 2017; **168**: 670-91. doi: 10.1016/j.cell.2016.11.037
- Bockhorn M, Jain RK, Munn LL. Active versus passive mechanisms in metastasis: do cancer cells crawl into vessels, or are they pushed? *Lancet Oncol* 2007; **8**: 444-8. doi: 10.1016/S1470-2045(07)70140-7
- Huang Q, Hu X, He W, Zhao Y, Hao S, Wu Q, et al. Fluid shear stress and tumor metastasis. *Am J Cancer Res* 2018; **8**: 763-77. PMID: 29888101
- Stott SL, Lee RJ, Nagrath S, Yu M, Miyamoto DT, Ulkus L, et al. Isolation and characterization of circulating tumor cells from patients with localized and metastatic prostate cancer. *Sci Transl Med* 2010; **2**: 25ra23. doi: 10.1126/scitranslmed.3000403
- Lou X-L, Sun J, Gong S-Q, Yu X-F, Gong R, Deng H. Interaction between circulating cancer cells and platelets: clinical implication. *Chin J Cancer Res* 2015; **27**: 450-60. doi: 10.3978/j.issn.1000-9604.2015.04.10
- Labelle M, Hynes RO. The initial hours of metastasis: the importance of cooperative host-tumor cell interactions during hematogenous dissemination. *Cancer Discov* 2012; **2**: 1091-9. doi: 10.1158/2159-8290.CD-12-0329
- Nieswandt B, Hafner M, Echtenacher B, Männel DN. Lysis of tumor cells by natural killer cells in mice is impeded by platelets. *Cancer Res* 1999; **59**: 1295-300. PMID: 10096562
- Franco AT, Corken A, Ware J. Platelets at the interface of thrombosis, inflammation, and cancer. *Blood* 2015; **126**: 582-8. doi: 10.1182/blood-2014-08-531582
- Placke T, Orgel M, Schaller M, Jung G, Rammensee HG, Kopp HG, et al. Platelet-derived MHC class I confers a pseudonormal phenotype to cancer cells that subverts the antitumor reactivity of natural killer immune cells. *Cancer Res* 2012; **72**: 440-8. doi: 10.1158/0008-5472.CAN-11-1872
- Kopp H-G, Placke T, Salih HR. Platelet-derived transforming growth factor - down-regulates NKG2D thereby inhibiting natural killer cell antitumor reactivity. *Cancer Res* 2009; **69**: 7775-83. doi: 10.1158/0008-5472.CAN-09-2123
- Labelle M, Begum S, Hynes RO. Direct signaling between platelets and cancer cells induces an epithelial-mesenchymal-like transition and promotes metastasis. *Cancer Cell* 2011; **20**: 576-90. doi: 10.1016/j.ccr.2011.09.009
- Mittal D, Gubin MM, Schreiber RD, Smyth MJ. New insights into cancer immunoediting and its three component phases - elimination, equilibrium and escape. *Curr Opin Immunol* 2014; **27**: 16-25. doi: 10.1016/j.coi.2014.01.004
- Vinay DS, Ryan EP, Pawelec G, Talib WH, Stagg J, Elkord E, et al. Immune evasion in cancer: mechanistic basis and therapeutic strategies. *Semin Cancer Biol* 2015; **35**: S185-98. doi: 10.1016/j.semcancer.2015.03.004
- Hiratsuka S, Watanabe A, Aburatani H, Maru Y. Tumour-mediated upregulation of chemoattractants and recruitment of myeloid cells predetermines lung metastasis. *Nat Cell Biol* 2006; **8**: 1369-75. doi: 10.1038/ncb1507
- Kim S, Takahashi H, Lin W-W, Descargues P, Grivennikov S, Kim Y, et al. Carcinoma-produced factors activate myeloid cells through TLR2 to stimulate metastasis. *Nature* 2009; **457**: 102-6. doi: 10.1038/nature07623

34. Szczerba BM, Castro-Giner F, Vetter M, Krol I, Gkountela S, Landin J, et al. Neutrophils escort circulating tumour cells to enable cell cycle progression. *Nature* 2016; **553**: 7. doi: 10.1038/s41586-019-0915-y
35. Hanna N. Role of natural killer cells in control of cancer metastasis. *Cancer Metastasis Rev* 1982; **1**: 45-64.
36. Brodbeck T, Nehmann N, Bethge A, Wedemann G, Schumacher U. Perforin-dependent direct cytotoxicity in natural killer cells induces considerable knockdown of spontaneous lung metastases and computer modelling-proven tumor cell dormancy in a HT29 human colon cancer xenograft mouse model. *Mol Cancer* 2014; **13**: 244. doi: 10.1186/1476-4598-13-244
37. Santos MF, Mannam VKR, Craft BS, Punecky LV, Sheehan NT, Lewis RE, et al. Comparative analysis of innate immune system function in metastatic breast, colorectal, and prostate cancer patients with circulating tumor cells. *Exp Mol Pathol* 2014; **96**: 367-74. doi: 10.1016/j.yexmp.2014.04.001
38. McDonald B, Spicer J, Giannais B, Fallavollita L, Brodt P, Ferri LE. Systemic inflammation increases cancer cell adhesion to hepatic sinusoids by neutrophil mediated mechanisms. *Int J Cancer* 2009; **125**: 1298-305. doi: 10.1002/ijc.24409
39. Spicer JD, McDonald B, Cools-Lartigue JJ, Chow SC, Giannais B, Kubes P, et al. Neutrophils promote liver metastasis via Mac-1-mediated interactions with circulating tumor cells. *Cancer Res* 2012; **72**: 3919-27. doi: 10.1158/0008-5472.CAN-11-2393
40. Huh SJ, Liang S, Sharma A, Dong C, Robertson GP. Transiently entrapped circulating tumor cells interact with neutrophils to facilitate lung metastasis development. *Cancer Res* 2010; **70**: 6071-82. doi: 10.1158/0008-5472.CAN-09-4442
41. Strell C, Lang K, Niggemann B, Zaenker KS, Entschladen F. Neutrophil granulocytes promote the migratory activity of MDA-MB-468 human breast carcinoma cells via ICAM-1. *Exp Cell Res* 2010; **316**: 138-48. doi: 10.1016/j.yexcr.2009.09.003
42. Auffray C, Fogg D, Garfa M, Elain G, Join-Lambert O, Kayal S, et al. Monitoring of blood vessels and tissues by a population of monocytes with patrolling behavior. *Science* 2007; **317**: 666-70. doi: 10.1126/science.1142883
43. Hanna RN, Cecik C, Sag D, Tacke R, Thomas GD, Nowyhed H, et al. Patrolling monocytes control tumor metastasis to the lung. *Science* 2015; **350**: 985-90. doi: 10.1126/science.aac9407
44. De Giorgi U, Mego M, Scarpi E, Giuliano M, Giordano A, Reuben JM, et al. Relationship between lymphocytopenia and circulating tumor cells as prognostic factors for overall survival in metastatic breast cancer. *Clin Breast Cancer* 2012; **12**: 264-9. doi: 10.1016/j.clbc.2012.04.004
45. Mego M, Gao H, Cohen EN, Anfossi S, Giordano A, Sanda T, et al. Circulating tumor cells (CTC) are associated with defects in adaptive immunity in patients with inflammatory breast cancer. *J Cancer* 2016; **7**: 1095-104. doi: 10.7150/jca.13098
46. Ye L, Zhang F, Li H, Yang L, Lv T, Gu W, et al. Circulating tumor cells were associated with the number of T lymphocyte subsets and NK cells in peripheral blood in advanced non-small-cell lung cancer. *Dis Markers* 2017; **2017**: 5727815. doi: 10.1155/2017/5727815
47. Mazel M, Jacot W, Pantel K, Bartkowiak K, Topart D, Cayrefourcq L, et al. Frequent expression of PD-L1 on circulating breast cancer cells. *Mol Oncol* 2015; **9**: 1773-82. doi: 10.1016/j.molonc.2015.05.009
48. Kallergi G, Vetsika E-K, Aggouraki D, Lagoudaki E, Koutsopoulos A, Koinis F, et al. Evaluation of PD-L1/PD-1 on circulating tumor cells in patients with advanced non-small cell lung cancer. *Ther Adv Med Oncol* 2018; **10**: 175883401775012. doi: 10.1177/1758834017750121
49. Oliveira-Costa JP, de Carvalho AF, da Silveira GG, Amaya P, Wu Y, Park KJ, et al. Gene expression patterns through oral squamous cell carcinoma development: PD-L1 expression in primary tumor and circulating tumor cells. *Oncotarget* 2015; **6**: 20902-20920. doi: 10.18632/oncotarget.3939
50. Yue C, Jiang Y, Li P, Wang Y, Xue J, Li N, et al. Dynamic change of PD-L1 expression on circulating tumor cells in advanced solid tumor patients undergoing PD-1 blockade therapy. *Oncimmunology* 2018; **7**: e1438111. doi: 10.1080/2162402X.2018.1438111
51. Nicolazzo C, Raimondi C, Mancini M, Caponnetto S, Gradilone A, Gandini O, et al. Monitoring PD-L1 positive circulating tumor cells in non-small cell lung cancer patients treated with the PD-1 inhibitor nivolumab. *Sci Rep* 2016; **6**: 31726. doi: 10.1038/srep31726
52. Guibert N, Delaunay M, Lusque A, Boubekour N, Rouquette I, Clermont E, et al. PD-L1 expression in circulating tumor cells of advanced non-small cell lung cancer patients treated with nivolumab. *Lung Cancer* 2018; **120**: 108-12. doi: 10.1016/j.lungcan.2018.04.001
53. Micalizzi DS, Maheswaran S, Haber DA. A conduit to metastasis: circulating tumor cell biology. *Genes Dev* 2017; **31**: 1827-40. doi: 10.1101/gad.305805.117
54. Reymond N, d'Água BB, Ridley AJ. Crossing the endothelial barrier during metastasis. *Nat Rev Cancer* 2013; **13**: 858-70. doi: 10.1038/nrc3628
55. Qian B, Deng Y, Im JH, Muschel RJ, Zou Y, Li J, et al. A distinct macrophage population mediates metastatic breast cancer cell extravasation, establishment and growth. *PLoS One*. 2009; **4**: e6562. doi: 10.1371/journal.pone.0006562
56. Schumacher D, Strilic B, Sivaraj KK, Wettschureck N, Offermanns S. Platelet-derived nucleotides promote tumor-cell transendothelial migration and metastasis via P2Y2 receptor. *Cancer Cell* 2013; **24**: 130-7. doi: 10.1016/j.ccr.2013.05.008
57. Kienast Y, von Baumgarten L, Fuhrmann M, Klinkert WE, Goldbrunner R, Herms J, et al. Real-time imaging reveals the single steps of brain metastasis formation. *Nat Med* 2010; **16**: 116-22. doi: 10.1038/nm.2072
58. Hiratsuka S, Goel S, Kamoun WS, Maru Y, Fukumura D, Duda DG, et al. Endothelial focal adhesion kinase mediates cancer cell homing to discrete regions of the lungs via E-selectin up-regulation. *Proc Natl Acad Sci* 2011; **108**: 3725-30. doi: 10.1073/pnas.1100446108
59. Balkwill FR. The chemokine system and cancer. *J Pathol* 2012; **226**: 148-57. doi: 10.1002/path.3029
60. Kukreja P, Abdel-Mageed AB, Mondal D, Liu K, Agrawal KC. Up-regulation of CXCR4 expression in PC-3 cells by stromal-derived factor-1 α (CXCL12) increases endothelial adhesion and transendothelial migration: role of MEK/ERK signaling pathway-dependent NF- κ B activation. *Cancer Res* 2005; **65**: 9891-8. doi: 10.1158/0008-5472.CAN-05-1293
61. Taichman RS, Cooper C, Keller ET, Pienta KJ, Taichman NS, McCauley LK. Use of the stromal cell-derived factor-1/CXCR4 pathway in prostate cancer metastasis to bone. *Cancer Res* 2002; **62**: 1832-7. <http://www.ncbi.nlm.nih.gov/pubmed/11912162>.
62. Hoeben A, Landuyt B, Highley MS, Wildiers H, Van Oosterom AT, De Bruijn EA. Vascular endothelial growth factor and angiogenesis. *Pharmacol Rev* 2004; **56**: 549-80. doi: 10.1124/pr.56.4.3
63. Drabsch Y, ten Dijke P. TGF- β signaling in breast cancer cell invasion and bone metastasis. *J Mammary Gland Biol Neoplasia* 2011; **16**: 97-108. doi: 10.1007/s10911-011-9217-1
64. Wan L, Pantel K, Kang Y. Tumor metastasis: moving new biological insights into the clinic. *Nat Med* 2013; **19**: 1450-64. doi: 10.1038/nm.3391
65. De Cock JM, Shibue T, Dongre A, Keckesova Z, Reinhardt F, Weinberg RA. Inflammation triggers Zeb1-dependent escape from tumor latency. *Cancer Res*. 2016; **76**: 6778-84. doi: 10.1158/0008-5472.CAN-16-0608
66. Li YC, Zou JM, Luo C, Shu Y, Luo J, Qin J, et al. Circulating tumor cells promote the metastatic colonization of disseminated carcinoma cells by inducing systemic inflammation. *Oncotarget* 2017; **8**: 28418-30. doi: 10.18632/oncotarget.16084
67. Fridlender ZG, Sun J, Kim S, Kapoor V, Cheng G, Ling L, et al. Polarization of tumor-associated neutrophil phenotype by TGF- β : "N1" versus "N2" TAN. *Cancer Cell* 2009; **16**: 183-94. doi: 10.1016/j.ccr.2009.06.017
68. Oskarsson T, Acharyya S, Zhang XH-F, Vanharanta S, Tavazoie SF, Morris PG, et al. Breast cancer cells produce tenascin C as a metastatic niche component to colonize the lungs. *Nat Med* 2011; **17**: 867-74. doi: 10.1038/nm.2379
69. Malanchi I, Santamaria-Martínez A, Susanto E, Peng H, Lehr HA, Delaloye JF, et al. Interactions between cancer stem cells and their niche govern metastatic colonization. *Nature* 2012; **481**: 85-9. doi: 10.1038/nature10694
70. Barkan D, El Touny LH, Michalowski AM, Smith JA, Chu I, Davis AS, et al. Metastatic growth from dormant cells induced by a Col1-enriched fibrotic environment. *Cancer Res* 2010; **70**: 5706-16. doi: 10.1158/0008-5472.CAN-09-2356
71. Costa-Silva B, Aiello NM, Ocean AJ, Singh S, Zhang H, Thakur BK, et al. Pancreatic cancer exosomes initiate pre-metastatic niche formation in the liver. *Nat Cell Biol* 2015; **17**: 816-26. doi: 10.1038/ncb3169

72. Zhang L, Ridgway LD, Wetzel MD, Ngo J, Yin W, Kumar D, et al. The identification and characterization of breast cancer CTCs competent for brain metastasis. *Sci Transl Med* 2013; **5**: 180ra48. doi: 10.1126/scitranslmed.3005109
73. Kang Y, Siegel PM, Shu W, Drobnjak M, Kakonen SM, Cordon-Cardo C, et al. A multigenic program mediating breast cancer metastasis to bone. *Cancer Cell* 2003; **3**: 537-49.
74. Minn AJ, Gupta GP, Siegel PM, Bos PD, Shu W, Giri DD, et al. Genes that mediate breast cancer metastasis to lung. *Nature* 2005; **436**: 518-24. doi: 10.1038/nature03799
75. Uhr JW, Pantel K. Controversies in clinical cancer dormancy. *Proc Natl Acad Sci* 2011; **108**: 12396-400. doi: 10.1073/pnas.1106613108
76. Braun S, Vogl FD, Naume B, Janni W, Osborne MP, Coombes RC, et al. A pooled analysis of bone marrow micrometastasis in breast cancer. *N Engl J Med* 2005; **353**: 793-802. doi: 10.1056/NEJMoa050434
77. Pantel K, Alix-Panabières C, Riethdorf S. Cancer micrometastases. *Nat Rev Clin Oncol* 2009; **6**: 339-51. doi: 10.1038/nrclinonc.2009.44
78. Krebs MG, Metcalf RL, Carter L, Brady G, Blackhall FH, Dive C. Molecular analysis of circulating tumour cells—biology and biomarkers. *Nat Rev Clin Oncol* 2014; **11**: 129-44. doi: 10.1038/nrclinonc.2013.253
79. Shen Z, Wu A, Chen X. Current detection technologies for circulating tumor cells. *Chem Soc Rev* 2017; **46**: 2038-56. doi: 10.1039/c6cs00803h
80. Saucedo-Zeni N, Mewes S, Niestroj R, Gasiorowski L, Murawa D, Nowaczyk P, et al. A novel method for the in vivo isolation of circulating tumor cells from peripheral blood of cancer patients using a functionalized and structured medical wire. *Int J Oncol* 2012; **41**: 1241-50. doi: 10.3892/ijo.2012.1557
81. Alix-Panabieres C, Pantel K. Circulating tumor cells: liquid biopsy of cancer. *Clin Chem* 2013; **59**: 110-8. doi: 10.1373/clinchem.2012.194258
82. Hao S-J, Wan Y, Xia Y-Q, Zou X, Zheng S-Y. Size-based separation methods of circulating tumor cells. *Adv Drug Deliv Rev* 2018; **125**: 3-20. doi:10.1016/j.addr.2018.01.002
83. Ferreira MM, Ramani VC, Jeffrey SS. Circulating tumor cell technologies. *Mol Oncol* 2016; **10**: 374-94. doi: 10.1016/j.molonc.2016.01.007
84. Laget S, Broncy L, Hormigos K, Dhingra DM, BenMohamed F, Capiod T, et al. Technical insights into highly sensitive isolation and molecular characterization of fixed and live circulating tumor cells for early detection of tumor invasion. *Plos One* 2017. **12**: e0169427. doi: 10.1371/journal.pone.0169427
85. Hvichia GE, Parveen Z, Wagner C, Janning M, Quidde J, Stein A, et al. A novel microfluidic platform for size and deformability based separation and the subsequent molecular characterization of viable circulating tumor cells. *Int J Cancer* 2016; **138**: 2894-904. doi: 10.1002/ijc.30007
86. Seal SH. Silicone flotation: A simple quantitative method for the isolation of free-floating cancer cells from the blood. *Cancer* 1959; **12**: 590-5.
87. Rawal S, Yang Y-P, Cote R, Agarwal A. Identification and quantitation of circulating tumor cells. *Annu Rev Anal Chem* 2017; **10**: 321-43. doi: 10.1146/annurev-anchem-061516-045405
88. Kulasinghe A, Zhou J, Kenny L, Papautsky I, Punyadeera C. Capture of circulating tumour cell clusters using straight microfluidic chips. *Cancers (Basel)* 2019; **11**: 89. doi: 10.3390/cancers11010089
89. Cabel L, Proudhon C, Gortais H, Lohrat D, Coussy F, Pierga JY, et al. Circulating tumor cells: clinical validity and utility. *Int J Clin Oncol* 2017; **22**: 421-30. doi: 10.1007/s10147-017-1105-2
90. Guo M, Li X, Zhang S, Song H, Zhang W, Shang X, et al. Real-time quantitative RT-PCR detection of circulating tumor cells from breast cancer patients. *Int J Oncol* 2015; **46**: 281-9. doi: 10.3892/ijo.2014.2732
91. Katseli A, Maragos H, Nezos A, Syrigos K, Koutsilieris M. Multiplex PCR-Based Detection of circulating tumor cells in lung cancer patients using CK19, PTHrP, and LUNX specific primers. *Clin Lung Cancer* 2013; **14**: 513-20. doi: 10.1016/j.clcc.2013.04.007
92. Riethdorf S, Fritsche H, Muller V, Rau T, Schindlbeck C, Rack B, et al. Detection of circulating tumor cells in peripheral blood of patients with metastatic breast cancer: a validation study of the CellSearch system. *Clin Cancer Res* 2007; **13**: 920-8. doi: 10.1158/1078-0432.CCR-06-1695
93. Bednarz-Knoll N, Alix-Panabières C, Pantel K. Plasticity of disseminating cancer cells in patients with epithelial malignancies. *Cancer Metastasis Rev* 2012; **31**: 673-87. doi: 10.1007/s10555-012-9370-z
94. Alix-Panabieres C, Pantel K. Clinical applications of circulating tumor cells and circulating tumor DNA as liquid biopsy. *Cancer Discov* 2016; **6**: 479-91. doi: 10.1158/2159-8290.CD-15-1483
95. Cristofanilli M, Budd GT, Ellis MJ, Stopeck A, Matera J, Miller MC, et al. Circulating tumor cells, disease progression, and survival in metastatic breast cancer. *N Engl J Med* 2004; **351**: 781-91. doi: 10.1056/NEJMoa040766
96. Pantel K, Deneve E, Nocca D, Coffy A, Vendrell JP, Maudelonde T, et al. Circulating epithelial cells in patients with benign colon diseases. *Clin Chem* 2012; **58**: 936-40. doi: 10.1373/clinchem.2011.175570
97. Davis JW, Nakanishi H, Kumar VS, Bhadkamkar VA, McCormack R, Fritsche HA, et al. Circulating tumor cells in peripheral blood samples from patients with increased serum prostate specific antigen: initial results in early prostate cancer. *J Urol* 2008; **179**: 2187-191. doi: 10.1016/j.juro.2008.01.102
98. Ilie M, Hofman V, Long-Mira E, Selva E, Vignaud JM, Padovani B, et al. "Sentinel" circulating tumor cells allow early diagnosis of lung cancer in patients with chronic obstructive pulmonary disease. Kalinichenko V V, ed. *PLoS One* 2014; **9**: e111597. doi: 10.1371/journal.pone.0111597
99. Fiorelli A, Accardo M, Carelli E, Angioletti D, Santini M, Di Domenico M. Circulating tumor cells in diagnosing lung cancer: clinical and morphologic analysis. *Ann Thorac Surg* 2015; **99**: 1899-905. doi: 10.1016/j.athoracsur.2014.11.049
100. UICC International Union Against Cancer. *TNM classification of malignant tumours. 7th edition*. Sobin LH, Gospodarowicz MK, Wittekind C, editors. Chichester: Wiley-Blackwell; 2011.
101. Huang X, Gao P, Song Y, Sun J, Chen X, Zhao J, et al. Meta-analysis of the prognostic value of circulating tumor cells detected with the CellSearch System in colorectal cancer. *BMC Cancer* 2015; **15**: 202. doi: 10.1186/s12885-015-1218-9
102. Vlaeminck-Guillem V. When prostate cancer circulates in the bloodstream. *Diagnostics*. 2015; **5**: 428-74. doi: 10.3390/diagnostics5040428
103. Krebs MG, Sloane R, Priest L, Lancashire L, Hou JM, Greystoke A, et al. Evaluation and prognostic significance of circulating tumor cells in patients with non-small-cell lung cancer. *J Clin Oncol* 2011; **29**: 1556-63. doi: 10.1200/JCO.2010.28.7045
104. Hou J-M, Krebs MG, Lancashire L, Sloane R, Backen A, Swain RK, et al. Clinical significance and molecular characteristics of circulating tumor cells and circulating tumor microemboli in patients with small-cell lung cancer. *J Clin Oncol* 2012; **30**: 525-32. doi: 10.1200/JCO.2010.33.3716
105. Janni WJ, Rack B, Terstappen LWMM, Pierga JY, Taran FA, Fehm T, et al. Pooled analysis of the prognostic relevance of circulating tumor cells in primary breast cancer. *Clin Cancer Res* 2016; **22**: 2583-93. doi: 10.1158/1078-0432.CCR-15-1603
106. Cohen SJ, Punt CJA, Iannotti N, Saidman BH, Sabbath KD, Gabrail NY, et al. Relationship of circulating tumor cells to tumor response, progression-free survival, and overall survival in patients with metastatic colorectal cancer. *J Clin Oncol* 2008; **26**: 3213-21. doi: 10.1200/JCO.2007.15.8923
107. Bidard FC, Huguet F, Louvet C, Mineur L, Bouche O, Chibaudel B, et al. Circulating tumor cells in locally advanced pancreatic adenocarcinoma: the ancillary CirCe 07 study to the LAP 07 trial. *Ann Oncol* 2013; **24**: 2057-61. doi: 10.1093/annonc/mdt176
108. Zhang L, Riethdorf S, Wu G, Wang T, Yang K, Peng G, et al. Meta-analysis of the prognostic value of circulating tumor cells in breast cancer. *Clin Cancer Res* 2012; **18**: 5701-10. doi: 10.1158/1078-0432.CCR-12-1587
109. Grobe A, Blessmann M, Hanken H, Friedrich RE, Schön G, Wikner J, et al. Prognostic relevance of circulating tumor cells in blood and disseminated tumor cells in bone marrow of patients with squamous cell carcinoma of the oral cavity. *Clin Cancer Res* 2014; **20**: 425-33. doi: 10.1158/1078-0432.CCR-13-1101
110. Tol J, Koopman M, Miller MC, Tibbe A, Cats A, Creemers GJM, et al. Circulating tumour cells early predict progression-free and overall survival in advanced colorectal cancer patients treated with chemotherapy and targeted agents. *Ann Oncol* 2010; **21**: 1006-12. doi: 10.1093/annonc/mdp463

111. Sastre J, Maestro ML, Gomez-Espana A, Rivera F, Valladares M, Massuti B, et al. Circulating tumor cell count is a prognostic factor in metastatic colorectal cancer patients receiving first-line chemotherapy plus bevacizumab: A Spanish Cooperative Group for the Treatment of Digestive Tumors Study. *Oncologist* 2012; **17**: 947-55. doi: 10.1634/theoncologist.2012-0048
112. de Bono JS, Scher HI, Montgomery RB, Parker C, Miller MC, Tissing H, et al. Circulating tumor cells predict survival benefit from treatment in metastatic castration-resistant prostate cancer. *Clin Cancer Res* 2008; **14**: 6302-9. doi: 10.1158/1078-0432.CCR-08-0872
113. Jansson S, Bendahl P-O, Larsson A-M, Aaltonen KE, Rydén L. Prognostic impact of circulating tumor cell apoptosis and clusters in serial blood samples from patients with metastatic breast cancer in a prospective observational cohort. *BMC Cancer* 2016; **16**: 433. doi: 10.1186/s12885-016-2406-y
114. Lu CY, Uen YH, Tsai HL, Chuang SC, Hou MF, Wu DC, et al. Molecular detection of persistent postoperative circulating tumour cells in stages II and III colon cancer patients via multiple blood sampling: prognostic significance of detection for early relapse. *Br J Cancer* 2011; **104**: 1178-84. doi: 10.1038/bjc.2011.40
115. Yamada T, Matsuda A, Koizumi M, Shinji S, Takahashi G, Iwai T, et al. Liquid biopsy for the management of patients with colorectal cancer. *Digestion* 2019; **99**: 39-45. doi: 10.1159/000494411
116. Goodman CR, Seagle B-LL, Friedl TWP, Rack B, Lato K, Fink V, et al. Association of circulating tumor cell status with benefit of radiotherapy and survival in early-stage breast cancer. *JAMA Oncol* 2018; **4**: e180163. doi: 10.1001/jamaoncol.2018.0163
117. Scher HI, Heller G, Molina A, Attard G, Danila DC, Jia X, et al. Circulating tumor cell biomarker panel as an individual-level surrogate for survival in metastatic castration-resistant prostate cancer. *J Clin Oncol* 2015; **33**: 1348-55. doi: 10.1200/JCO.2014.55.3487
118. Bidard F-C, Peeters DJ, Fehm T, Nolé F, Gisbert-Criado R, Mavroudis D, et al. Clinical validity of circulating tumour cells in patients with metastatic breast cancer: a pooled analysis of individual patient data. *Lancet Oncol* 2014; **15**: 406-14. doi: 10.1016/S1470-2045(14)70069-5
119. Yu M, Bardia A, Aceto N, Bersani F, Madden MW, Donaldson MC, et al. Ex vivo culture of circulating breast tumor cells for individualized testing of drug susceptibility. *Science* 2014; **345**: 216-20. doi: 10.1126/science.1253533
120. Gates JD, Benavides LC, Stojadinovic A, Mittendorf EA, Holmes JP, Carmichael MG, et al. Monitoring circulating tumor cells in cancer vaccine trials. *Hum Vaccin* 2008; **4**: 389-92.
121. Lin M, Liang S-Z, Shi J, Niu LZ, Chen JB, Zhang MJ, et al. Circulating tumor cell as a biomarker for evaluating allogenic NK cell immunotherapy on stage IV non-small cell lung cancer. *Immunol Lett* 2017; **191**: 10-5. doi: 10.1016/j.imlet.2017.09.004
122. Kalinsky K, Mayer JA, Xu X, Pham T, Wong KL, Villarín E, et al. Correlation of hormone receptor status between circulating tumor cells, primary tumor, and metastasis in breast cancer patients. *Clin Transl Oncol* 2015; **17**: 539-46. doi: 10.1007/s12094-015-1275-1
123. Lee JS, Magbanua MJM, Park JW. Circulating tumor cells in breast cancer: applications in personalized medicine. *Breast Cancer Res Treat* 2016; **160**: 411-24. doi: 10.1007/s10549-016-4014-6
124. Tewes M, Aktas B, Welt A, Mueller S, Hauch S, Kimmig R, et al. Molecular profiling and predictive value of circulating tumor cells in patients with metastatic breast cancer: an option for monitoring response to breast cancer related therapies. *Breast Cancer Res Treat* 2009; **115**: 581-90. doi: 10.1007/s10549-008-0143-x
125. Aktas B, Müller V, Tewes M, Zeitz J, Kasimir-Bauer S, Loehberg CR, et al. Comparison of estrogen and progesterone receptor status of circulating tumor cells and the primary tumor in metastatic breast cancer patients. *Gynecol Oncol* 2011; **122**: 356-60. doi: 10.1016/j.ygyno.2011.04.039
126. Somlo G, Lau SK, Frankel P, Hsieh HB, Liu X, Yang L, et al. Multiple biomarker expression on circulating tumor cells in comparison to tumor tissues from primary and metastatic sites in patients with locally advanced/inflammatory, and stage IV breast cancer, using a novel detection technology. *Breast Cancer Res Treat* 2011; **128**: 155-63. doi: 10.1007/s10549-011-1508-0
127. Paoletti C, Muñoz MC, Thomas DG, Griffith KA, Kidwell KM, Tokudome N, et al. Development of circulating tumor cell-endocrine therapy index in patients with hormone receptor-positive breast cancer. *Clin Cancer Res* 2015; **21**: 2487-98. doi: 10.1158/1078-0432.CCR-14-1913
128. Jaeger BAS, Neugebauer J, Andergassen U, Melcher C, Schochter F, Mouarrawy D, et al. The HER2 phenotype of circulating tumor cells in HER2-positive early breast cancer: A translational research project of a prospective randomized phase III trial. *PLoS One* 2017; **12**: e0173593. doi: 10.1371/journal.pone.0173593
129. Georgoulas V, Bozionelou V, Agelaki S, Perraki M, Apostolaki S, Kallergi G, et al. Trastuzumab decreases the incidence of clinical relapses in patients with early breast cancer presenting chemotherapy-resistant CK-19mRNA-positive circulating tumor cells: results of a randomized phase II study. *Ann Oncol* 2012; **23**: 1744-50. doi: 10.1093/annonc/mds020
130. Kulasinghe A, Kapeleris J, Kimberley R, Mattarollo SR, Thompson EW, Thiery JP, et al. The prognostic significance of circulating tumor cells in head and neck and non-small-cell lung cancer. *Cancer Med* 2018; **7**: 5910-19. doi: 10.1002/cam4.1832
131. Antonarakis ES, Lu C, Luber B, Wang H, Chen Y, Nakazawa M, et al. Androgen receptor splice variant 7 and efficacy of taxane chemotherapy in patients with metastatic castration-resistant prostate cancer. *JAMA Oncol* 2015; **1**: 582. doi: 10.1001/jamaoncol.2015.1341
132. Payne RE, Yagüe E, Slade MJ, Apostolopoulos C, Jiao LR, Ward B, et al. Measurements of EGFR expression on circulating tumor cells are reproducible over time in metastatic breast cancer patients. *Pharmacogenomics* 2009; **10**: 51-7. doi: 10.2217/14622416.10.1.51
133. Nadal R, Ortega FG, Salido M, Lorente JA, Rodríguez-Rivera M, Delgado-Rodríguez M, et al. CD133 expression in circulating tumor cells from breast cancer patients: potential role in resistance to chemotherapy. *Int J Cancer* 2013; **133**: 2398-407. doi: 10.1002/ijc.28263
134. Baccelli I, Schneeweiss A, Riethdorf S, Stenzinger A, Schillert A, Vogel V, et al. Identification of a population of blood circulating tumor cells from breast cancer patients that initiates metastasis in a xenograft assay. *Nat Biotechnol* 2013; **31**: 539-44. doi: 10.1038/nbt.2576
135. Tellez-Gabriel M, Cochonneau D, Cadé M, Jubellin C, Heymann MF, Heymann D. Circulating tumor cell-derived pre-clinical models for personalized medicine. *Cancers (Basel)* 2018; **11**: 19. doi: 10.3390/cancers11010019
136. Whittle JR, Lewis MT, Lindeman GJ, Visvader JE. Patient-derived xenograft models of breast cancer and their predictive power. *Breast Cancer Res* 2015; **17**: 17. doi: 10.1186/s13058-015-0523-1
137. Lallo A, Gulati S, Schenk MW, Khandelwal G, Berglund UW, Pateras IS, et al. Ex vivo culture of cells derived from circulating tumour cell xenograft to support small cell lung cancer research and experimental therapeutics. *Br J Pharmacol* 2018; **176**: 436-50. doi: 10.1111/bph.14542
138. Pereira-Veiga T, Abreu M, Robledo D, Matias-Guiu X, Santacana M, Sánchez L, et al. CTCs-derived xenograft development in a triple negative breast cancer case. *Int J Cancer* 2019; **144**: 2254-65. doi: 10.1002/ijc.32001
139. Williams ES, Rodriguez-Bravo V, Chippada-Venkata U, Iglesia-Vicente JDI, Gong Y, Galsky M, et al. Generation of prostate cancer patient derived xenograft models from circulating tumor cells. *J Vis Exp* 2015; **104**: e53182. doi: 10.3791/53182
140. Pierga JY, Hajage D, Bachelot T, Delaloge S, Brain E, Campone M, et al. High independent prognostic and predictive value of circulating tumor cells compared with serum tumor markers in a large prospective trial in first-line chemotherapy for metastatic breast cancer patients. *Ann Oncol* 2012; **23**: 618-24. doi: 10.1093/annonc/mdr263
141. Cristofanilli M, Hayes DF, Budd GT, Ellis MJ, Stopeck A, Reuben JM, et al. Circulating tumor cells: a novel prognostic factor for newly diagnosed metastatic breast cancer. *J Clin Oncol* 2005; **23**: 1420-30. doi: 10.1200/JCO.2005.08.140
142. Dawood S, Broglio K, Valero V, Reuben J, Handy B, Islam R, et al. Circulating tumor cells in metastatic breast cancer. *Cancer* 2008; **113**: 2422-30. doi: 10.1002/cncr.23852
143. Hayes DF, Cristofanilli M, Budd GT, Ellis MJ, Stopeck A, Miller MC, et al. Circulating tumor cells at each follow-up time point during therapy of metastatic breast cancer patients predict progression-free and overall survival. *Clin Cancer Res* 2006; **12**: 4218-24. doi: 10.1158/1078-0432.CCR-05-2821
144. Nole F, Munzone E, Zorzino L, Minchella I, Salvatici M, Botteri E, et al. Variation of circulating tumor cell levels during treatment of metastatic breast cancer: prognostic and therapeutic implications. *Ann Oncol* 2008; **19**: 891-7. doi: 10.1093/annonc/mdm558

145. Paoletti C, Li Y, Muniz MC, Kidwell KM, Aung K, Thomas DG, et al. Significance of circulating tumor cells in metastatic triple-negative breast cancer patients within a randomized, phase II trial: TBCRC 019. *Clin Cancer Res* 2015; **21**: 2771-9. doi: 10.1158/1078-0432.CCR-14-2781
146. Yan WT, Cui X, Chen Q, Li YF, Cui YH, Wang, Y, et al. Circulating tumor cell status monitors the treatment responses in breast cancer patients: a meta-analysis. *Sci Rep* 2017; **7**: 43464. doi: 10.1038/srep43464
147. Giuliano M, Giordano A, Jackson S, Hess KR, De Giorgi U, Mego M, et al. Circulating tumor cells as prognostic and predictive markers in metastatic breast cancer patients receiving first-line systemic treatment. *Breast Cancer Res* 2011; **13**: R67. doi: 10.1186/bcr2907
148. Budd GT, Cristofanilli M, Ellis MJ, Stopeck A, Borden E, Miller MC, et al. Circulating tumor cells versus imaging--predicting overall survival in metastatic breast cancer. *Clin Cancer Res* 2006; **12**: 6403-9. doi: 10.1158/1078-0432.CCR-05-1769
149. Mego M, De Giorgi U, Dawood S, Wang X, Valero V, Andreopoulou E, et al. Characterization of metastatic breast cancer patients with nondetectable circulating tumor cells. *Int J Cancer* 2011; **129**: 417-23. doi: 10.1002/ijc.25690
150. Smerage JB, Barlow WE, Hortobagyi GN, Winer EP, Leyland-Jones B, Srkalovic G, et al. Circulating tumor cells and response to chemotherapy in metastatic breast cancer: SWOG S0500. *J Clin Oncol* 2014; **32**: 3483-89. doi: 10.1200/JCO.2014.56.2561
151. Thiery JP, Lim CT. Tumor Dissemination: An EMT Affair. *Cancer Cell* 2013; **23**: 272-3. doi: 10.1016/j.ccr.2013.03.004
152. Mooney SM, Talebian V, Jolly MK, Jia D, Gromala M, Levine H, et al. The GRHL2/ZEB feedback loop-a key axis in the regulation of EMT in breast cancer. *J Cell Biochem* 2017; **118**: 2559-70. doi: 10.1002/jcb.25974
153. Pattabiraman DR, Weinberg RA. Targeting the epithelial-to-mesenchymal transition: the case for differentiation-based therapy. *Cold Spring Harb Symp Quant Biol* 2016; **81**: 11-9. doi: 10.1101/sqb.2016.81.030957
154. Giordano A, Giuliano M, De Laurentis M, Arpino G, Jackson S, Handy BC, et al. Circulating tumor cells in immunohistochemical subtypes of metastatic breast cancer: lack of prediction in HER2-positive disease treated with targeted therapy. *Ann Oncol* 2012; **23**: 1144-50. doi: 10.1093/annonc/mdr434
155. Lu Y, Wang P, Wang X, Peng J, Zhu Y, Shen N. The significant prognostic value of circulating tumor cells in triple-negative breast cancer: a meta-analysis. *Oncotarget* 2016; **7**: 37361-9. doi: 10.18632/oncotarget.8156
156. Riethdorf S, O'Flaherty L, Hille C, Pantel K. Clinical applications of the CellSearch platform in cancer patients. *Adv Drug Deliv Rev* 2018; **125**: 102-21. doi: 10.1016/j.addr.2018.01.011
157. Rack B, Schindlbeck C, Jückstock J, Andergassen U, Hepp P, Zwingers T, et al. Circulating tumor cells predict survival in early average-to-high risk breast cancer patients. *JNCI J Natl Cancer Inst* 2014; **106**: 5. doi: 10.1093/jnci/dju066
158. Sandri MT, Zorzino L, Cassatella MC, Bassi F, Luini A, Casadio C, et al. Changes in circulating tumor cell detection in patients with localized breast cancer before and after surgery. *Ann Surg Oncol* 2010; **17**: 1539-45. doi: 10.1245/s10434-010-0918-2
159. Krishnamurthy S, Cristofanilli M, Singh B, Anfossi S, Khoury J, Hess K, et al. Detection of minimal residual disease in blood and bone marrow in early stage breast cancer. *Cancer* 2010; **116**: 3330-7. doi: 10.1002/cncr.25145
160. Lucci A, Hall CS, Lodhi AK, Bhattacharyya A, Anderson AE, Xiao L, et al. Circulating tumour cells in non-metastatic breast cancer: a prospective study. *Lancet Oncol* 2012; **13**: 688-95. doi: 10.1016/S1470-2045(12)70209-7
161. Hall CS, Karhade MG, Bowman Bauldry JB, Valad LM, Kuerer HM, DeSnyder SM, et al. Prognostic value of circulating tumor cells identified before surgical resection in nonmetastatic breast cancer patients. *J Am Coll Surg* 2016; **223**: 20-9. doi: 10.1016/j.jamcollsurg.2016.02.021
162. Hartkopf AD, Wallwiener M, Hahn M, Fehm TN, Brucker SY, Taran FA. Simultaneous detection of disseminated and circulating tumor cells in primary breast cancer patients. *Cancer Res Treat* 2016; **48**: 115-24. doi: 10.4143/crt.2014.287
163. Riethdorf S, Müller V, Loibl S, Nekljudova V, Weber K, Huober J, et al. Prognostic impact of circulating tumor cells for breast cancer patients treated in the neoadjuvant »Geparquattro« trial. *Clin Cancer Res* 2017; **23**: 5384-93. doi: 10.1158/1078-0432.CCR-17-0255
164. Riethdorf S, Müller V, Zhang L, Rau T, Loibl S, Komor M, et al. Detection and HER2 expression of circulating tumor cells: prospective monitoring in breast cancer patients treated in the neoadjuvant GeparQuattro trial. *Clin Cancer Res* 2010; **16**: 2634-45. doi: 10.1158/1078-0432.CCR-09-2042
165. Pierga JY, Bidard FC, Mathiot C, Brain E, Delaloge S, Giachetti S, et al. Circulating tumor cell detection predicts early metastatic relapse after neoadjuvant chemotherapy in large operable and locally advanced breast cancer in a phase II randomized trial. *Clin Cancer Res* 2008; **14**: 7004-10. doi: 10.1158/1078-0432.CCR-08-0030
166. Scher HI, Jia X, de Bono JS, Fleisher M, Pienta KJ, Raghavan D, et al. Circulating tumour cells as prognostic markers in progressive, castration-resistant prostate cancer: a reanalysis of IMMC38 trial data. *Lancet Oncol* 2009; **10**: 233-9. doi: 10.1016/S1470-2045(08)70340-1
167. Goodman OB, Fink LM, Symanowski JT, Wong B, Grobaski B, Pomerantz D, et al. Circulating tumor cells in patients with castration-resistant prostate cancer baseline values and correlation with prognostic factors. *Cancer Epidemiol Biomarkers Prev* 2009; **18**: 1904-13. doi: 10.1158/1055-9965.EPI-08-1173
168. Okegawa T, Itaya N, Hara H, Tambo M, Nutahara K. Circulating tumor cells as a biomarker predictive of sensitivity to docetaxel chemotherapy in patients with castration-resistant prostate cancer. *Anticancer Res* 2014; **34**: 6705-10.
169. Vogelzang NJ, Fizazi K, Burke JM, De Wit R, Bellmunt J, Hutson TE, et al. Circulating tumor cells in a phase 3 study of docetaxel and prednisone with or without lenalidomide in metastatic castration-resistant prostate cancer. *Eur Urol* 2017; **71**: 168-71. doi: 10.1016/j.eururo.2016.07.051
170. Goldkorn A, Ely B, Quinn DI, Tangen CM, Fink LM, Xu T, et al. Circulating tumor cell counts are prognostic of overall survival in SWOG S0421: a phase III trial of docetaxel with or without atrasentan for metastatic castration-resistant prostate cancer. *J Clin Oncol* 2014; **32**: 1136-42. doi: 10.1200/JCO.2013.51.7417
171. Scher HI, Morris MJ, Stadler WM, Higano C, Basch E, Fizazi K, et al. Trial design and objectives for castration-resistant prostate cancer: updated recommendations from the Prostate Cancer Clinical Trials Working Group 3. *J Clin Oncol* 2016; **34**: 1402-18. doi: 10.1200/JCO.2015.64.2702
172. Danila DC, Heller G, Gignac GA, Gonzalez-Espinoza R, Anand A, Tanaka E, et al. Circulating tumor cell number and prognosis in progressive castration-resistant prostate cancer. *Clin Cancer Res* 2007; **13**: 7053-8. doi: 10.1158/1078-0432.CCR-07-1506
173. Thalgott M, Rack B, Horn T, Heck MM, Eiber M, Kübler H, et al. Detection of circulating tumor cells in locally advanced high-risk prostate cancer during neoadjuvant chemotherapy and radical prostatectomy. *Anticancer Res* 2015; **35**: 5679-85.
174. Meyer CP, Pantel K, Tennstedt P, Stroelin P, Schlomm T, Heinzer H, et al. Limited prognostic value of preoperative circulating tumor cells for early biochemical recurrence in patients with localized prostate cancer. *Urol Oncol Semin Orig Investig* 2016; **34**: 235.e11-235.e16. doi: 10.1016/j.urolonc.2015.12.003
175. Loh J, Jovanovic L, Lehman M, Capp A, Pryor D, Harris M, et al. Circulating tumor cell detection in high-risk non-metastatic prostate cancer. *J Cancer Res Clin Oncol* 2014; **140**: 2157-62. doi: 10.1007/s00432-014-1775-3
176. Okegawa T, Nutahara K, Higashihara E. Immunomagnetic quantification of circulating tumor cells as a prognostic factor of androgen deprivation responsiveness in patients with hormone naive metastatic prostate cancer. *J Urol* 2008; **180**: 1342-7. doi: 10.1016/j.juro.2008.06.021
177. Goodman OB, Symanowski JT, Loudy A, Fink LM, Ward DC, Vogelzang NJ. Circulating tumor cells as a predictive biomarker in patients with hormone-sensitive prostate cancer. *Clin Genitourin Cancer* 2011; **9**: 31-8. doi: 10.1016/j.clgc.2011.04.001
178. Resel Folkersma L, San José Manso L, Galante Romo I, Moreno Sierra J, Olivier Gómez C. Prognostic significance of circulating tumor cell count in patients with metastatic hormone-sensitive prostate cancer. *Urology* 2012; **80**: 1328-32. doi: 10.1016/j.urology.2012.09.001
179. Rink M, Chun FKH, Minner S, Friedrich M, Mauermann O, Heinzer H, et al. Detection of circulating tumour cells in peripheral blood of patients with advanced non-metastatic bladder cancer. *BJU Int* 2011; **107**: 1668-75. doi: 10.1111/j.1464-410X.2010.09562.x

180. Rink M, Chun FK, Dahlem R, Soave A, Minner S, Hansen J, et al. Prognostic role and HER2 expression of circulating tumor cells in peripheral blood of patients prior to radical cystectomy: a prospective study. *Eur Urol* 2012; **61**: 810-7. doi: 10.1016/j.eururo.2012.01.017
181. Soave A, Riethdorf S, Dahlem R, Minner S, Weisbach L, Engel O, et al. Detection and oncological effect of circulating tumour cells in patients with variant urothelial carcinoma histology treated with radical cystectomy. *BJU Int* 2017; **119**: 854-61. doi: 10.1111/bju.13782
182. Nastaly P, Ruf C, Becker P, Bednarz-Knoll N, Stoupiec M, Kavsar R, et al. Circulating tumor cells in patients with testicular germ cell tumors. *Clin Cancer Res* 2014; **20**: 3830-41. doi: 10.1158/1078-0432.CCR-13-2819
183. Gorin MA, Verdone JE, van der Toom E, Bivalacqua TJ, Allaf ME, Pienta KJ. Circulating tumour cells as biomarkers of prostate, bladder and kidney cancer. *Nat Rev Urol* 2017; **14**: 90-7. doi: 10.1038/nrurol.2016.224
184. Gradilone A, Iacovelli R, Cortesi E, Raimondi C, Gianni W, Nicolazzo C, et al. Circulating tumor cells and »suspicious objects« evaluated through CellSearch® in metastatic renal cell carcinoma. *Anticancer Res* 2011; **31**: 4219-21.
185. van Dalum G, Stam GJ, Scholten LF, Mastboom WJ, Vermes I, Tibbe AG, et al. Importance of circulating tumor cells in newly diagnosed colorectal cancer. *Int J Oncol* 2015; **46**: 1361-8. doi: 10.3892/ijo.2015.2824
186. Bissolati M, Sandri MT, Burtulo G, Zorzino L, Balzano G, Braga M. Portal vein-circulating tumor cells predict liver metastases in patients with resectable pancreatic cancer. *Tumor Biol* 2015; **36**: 991-6. doi: 10.1007/s13277-014-2716-0
187. Khoja L, Backen A, Sloane R, Menasce L, Ryder D, Krebs M, et al. A pilot study to explore circulating tumour cells in pancreatic cancer as a novel biomarker. *Br J Cancer* 2012; **106**: 508-16. doi: 10.1038/bjc.2011.545
188. Yang JD, Campion MB, Liu MC, Chaiteerakij R, Giama NH, Mohammed HA, et al. Circulating tumor cells are associated with poor overall survival in patients with cholangiocarcinoma. *Hepatology* 2016; **63**: 148-58. doi: 10.1002/hep.27944
189. Naito T, Tanaka F, Ono A, Yoneda K, Takahashi T, Murakami H, et al. Prognostic impact of circulating tumor cells in patients with small cell lung cancer. *J Thorac Oncol* 2012; **7**: 512-9. doi: 10.1097/JTO.0b013e31823f125d
190. Hiltermann TJN, Pore MM, van den Berg A, Timens W, Boezen HM, Liesker JJW, et al. Circulating tumor cells in small-cell lung cancer: a predictive and prognostic factor. *Ann Oncol* 2012; **23**: 2937-42. doi: 10.1093/annonc/mds138
191. Komine K, Inoue M, Otsuka K, Fukuda K, Nanjo H, Shibata H. Utility of measuring circulating tumor cell counts to assess the efficacy of treatment for carcinomas of unknown primary origin. *Anticancer Res* 2014; **34**: 3165-8.

Cisplatin and beyond: molecular mechanisms of action and drug resistance development in cancer chemotherapy

Tomaz Makovec

Institute of Biochemistry, Faculty of Medicine, University of Ljubljana, Ljubljana, Slovenia

Radiol Oncol 2019; 53(2): 148-158.

Received 20 July 2018

Accepted 5 September 2018

Correspondence to: Tomaz Makovec, Ph.D., Institute of Biochemistry, Faculty of Medicine, University of Ljubljana, Vrazov trg 2, SI-1000 Ljubljana, Slovenia. Phone: +386 (0)1 543 640; Fax: +386 (0)1 5437 641; E-mail: tomaz.makovec@mf.uni-lj.si

Disclosure: No potential conflicts of interest were disclosed.

Background. Platinum-based anticancer drugs are widely used in the chemotherapy of human neoplasms. The major obstacle for the clinical use of this class of drugs is the development of resistance and toxicity. It is therefore very important to understand the chemical properties, transport and metabolic pathways and mechanism of actions of these compounds. There is a large body of evidence that therapeutic and toxic effects of platinum drugs on cells are not only a consequence of covalent adducts formation between platinum complexes and DNA but also with RNA and many proteins. These processes determine molecular mechanisms that underlie resistance to platinum drugs as well as their toxicity. Increased expression levels of various transporters and increased repair of platinum-DNA adducts are both considered as the most significant processes in the development of drug resistance. Functional genomics has an increasing role in predicting patients' responses to platinum drugs. Genetic polymorphisms affecting these processes may play an important role and constitute the basis for individualized approach to cancer therapy. Similar processes may also influence therapeutic potential of nonplatinum metal compounds with anticancer activity.

Conclusions. Cisplatin is the most frequently used platinum based chemotherapeutic agent that is clinically proven to combat different types of cancers and sarcomas.

Key words: cisplatin; molecular mechanisms; chemotherapy; resistance

Introduction

Drug resistance is a wide spread and well known phenomenon among anticancer medications and platinum drugs are not exceptions. The use of these drugs in chemotherapy is hampered by extrinsic and intrinsic resistance of cells. Although many cancer cells are initially susceptible to chemotherapy with platinum drugs, over time they may develop resistance through more efficient DNA damage repair, drug inactivation with glutathione and metallothioneins and drug efflux with various transport systems located in cell membrane. In this review the chemical properties, metabolism and transport of platinum and similar compounds and how they are implicated in the developing in cell resistance and toxicity are described. The knowl-

edge of mechanism of action of these drugs reveals mechanisms of resistance and toxicity. The aim of this review is also to provide recent data concerning hypersensitivity reactions to platinum-containing chemotherapy agents. To minimize toxicity, resistance and hypersensitivity reactions to platinum drugs the new metallodrugs were developed. A brief summary of these agents is also presented.

The discovery of platinum compounds as anticancer agents

Until the mid-1960s, cancer chemotherapy was based on purely organic compounds. An accidental discovery of anticancer properties of inorganic co-

the chloride ion is about 105 mM and, according to Le Chatelier's principle, the loss of the chloride ion from cisplatin is suppressed by the chloride ion in solution; the reaction shown in Figure 1 does not progress very far to the right (from **1** to **2**). According to the first order kinetics for conversion from **1** to **2**, the half-life for cisplatin at 35.5 °C is 1.05 h. The binding of a water molecule to the Pt²⁺ ion makes water very acidic and monoaqua species **3** is dissociated in the monohydroxo complex **4**. So in an aqueous solution with the high chloride concentration the forms **1**, **2** and **4** predominate. In the cytoplasm, where chloride ion concentration is only 4 mM, the equilibria is shifted to the right and forms **3**, **5** and **6** predominate. A common route of cisplatin administration is the infusion of the solutions such as Platinol® and Plationol®AQ, which contain 3.3 mM cisplatin (1 mg/ml) and 154 mM sodium chloride, NaCl (normal saline solution). Since the pH is adjusted to pH about 4 solution in Platinol contains mainly (95%) of species **1** and only smaller amounts of **3** and **4**.

Uptake and removal of cisplatin from cells

Cisplatin in blood

Since the concentration of chloride in blood is lower than in the infusion solution (105 versus 154 mM), the equilibria (Figure 1) is shifted to the right. Because the carbonate and phosphate ions react with aquated cisplatin forms and because some platinum binds to protein that is being eliminated in significant amounts via the urine during the infusion, it is impossible to predict the composition of species **1** – **6** according to the data in Figure 1. This system is far from the chemical equilibrium. A major part (68 – 98%) of cisplatin is bound to the blood plasma proteins, especially on human serum albumin (HSA)⁶. One molecule of HSA binds five molecules of cisplatin. *cis*-[PtCl(NH₃)₂]⁺ is bound to nitrogen atom from His105 and His288 and sulphur atoms from Met329, Met298 and Met548. Treatment of HSA with cisplatin also leads to the formation of adduct between *cis*-[Pt(NH₃)₂]²⁺ and His67 and His247. Since both histidine residues are involved in the transport of Zn²⁺ ions to the cell by HSA⁷, this may be the reason why some patients on therapy with cisplatin have zinc imbalance in their body.⁸ For study of binding of platinum compounds to human serum proteins a novel method for accessing of Pt using conjoint liquid chromatography has also been developed.⁹

Cisplatin uptake from blood into a cell

The first step for platinum drugs to exert their therapeutic as well as toxic effects is to enter the cells. This process is complex and not completely understood. Cisplatin enters a cell mainly by passive diffusion. Uptake of cisplatin by cells was proportional to the total concentration of cisplatin in the cell culture medium up to 3 mM concentration and was not saturable.¹⁰ The most likely candidates for passive diffusion through hydrophobic lipid bilayer are neutral species without the charge such as cisplatin and monohydroxo form (**1** and **4**, respectively in Figure 1). But studies with the inhibitors of active transporters suggested that there must also be other uptake mechanisms.¹¹ Recently, a lot of attention has been given to the active modes of the uptake.¹² The most likely candidates for the transport of cisplatin into a cell by facilitated diffusion are the copper transporters Ctr1 (SLC31A1) and Ctr2 (SLC31A2, copper importer).¹³ This transmembrane protein has an extracellular domain that is rich in methionine and histidine residues. It has been suggested that both metals, platinum and copper, use Ctr1 as their entry route into the cell although the chemistry of these two metals is quite different. Switching between different oxidation states has pivotal role in the transport of copper. Whereas copper exists in two biological oxidation states as Cu⁺ and Cu²⁺ ions, the cisplatin exists only in one stable biologically accessible oxidation state with Pt²⁺ ion. Because platinum cannot switch between different oxidation states, the uptake of cisplatin into the cell by this protein might be blocked. An additional factor that throws doubt on Ctr (**1** and **2**) as a main transporter of cisplatin is the reaction of extracellular methionine residue with Pt²⁺ resulting in formation of a stable Pt²⁺-S bond, similar to the bond between Pt²⁺ and methionine residues in HSA. Since the transport of Pt²⁺ ion through Ctr would require a facile breaking and reforming of the Pt²⁺-S bond, the thermodynamic and kinetic parameters of this bond would exclude the Ctr as an entry route for cisplatin. Furthermore, *cis*-ammonia molecules would be lost during cisplatin transfer with Ctr due to *trans* effect. Additionally, excessive copper in extracellular fluid triggers an internalization and degradation of Ctr protein. This acute regulatory response has also been reported following exposure of human ovarian carcinoma cells to cisplatin, but such response was not observed in other types of cancer cells.¹⁴ Although many studies have shown that cisplatin can bind to Ctr, none has shown that Pt²⁺

ion can actually be transported into a cell by this mechanism.¹⁵ Arnesano and Natile¹⁶ hypothesized that the interaction of cisplatin with Ctr leads to pinocytosis and vesicular transport of cisplatin into the cell, thus protecting the drug from inactivation with glutathione (GSH) and metallothioneins (MT) which are present in cells.

As forms 2, 3 and 5 shown in Figure 1 are cations, led investigators to examine the involvement of organic cation transporters (OCTs, SLC22A) in cisplatin transport across the membrane. This assumption was strengthened by the observation that OCTs are expressed in tissues sensitive to cisplatin toxicity. It was shown that both OCT1 (SLC22A1) and OCT2 (SLC22A2) are implicated in transport of cisplatin into the HEK 293 cells as well as the other cell lines.¹⁷ Under physiological conditions, cisplatin may also undergo a transformation in cisplatin carbonato complexes, which are anionic species and these forms may be transported into the cell by organic anion transporters (OATs, SLC22A). The transport of platinum drugs by OAT may also explain the nephrotoxicity of these substances.¹⁸ Both OCT and OAT mediated cisplatin nephrotoxicities are observed in 30% of patients. OCT2 is specifically expressed in the kidneys and for this reason it is a suitable target for the investigating of the protection against nephrotoxicity. The tissue specific expression of OCT may be also critical for the development of ototoxicity as well as peripheral neurotoxicity.¹⁹

Cisplatin transport out of the cells

Since the therapeutic range of cisplatin is narrow we cannot overcome the cell resistance simply by increasing the dose. Resistance to cisplatin is a consequence of the enhanced removal of the drug that enters a cell and the efficiency of DNA repair mechanisms, which remove lethal adducts between DNA and cisplatin. Another copper transporter, *ATP7A* and closely related *ATP7B*, which deliver copper into the organelles and are responsible for removing the excess copper out of a cell, may also be involved in the cisplatin-induced resistance.²⁰ Mutation in *ATP7B* gene produces accumulation of copper in the body, a state known as Wilson's disease²¹, while the mutation in *ATP7A* gene has the opposite effect and is responsible for a copper deficiency, known as the Menkes disease.²² Both *ATP7A* and *ATP7B* can bind cisplatin at cysteine residue in their N-terminal metal binding domains forming a stable Pt^{2+} -S bond. Elevated levels of these proteins correlate with a diminished

accumulation of cisplatin and consequently with lower cytotoxicity.²³

Beside the copper-transporting proteins GSH and metallothioneins may also influence cisplatin transport. These cysteine rich, low molecular weight proteins are involved in intracellular inactivation of platinum and other similar drugs through coordination to thiol groups. An overexpression of metallothionein in the tumour cells is present in 70% of the patients with oesophageal cancer and it is correlated with resistance to cisplatin.²⁴ It was shown that GSH and cisplatin form anionic *bis* Pt^{2+} -GSH complexes which can be refluxed from leukaemia cells in the presence of ATP.²⁵ Later it was shown that multidrug resistance-associated protein MRP2 (ABCC2) and OAT were responsible for the efflux of this complex.²⁶ Since the formation of the adduct between cisplatin and two deprotonated forms of GSH prevents the drug from reacting with DNA and other targets, MRP2 and OAT are important factors in detoxification of the cell from cisplatin. Due to combination of uptake and export transporters only 1% of administered drug reaches the site of action within the cells. Cellular traffic of cisplatin is summarized in Figure 2.

Clinical applications

Genetic background as a determinant of cisplatin-based drug response

The inter-individual variability of the efficacy of platinum based chemotherapy as well as its toxic-

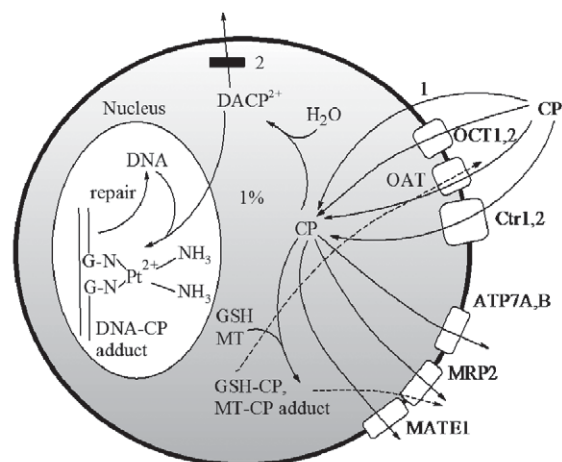


FIGURE 2. Traffic of cisplatin (CP). 1, passive diffusion, 2, passive diffusion blocked. See text for explanations. CP: cisplatin, DACP: diaqua cisplatin, OCT: organic cation transporter, OAT: organic anion transporter, Ctr: copper transporter, MRP: multidrug resistance-associated protein, ATP7: copper-transporting P-type ATPase, MATE: multidrug extrusion transporter, GSH: glutathione, MT: metallothionein.

TABLE 1. Polymorphisms of transporters that influence the efficacy of platinum drugs

Protein	Gene	Genetic polymorphisms or expression level (EL) that influences the outcome of platinum-based therapy
Uptake of platinum drugs		
OCT1	SLC22A1	c.181C > T, c.480C > G, c.1022C > T, c.1222A > G, c.1390G > A, c.1463G > T
OCT2	SLC22A2	c.160C > T, c.481 T > C, c.493A > G, c.495G > A, c.808G > T, c.890C > G, c.1198C > T, c.1294A > C
OCT3	SLC22A3	EL
CTR1	SLC31A1	rs10981694 A>C
CTR2	SLC31A2	
Efflux of platinum drugs		
MATE1	SLC47A1	p.Gly64Asp and p.Val480Met: reduced transport of oxaliplatin
MATE2	SLC47A2	p.Gly211Val
ATP7A	ATP7A (MNK)	c.2299G > C (p.Val767Leu) and c.4390A > G (p.Ile1464Val)
ATP7B	ATP7B (WND)	c.1216G > T (p.Ala406Ser), c.1366G > C (p.Val456Leu), c.2495A > G (p.KLys32Arg), c.2785A > G (p.Ile929Val), c.2855G > A (p.Arg952Lys), c.2871delC (P957PfsX9), c.3419 T > C (p.Val1140Ala), c.3836A > G (p.Asp1279Gly), c.3886G > A (p.Asp1296Asn) and c.3889G > A (p.Val1297Ile)

EL = expression level

TABLE 2. Polymorphisms of DNA-platinum drug adducts repairing enzymes

Protein	Gene	Polymorphisms
DNA-adduct repair system		
ERCC1	ERCC1	c.8092C>A, c.C354T
XRCC1	XRCC1	c.C580T, c.A1196G
XRCC3	XRCC2	p.Thr241Met, c.C241T
XPD	XPD	p.Lys751Gln, c.A2251C, c.C2133T
XPG		c.T242C
XPA		5'UTR
Metabolism of platinum-based drugs		
MDR1		c.T3435C
GSTP1	GSTP1 (FAEES3)	c.A313G

ity is the result of the genetic variability in genes involved in drug metabolism, drug transport and DNA repair. Therefore, the determination of genetic markers such as genetic polymorphisms in these genes may provide the hints about the optimal cisplatin regimens for personalized therapy.

Both uptake and efflux transporters are subject to genetic variability. Polymorphic transporters are involved in processes that increase the intracellular level of the drug: transport with copper transporters Ctr1 and 2 and organic cation transporters OCT 1 and 2. The same is true for the transporters that are involved in the efflux of cisplatin from the cell and resistance, copper-transporting ATPases ATP7A and ATP7B, organic anion transporters, OAT, glutathione and metallothionein, multidrug resistance-associated protein MRP2 as well as multidrug extrusion transporter-1 (MATE1).²⁷

The presence of single nucleotide polymorphisms in all transporters shown in Figure 2 influence the response of patients to platinum drugs in a great extent and this influence is dependent on both, the type of platinum drug and the type of cancer cells.²⁸ The data on these polymorphisms are summarized in the Table 1.

The main mechanism of resistance is a DNA-platinum drug adducts repairing system. Polymorphisms of DNA-adduct repair enzymes also play a role in sensitivity towards platinum-based chemotherapy (Table 2). X-ray repair cross-complementing group 1 (XRCC1), excision repair cross complementation 1 (ERCC1) and xeroderma pigmentosum complementary group (XPA, XPD and XPG) are enzymes that play the crucial role in these processes. The polymorphic A1196G allele in XRCC1 gene is present in 20-38% of lung cancer patients.²⁹ A number of studies have been performed to investigate the association of XRCC1 gene polymorphisms with platinum drug efficacy but the results are inconsistent.

Recent studies also investigated Major Vault Protein (MVP) present as the main component of the vault in normal tissues as well as in malignant cells, including ovarian cancer, colon carcinoma and acute myeloid leukaemia.³⁰ Although MVP has been linked to the development of multidrug resistance in cancer cells, several studies have reported conflicting results.³¹ The association between polymorphisms in MVP gene and platinum resistance has not yet been confirmed probably due to the limited number of patients.³²

Allergic reactions to cisplatin

Although allergic reactions to cisplatin are rare, with later cisplatin derivatives, carboplatin and oxaliplatin the allergic reactions are more common. Still they are less frequent than with anticancer drugs which names end with “mab” and other drugs that contain proteins. Hypersensitivity reactions to platinum generally occur after multiple cycles of therapy – they are acquired and are consistent with type 1 IgE-mediated hypersensitivity. In patients presenting with severe hypersensitivity reactions to carboplatin it is feasible to replace it with cisplatin. Overall incidence of hypersensitivity to platinum agents is 5 – 20% for cisplatin and occurs mostly between 4th-8th course of infusion. The incidence is 1 – 44% for carboplatin and 10 – 20% for oxaliplatin.³³ The most striking difference between carboplatin hypersensitivity, compared to hypersensitivity to nonplatinum drugs, is that the cumulative risk of hypersensitivity reactions increases with the number of infusions and there is no evidence of plateau.³⁴ Hypersensitivity reactions occur more frequently in patients receiving certain drug combinations such as carboplatin – paclitaxel as compared to carboplatin in combination with pegylated liposomal doxorubicin.³⁵

Cisplatin and multimodal treatment and novel approaches

Since hyperthermia enhances cytotoxic effects of cisplatin, the trimodal combination of platinum drugs with hyperthermia and radiation can lead to potent synergistic interaction.³⁶ There is a synergistic effect of regional hyperthermia (39-43°C) and cisplatin anti-tumour efficacy, if cisplatin is encapsulated in temperature-sensitive liposomes used for targeted drug delivery. It is hypothesized that hyperthermia increases cisplatin accumulation in part by increasing Ctr1 multimerization and thus greater cisplatin accumulation. Increased Ctr1 multimerization following hyperthermia treatment (41°C) *in vitro*, compared to normothermic controls (37°C), was observed suggesting that there may be a mechanism for an increased cisplatin uptake in heat-treated cells. Hyperthermia enhanced cisplatin-mediated cytotoxicity in wild type (WT) cells with a dose modifying factor (DMF) of 1.8 compared to 1.4 in Ctr1-/- cells because WT cells contained greater levels of platinum compared to Ctr1-/- cells.³⁷

Since the atomic number of platinum is high, 78, it is possible to produce Auger electrons and/

or Auger radiation upon treating the platinum drug with ionizing radiation. Treatment of cervical cancer with a conjunction of cisplatin and ionizing radiation increased survival and disease free intervals and became a part of standard care for the treatment of cervical cancers.³⁸ The »Trojan horse« treatment of glioblastoma involves gold (atomic number 79) nanoparticles and attached molecules of cisplatin. Treated cultured glioblastoma cells in preclinical studies absorb nanoparticles and DNA binds platinum attached to nanoparticles. After radiation, both gold and platinum serve as high atomic number radio sensitizers that emit Auger electrons and radiation. The resulting assembly of gold nanoparticles with attached cisplatin and antibodies after radiation exhibit both chemotherapeutic power to cancer cells as well as Auger-mediated secondary electron emission, which cause DNA double strand breaks adjacent to the cisplatin bound to DNA.³⁹ Binding cisplatin to gold nanoparticles is also a strategy to enhance the delivery of cisplatin through the blood brain barrier. A combination with a magnetic resonance-guided ultrasound intensifies glioblastoma treatment. It is demonstrated that the assembly of gold nanoparticles and cisplatin greatly inhibits the growth of glioblastoma cells compared to the free cisplatin and synergy with radiation therapy.⁴⁰ An important reactive oxygen species (ROS) scavenger DJ-1 protein (PARK7) modulates different oncogenic pathways that support the growth and invasion of ovarian cancer cells. This cancer targeted nanoplat-form based on siRNA-mediated suppression of DJ-1 protein outperforms cisplatin alone. Three cycles of siRNA-mediated DJ-1 therapy combined with a low dose of cisplatin completely eradicated ovarian cancer tumours from the mice without recurrence during a 35-week long study.⁴¹

The next step in the research includes the attachment of the transport system for delivering nanoparticles with cisplatin to the target.⁴² Mice treated with hyaluronic-acid conjugated mesoporous silica nanoparticles carried TWIST-siRNA and cisplatin exhibited specific tumour targeting and reduction of tumour burden.⁴³

Another important aspect of novel approaches to cisplatin chemotherapy is to reduce cisplatin toxicity. The two other approved platinum-based chemotherapeutics, carboplatin and oxaliplatin exhibit improved nephrotoxicity⁴⁴ and ototoxicity⁴⁵ profiles, but are also less efficient than cisplatin. This challenge could be addressed by harnessing a nanotechnology-based strategy. An example of the cisplatin toxicity prevention on the reproduc-

tive system is the use of selenium nanoparticles (Nano-Se). Nano-Se particles, due to their strong antioxidant potential are suitable to prevent cisplatin induced gonadotoxicity. Co-administration with cisplatin significantly improves the sperm quality, serum testosterone and spermatogenesis in male rats.⁴⁶ Lipoplatin is another example of bi-as cisplatin toxicity. These nanoparticles of 110 nm average diameter are composed of lipids and cisplatin. After intravenous administration it escapes clearance from macrophages and the half-life of lipoplatin is 120 h.⁴⁷ Attachment of platinum drugs to nanoparticles passively targets solid tumours through the enhanced permeability. Lipoplatin exerted negligible nephrotoxicity, ototoxicity and neurotoxicity in Phase I human studies.⁴⁸

For poorly permeable platinum drugs such as cisplatin and similar low lipophilic analogues, a higher doses are needed to exert therapeutic effect and consequently toxicity is more pronounced. To mitigate this effect an enhanced influx into the cancer cells can be achieved with electroporation in the process of electrochemotherapy.^{49,50,51} This method increases the cytotoxicity up to 80-fold in cisplatin-sensitive as well as cisplatin-resistant tumour types.⁵² Other approach include the synthesis of novel platinum compounds with more lipophilic leaving groups with potential antitumor effect. One such candidate is trans-[PtCl₂(3-hydroxyethylpyridine)₂] applied with electroporation as drug delivery method⁵³.

Non-DNA targets for cisplatin

The principle target of cisplatin is the DNA as the platination of the DNA is lethal to the cell. However, the other targets are also very important and may contribute to the lethal effect on the cell. Cisplatin, among others, attacks mitochondria and triggers the production of ROS, destroys lysosomes inducing the release of lysosomal proteases and degrades endoplasmic reticulum which results in the deregulation of calcium storage and in the misfolded proteins.⁵⁴ Beside the DNA in mitochondria, cisplatin attacks other organelles by forming adducts with functional groups on proteins, especially with the sulphur atom in cysteine and methionine side chains.

A membrane-bound Na⁺/H⁺ exchanger protein (NHE) is one of the non-DNA targets for cisplatin. When cisplatin binds to this protein in human colon cancer cells, it causes intracellular acidosis, increases fluidity of membrane through promotion

of lipid rafts and the induction of apoptosis via *fas* pathway and cell death.⁵⁵ Since the membrane is the first barrier that cisplatin must cross, NHE may be the first target for cisplatin in cancer cells. Adducts between NHE and cisplatin occur in a few minutes after adding cisplatin to the culture medium, whereas cisplatin-DNA adducts occur at a much slower rate after about an hour.

Zinc fingers that bind to the DNA and regulate gene expression are also cisplatin targets. An example is 31-amino-amino-acid long zinc finger, that is the DNA-binding domain of the enzyme DNA-polymerase- α , a very important enzyme for accurate synthesis of genetic information.⁵⁶ Four thiolate groups from cysteine residues coordinate the zinc atom in zinc fingers. Cisplatin reacts with the Zn²⁺ ion in a stepwise manner to substitute the coordinated Zn²⁺ ion from the finger. The reaction between a zinc finger and cisplatin is faster than between cisplatin and DNA. That means that the zinc fingers could be the targets for platinum drugs. Cisplatin changes the structure of DNA-polymerase- α and this could be the mechanism by which the drug blocks DNA replication and causes cell death.

Another protein target is tubulin. These 50 kDa proteins must be assembled into microtubules and disassembled rapidly during mitosis and molecules that interfere with this process can push the cell into a cell-cycle arrest and the cell dies. Even in the presence of an anticancer drug paclitaxel, which stabilizes and prevents disassembly of microtubules into tubulin, the nonfilamentous structures appear only if the diaqua derivative of cisplatin is present. GTP is required for the formation of filaments and since platinum drugs react readily with N7-atom in guanine, this is the mechanism of the deprivation of the necessary energy for the microtubule formation.⁵⁷

Thioredoxin reductase (TrxR) has selenocysteine residue at the C-terminus that is an excellent target for platinum drugs. Both cisplatin and transplatin can irreversibly inactivate this enzyme. Since a large percent of cisplatin in the cell is inactivated by GSH into GS-Pt, Ishikawa surprisingly found that GS-Pt can also inactivate TrxR.⁵⁸ In the presence of cisplatin, cells also produce increased level of stress response and DNA-binding proteins.

RNA is another molecule that has been largely overlooked as a possible candidate for the cisplatin attack and also contains suitable positioned bases. DeRose with the co-workers have shown that 4 to 20-fold more platinum binds to RNA compared to DNA.⁵⁹ Helix 18 of 18S rRNA binds three platinum

ions. One of them is bridging opposing strands of RNA in an interstrand crosslink.

Cytotoxic metals

The problem with cisplatin is that it may be inactivated into transplatin during the uptake into the cell via Ctr1 transporter. To avoid this problem other derivatives of platinum drugs have been synthesized, where two ligands are interconnected and *trans* effect is decreased. Oxaliplatin, nedaplatin, lobaplatin, heptaplatin and carboplatin have both oxygen ligands in one molecule as bidentate ligand. Oxaliplatin, lobaplatin and heptaplatin have also nonleaving amino ligands as parts of the bidentate molecule.

The next generation of cisplatin-like drugs tend to be structurally similar to the approved drugs and they are expected to operate via a similar mechanism of action. More than five thousand distinct compounds with general formula $cis-PtA_2X_2$, where A is the symbol for ammine or a substituted ammine and X is anionic bidentate ligand, have been synthesized until now. The effort put into the elucidation of mechanisms of tumour resistance to cisplatin and other platinum based drugs triggered the boom also in other metal based cytostatics.

During a 40-year-long period between the development and the final approval of cis-, carbo- and oxaliplatin, the search for nonplatinum anticancer drugs yielded some interesting compounds. Better understanding of their chemistry and mode of action may facilitate the development of anticancer drugs based on these compounds.

Ruthenium Organometallic ruthenium (II) arene compounds are emerging as a new class of promising anticancer drugs. They show selective activity against certain cancer cells and low toxicity. Due to octahedral coordination sphere, ruthenium complexes have higher degree of specificity and size discrimination and exert lower toxicity and faster elimination from the body, in contrast to square planar geometry of platinum (II) compounds. Well known species NAMI-A and KP1019, which are currently in clinical trials, is opening new approaches in cancer treatment. The cellular targets of ruthenium compounds have not yet been identified with certainty. Despite the fact that DNA has been assumed to be the primary target, recent results show that several proteins have been recognized as the binding partners.⁶⁰ In particular, these proteins are glutathione S-transferase, HSA and transferrin.⁶¹ NAMI-A binds to the exposed imida-

zole (histidine) on HSA and apo-transferrin, but only weakly on DNA and RNA. The main effect of NAMI-A is to stop a tumour from spreading, a process known as metastasis.⁶⁰

Gold, palladium. In arthritic patients receiving gold +3 and +1 compounds as therapy it was observed that gold possesses anticancer activity.⁶² The mechanism of the action of gold compounds, for example a gold phosphine ligands $[Au(dppe)_2]^+$, is still unknown, although, most researchers believe that the site of action of this compound is the mitochondria in the cells. Such compounds also produce breaks in DNA and also serve as a bridge between protein and DNA. Complexes with gold and palladium, depending on dose, reduce the proliferation of ovarian and breast cancer as well as myeloid leukaemia and lymphatic cell line. Compounds with selenium ligands in general induce stronger effects than compounds with sulphur ligands. The IC₅₀ for proliferation of SUP-B15 cells was 50% lower with Au-Se compounds in comparison with Au-S compounds and around a quarter lower in the case of Ru-Se and Pd-Se compounds in comparison with Ru-S and Pd-S compounds.⁶³ The mechanism of action is composed of the inhibition of metabolism and proliferation and it also includes apoptosis and oxidative stress by ROS production.

In **titanium**, as in cisplatin, there are two chloride-leaving ligands in *cis* position present in titanocene dichloride and the molecule is neutral in charge. Since this compound showed no nephro- or myelotoxicity in preclinical studies, it was entered into clinical trials.⁶⁴ The trials revealed that the compound was active against colon 38 carcinoma and B16 melanoma cells. In treating ovarian cancer cells, titanocene dichloride displayed higher activity than cisplatin. While investigating the mechanism of action, a far more complicated picture has appeared indicating multiple cellular processes that can be triggered by titanium anticancer compounds.⁶⁵ The exact site of binding is not established, but since Ti^{4+} is a hard base, negatively charged oxygens on the phosphate groups of DNA form bonds with the ion and thus disable DNA.⁶⁶

Vanadium, niobium, molybdenum and rhenium complexes – early transition metal based antitumor drugs and a large spectrum of other transition metals have also been tested for anticancer activity. For most of them, the intercalation with DNA atoms is not required for activity. Proteins, such as human topoisomerase 1 and thioredoxin reductase, are only a few of the possible targets of these transition metal complexes.⁶⁷

Conclusions

In the last decade, several of platinum and other metal complexes have been created and tested for anticancer activity in order to bypass the drawback of existing metal anticancer chelates. The enormous spectrum of transition metal combinations and a plethora of ligands combinations have produced extremely broad spectrum of anticancer complexes – more than 5000 only with platinum. Each of them has its own mechanism of action and the continuation of work on this field could produce metal complexes which can outperform the existing drugs and provide more effective chemotherapy and less toxicity.

The other field of intensive research is the investigation of genetic polymorphisms as an approach to the optimal metal-based chemotherapy for a particular individual and probably it represents the plateau of this type of treatment. The solid knowledge of the molecular mechanisms of action and genetic basis of interindividual variability of response to cisplatin and other metal based compounds summarized in this review may therefore help the oncologist to better understand the mechanism of their cytostatic action.

References

- Rosenberg B, Van Camp L, Grimley EB, Thomson AJ. The inhibition of growth or cell division in *Escherichia coli* by different ionic species of platinum(IV) complexes. *J Biol Chem* 1967; **242**: 1347-52. PMID: 5337590
- Rosenberg B, Van Camp L, Trosko JE, Mansour VH. Platinum compounds: a new class of potent antitumor agents. *Nature* 1969; **222**: 385-6. PMID: 5782119
- Peyrone M. Über die einwirkungdes ammoniaks auf platichlorür. *Annalen der chemie und pharmacie* 1844; **51**: 1-29. doi: 10.1002/jlac.18440510102
- Rosenberg B. Some biological effects of platinum compounds. New agents for the control of tumours. *Platinum Met Rev* 1971; **15**: 42-51.
- Apps MG, Choi EHY, Wheate NJ. The state-of-play and future of platinum drugs. *Endocr Relat Cancer* 2015; **22**: R219-33. doi: 10.1530/ERC-15-0237
- Dabrowiak JC. *Metals in medicine*. 2nd edition. John Wiley & Sons Ltd; 2017. p. 94-5.
- Sooriyaarachchi M, Narendran A, Gailer J. Comparative hydrolysis and plasma protein binding of cisplatin and carboplatin in human plasma in vitro. *Metallomics* 2011; **3**: 49-55. doi: 10.1039/c0mt00058b
- Handing KB, Shabalín IG, Kassaar O, Khazaipoul S, Blindauer CA, Stewart AJ, et al. Circulatory zinc transport is controlled by distinct interdomain sites on mammalian albumins. *Chem Sci Chem* 2016; **7**: 6635-48. doi: 10.1039/c6sc02267g
- Hu W, Luo Q, Wu K, Li X, Wang F, Chen Y, et al. The anticancer drug cisplatin can crosslink the interdomain zinc site on human albumin. *Chem Commun (Camb)* 2011; **47**: 6006-8. doi: 10.1039/c1cc11627d
- Martinčić A, Cemazar M, Serša G, Kovač V, Milačić R, Ščančar J. A novel method for speciation of Pt in human serum incubated with cisplatin, oxaliplatin and carboplatin by conjoint liquid chromatography on monolithic disks with UV and ICP-MS detection. *Talanta* 2013; **116**: 141-8. doi: 10.1016/j.talanta.2013.05.016
- Eljack ND, Ma HY, Drucker J, Shen C, Hambley TW, New EJ, et al. Mechanisms of cell uptake and toxicity of the anticancer drug cisplatin. *Metallomics* 2014; **6**: 2126-33. doi: 10.1039/c4mt00238e
- Hall MD, Okabe M, Shen DW, Liang XJ, Gottesman MM. The role of cellular accumulation in determining sensitivity to platinum-based chemotherapy. *Annu Rev Pharmacol Toxicol* 2008; **48**: 495-535. doi: 10.1146/annurev.pharmtox.48.080907.180426
- Eljack ND, Ma MH, Drucker J, Shen C, Hambley TW, New JE, et al. Mechanisms of cell uptake and toxicity of the anticancer drug cisplatin. *Metallomics* 2014; **6**: 2126-33. doi: 10.1039/c4mt00238e
- Lasorsa A, Natile G, Rosato A, Tadini-Buoninsegni F, Arnesano F. Monitoring interactions inside cells by advanced spectroscopies: overview of copper transporters and cisplatin. *Curr Med Chem* 2018; **25**: 462-77. doi: 10.2174/0929867324666171110141311
- Holzer AK, Howell SB. The internalization and degradation of human copper transporter 1 following cisplatin exposure. *Cancer Res* 2006; **66**: 10944-52. doi: 10.1158/0008-5472.CAN-06-1710
- Ivy KD, Kaplan JH. A re-evaluation of the role of hCTR1, the human high-affinity copper transporter, in platinum-drug entry into human cells. *Mol Pharmacol* 2013; **83**: 1237-46. doi: 10.1124/mol.113.085068.
- Arnesano F, Seintilla S, Natile G. Interaction between platinum complexes and a methionine motif found in copper transport proteins. *Angew Chem Int Ed Engl* 2007; **46**: 9062-4. doi: 10.1002/anie.200703271
- Yonezawa A, Masuda S, Yokoo S, Katsura T, Inui K. Cisplatin and oxaliplatin, but not carboplatin and nedaplatin, are substrates for human organic cation transporters (SLC22A1-3 and multidrug and toxin extrusion family). *J Pharmacol Exp Ther* 2006; **319**: 879-86. doi: 10.1124/jpet.106.110346
- Nieskens T, Peters JGP, Dabaghie D, Korte D, Jansen K, Van Asbeck AH, et al. Expression of organic anion transporter 1 or 3 in human kidney proximal tubule cells reduces cisplatin sensitivity. *Drug Metab Dispos* 2018; **46**: 592-9. doi: 10.1124/dmd.117.079384
- Ciarimboli G. Membrane transporters as mediators of cisplatin side-effects. *Anticancer Res* 2014; **34**: 547-50. PMID: 24403515.
- Calandrini V, Arnesano F, Galliani A, Nguyen TH, Ippoliti E, Carloni P, et al. Platination of the copper transporter ATP7A involved in anticancer drug resistance. *Dalton Trans* 2014; **43**: 12085-94. doi: 10.1039/c4dt01339e
- Aggarwal A, Bhatt M. Advances in treatment of Wilson disease. *Tremor Other Hyperkinet Mov (NY)* 2018; **8**: 525. doi: 10.7916/D841881D
- Ferreira CR, Gahl WA. Disorders of metal metabolism. *Transl Sci Rare Dis* 2017; **2**: 101-39. doi: 10.3233/TRD-170015
- Tadini-Buoninsegni F, Bartolommei G, Moncelli MR, Inesi G, Galliani A, Sinisi M, et al. Translocation of platinum anticancer drugs by human copper ATPases ATP7A and ATP7B. *Angew Chem Int Ed Engl* 2014; **53**: 1297-301. doi: 10.1002/anie.201307718
- Hishikawa Y, Abe S, Kinugasa S, Yoshimura H, Monden N, Igarashi M, et al. Overexpression of metallothionein correlates with chemo resistance to cisplatin and prognosis in oesophageal cancer. *Oncology* 1997; **54**: 342-7. doi: 10.1159/000227714
- Ishikawa T, Ali-Osman F. Glutathione-associated cis-diamminedichloroplatinum(II) metabolism and ATP-dependent efflux from leukaemia cells. Molecular characterization of glutathione-platinum complex and its biological significance. *J Biol Chem* 1993; **268**: 20116-25. PMID: 8376370.
- Chen HH, Kuo MT. Role of glutathione in the regulation of cisplatin resistance in cancer chemotherapy. *Met Based Drugs* 2010; pii: 430939. doi: 10.1155/2010/430939
- Sauzay C, White-Koning M, Hennebelle I, Deluche T, Delmas C, Imbs DC, et al. Inhibition of OCT2, MATE1 and MATE2-K as a possible mechanism of drug interaction between pazopanib and cisplatin. *Pharmacol Res* 2016; **110**: 89-95. doi: 10.1016/j.phrs.2016.05.012
- Sprowl JA, Ness RA, Sparreboom A. Polymorphic transporters and platinum pharmacodynamics. *Drug Metab Pharmacokinet* 2013; **28**: 19-27. PMID: 22986709
- Filipski KK, Mathijssen RH, Mikkelsen TS, Schinkel AH, Sparreboom A. Contribution of organic cation transporter 2 (OCT2) to cisplatin-induced nephrotoxicity. *Clin Pharmacol Ther* 2009; **86**: 396-402. doi: 10.1038/clpt.2009.139

31. Tzvetkov MV, Behrens G, O'Brien VP, Hohloch K, Brockmüller J, Benöhr P. Pharmacogenetic analyses of cisplatin-induced nephrotoxicity indicate a renoprotective effect of ERCC1 polymorphisms. *Pharmacogenomics* 2011; **12**: 1417-27. doi: 10.2217/pgs.11.93
32. Hsu CM, Lin PM, Chang JG, Lin HC, Li SH, Lin SF, et al. Upregulated SLC22A3 has a potential for improving survival of patients with head and neck squamous cell carcinoma receiving cisplatin treatment. *Oncotarget* 2017; **8**: 74348-58. doi: 10.18632/oncotarget.20637
33. Chen Y, Teranishi K, Li S, Yee SW, Hesselson S, Stryke D, et al. Genetic variants in multidrug and toxic compound extrusion-1, hMATE1, alter transport function. *Pharmacogenomics* 2009; **9**: 127-36. doi: 10.1038/tj.2008.19
34. Au WW, Salama SA, Sierra-Torres CH. Functional characterization of polymorphisms in DNA repair genes using cytogenetic challenge assays. *Environ Health Perspect* 2003; **111**: 1843-50. doi: 10.1289/ehp.6632
35. Osawa K. Gene polymorphisms and chemotherapy in non-small cell lung cancer. *Zhongguo Fei Ai Za Zhi* 2009; **12**: 837-40. doi: 10.3779/j.issn.1009-3419.2009.08.01
36. de las Peñas R, Sanchez-Ronco M, Alberola V, Taron M, Camps C, Garcia-Carbonero R, et al. Polymorphisms in DNA repair genes modulate survival in cisplatin/gemcitabine-treated non-small-cell lung cancer patients. *Ann Oncol* 2006; **17**(4): 668-75. doi: 10.1093/annonc/mdj135
37. Saldívar JS, Lu KH, Liang D, Gu J, Huang M, Vlastos AT, et al. Moving toward individualized therapy based on NER polymorphisms that predict platinum sensitivity in ovarian cancer patients. *Gynecol Oncol* 2007; **107**(1 Suppl 1): S223-9. doi: 10.1016/j.ygyno.2007.07.024
38. Goričar K, Kovač V, Jazbec J, Zakotnik B, Lamovec J, Dolžan V. Genetic variability of DNA repair mechanisms and glutathione-S-transferase genes influences treatment outcome in osteosarcoma. *Cancer Epidemiol* 2015; **39**: 182-8. doi: 10.1016/j.canep.2014.12.009
39. Deng JH, Deng J, Shi DH, Uuyang XN, P-G. Niu PG. Clinical outcome of cisplatin-based chemotherapy is associated with the polymorphisms of GSTP1 and XRCC1 in advanced nonsmall cell lung cancer patients. *Clin Transl Oncol* 2015; **17**: 720-6. doi: 10.1007/s12094-015-1299-6
40. Izquierdo MA, Scheffer GL, Flens MJ, Giaccone G, Broxterman HJ, Meijer CJ, et al. Broad distribution of the multidrug resistance-related vault lung resistance protein in normal human tissues and tumours. *Am J Pathol* 1996; **148**: 877-87. PMID: 8774142.
41. Sedláková I, Laco J, Caltová K, Červinka M, Tošner J, Řezáč A, et al. Clinical significance of the resistance proteins LRP, Pgp, MRP1, MRP3, and MRP5 in epithelial ovarian cancer. *Int J Gynecol Cancer* 2015; **25**(2): 236-43. doi: 10.1097/JG.C.0000000000000354
42. Zhao YN, He DN, Wang YD, Li JJ, Ha MW. Association of single nucleotide polymorphisms in the MVP gene with platinum resistance and survival in patients with epithelial ovarian cancer. *Oncol Lett* 2016; **11**(4): 2925-33. doi: 10.3892/ol.2016.4311
43. Makrilia N, Syrigou E, Kaklamanos I, Manolopoulos L, Wasif Saif M. Hypersensitivity reactions associated with platinum antineoplastic agents: a systematic review. *Metal-Based Drugs* 2010; **20**(10): 1-11. doi: 10.1155/2010/207084
44. Lafay-Cousin L, Sung L, Carret AS, Hukin J, Wilson B, Johnston DL, et al. Carboplatin hypersensitivity reaction in paediatric patients with low-grade glioma: a Canadian paediatric brain tumour consortium experience. *Cancer* 2008; **112**: 892-9. doi: 10.1002/cncr.23249
45. Markman M, Moon J, Wilczynski S, Lopez AM, Rowland KM Jr, Michelin DP, et al. Single agent carboplatin versus carboplatin plus PEGylated liposomal doxorubicin in recurrent ovarian cancer: final survival results of a SWOG (S0200) phase 3 randomized trial. *Gynecol Oncol* 2010; **116**: 323-5. doi: 10.1016/j.ygyno.2009.11.026
46. van Meerten E, Franckena M, Wiemer E, van Doorn L, Kraan J, Westermann A, et al. Phase I study of cisplatin, hyperthermia, and lapatinib in patients with recurrent carcinoma of the uterine cervix in a previously irradiated area. *Oncologist* 2015; **20**: 241-2. doi: 10.1634/theoncologist.2014-0365
47. Landon CD. Enhancing cisplatin delivery and anti-tumour efficacy using hyperthermia. [Dissertation]. Durham: Duke University; 2013.
48. Rose PG, Bundy BN, Watkins EB, Thigpen JT, Deppe G, Maiman MA, et al. Concurrent cisplatin-based radiotherapy and chemotherapy for locally advanced cervical cancer. *N Engl J Med* 1999; **340**: 3144-53. doi: 10.1056/NEJM199904153401502
49. Biston MC, Joubert A, Adam JF, Elleaume H, Bohic S, Charvet AM, et al. Cure of Fisher rats bearing radio resistant F98 glioma treated with cis-platinum and irradiated with monochromatic synchrotron X-rays. *Cancer Res* 2004; **64**: 2317-23. doi: 10.1158/0008-5472.CAN-03-3600
50. Coluccia D, Figueiredo CA, Wu MY, Riemenschneider AN, Diaz R, Luck A, et al. Enhancing glioblastoma treatment using cisplatin-gold-nanoparticle conjugates and targeted delivery with magnetic resonance-guided focused ultrasound. *Nanomedicine* 2018; **14**: 1137-48. doi: 10.1016/j.nano.2018.01.021
51. Schumann C, Chan S, Millar JA, Bortnyak Y, Carey K, Fedchyk A, et al. Intraperitoneal nanotherapy for metastatic ovarian cancer based on siRNA-mediated suppression of DJ-1 protein combined with a low dose of cisplatin. *Nanomedicine* 2018; **14**: 1395-405. doi: 10.1016/j.nano.2018.03.005
52. Setua S, Ouberai M, Piccirillo SG, Watts C, Welland M. Cisplatin-tethered gold nanospheres for multimodal chemo-radiotherapy of glioblastoma. *Nanoscale* 2014; **6**: 10865-73. doi: 10.1039/c4nr03693j
53. Shahin SA, Wang R, Simargi SI, Glackin CA. Hyaluronic acid conjugated nanoparticle delivery of siRNA against TWIST reduces tumour burden and enhances sensitivity to cisplatin in ovarian cancer. *Nanomedicine* 2017; **13**: 965-76. doi: 10.1016/j.nano.2018.04.00
54. Joybari AY, Sarbaz S, Azadeh P, Mirafsharieh SA, Rahbari A, Farasatinasab M, et al. Oxaliplatin-induced renal tubular vacuolization. *Ann Pharmacother* 2014; **4**: 796-800. doi: 10.1177/1060028014526160
55. Hellberg V, Wallin I, Eriksson S, Hernlund E, Jerremalm E, Berndtsson M, et al. Cisplatin and oxaliplatin toxicity: importance of cochlear kinetics as a determinant for ototoxicity. *J Natl Cancer Inst* 2009; **101**: 37-47. doi: 10.1093/jnci/djn418
56. Hosnedlova B, Kepinska M, Skalickova S, Fernandez C, Ruttkay-Nedecky B, Peng Q, et al. Nano-selenium and its nanomedicine applications: a critical review. *Int J Nanomedicine* 2018; **13**: 2107-28. doi: 10.2147/IJN.S157541
57. Bouliskas T, Stathopoulos GP, Volakakis N, Vougiouka M. Systemic Lipoplatin infusion results in preferential tumor uptake in human studies. *Anticancer Res* 2005; **25**: 3031-40. PMID: 16080562
58. Serinan E, Altun Z, Aktaş S, Çeçen E, Olgun N. Comparison of cisplatin with lipoplatin in terms of ototoxicity. *J Int Adv Otol* 2018; **14**: 211-5. doi: 10.5152/iao.2018.4097
59. Serša G, Čemažar M, Miklavčič D. Antitumor effectiveness of electrochemotherapy with cis-diamminedichloroplatinum(II) in mice. *Cancer Res* 1995; **55**: 3450-5. PMID: 7614485
60. Serša G, Stabuc B, Cemazar M, Miklavcic D, Rudolf Z. Electrochemotherapy with cisplatin: Clinical experience in malignant melanoma patients. *Clin Cancer Res* 2000; **6**: 863-7. PMID: 107417
61. Gehl J, Sersa G, Wichmann Matthiessen L, Muir T, Soden D, Occhini A, et al. Updated standard operating procedures for electrochemotherapy of cutaneous tumours and skin metastases. *Acta Oncol* 2018; **57**: 874-882. doi: 10.1080/0284186X.2018.1454602.
62. Kranjc S, Cemazar M, Sersa G, Scancar J, Grabner S. *In vitro* and *in vivo* evaluation of electrochemotherapy with trans-platinum analogue trans-[PtCl₂(3-Hmpy)₂]. *Radial Oncol* 2017; **51**: 295-306. doi: 10.1515/raon-2017-0034
63. Grabner S, Modec B, Bukovec N, Bukovec P, Čemažar M, Kranjc S, et al. Cytotoxic trans-platinum(II) complex with 3-hydroxymethylpyridine: Synthesis, X-ray structure and biological activity evaluation. *J Inorg Biochem* 2016; **161**: 40-51. doi: 10.1016/j.jinorgbio.2016.04.031
64. Sancho-Martínez SM, Prieto-García L, Prieto M, López-Novoa JM, López-Hernández FJ. Subcellular targets of cisplatin cytotoxicity: an integrated view. *Pharmacol Ther* 2012; **136**: 35-55. doi: 10.1016/j.pharmthera.2012.07.003
65. Rebillard A, Tekpli X, Meurette O, Sergent O, LeMoigne-Muller G, Vernhet L, et al. Cisplatin-induced apoptosis involves membrane fluidification via inhibition of NHE1 in human colon cancer cells. *Cancer Res* 2007; **67**: 7865-74. doi: 10.1158/0008-5472.CAN-07-0353
66. Bose RN, Yang WW, Evanics F. Structural perturbation of a C4 zinc-finger module by cis-diamminedichloroplatinum(II): insights into the inhibition of transcription processes by the antitumor drug. *Inorganica Chim Acta* 2005; **358**: 2844-54. doi: org/10.1016/j.ica.2004.06.052
67. Huang X, Huang R, Gou S, Wang Z, Liao Z, Wang H. Combretastatin A-4 analogue: a dual-targeting and tubulin inhibitor containing antitumor Pt(IV) moiety with a unique mode of action. *Bioconjugate Chem* 2016; **27**: 2132-48. doi: 10.1021/acs.bioconjugchem.6b00353

68. Ishikawa T, Ali-Osman F. Glutathione-associated cis-diamminedichloroplatinum(II) metabolism and ATP-dependent efflux from leukaemia cells. Molecular characterization of glutathione-platinum complex and its biological significance. *J Biol Chem* 1993; **268**: 20116-25. PMID: 8376370
69. Hostetter AA, Osborn MF, DeRose VJ. RNA-Pt adducts following cisplatin treatment of *Saccharomyces cerevisiae*. *ACS Chem Biol* 2012; **7**: 218-25. doi: 10.1021/cb200279p
70. Wolters DA, Stefanopoulou M, Dyson PJ, Groessl M. Combination of metalomics and proteomics to study the effects of the metalloid drug RAPTA-T on human cancer cells. *Metallomics* 2012; **4**: 1185-96. doi: 10.1039/c2mt20070h
71. Palermo G, Magistrato A, Riedel T, von Erlach T, Davey CA, Dyson PJ, et al. Fighting cancer with transition metal complexes: from naked DNA to protein and chromatin targeting strategies. *Chem Med Chem* 2016; **11**: 1199-210. doi: 10.1002/cmdc.201500478
72. Zou T, Lum CT, Lok CN, Zhang JJ, Che CM. Chemical biology of anticancer gold(III) and gold(I) complexes. *Chem Soc Rev* 2015; **44**: 8786-801. doi: 10.1039/c5cs00132c
73. Molter A, Kathrein S, Kircher B, Mohr F. Anti-tumour active gold(I), palladium(II) and ruthenium(II) complexes with thio- and selenoureato ligands: a comparative study. *Dalton Trans* 2018; **47**: 5055. doi: 10.1039/C7DT04180B
74. Tshuva EY, Miller M. Coordination complexes of titanium(IV) for anticancer therapy. *Met Ions Life Sci* 2018; **18**. doi: 10.1515/9783110470734-014
75. Cini M, Bradshaw TD, Woodward S. Using titanium complexes to defeat cancer: the view from the shoulders of titans. *Chem Soc Rev* 2017; **4**: 1040-51. doi: 10.1039/c6cs00860g
76. Meléndez E. Titanium complexes in cancer treatment. *Crit Rev Oncol Hematol* 2002; **42**: 309-15. doi: 10.1016/S1040-8428(01)00224-4
77. Ang DL, Gordon CP, Aldrich-Wright JR. Transition metal intercalators as anti-cancer agents - recent advances. *Int J Mol Sci* 2016; **17**: 1-17. doi: 10.3390/ijms17111818

review

Multiparametric MRI - local staging of prostate cancer and beyond

Iztok Caglic^{1,2}, Viljem Kovac^{2,3}, Tristan Barrett^{4,5}

¹ Department of Radiology, Norfolk and Norwich University Hospital, Norwich, UK

² Faculty of Medicine, University of Ljubljana, Slovenia

³ Institute of Oncology Ljubljana, Ljubljana, Slovenia

⁴ Department of Radiology, Addenbrooke's Hospital and University of Cambridge, Cambridge, UK

⁵ CamPARI Clinic, Addenbrooke's Hospital and University of Cambridge, Cambridge, UK

Radiol Oncol 2019; 53(2): 159-170.

Received 29 March 2019

Accepted 15 April 2019

Correspondence to: Assoc. Prof. Viljem Kovač, M.D., Ph.D., Institute of Oncology Ljubljana, Zaloška 2, 1000 Ljubljana, Slovenia.

Phone: +386 1 5879 117; Fax: 386 1 5879 400. E-mail: vkovac@onko-i.si

Disclosure: No potential conflicts of interest were disclosed.

Background. Accurate local staging is critical for treatment planning and prognosis in patients with prostate cancer (PCa). The primary aim is to differentiate between organ-confined and locally advanced disease with the latter carrying a worse clinical prognosis. Multiparametric MRI (mpMRI) is the imaging modality of choice for the local staging of PCa and has an incremental value in assessing pelvic nodal disease and bone involvement. It has shown superior performance compared to traditional staging based on clinical nomograms, and provides additional information on the site and extent of disease. MRI has a high specificity for diagnosing extracapsular extension (ECE), seminal vesicle invasion (SVI) and lymph node (LN) metastases, however, sensitivity remains poor. As a result, extended pelvic LN dissection remains the gold standard for assessing pelvic nodal involvement, and there has been recent progress in developing advanced imaging techniques for more distal staging.

Conclusions. T2W-weighted imaging is the cornerstone for local staging of PCa. Imaging at 3T and incorporating both diffusion weighted and dynamic contrast enhanced imaging can further increase accuracy. "Next generation" imaging including whole body MRI and PET-MRI imaging using prostate specific membrane antigen (⁶⁸Ga-PSMA), has shown promising for assessment of LN and bone involvement as compared to the traditional work-up using bone scintigraphy and body CT.

Key words: multiparametric MRI; prostate cancer; staging

Introduction

Accurate staging of prostate cancer is essential to inform prognosis and to stratify patients for appropriate management. MRI affords excellent soft tissue differentiation making it the most accurate modality for preoperative local T-staging of prostate cancer.¹ According to European Association of Urology (EAU) guidelines, local staging investigations are only indicated for intermediate and high-risk patient groups.¹ The high accuracy of multiparametric MRI (mpMRI) for detection of index lesions can aid T-staging, and can also identify tumours

that may be missed by systematic biopsies, enabling early re-biopsy and accurate risk stratification.²

For the purposes of prognosis and management the primary aim is to differentiate organ-confined disease from locally advanced disease. Extracapsular disease and seminal vesicle invasion carry a worse prognosis due to a greater risk of positive surgical margins leading to biochemical recurrence^{3,4} and an increased risk of lymph node (LN) metastases, respectively.⁵ Nodal disease on its own is associated with a higher risk of progression to metastatic disease and thus a higher rate of cancer specific mortality.⁶⁻⁸

Traditionally, staging of prostate cancer has been performed using nomograms such as Partin tables which are based on digital rectal examination (DRE), prostate-specific antigen (PSA) levels, Gleason score and percentage core involvement as a surrogate of lesion volume.⁹⁻¹¹ This approach often underestimates the true stage of the disease and has been shown to be inferior to MRI¹², with the combination of MRI findings and nomograms showing significant added value for predicting adverse pathology in prostate cancer.¹³ In addition to improving accuracy, MRI also provides information on the site and extent of disease, which helps surgical planning, informing decision making on taking wider surgical margins to decrease the rate of positive margins, or performing nerve-sparing surgery to decrease morbidity. In case of a gross extracapsular extension or seminal vesicle invasion on MRI, external beam radiotherapy is a recom-

mended approach over brachytherapy or surgery, to avoid under dosing or positive surgical margins, respectively.¹⁴ As MR imaging currently does not offer sufficient diagnostic performance, extended pelvic lymph node dissection (ePLND) remains the gold standard for N-staging.¹ However, ePLND has its own disadvantages including higher morbidity, with worse intraoperative and perioperative outcomes, and may result in under-sampling, thus its direct therapeutic effect is equivocal.¹⁵

This review aims to summarize the role of MRI in staging prostate cancer and focuses mainly on exploring the current evidence and providing a practical approach to assessment of extracapsular extension, seminal vesicle invasion and nodal disease.

Staging of prostate cancer

The most widely used system for staging of prostate cancer is the tumour, nodes, and metastases (TNM) staging system developed by the American Joint Committee on Cancer (AJCC). The current version of the TNM staging of prostate cancer (8th edition) was implemented in January 2018 introducing grade groups and simplifying organ-confined disease to pathological stage pT2 and omitting pT2a–pT2c, however, this sub-classification is retained for clinical staging (Table 1).¹⁶ In addition, Cancer-group staging of prostate cancer (stage I–IV) is determined by TNM, PSA levels at diagnosis, and histologic Grade Groups.¹⁷

Locally confined disease (T1–T2) is further divided into stage T1a and T1b tumours which are not apparent clinically and are found incidentally, typically at transurethral resection. From the radiological standpoint, the more relevant categories are stage T1c and T2 (a–c) as histologically they both represent a biopsy proven carcinoma albeit with an important difference: T1c cancer is by definition not visualised at MRI. This is relevant to active surveillance studies (AS) cohorts, with the term “non-visible lesion” (T1c) being introduced, based on the predictive nature of this feature, with a significantly increased progression free survival for non-visible lesions when compared with the MRI-visible lesions (T2).¹⁸

Locally advanced prostate cancer carries a worse prognosis than organ-confined disease. T3a disease describes extraprostatic extension, T3b seminal vesicle invasion, and T4 disease direct invasion of adjacent organs/structures (Table 1). In clinical practice those undergoing prostate mpMRI will

TABLE 1. Summary of TNM guidelines for the staging of prostate cancer

Category	Definition
Tumour	
Tx	Primary tumour cannot be assessed (e.g. CT study, severe artefacts on MRI)
T1a–T1b	Tumour incidental histologic finding
T1c	Tumour identified by needle biopsy but not visible by imaging
T2	Organ confined disease
T2a	The tumour involves up to one half of 1 side of the prostate
T2b	The tumour involves more than one half of 1 side of the prostate
T2c	The tumour involves both sides of the prostate
T3	Extraprostatic extension
T3a	Extraprostatic extension (unilateral or bilateral) or microscopic invasion of the bladder neck
T3b	Tumour invades seminal vesicle(s)
T4	Tumour invades adjacent structures other than seminal vesicles, such as external sphincter, rectum, bladder, levator muscles, and/or pelvic wall
Node	
Nx	Regional lymph nodes were not assessed
N0	No positive regional lymph nodes
N1	Metastases in regional lymph node(s)
Metastasis	
Mx	M staging not assessed (e.g. MRI with pelvic only coverage)
M0	No distant metastasis
M1	Distant metastasis
M1a	Nonregional lymph node(s)
M1b	Bones
M1c	Other site(s) with or without bone disease

have at least one sequence where the field of view covers the pelvis to the level of aortic bifurcation¹⁹ in order to evaluate the common iliac and bifurcation nodes (M1a) and from which partial M staging of the bony pelvis (M1b) can be performed.

MR imaging

MRI scanners

The Prostate Imaging-Reporting and Data System (PI-RADS) guidelines¹⁹ are aimed at standardizing MRI acquisition and interpretation and recommend MRI to be performed at 3T in order to increase signal-to-noise ratio (SNR) and spatial resolution, and decrease acquisition times.^{20,21} If acquisition protocols are optimized and contemporary technology is employed, then 1.5T scanners are also able to provide sufficient diagnostic performance. 1.5T scanning may also be preferential when a patient has an implant non-compatible at higher field strengths, or with bilateral hip replacements in order to minimise artefact.^{22,23} The routine use of an endorectal coil (ERC) is no longer recommended.¹⁹ 3T scanners or contemporary 1.5T scanners can provide sufficient imaging quality and although ERC increases SNR bring disadvantages, including deformation of the gland contour, near field coil flare, increased cost and time of examination as well as higher patient discomfort.^{19,21}

MRI protocol

Standard prostate MRI protocols should incorporate anatomical T1W and T2W imaging in combination with the two functional sequences of diffusion weighted imaging (DWI) and dynamic contrast enhanced imaging (DCE).²⁴ A set of minimal technical parameters for each of these sequences is outlined in Table 2²⁵, although institutions are encouraged to optimize imaging protocols based on their own equipment, capacity and expertise. It is mandatory for axial T2W, DWI and DCE to be acquired in the same location, angle, slice thickness and gap to allow for synchronous scrolling through the images and direct evaluation of suspicious findings between the sequences. Axial T1W1 is essential to assess post-biopsy haemorrhage, and is typically employed as the sequence to cover the pelvis to the aortic bifurcation to enable bone and nodal assessment.

T2W imaging is the key sequence for local T-staging of the prostate. The high in-plane spatial resolution allows for accurate evaluation of extra-

TABLE 2. PI-RADS v2.1 recommended MR imaging protocols

Imaging sequence	Technical parameters
T2 imaging	Axial plane and a minimum of one additional orthogonal plane (either sagittal or coronal) Straight axial plane to the patient or to the long axis of the prostate FOV: 12-20 cm to image the entire prostate gland and seminal vesicles Section thickness/gap: 3 mm/0 mm In-plane resolution: ≤ 0.7 mm (phase) x ≤ 0.4 mm (frequency)
DW imaging	Axial plane (same locations as for T2WI) Free-breathing spin echo EPI sequence combined with spectral fat saturation is recommended Section thickness/gap: 3 mm/0 mm TE: ≤ 90 ms; TR: > 3000 ms FOV: 16-22 cm In plane dimension: ≤ 2.5 mm phase and frequency ADC map calculation: low b-value should be set at 0–100 s/mm ² , high b-value should be < 1000 s/mm ² "High b-value": b-value of ≥ 1400 sec/mm ² ; it can be acquired by scanning or calculated
DCE	Axial plane (same locations as for T2WI) Fat suppression and/or subtraction is recommended 2D or 3D T1 GRE sequence (preferred) Section thickness/gap: 3 mm/0 mm Injection rate: 2-3 ml/s TR/TE: < 100 ms/ < 5 ms In-plane dimension: ≤ 2 mm X ≤ 2 mm Temporal resolution: ≤ 15 s Total observation: > 2 min

2D = two-dimensional; 3D = three-dimensional; ADC = apparent diffusion coefficient; EPI = echo planar imaging; DW = diffusion weighted; FOV = field of view; GRE = gradient echo T2W = T2 weighted; TE = echo time; TR = repetition time

capsular extension, neurovascular bundle assessment and seminal vesicle invasion. Fast-spin-echo (FSE) or turbo-spin-echo (TSE) imaging should be obtained in the axial plane and in at least one additional orthogonal plane (sagittal or coronal) with the highest quality possible and thin slices at 3 mm with no gap.²⁵ 3D T2 weighted imaging with isotropic voxels and slice thickness at 1 mm may be obtained, with evidence suggesting utility for assessment of extraprostatic extension²⁶ and for nodal and bone staging when combined with DWI of the entire pelvis (b-values 0–1000 s/mm²).²⁷

Limitations

Motion artefact. Bowel peristalsis is a well-known cause of motion artefact in abdominal imaging,

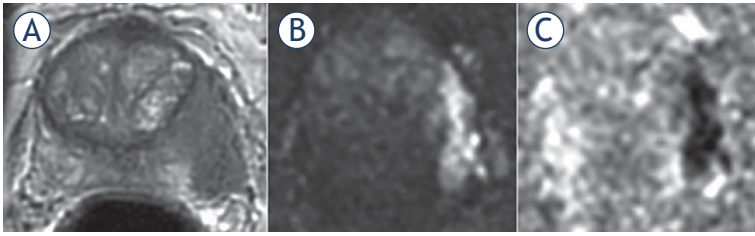


FIGURE 1. 65-yr-old man with PSA 19.5 ng/ml. Invasion of the periprostatic fat and neurovascular bundle (NVB) infiltration at the left midgland consistent with T3a disease. Biopsy showed Gleason score (GS) 4 + 4 = 8. Radical retropubic prostatectomy (RRP) confirmed GS 4 + 4 = 8 and showed established T3a disease with a clear surgical margin (at least 1 mm).

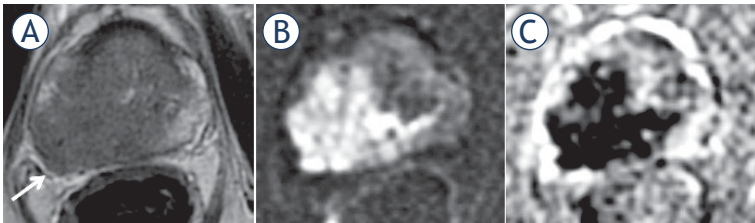


FIGURE 2. 77-yr-old man with PSA 38.2 ng/ml. (A) T2 weighted (T2W) imaging; (B) diffusion weighted (DW) imaging; (C) apparent diffusion coefficient (ADC) map. T3a at the right mid gland with bulging and asymmetrical thickening of the right neurovascular bundle (arrow). Gleason score (GS) = 9 with extracapsular extension and clear surgical margins was confirmed at radical prostatectomy.

but the relatively low position of the prostate, remote from small bowel combined with limited evidence prior to PIRADS version 2 means that anti-spasmodic agents are not recommended in current guidelines. However, recent studies have shown use of anti-peristaltic agents significantly improves image quality of T2W imaging^{28, 29} with better depiction of anatomical details (e.g. prostatic capsule and neurovascular bundles) as well as reducing non-diagnostic MRI to < 1%.²⁹ Routine use of antiperistaltic agents (recommended dose 20 mg HBB *i.v.* or 1 mg glucagon) prior to prostate mp-

TABLE 3. PI-RADS v2 criteria for predicting extraprostatic extension

Capsular abutment
Capsular irregularity, spiculation or retraction
Neurovascular bundle asymmetry or thickening
Obliteration of the rectoprostatic angle
Tumour-capsular contact > 10 mm
Bulge or loss of capsule
Measurable extracapsular disease

MRI may therefore be beneficial for optimisation of T2W image quality, a key sequence of mpMRI for local staging.³⁰ The risk of side-effects with these agents is low and these are usually minor and self-limiting.³¹

T-staging

T3a disease

Extension of the tumour into the periprostatic fat is defined as T3a disease, termed extracapsular extension (ECE). Of note, however, in a strict sense the prostate lacks a true capsule as an anatomic structure that encloses the gland but has rather an outer fibromuscular layer which is inseparable component of the prostatic stroma.^{32,33} T3a disease also incorporates invasion into the neurovascular bundle, internal sphincter and bladder neck.¹ Histopathologically, extracapsular extension (ECE) is sub-classified into focal and established with the latter carrying a worse prognosis.³⁴ However, there is currently no clear consensus on the exact definitions of these, which can vary from a few glands beyond the capsule to cancer extending up to 0.5 mm radially from the capsule.¹ In addition, focal ECE cannot be detected by MRI due to inherent resolution limits.³⁵

Extracapsular extension has traditionally been evaluated by clinical criteria and nomograms such as Partin tables, which are based on PSA, DRE and Gleason score at biopsy.³⁶ However, nomograms represent a patient level risk score alone, have been shown to be inferior to MRI^{11,37}, and unlike MRI offer no information on location and extent of ECE. A meta-analysis by de Rooij *et al.* in 2016 showed MRI to have a high specificity of 91% but only moderate sensitivity at 57% in diagnosing ECE. Of note, this analysis included studies with both uni- and multiparametric protocols at both 1.5T and 3T, and sub-analysis of 3T studies improved overall performance with specificity 86% and sensitivity 68%.³⁸ The main reasons for improvement being higher spatial resolution at 3T and improved lesion identification with a multiparametric approach, allowing interrogation of the capsule and neurovascular bundle in the adjacent region (Figure 2).³⁹

Several approaches have been proposed and explored in order to increase diagnostic accuracy for the evaluation of ECE. Prostate imaging-reporting and data system (PI-RADS) guidelines recommends various morphologic criteria (Table 3).¹⁹ These have been evaluated and demonstrated sensitivity and specificity between 60%–81% and

75%–78%, respectively, and showed moderate inter-reader agreement ($K = 0.45$) for the prediction of T3a disease.^{40,41}

In addition, the length of tumour contact with the capsule at MRI (Figure 3) has also been shown to be a strong predictor of ECE^{35,42,43} with good to excellent inter-reader agreement^{26,35} (Figure 3).^{26,35} However, a reliable threshold is yet to be established, with reported rates varying from 6–20 mm, the PI-RADS v2 guidelines recommend an arbitrary threshold of 10 mm¹⁹, which pre-dates many of these studies. The reason for variability is likely multifactorial with different methodology employed and variations in scanner strength, vendor and protocols. For instance, Rosenkrantz *et al.* measured the length in a linear rather than curvilinear fashion which likely explains their lower reported threshold of 6 mm.³⁵ In addition, a more recent study suggests that thresholds differ between low- (Grade Group 1–2) and high-grade (Grade Group 3–5) cancers, with the former having a positive predictive values (PPV) of 90.4% for ECE at 12.5 mm and the optimal cut-off for the latter being 5 mm.²⁶ This finding was further confirmed by Matsuoka *et al.* who reported significantly increased upstaging in low- versus high-grade cancers when the same threshold (10 mm) was applied.⁴⁴ Given that lower apparent diffusion coefficient (ADC) values in prostate cancer correlate with higher Gleason score^{45,46}, this could potentially be exploited as an adjunct for more accurate diagnosis of T3a disease prior to biopsy results. To date however, there have been mixed results when applying ADC values for stage assessment, which may relate to difficulties in applying uniform quantitative values.^{39,47–50}

Another potential approach to improve sensitivity is utilisation of an isovolumetric 3D T2 imaging sequence to acquire thinner slices with less partial voluming and reformatting of isotropic images in multiple planes. Studies using 3D-T2 sequence have reported encouraging results with sensitivity and specificity ranging from 58.3%–84% and 73.1%–89%, respectively.^{44,51–53} In addition, Caglic *et al.* proposed a new criterion of 3D Contact which significantly improved detection of ECE (sensitivity, specificity: 73.7% and 87.8%) when compared to the length of capsular contact measured on conventional T2 imaging in axial plane (sensitivity, specificity: 59.6%, 87.8%).²⁶ This approach exploited the reduced partial voluming due to thinner slices (Figure 4) and reconstruction of images in multiple planes in order to measure the more representative a truer length of capsular contact. Although not supported by work of Jäderling *et*

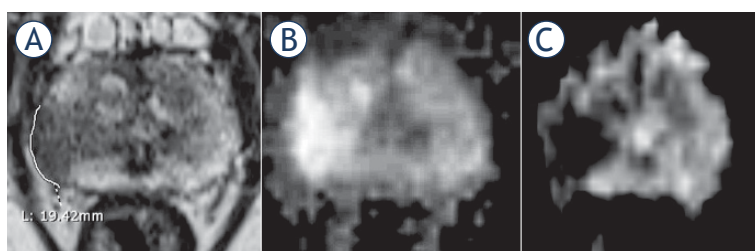


FIGURE 3. 74-yr-old man with PSA 35.2 ng/ml. (A) T2 weighted (T2W) imaging, (B) diffusion weighted (DW) imaging, (C) apparent diffusion coefficient (ADC) map. T3a at the right mid gland as suggested by a broad capsular contact at 19.4 mm. Biopsy showed Gleason score (GS) 4 + 4 = 8 disease. Patient underwent radiotherapy.

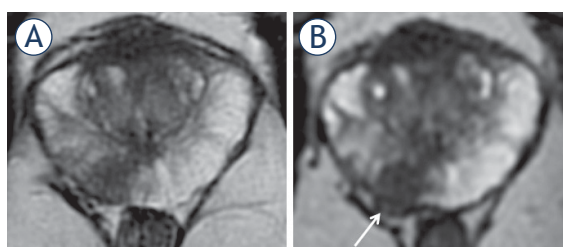


FIGURE 4. 57-yr-old man with PSA 26 ng/ml. (A) Axial T2 weighted imaging (T2WI) shows mid gland right peripheral zones (PZ) lesion (arrow) with capsular contact but no tumour extension beyond it. (B) axial thin-sliced cube reformat suggests capsular breach and right neurovascular bundle involvement (arrow). Prostatectomy showed tumour in the right mid gland, Gleason score 4 + 5 = 9, with established extracapsular extension (ECE) (pT3a).

al. using 3D-T2 reconstructions, it should be noted that their analysis was based on morphological criteria and not on quantifying capsular contact.⁵⁴

Although diagnostic accuracy for early ECE is improving, sensitivity remains relatively poor, and it should be noted that these results come from experienced centres, utilizing modern equipment and optimised protocols. As a result, equivocal MRI findings should not change the planned treatment course, but rather ensure discussion between radiologists and urologists at multidisciplinary meetings on a case-by-case basis. Practical advice would be to flag indeterminate features of ECE, to allow wider surgical margins to be taken in the corresponding region.¹⁰ Furthermore, reporting the exact location of T3a disease is important, as clear margins are harder to obtain at the apex whereas tumours remote from the neurovascular bundle (NVB) such as in the anterior location will allow nerve sparing surgery and reduce resultant morbidity from urinary incontinence or erectile dysfunction.

T3b disease

T3b disease is defined as involvement of one or both seminal vesicles (SV) by prostate cancer, with the prevalence of SV invasion in surgical series being reported at 4–23%.^{55,56} Patients with T3b disease carry an increased risk of lymph node involvement, local recurrence and distant metastases⁵⁷, making preoperative identification of SV involvement an important factor for prognosis and treatment planning. Patients with T3b disease are typically not offered radical prostatectomy or brachytherapy unless as part of a multimodal approach, and are usually offered external beam radiotherapy (EBRT) and androgen deprivation therapy (ADT).

MRI has been shown to outperform clinical risk assessment tools such as Kattan nomogram and Partin tables in predicting SV involvement^{13,58}, with meta-analyses showing moderate sensitivity of 73% and specificity of 95% for multiparametric MRI studies at 3T.³⁸ Recent work by Grivas *et al.* including 527 patients at 3T mpMRI achieved similar results with sensitivity, specificity, PPV and negative predictive values (NPV) at 75.9%, 94.7%, 62% and 97%, respectively.⁵⁹

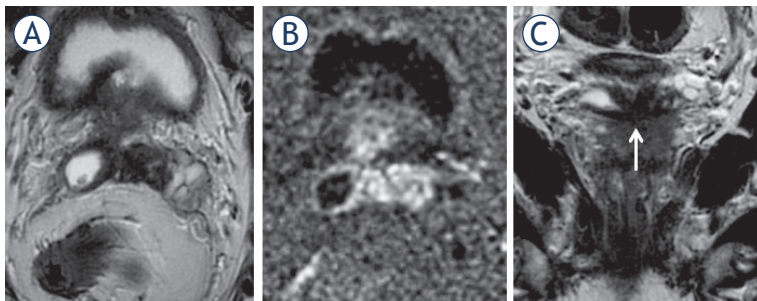


FIGURE 5. 65-yr-old-man with PSA = 15.3 ng/ml and Gleason score 4 + 4 = 8 at biopsy. Axial (A) and coronal (C) T2 weighted imaging (T2WI) and diffusion weighted imaging (DWI) (B). T3b involving both seminal vesicles via ejaculatory ducts, shown in the coronal plane (arrow).

Histopathologically, SV invasion is defined as prostate cancer penetrating the SV muscular wall, with tumour involving the extraprostatic portion of the vesicles rather than the intraprostatic ejaculatory ducts.⁵⁷ Three routes of invasion have been described, Type I: direct spread via the ejaculatory duct complex (Figure 5), Type II: extracapsular spread of disease with invasion via the outer seminal vesicle wall and type III: metastatic involvement from a remote intraprostatic lesion (Figure 6). The first two types individually or in combination account for more than 95% of cases, with type III spread being extremely rare.^{60,61}

Seminal vesicles are best evaluated on T2W imaging in combination with functional imaging. Coronal or sagittal reformats are especially useful in demonstrating the type of spread. In Type I invasion, invasion *via* the erectile dysfunction (ED) causes SV expansion with a low signal intraluminal mass and may cause diffuse or focal wall thickening. In Type II involvement, there is obliteration of the angle between the base of the prostate and SV.⁶⁰ In addition, in 2009 Jung *et al.* proposed a novel six-tier classification system for SV invasion based on morphological appearance of SV on T2W imaging (Class 0 = normal SV appearance, Class 5 = apparent mass lesion with destructive architecture) showing sensitivity and specificity of 71.4 and 96.6%, respectively.⁶² More recent work incorporating functional sequences has further increased accuracy, with DWI proving to be of more incremental value than DCE.^{56,63}

There are known pitfalls to be aware of when assessing for SV involvement, such as diffuse wall thickening due to SV atrophy or asymmetry. In addition, there can be large variation with a mean right - left asymmetry of 20% and surgical series suggesting SV length between sides can vary up to 9-fold.⁶⁴ Post-biopsy haemorrhage can mimic the low T2 signal of prostate cancer and review

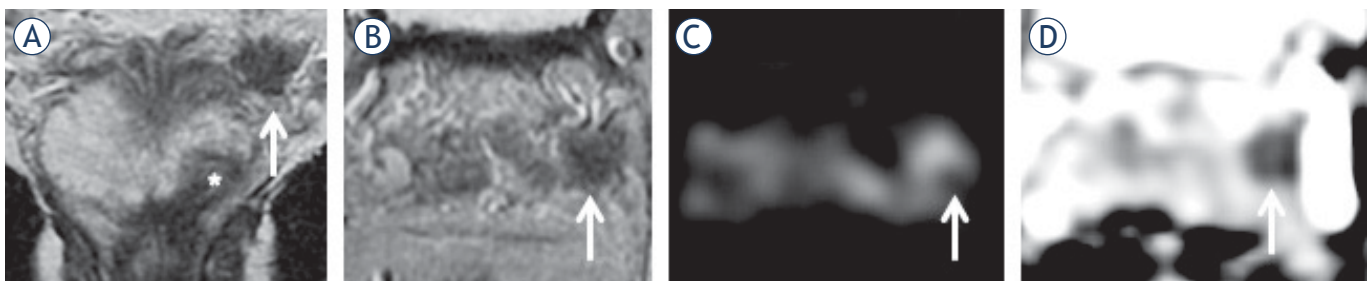


FIGURE 6. 67-yr-old man with raising PSA = 12.7 ng/ml. (A) (coronal) and (B) (axial) T2 weighted (T2W) imaging shows index lesion in the left apex (*) and a low signal focus in the left seminal vesicle (arrow) with corresponding restricted diffusion on diffusion weighted imaging (DWI) ((C); arrow) and apparent diffusion coefficient (ADC) map ((D); arrow).

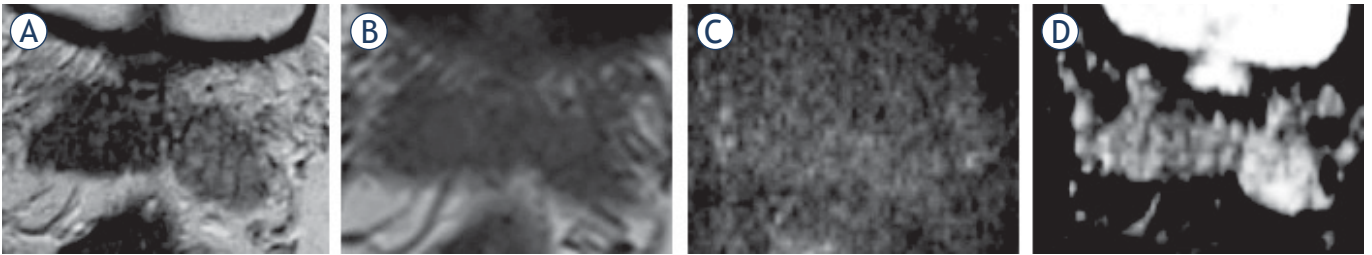


FIGURE 7. 55-yr-old-man with PSA 32 ng/ml. (A) T2 weighted (T2W) imaging, (B) T1 weighted (T1W) imaging, (C) diffusion weighted (DW) imaging, (D) apparent diffusion coefficient (ADC) map. Low T2 signal in the right seminal vesicle is mimicking prostate cancer (D), however, there is no restricted diffusion. Biopsy of the right seminal vesicle showed amyloidosis which was confirmed at radical prostatectomy. Index tumour with Gleason score 4 + 3 = 7 was in the left peripheral zone.

of T1W imaging for high signal within the SV is therefore essential. Another important mimic of prostate cancer is amyloidosis which exhibits low T2 signal but does not show diffusion restriction (Figure 7). In cases with equivocal SV findings on prebiopsy MRI, patients can undergo subsequent targeted biopsy in order to correctly stage the disease (Figure 7).⁶⁵

Although PI-RADS v2 does not recommend abstinence from ejaculation prior to prostate mpMRI¹⁹, some centres require patients to refrain from ejaculation prior to imaging in order to achieve maximal distension. Recent studies suggest 72 hours abstinence as the recommended interval to achieve maximal seminal vesicle distension.⁶⁶⁻⁶⁹ This may be beneficial in evaluation of seminal vesicle invasion but further prospective studies including patients with prostate cancer are required to determine the effect on local staging accuracy.

N-Staging

EAU guidelines recommend N-staging should be performed on prebiopsy MRI in patients from all risk groups.¹ This is in line with PI-RADS v2 guidelines which recommend that the prostate MRI protocol, which is primarily aimed at evaluating gland-confined and locally advanced disease, should also incorporate an additional sequence for the purpose of pelvic nodal staging from the level of aortic bifurcation.²⁴ PCa spreads primarily to four pelvic nodal stations, considered regional nodes: the obturator, internal and external iliac and presacral LNs. Involvement of any regional node is classified as N1 stage, whilst involvement of non-regional stations (para-aortic or paracaval LNs) represents M1a disease.^{17,70} Nodal mapping studies have shown that approximately 75% of pelvic nodal metastases are distributed between the ob-

turator fossa, internal and external iliac chain and the remaining 25% between the presacral, common iliac or aortic bifurcation group.^{71,72}

MRI has traditionally relied on size and morphological criteria in LN assessment including an enlarged size (> 8 mm), loss of fatty hilum, rounded shape, low T2W signal similar to primary tumour, or an irregular border. This is of limited diagnostic accuracy mainly due to low sensitivity, with a meta-analysis from 2008 incorporating anatomical imaging studies alone (T2W and T1W) reporting a sensitivity of only 39% (specificity 82%).⁷³ Size criteria in isolation is unhelpful, with a recent study showing the majority (68%) of metastatic nodes to have a short axis diameter < 5 mm.²⁷ More recent studies have tried to establish whether an ADC threshold can be applied for discrimination of benign from malignant LNs.^{27,74-78} Although malignant LNs typically exhibit lower ADC values, there is significant overlap between normal and pathological LNs as well as large variation in the reported thresholds, limiting the value of quantitative ADC measures at an individual patient level.⁷⁹ Reasons for poor discrimination include micro metastasis being unlikely to lower the overall ADC value of a node, whilst some benign conditions (lipomatosis, sinus histiocytosis, and follicular hyperplasia)²⁷ as well as inflammation (sarcoidosis and catch scratch disease) can also result in restricted diffusion within LNs.^{80,81} In addition, reproducibility of ADC measurements in small structures such as LNs may be insufficient and differences in acquisition protocols between centres further inhibits establishment of an absolute threshold.⁸²⁻⁸⁵ Consequently, some studies have focused on qualitative assessment of DWI using high b-value imaging in combination with anatomical T2W and reported improved performance with sensitivities of 55–73% and specificities of 86–90%.^{27,86} Normal LNs have an inherent relatively long T2 relaxation time and will there-

fore appear as high signal intensity structures on high b-value imaging (Figure 8), which is especially useful in depicting LNs as a “nodal map” when these do not meet size criteria. Detected nodes should then be carefully evaluated on T2W imaging in order to avoid false positive results due to structures which also appear bright on high b-value DWI (bowel mucosa, vessels, nerves)⁸⁷ and to assess morphological features of malignancy.

Current diagnostic performance of MRI in nodal staging is sub-optimal, thus ePLND remains the gold standard. Due to the limited sensitivity (high false negative rate) of MRI, negative findings should not deter surgeons from performing lymphadenectomy in patients with a high clinical risk for LN involvement. Conversely, the specificity of MRI is high (low false positive rate) and LNs considered to be suspicious at MRI warrant resection.

Further work and development of imaging techniques with a high diagnostic performance is needed in order to more efficiently and less invasively identify patients with metastatic LNs. Initial clinical trials with prostate specific membrane antigen (⁶⁸Ga-PSMA) PET-MRI have shown promising results for detection of LN metastases^{88,89}, resulting in change of treatment (either to systemic treat-

ment or active surveillance) in approximately one third of patients.⁹⁰ MR lymphangiography (MRL) with ultra-small superparamagnetic iron oxide (USPIO) has also demonstrated encouraging results with studies reporting sensitivity of 65–100% and specificity of 93–100% on a per patient basis.^{91–93} However, USPIO is currently not licenced for general clinical use, with only the Netherlands producing it (commercially known as Combidex) and licensing it mainly for the research purposes in patients with PCa.⁹⁴

M-Staging

EAU guidelines recommend staging for metastatic disease (M1a–M1c) in patients with unfavourable intermediate (International Society of Urological Pathology [ISUP] grade group 3) or high-risk (ISUP grade group 4–5) disease.¹ Current guidelines recommend evaluation of non-regional LNs and visceral metastases (M1a and M1c disease, respectively) by CT abdomen/pelvis imaging, combined with bone scintigraphy (BS) for evaluation of bone metastases (M1b disease) (Figure 9).⁹⁵

Several studies have shown MRI (either whole-body MRI or axial skeleton only MRI) to significantly outperform BS for assessment of M1b disease, with a thorough meta-analysis from 2014 reporting MRI sensitivity and specificity to be 97% and 95% compared to BS at 79% and 82%, respectively.⁹⁶ MRI is not incorporated into current guidelines mainly due to its limited availability and lower cost effectiveness.⁹⁶ However, over the last decade whole body MRI (WB-MRI) has been gradually gaining attention due to its ability to detect bone marrow infiltration by malignant cells before bone remodelling occurs and therefore becomes visible on BS.⁹⁷ The METastasis Reporting and Data System for Prostate (MET-RADS-P) is aimed at practical guidance for acquisition, interpretation, and reporting of WB-MRI in advanced prostate cancer.⁹⁸ The recommended protocol consists of a combination of anatomical and functional sequences (T1W, short tau inversion recovery [STIR] or fat suppressed T2W and DW imaging). Bone metastases appear as low signal on T1W imaging, bright on STIR or fat suppressed T2W and with restricted diffusion. Beside bone assessment, WB-MRI can also provide N-staging and assess for involvement of visceral organs.^{99,100} Whilst the diagnostic potential of WB-MRI is promising, there are barriers to widespread adoption, including additional coils required, increased scanning time, the

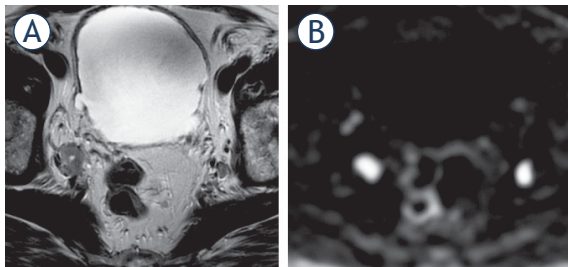


FIGURE 8. 77-yr-old man with PSA = 38.2 ng/ml. Enlarged nodes bilaterally consistent with metastatic involvement on T2 weighted imaging (T2WI) (A), more conspicuous on diffusion weighted imaging (DWI) (B).

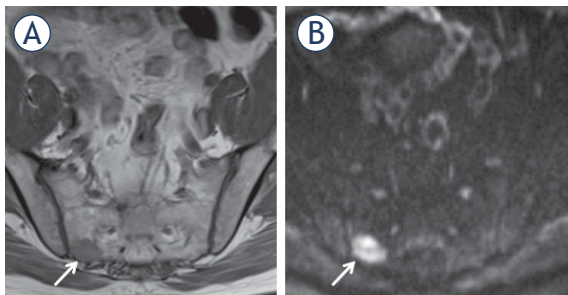


FIGURE 9. 61-yr-old man with PSA = 12.7 ng/ml. Bone metastasis (arrow) in the right sacrum shown as low signal on T1 weighted (T1W) imaging (A); more conspicuous as high signal on diffusion weighted imaging (DWI) (B).

need for sub-specialised knowledge, and increased reporting time. A recent study from 2018 by Larbi *et al.* has shown a possible means of overcoming some of these disadvantages by demonstrating that the combination of either T1-DWI or T1-STIR is non-inferior to a full protocol (Figure 9), whilst at the same time showing good interobserver agreement.¹⁰¹

Conclusions

MpMRI is the recommended modality for the local staging of prostate cancer. It has shown superior performance compared to traditional staging based on clinical nomograms, and provides additional information on the site and extent of disease. T2W-weighted imaging remains the cornerstone for ECE and SV invasion assessment, however, improved accuracy can be achieved by scanning on 3T devices with the incorporation of diffusion weighted and dynamic contrast enhanced imaging. Whilst its role in nodal and bone staging outside academic centres is currently limited, there are emerging “next generation” imaging modalities including ⁶⁸Ga-PSMA-PET/MRI and whole-body MRI offer potential to become the future standard of care for evaluation, having shown superior results for distal staging in comparison to the traditional work-up with bone scintigraphy and body CT. Despite the advantages of mpMRI there remain limitations which should be known to radiologists and other members of the multidisciplinary team in order to jointly decide on the best treatment options for prostate cancer patients on an individual basis.

Acknowledgements

The authors acknowledge grant support from the Evelyn Trust UK and research support from Cancer Research UK, National Institute of Health Research Cambridge Biomedical Research Centre, Cancer Research UK and the Engineering and Physical Sciences Research Council Imaging Centre in Cambridge and Manchester and the Cambridge Experimental Cancer Medicine Centre.

References

- Mottet N, van den Bergh RCN, Briers E, Bourke L, Cornford P, De Santis M, et al. EAU - ESTRO - ESUR - SIOG guidelines on prostate cancer 2018. In: *European Association of Urology guidelines 2018 Edition*. Arnhem, The Netherlands: European Association of Urology Guidelines Office; 2018.
- Brizomohun Appayya M, Adsheed J, Ahmed HU, Allen C, Bainbridge A, Barrett T, et al. National implementation of multi-parametric magnetic resonance imaging for prostate cancer detection - recommendations from a UK consensus meeting. *BJU Int* 2018; **122**: 13-25. doi: 10.1111/bju.14361
- Swanson GP, Riggs M, Hermans M. Pathologic findings at radical prostatectomy: risk factors for failure and death. *Urol Oncol* 2007; **25**: 110-4. doi: 10.1016/j.urolonc.2006.06.003
- Godoy G, Tareen BU, Lepor H. Site of positive surgical margins influences biochemical recurrence after radical prostatectomy. *BJU Int* 2009; **104**: 1610-4. doi: 10.1111/j.1464-410X.2009.08688.x
- Epstein JI, Partin AW, Potter SR, Walsh PC. Adenocarcinoma of the prostate invading the seminal vesicle: prognostic stratification based on pathologic parameters. *Urology* 2000; **56**: 283-8. doi: 10.1016/S0090-4295(00)00640-3
- Cagiannos I, Karakiewicz P, Eastham JA, Ohori M, Rabbani F, Gerigk C, et al. A preoperative nomogram identifying decreased risk of positive pelvic lymph nodes in patients with prostate cancer. *J Urol* 2003; **170**: 1798-803. doi: 10.1097/01.ju.0000091805.98960.13
- Gervasi LA, Mata J, Easley JD, Wilbanks JH, Seale-Hawkins C, Carlton CE, et al. Prognostic significance of lymph nodal metastases in prostate cancer. *J Urol* 1989; **142**: (2 Part 1)332-6. doi: 10.1016/S0022-5347(17)38748-7
- Eggerer SE, Scardino PT, Walsh PC, Han M, Partin AW, Trock BJ, et al. Predicting 15-year prostate cancer specific mortality after radical prostatectomy. *J Urol* 2011; **185**: 869-75. doi: 10.1016/j.juro.2010.10.057
- Morlacco A, Sharma V, Viers BR, Rangel LJ, Carlson RE, Froemming AT, et al. The incremental role of magnetic resonance imaging for prostate cancer staging before radical prostatectomy. *Eur Urol* 2017; **71**: 701-4. doi: 10.1016/j.eururo.2016.08.015
- Ward JF, Slezak JM, Blute ML, Bergstralh EJ, Zincke H. Radical prostatectomy for clinically advanced (cT3) prostate cancer since the advent of prostate-specific antigen testing: 15-year outcome. *BJU Int* 2005; **95**: 751-6. doi: 10.1111/j.1464-410X.2005.05394.x
- Augustin H, Fritz GA, Ehammer T, Auprich M, Pummer K. Accuracy of 3-Tesla magnetic resonance imaging for the staging of prostate cancer in comparison to the partin tables. *Acta Radiol* 2009; **50**: 562-9. doi: 10.1080/02841850902889846
- Gupta RT, Faridi KF, Singh AA, Passoni NM, Garcia-Reyes K, Madden JF, et al. Comparing 3-T multiparametric MRI and the Partin tables to predict organ-confined prostate cancer after radical prostatectomy. *Urol Oncol Semin Orig Investig* 2014; **32**: 1292-9. doi: 10.1016/j.urolonc.2014.04.017
- Rayn KN, Bloom JB, Gold SA, Hale GR, Baiocco JA, Mehrilvand S, et al. Added value of multiparametric magnetic resonance imaging to clinical nomograms for predicting adverse pathology in prostate cancer. *J Urol* 2018; **200**: 1041-7. doi: 10.1016/j.juro.2018.05.094
- Boehmer D, Maingon P, Poortmans P, Baron M-H, Miralbell R, Remouchamps V, et al. Guidelines for primary radiotherapy of patients with prostate cancer. *Radiother Oncol* 2006; **79**: 259-69. doi: 10.1016/j.radonc.2006.05.012
- Mottet N, van der Poel HG, Rouvière O, Matveev VB, Schoots IG, Briers E, et al. The benefits and harms of different extents of lymph node dissection during radical prostatectomy for prostate cancer: a systematic review. *Eur Urol* 2017; **72**: 84-109. doi: 10.1016/j.eururo.2016.12.003
- Buyyounouski MK, Choyke PL, McKenney JK, Sartor O, Sandler HM, Amin MB, et al. Prostate cancer - major changes in the American Joint Committee on Cancer eighth edition cancer staging manual. *CA Cancer J Clin* 2017; **67**: 245-53. doi: 10.3322/caac.21391
- Amin MB, Edge SB, Greene FL, Byrd DR, Brookland RK, Washington MK, et al, editors. *AJCC cancer staging manual*. 8th edition. New York: Springer; 2017.
- Giganti F, Moore CM, Punwani S, Allen C, Emberton M, Kirkham A. The natural history of prostate cancer on MRI: lessons from an active surveillance cohort. *Prostate Cancer Prostatic Dis* 2018; **21**: 556-63. doi: 10.1038/s41391-018-0058-5
- Weinreb JC, Barentsz JO, Choyke PL, Cornud F, Haider MA, Macura KJ, et al. PI-RADS prostate imaging - reporting and data system: 2015, Version 2. *Eur Urol* 2016; **69**: 16-40. doi: 10.1016/j.eururo.2015.08.052
- Rouvière O, Hartman RP, Lyonnet D. Prostate MR imaging at high-field strength: evolution or revolution? *Eur Radiol* 2006; **16**: 276-84. doi: org/10.1007/s00330-005-2893-8

21. Turkbey B, Merino MJ, Gallardo EC, Shah V, Aras O, Bernardo M, et al. Comparison of endorectal coil and nonendorectal coil T2W and diffusion-weighted MRI at 3 Tesla for localizing prostate cancer: correlation with whole-mount histopathology. *J Magn Reson Imaging* 2014; **39**: 1443-8. doi: 10.1002/jmri.24317
22. Czarniecki M, Caglic I, Grist JT, Gill AB, Lorenc K, Slough RA, et al. Role of PROPELLER-DWI of the prostate in reducing distortion and artefact from total hip replacement metalwork. *Eur J Radiol* 2018; **102**: 213-9. doi: org/10.1016/j.ejrad.2018.03.021
23. Gill AB, Czarniecki M, Gallagher FA, Barrett T. A method for mapping and quantifying whole organ diffusion-weighted image distortion in MR imaging of the prostate. *Sci Rep* 2017; **7**: 12727. doi: 10.1038/s41598-017-13097-6
24. Barrett T, Turkbey B, Choyke PL. PI-RADS version 2: what you need to know. *Clin Radiol* 2015; **70**: 1165-76. doi: 10.1016/j.crad.2015.06.093
25. Turkbey B, Rosenkrantz AB, Haider MA, Padhani AR, Villeirs G, Macura KJ, et al. Prostate Imaging Reporting and Data System Version 2.1: 2019 update of Prostate Imaging Reporting and Data System Version 2. *Eur Urol* 2019; **0232**: 1-12. doi: 10.1016/j.eururo.2019.02.033
26. Caglic I, Povalej Brzan P, Warren AY, Bratt O, Shah N, Barrett T. Defining the incremental value of 3D T2-weighted imaging in the assessment of prostate cancer extracapsular extension. *Eur Radiol* 2019. [Epub ahead of print]. doi: 10.1007/s00330-019-06070-6
27. Thoeny HC, Froehlich JM, Triantafyllou M, Huesler J, Bains LJ, Vermathen P, et al. Metastases in normal-sized pelvic lymph nodes: detection with diffusion-weighted MR imaging. *Radiology* 2014; **273**: 125-35. doi: 10.1148/radiol.14132921
28. Slough RA, Caglic I, Hansen NL, Patterson AJ, Barrett T. Effect of hyoscine butylbromide on prostate multiparametric MRI anatomical and functional image quality. *Clin Radiol* 2018; **73**: 216.e9-14. doi: 10.1016/j.crad.2017.07.013
29. Ullrich T, Quentin M, Schmaltz AK, Arsov C, Rubbert C, Blondin D, et al. Hyoscine butylbromide significantly decreases motion artefacts and allows better delineation of anatomic structures in mp-MRI of the prostate. *Eur Radiol* 2018; **28**: 17-23. doi: org/10.1007/s00330-017-4940-7
30. Caglic I, Barrett T. Optimising prostate mpMRI: prepare for success. *Clin Radiol* 2019. [Epub ahead of print]. doi: 10.1016/j.crad.2018.12.003
31. Dyde R, Chapman AH, Gale R, Mackintosh A, Tolan DJM. Precautions to be taken by radiologists and radiographers when prescribing hyoscine-N-butylbromide. *Clin Radiol* 2008; **63**: 739-43. doi: org/10.1016/j.crad.2008.02.008
32. Ayala AG, Ro JY, Babaian R, Troncoso P, Grignon DJ. The prostatic capsule. *Am J Surg Pathol* 1989; **13**: 21-7. doi: 10.1097/00000478-198901000-00003
33. McNeal JE. Normal histology of the prostate. *Am J Surg Pathol* 1988; **12**: 619-33. doi: 10.1097/00000478-198808000-00003
34. Ball MW, Partin AW, Epstein JI. Extent of extraprostatic extension independently influences biochemical recurrence-free survival: evidence for further PT3 subclassification. *Urology* 2015; **85**: 161-4. doi: org/10.1016/j.urology.2014.08.025
35. Rosenkrantz AB, Shanbhogue AK, Wang A, Kong MX, Babb JS, Taneja SS. Length of capsular contact for diagnosing extraprostatic extension on prostate MRI: assessment at an optimal threshold. *J Magn Reson Imaging* 2016; **43**: 990-7. doi: 10.1002/jmri.25040
36. Eifler JB, Feng Z, Lin BM, Partin MT, Humphreys EB, Han M, et al. An updated prostate cancer staging nomogram (Partin tables) based on cases from 2006 to 2011. *BJU Int* 2013; **111**: 22-9. doi: 10.1111/j.1464-410X.2012.11324.x
37. Turkbey B, Mani H, Aras O, Ho J, Hoang A, Rastinehad AR, et al. Prostate cancer: can multiparametric MR imaging help identify patients who are candidates for active surveillance? *Radiology* 2013; **268**: 144-52. doi: 10.1148/radiol.13121325
38. de Rooij M, Hamoen E, Witjes JA, Barentsz JO, Rovers MM. Accuracy of magnetic resonance imaging for local staging of prostate cancer: a diagnostic meta-analysis. *Eur Urol* 2016; **70**: 233-45. doi: 10.1016/j.eururo.2015.07.029
39. Lawrence EM, Gallagher FA, Barrett T, Warren AY, Priest AN, Goldman DA, et al. Preoperative 3-T diffusion-weighted MRI for the qualitative and quantitative assessment of extracapsular extension in patients with intermediate- or high-risk prostate cancer. *AJR Am J Roentgenol* 2014; **203**: W280-6. doi: 10.2214/AJR.13.11754
40. Boesen L, Chabanova E, Løgager V, Balslev I, Mikines K, Thomsen HS. Prostate cancer staging with extracapsular extension risk scoring using multiparametric MRI: a correlation with histopathology. *Eur Radiol* 2015; **25**: 1776-85. doi: 10.1007/s00330-014-3543-9
41. Schieda N, Quon JS, Lim C, El-Khodary M, Shabana W, Singh V, et al. Evaluation of the European Society of Urogenital Radiology (ESUR) PI-RADS scoring system for assessment of extra-prostatic extension in prostatic carcinoma. *Eur J Radiol* 2015; **84**: 1843-8. doi: 10.1016/j.ejrad.2015.06.016
42. Baco E, Rud E, Vlatkovic L, Svindland A, Eggesbø HB, Hung AJ, et al. Predictive value of magnetic resonance imaging determined tumor contact length for extracapsular extension of prostate cancer. *J Urol* 2015; **193**: 466-72. doi: 10.1016/j.juro.2014.08.084
43. Woo S, Kim SY, Cho JY, Kim SH. Length of capsular contact on prostate MRI as a predictor of extracapsular extension: which is the most optimal sequence? *Acta Radiol* 2017; **58**: 489-97. doi: 10.1177/0284185116658684
44. Matsuoka Y, Ishioka J, Tanaka H, Kimura T, Yoshida S, Saito K, et al. Impact of the Prostate Imaging Reporting and Data System, Version 2, on MRI diagnosis for extracapsular extension of prostate cancer. *AJR Am J Roentgenol* 2017; **209**: W76-84. doi: org/10.2214/AJR.16.17163
45. Hambrock T, Somford DM, Huisman HJ, van Oort IM, Witjes JA, Hulsbergen-van de Kaa CA, et al. Relationship between apparent diffusion coefficients at 3.0-T MR imaging and Gleason grade in peripheral zone prostate cancer. *Radiology* 2011; **259**: 453-61. doi: 10.1148/radiol.11091409
46. Verma S, Rajesh A, Morales H, Lemen L, Bills G, Delworth M, et al. Assessment of aggressiveness of prostate cancer: correlation of apparent diffusion coefficient with histologic grade after radical prostatectomy. *AJR Am J Roentgenol* 2011; **196**: 374-81. doi: 10.2214/AJR.10.4441
47. Kim CK, Park SY, Park JJ, Park BK. Diffusion-weighted MRI as a predictor of extracapsular extension in prostate cancer. *AJR Am J Roentgenol* 2014; **202**: W270-6. doi: 10.2214/AJR.13.11333
48. Woo S, Cho JY, Kim SY, Kim SH. Extracapsular extension in prostate cancer: added value of diffusion-weighted MRI in patients with equivocal findings on T2-weighted imaging. *AJR Am J Roentgenol* 2015; **204**: W168-75. doi: 10.2214/AJR.14.12939
49. Giganti F, Coppola A, Ambrosi A, Ravelli S, Esposito A, Freschi M, et al. Apparent diffusion coefficient in the evaluation of side-specific extracapsular extension in prostate cancer: development and external validation of a nomogram of clinical use. *Urol Oncol Semin Orig Investig* 2016; **34**: 291.e9-17. doi: 10.1016/j.urolonc.2016.02.015
50. Barrett T, Priest AN, Lawrence EM, Goldman DA, Warren AY, Gnanapragasam VJ, et al. Ratio of tumor to normal prostate tissue apparent diffusion coefficient as a method for quantifying DWI of the prostate. *AJR Am J Roentgenol* 2015; **205**: W585-93. doi: 10.2214/AJR.15.14338
51. Rosenkrantz AB, Neil J, Kong X, Melamed J, Babb JS, Taneja SS, et al. Prostate cancer: comparison of 3D T2-weighted with conventional 2D T2-weighted imaging for image quality and tumor detection. *AJR Am J Roentgenol* 2010; **194**: 446-52. doi: 10.2214/AJR.09.3217
52. Itatani R, Namimoto T, Takaoka H, Katahira K, Morishita S, Kitani K, et al. Extracapsular extension of prostate cancer: diagnostic value of combined multiparametric magnetic resonance imaging and isovoxel 3-dimensional T2-weighted imaging at 1.5 T. *J Comput Assist Tomogr* 2015; **39**: 37-43. doi: 10.1097/RCT.0000000000000172
53. Liberatore M, Delongchamps NB, Eiss D, Beuvon F, Zerbib M, Flam T, et al. Endorectal 3D T2-weighted 1mm-slice thickness MRI for prostate cancer staging at 1.5Tesla: should we reconsider the indirect signs of extracapsular extension according to the D'Amico tumor risk criteria? *Eur J Radiol* 2011; **81**: e591-7. doi: 10.1016/j.ejrad.2011.06.056
54. Jäderling F, Nyberg T, Öberg M, Carlsson S, Skorpil M, Blomqvist L. Accuracy in local staging of prostate cancer by adding a three-dimensional T2-weighted sequence with radial reconstructions in magnetic resonance imaging. *Acta Radiol Open* 2018; **7**: 205846011875460. doi: 10.1177/2058460118754607

55. Peng Y, Schmid-Tannwald C, Wang S, Antic T, Jiang Y, Eggner S, et al. Seminal vesicle invasion in prostate cancer: evaluation by using multiparametric endorectal MR imaging. *Radiology* 2013; **267**: 797-806. doi: 10.1148/radiol.13121319
56. Chan KK, Choi D, Byung KP, Ghee YK, Hyo KL. Diffusion-weighted MR imaging for the evaluation of seminal vesicle invasion in prostate cancer: initial results. *J Magn Reson Imaging* 2008; **28**: 963-9. doi: 10.1002/jmri.21531
57. Potter SR, Epstein JI, Partin AW. Seminal vesicle invasion by prostate cancer: prognostic significance and therapeutic implications. *Rev Urol* 2000; **2**: 190-5. PMID: 16985773
58. Wang L, Hricak H, Kattan MW, Chen HN, Kuroiwa K, Eisenberg HF, et al. Prediction of seminal vesicle invasion in prostate cancer: incremental value of adding endorectal MR imaging to the Kattan nomogram. *Radiology* 2007; **242**: 182-8. doi: 10.1148/radiol.2421051254
59. Grivas N, Hinnen K, de Jong J, Heemsbergen W, Moonen L, Witteveen T, et al. Seminal vesicle invasion on multi-parametric magnetic resonance imaging: correlation with histopathology. *Eur J Radiol* 2018; **98**: 107-12. doi: 10.1016/j.ejrad.2017.11.013
60. Roethke M, Kaufmann S, Kniess M, Ketelsen D, Claussen CD, Schlemmer HP, et al. Seminal vesicle invasion: accuracy and analysis of infiltration patterns with high-spatial resolution T2-weighted sequences on endorectal magnetic resonance imaging. *Urol Int* 2014; **92**: 294-9. doi: 10.1159/000353968
61. Ohori M, Scardino PT, Lapin SL, Seale-Hawkins C, Link J, Wheeler TM. The mechanisms and prognostic significance of seminal vesicle involvement by prostate cancer. *Am J Surg Pathol* 1993; **17**: 1252-61. doi: 10.1097/0000478-199312000-00006
62. Jung DC, Lee HJ, Kim SH, Choe GY, Lee SE. Preoperative MR imaging in the evaluation of seminal vesicle invasion in prostate cancer: pattern analysis of seminal vesicle lesions. *J Magn Reson Imaging* 2008; **28**: 144-50. doi: 10.1002/jmri.21422
63. Soylu FN, Peng Y, Jiang Y, Wang S, Schmid-Tannwald C, Sethi I, et al. Seminal vesicle invasion in prostate cancer: evaluation by using multiparametric endorectal MR imaging. *Radiology* 2013; **267**: 797-806. doi: 10.1148/radiol.13121319
64. Gofrit ON, Zorn KC, Taxy JB, Zagaja GP, Steinberg GD, Shalhav AL. The dimensions and symmetry of the seminal vesicles. *J Robot Surg* 2009; **3**: 29-33. doi: 10.1007/s11701-009-0134-x
65. Saliken JC, Gray RR, Donnelly BJ, Owen R, White LJ, Ali-Ridha N, et al. Extraprostatic biopsy improves the staging of localized prostate cancer. *Can Assoc Radiol J* 2000; **51**: 114-20. PMID: 10786920
66. Barrett T, Tanner J, Gill AB, Slough RA, Watson J, Gallagher FA. The longitudinal effect of ejaculation on seminal vesicle fluid volume and whole-prostate ADC as measured on prostate MRI. *Eur Radiol* 2017; **27**: 5236-43. doi: 10.1007/s00330-017-4905-x
67. Medved M, Sammet S, Yousuf A, Oto A. MR Imaging of the prostate and adjacent anatomic structures before, during, and after ejaculation: qualitative and quantitative evaluation. *Radiology* 2014; **271**: 452-60. doi: 10.1148/radiol.14131374
68. Shin T, Kaji Y, Shukuya T, Nozaki M, Soh S, Okada H. Significant changes of T2 value in the peripheral zone and seminal vesicles after ejaculation. *Eur Radiol* 2018; **28**: 1009-15. doi: 10.1007/s00330-017-5077-4
69. Kabakus IM, Borofsky S, Merten FV, Greer M, Daar D, Wood BJ, et al. Does abstinence from ejaculation before prostate MRI improve evaluation of the seminal vesicles? *AJR Am J Roentgenol* 2016; **207**: 1205-9. doi: 10.2214/AJR.16.16278
70. McMahon CJ, Rofsky NM, Pedrosa I. Lymphatic metastases from pelvic tumors: anatomic classification, characterization, and staging. *Radiology* 2010; **254**: 31-46. doi: 10.1148/radiol.2541090361
71. Joniau S, Van den Bergh L, Lerut E, Deroose CM, Haustermans K, Oyen R, et al. Mapping of pelvic lymph node metastases in prostate cancer. *Eur Urol* 2013; **63**: 450-8. doi: 10.1016/j.eururo.2012.06.057
72. Briganti A, Suardi N, Capogrosso P, Passoni N, Freschi M, Di Trapani E, et al. Lymphatic spread of nodal metastases in high-risk prostate cancer: the ascending pathway from the pelvis to the retroperitoneum. *Prostate* 2012; **72**: 186-92. doi: 10.1002/pros.21420
73. Barentsz JO, Severens JL, Hoogeveen YL, Hövels AM, Adang EM, Jager GJ, et al. The diagnostic accuracy of CT and MRI in the staging of pelvic lymph nodes in patients with prostate cancer: a meta-analysis. *Clin Radiol* 2008; **63**: 387-95. doi: 10.1016/j.crad.2007.05.022
74. Vag T, Heck MM, Beer AJ, Souvatzoglou M, Weirich G, Holzapfel K, et al. Preoperative lymph node staging in patients with primary prostate cancer: comparison and correlation of quantitative imaging parameters in diffusion-weighted imaging and 11C-choline PET/CT. *Eur Radiol* 2014; **24**: 1821-6. doi: 10.1007/s00330-014-3240-8
75. Eiber M, Beer AJ, Holzapfel K, Tauber R, Ganter C, Weirich G, et al. Preliminary results for characterization of pelvic lymph nodes in patients with prostate cancer by diffusion-weighted MR-imaging. *Invest Radiol* 2010; **45**: 15-23. doi: 10.1097/RLI.0b013e3181bbdc2f
76. Beer AJ, Eiber M, Souvatzoglou M, Holzapfel K, Ganter C, Weirich G, et al. Restricted water diffusibility as measured by diffusion-weighted MR imaging and choline uptake in 11C-choline PET/CT are correlated in pelvic lymph nodes in patients with prostate cancer. *Mol Imaging Biol* 2011; **13**: 352-61. doi: 10.1007/s11307-010-0337-6
77. Vallini V, Ortori S, Boraschi P, Manassero F, Gabelloni M, Faggioni L, et al. Staging of pelvic lymph nodes in patients with prostate cancer: usefulness of multiple b value SE-EPI diffusion-weighted imaging on a 3.0 T MR system. *Eur J Radiol Open* 2016; **3**: 16-21. doi: 10.1016/j.ejro.2015.11.004
78. Roy C, Bierry G, Matau A, Bazille G, Pasquali R. Value of diffusion-weighted imaging to detect small malignant pelvic lymph nodes at 3 T. *Eur Radiol* 2010; **20**: 1803-11. doi: 10.1007/s00330-010-1736-4
79. Caglic I, Barrett T. Diffusion-weighted imaging (DWI) in lymph node staging for prostate cancer. *Transl Androl Urol* 2018; **7**: 814-23. doi: 10.21037/tau.2018.08.04
80. Abdel Razeq AAK, Soliman NY, Elkhamary S, Alsharaway MK, Tawfik A. Role of diffusion-weighted MR imaging in cervical lymphadenopathy. *Eur Radiol* 2006; **16**: 1468-77. doi: 10.1007/s00330-005-0133-x
81. Muenzel D, Duetsch S, Fauser C, Slotta-Huspenina J, Gaa J, Rummeny EJ, et al. Diffusion-weighted magnetic resonance imaging in cervical lymphadenopathy: report of three cases of patients with bartonella henselae infection mimicking malignant disease. *Acta Radiol* 2009; **50**: 914-6. doi: 10.1080/02841850903061445
82. Kwee TC, Takahara T, Luijten PR, Nievelstein RAJ. ADC measurements of lymph nodes: inter- and intra-observer reproducibility study and an overview of the literature. *Eur J Radiol* 2010; **75**: 215-20. doi: 10.1016/j.ejrad.2009.03.026
83. Braithwaite AC, Dale BM, Boll DT, Merkle EM. Short- and midterm reproducibility of apparent diffusion coefficient measurements at 3.0-T diffusion-weighted imaging of the abdomen. *Radiology* 2009; **250**: 459-65. doi: 10.1148/radiol.2502080849
84. Rosenkrantz AB, Oei M, Babb JS, Niver BE, Taouli B. Diffusion-weighted imaging of the abdomen at 3.0 Tesla: image quality and apparent diffusion coefficient reproducibility compared with 1.5 Tesla. *J Magn Reson Imaging* 2011; **33**: 128-35. doi: 10.1002/jmri.22395
85. Sadinski M, Medved M, Karademir I, Wang S, Peng Y, Jiang Y, et al. Short-term reproducibility of apparent diffusion coefficient estimated from diffusion-weighted MRI of the prostate. *Abdom Imaging* 2015; **40**: 2523-8. doi: 10.1007/s00261-015-0396-x
86. von Below C, Daouacher G, Wassberg C, Grzegorek R, Gestblom C, Sörensen J, et al. Validation of 3 T MRI including diffusion-weighted imaging for nodal staging of newly diagnosed intermediate- and high-risk prostate cancer. *Clin Radiol* 2016; **71**: 328-34. doi: 10.1016/j.crad.2015.12.001
87. Sushentsev N, Martin H, Rimmer Y, Barrett T. Added value of diffusion-weighted MRI for nodal radiotherapy planning in pelvic malignancies. *Clin Transl Oncol* 2019. [Epub ahead of print]. doi.org/10.1007/s12094-019-02068-0
88. Zacharias C, Kunder C, Giesel F, Daniel B, Hatami N, Harrison C, et al. Gallium 68 PSMA-11 PET/MR imaging in patients with intermediate- or high-risk prostate cancer. *Radiology* 2018; **288**: 495-505. doi: org/10.1148/radiol.2018172232
89. Freitag MT, Radtke JP, Hadaschik BA, Kopp-Schneider A, Eder M, Kopka K, et al. Comparison of hybrid 68Ga-PSMA PET/MRI and 68Ga-PSMA PET/CT in the evaluation of lymph node and bone metastases of prostate cancer. *Eur J Nucl Med Mol Imaging* 2016; **43**: 70-83. doi: 10.1007/s00259-015-3206-3
90. Baltzer P, Kenner L, Hartenbach M, Mitterhauser M, Goldner GM, Grahovac M, et al. PSMA Ligand PET/MRI for primary prostate cancer: staging performance and clinical impact. *Clin Cancer Res* 2018; **24**: 6300-7. doi: 10.1158/1078-0432.ccr-18-0768

91. Harisinghani MG, Barentsz J, Hahn PF, Deserno WM, Tabatabaei S, van de Kaa CH, et al. Noninvasive detection of clinically occult lymph-node metastases in prostate cancer. *N Engl J Med* 2003; **348**: 2491-9. doi: 10.1056/NEJMoa022749
92. Birkhäuser FD, Studer UE, Froehlich JM, Triantafyllou M, Bains LJ, Petralia G, et al. Combined ultrasmall superparamagnetic particles of iron oxide-enhanced and diffusion-weighted magnetic resonance imaging facilitates detection of metastases in normal-sized pelvic lymph nodes of patients with bladder and prostate cancer. *Eur Urol* 2013; **64**: 953-60. doi: 10.1016/j.eururo.2013.07.032
93. Thoeny HC, Triantafyllou M, Birkhaeuser FD, Froehlich JM, Tshering DW, Binsler T, et al. Combined ultrasmall superparamagnetic particles of iron oxide-enhanced and diffusion-weighted magnetic resonance imaging reliably detect pelvic lymph node metastases in normal-sized nodes of bladder and prostate cancer patients. *Eur Urol* 2009; **55**: 761-9. doi: 10.1016/j.eururo.2008.12.034
94. Fortuin AS, Brüggemann R, van der Linden J, Panfilov I, Israël B, Scheenen TWJ, et al. Ultra-small superparamagnetic iron oxides for metastatic lymph node detection: back on the block. *Wiley Interdiscip Rev Nanomedicine Nanobiotechnology* 2018; **10**: e1471. doi: 10.1002/wnan.1471
95. National Institute for Health and Care Excellence. Prostate cancer: diagnosis and management, clinical guideline [CG175], 2014. [cited 2019 March 28]. Available at: <http://www.nice.org.uk/guidance/cg175/chapter/1-recommendations>
96. Shen G, Deng H, Hu S, Jia Z. Comparison of choline-PET/CT, MRI, SPECT, and bone scintigraphy in the diagnosis of bone metastases in patients with prostate cancer: a meta-analysis. *Skeletal Radiol* 2014; **43**: 1503-13. doi: 10.1007/s00256-014-1903-9
97. Padhani AR, Koh D-M, Collins DJ. Whole-body diffusion-weighted MR imaging in cancer: current status and research directions. *Radiology* 2011; **261**: 700-18. doi: 10.1148/radiol.11110474
98. Padhani AR, Lecouvet FE, Tunariu N, Koh D-M, De Keyzer F, Collins DJ, et al. METastasis Reporting and Data System for Prostate Cancer: practical guidelines for acquisition, interpretation, and reporting of whole-body magnetic resonance imaging-based evaluations of multiorgan involvement in advanced prostate cancer. *Eur Urol* 2017; **71**: 81-92. doi: 10.1016/j.eururo.2016.05.033
99. Lecouvet FE, El Mouedden J, Collette L, Coche E, Danse E, Jamar F, et al. Can whole-body magnetic resonance imaging with diffusion-weighted imaging replace Tc 99m bone scanning and computed tomography for single-step detection of metastases in patients with high-risk prostate cancer? *Eur Urol* 2012; **62**: 68-75. doi: 10.1016/j.eururo.2012.02.020
100. Pasoglou V, Michoux N, Peeters F, Larbi A, Tombal B, Selleslagh T, et al. Whole-body 3D T1-weighted MR imaging in patients with prostate cancer: feasibility and evaluation in screening for metastatic disease. *Radiology* 2015; **275**: 155-66. doi: 10.1148/radiol.14141242
101. Larbi A, Pasoglou V, Triqueneaux P, Cyteval C, Tombal B, Omoumi P, et al. Whole-body MRI to assess bone involvement in prostate cancer and multiple myeloma: comparison of the diagnostic accuracies of the T1, short tau inversion recovery (STIR), and high b-values diffusion-weighted imaging (DWI) sequences. *Eur Radiol* 2018. [Epub ahead of print]. doi: 10.1007/s00330-018-5796-1

Evaluation of MRI accuracy after primary systemic therapy in breast cancer patients considering tumor biology: optimizing the surgical planning

Alberto Bouzón¹, Ángela Iglesias², Benigno Acea¹, Cristina Mosquera¹, Paz Santiago³, Joaquín Mosquera²

¹ Department of Surgery, Breast Unit, Complejo Hospitalario Universitario A Coruña, Spain

² Department of Radiology, Breast Unit, Complejo Hospitalario Universitario A Coruña, Spain

³ Department of Pathology, Breast Unit, Complejo Hospitalario Universitario A Coruña, Spain

Radiol Oncol 2019; 53(2): 171-177.

Received 25 December 2018

Accepted 18 April 2019

Correspondence to: Alberto Bouzón, M.D., Ph.D., Travesía Modesta Goicouría, N°5, 16 izquierda, 15004, A Coruña, Spain.
E-mail: dr.alberto@aecirujanos.es

Disclosure: No potential conflicts of interest were disclosed.

Background. We analyzed the accuracy of magnetic resonance imaging (MRI) after primary systemic therapy (PST) according to tumor subtype.

Patients and methods. Two-hundred and four breast cancer patients treated with PST were studied. MRI findings after PST were compared with pathologic findings, and results were stratified based on tumor subtype.

Results. Of the two-hundred and four breast cancer patients, eighty-four (41.2%) achieved a pathologic complete response (pCR) in the breast. The MRI accuracy for predicting pCR was highest in triple-negative (TN) and HER2-positive (non-luminal) breast cancer (83.9 and 80.9%, respectively). The mean size discrepancy between MRI-measured and pathologic residual tumor size was lowest in TN breast cancer and highest in luminal B-like (HER2-negative) breast cancer (0.45cm vs. 0.98 cm, respectively; $p = 0.003$). After breast conserving surgery (BCS), we found a lower rate of positive margins in TN breast cancer and a higher rate of positive margins in luminal B-like (HER2-negative) breast cancer (2.4% vs. 23.6%, respectively).

Conclusions. If tumor response after PST is assessed by MRI, tumor subtype should be considered when BCS is planned. The accuracy of MRI is highest in TN breast cancer.

Key words: MRI; breast cancer; primary systemic therapy; tumor subtype

Introduction

Breast cancer is a heterogeneous disease stratified into several molecular subtypes with different behavior and prognosis.^{1,2} In clinical setting, breast cancer is routinely classified into approximated subtypes using immunohistochemistry according to hormone receptor (HR) and human epidermal growth factor 2 receptor (HER2) status.

Primary systemic therapy (PST) is the standard of care for locally advanced breast cancer, and it is increasingly being used for early breast cancer to

improve cosmetic outcome after breast-conserving surgery (BCS). However, the primary goal of PST is to achieve pathologic complete response (pCR) prior to surgical treatment, which has been shown to predict favorable prognosis.³⁻⁵

Over the past few years, the highest use of PST was seen among HER2-positive and triple-negative breast cancer (TNBC) patients.⁶ Women with these tumor subtypes have the highest rates of BCS and pCR after PST.⁷ Furthermore, prognostic impact of pCR is highest in HER2-positive and TNBC.⁸⁻¹⁰

Currently, although the nuclear imaging techniques are promising, magnetic resonance imaging (MRI) is accepted as the most accurate imaging modality for assessment of tumor response and residual tumor size after PST in breast cancer patients.¹¹ However, breast MRI is less effective for predicting pCR.¹²⁻¹⁶ Therefore, in patients with absence of disease on MRI, surgical resection of the original tumor bed is required.

The purpose of the present study was to investigate the MRI diagnostic accuracy after PST in breast cancer patients focusing on tumor biology and its impact on margins after BCS. We also aimed to update the clinicopathologic factors affecting MRI accuracy to determine residual tumor size.

Patients and methods

Patients

A total of 204 patients with primary operable breast cancer treated with PST from October 2006 to September 2016 were included in this retrospective study. MRI was performed before and after PST to evaluate tumor response and residual tumor extent. A clip marker was placed at the tumor site prior to PST for surgical detection of the tumor bed. Patients with luminal A-like tumors were excluded due to their worse response to PST. Furthermore, in our previous study, the tumor size discrepancy between MRI and pathology was higher in this tumor subtype.¹⁶

Subtype classification

Breast cancer was classified into 5 approximate subtypes based on tumor characteristics using immunohistochemistry (HR status, HER2 status and ki-67 status). The five categories of tumor subtypes were: luminal A-like, luminal B-like (HER2-negative), luminal B-like (HER2-positive), HER2 positive (non-luminal) and TN subtype.¹⁷ The cut-off of ki-67 expression level was established at 20% to distinguish between luminal A-like and luminal B-like (HER2-negative) subtypes, so that a threshold of $\geq 20\%$ was indicative of high ki-67 status.

Chemotherapy regimen of PST

62.2% of patients received an anthracycline/taxane-based PST. All HER2-positive breast cancer patients except one received trastuzumab-based PST (36.3%), in combination with an anthracycline/taxane-based regimen. Three patients received a

nanoparticle albumin-bound paclitaxel regimen (1.5%).

MRI protocol and assessment

Residual tumor extent after PST was measured by MRI as the longest dimension of the enhancing lesion. MRI examinations were performed with patients in prone position using a 1.5T MRI scanner (Best, The Netherlands) with breast-surface coils. The protocol included an axial T1-weighted sequence (repetition time [TR]: 494 msec, echo time [TE]: 8 msec, number of acquired signals: 2, slice thickness: 3 mm, interval: 0.03 mm) and T2-weighted sequence (TR: 5000 msec, TE: 120 msec, number of acquired signals: 2, slice thickness: 3 mm, interval: 0.03 mm), followed by diffusion-weighted images performed at different b values ($b = 0$ and $b = 1000$).

A dynamic study (3D T1-weighted fast spoiled gradient-echo sequence) in the axial plane was performed before and 90, 180, 270, 360 and 450 sec after starting intravenous injection of 0.1 mmol/kg of gadoterate meglumine (Gd-DOTA, DOTAREM, Guerbet) at a rate of 2 mL/s, followed by a 20 mL saline flush.

All images were processed at a workstation for the analysis of contrast enhancement, time-signal intensity curves and restriction to the diffusion.

Imaging complete response (iCR) was defined as the absence of a clear enhancement visible on post-treatment MRI. Non-iCR was defined as the presence of any amount of tissue enhancement within the previous tumor bed visible on dynamic MRI after PST.

Surgical management of breast tumors

Surgery was performed within four weeks after completion of the neoadjuvant therapy. BCS was performed when the breast-tumor size index was favorable, considering patient's preference and multifocality. In non-palpable lesions after PST, a wire-guided resection of the clip containing breast area was performed. All patients undergoing BCS received adjuvant whole-breast irradiation with tangential fields.

Pathological examination of surgical specimens

All surgical specimens were fixed after gross evaluation in 10% neutral-buffered formalin for 24 hours, and then serially cut into 5 mm thick sections. If

residual tumor was clearly visible a gross measurement was made. If no evident tumor was identified, the clip marker placed prior to PST was found, and slides from the block containing the marker as well as the adjacent blocks were microscopically examined. Surgical specimens were stained with hematoxylin and eosin for the histological examination. The largest tumor diameter provided by the pathologist was used in the comparative study. If no invasive cancer was found in the surgical specimen after PST, regardless of the presence of carcinoma in situ, a breast pCR was considered. Negative resection margins were defined as no ink on tumor for invasive carcinoma and 2 mm clean margins for ductal carcinoma in situ.

Statistical analysis

Analyses were performed using SPSS version 23.0. Descriptive statistics of the variables included in the study were obtained. Continuous variables were expressed as mean (standard deviation) and median (range), and categorical variables were expressed as absolute values and percentages with their estimated 95% confidence interval. Student's T test or Mann-Whitney U Test were used to compare continuous variables. Moreover, chi-square test or Fisher's exact test were used to compare categorical variables. Multiple linear regression models were used to identify variables associated with MRI/pathologic tumor size discrepancy. Variables found to be significant on univariate analysis were included for the multivariate analysis. The diagnostic ability of MRI to detect residual disease after PST was quantified by the measures of diagnostic accuracy: sensitivity, specificity, positive predictive value (PPV), negative predictive value (NPV) and overall accuracy.

Ethical issues

Considering the Helsinki Declaration principles, the Institutional Research Ethics Committee approved this retrospective study (No. 2016/457).

Results

Patient and tumor characteristics

Baseline patient and tumor characteristics for the 204 breast cancer patients are described in Table 1. The median age of the patient cohort was 47 years (range, 30-82 years). Mean initial tumor size determined by MRI was 3.9 cm (72% of patients had T2

TABLE 1. Clinical and tumoral characteristics

Variables	Mean	SD	Median	Range
Age (years)	49.4	11.6	47.0	30.0–82.0
Baseline tumor size (cm)	3.9	1.9	3.4	1.2–12.0
		n	%	95% CI
Clinical tumor stage	T1	21	10.3	5.9–14.7
	T2	147	72.1	65.7–78.5
	T3	34	16.7	11.3–22.0
	T4	2	0.9	0.1–3.5
Histological type	IDC	196	96.1	93.2–99.0
	ILC	8	3.9	1.0–6.8
Histological grade	low-medium	60	30.0	23.4–36.6
	high	140	70.0	63.4–76.6
	NA	4		
Hormonal receptor status	positive	122	59.8	52.8–66.8
	negative	82	40.2	33.2–47.2
HER2 status	positive	75	36.8	29.9–43.6
	negative	129	63.2	56.4–70.1
Tumor subtype	luminal B/HER2-	77	37.7	30.8–44.6
	luminal B/HER2+	45	22.1	16.1–28.0
	HER2+	30	14.7	9.6–19.8
	triple negative	52	25.5	19.3–31.7
Baseline axillary status	positive	113	55.4	48.3–62.5
	negative	91	44.6	37.5–51.7

CI = confidence interval; IDC = invasive ductal carcinoma; ILC = invasive lobular carcinoma; NA = not available; SD = standard deviation

tumors). Patients enrolled by tumor subtype were 77 luminal B-like (HER2-negative) (37.7%), 45 luminal B-like (HER2-positive) (22.1%), 30 HER2 positive (non-luminal) (14.7%) and 52 TN (25.5%). The axillary nodal status before PST was positive in 55.4% of cases.

Response rate of the primary breast tumor to PST

84 patients (41.2%) achieved pCR in the breast after PST. The pCR rates differed significantly among tumor subtypes: 13% for luminal B-like (HER2-negative), 42.2% for luminal B-like (HER2-positive), 76.6% for HER2 positive (non-luminal) and 61.5% for TN. The iCR rate was 56.4% (115/204). The average pathologic tumor size was 1.10 cm and the average tumor size by post-treatment MRI was 1.03 cm.

TABLE 2. Diagnostic accuracy of MRI to detect residual disease

	S (%)	SP (%)	PPV (%)	NPV (%)	ACC (%)
Total	62.5	83.3	84.3	60.9	71.1
Luminal B/HER2-	64.2	100.0	100.0	29.4	68.8
Luminal B/HER2+	53.8	89.5	87.5	58.6	68.9
HER2+	42.9	73.9	33.3	80.9	66.7
Triple negative	75.0	81.2	71.4	83.9	78.8

ACC = accuracy; NPV = negative predictive value; PPV = positive predictive value; S = sensitivity; SP = specificity

Accuracy of MRI after PST

The diagnostic accuracy of MRI to detect residual invasive disease in the breast for all patients and by tumor subtypes is summarized in Table 2. The overall accuracy was 71.1%. The NPV and PPV were 60.9% and 84.3%, respectively. Among the different tumor subtypes, the highest diagnostic accuracy of MRI was observed in TNBC patients (78.8%). The ability of MRI to predict pCR was highest for the TN and HER2 positive (non-luminal) subtypes (83.9% and 80.9%, respectively).

The mean size difference between post-treatment MRI and pathology was significantly lower in TN tumors as compared with luminal B-like (HER2-negative) tumors (0.45 cm vs. 0.98; $p = 0.003$) (Figure 1).

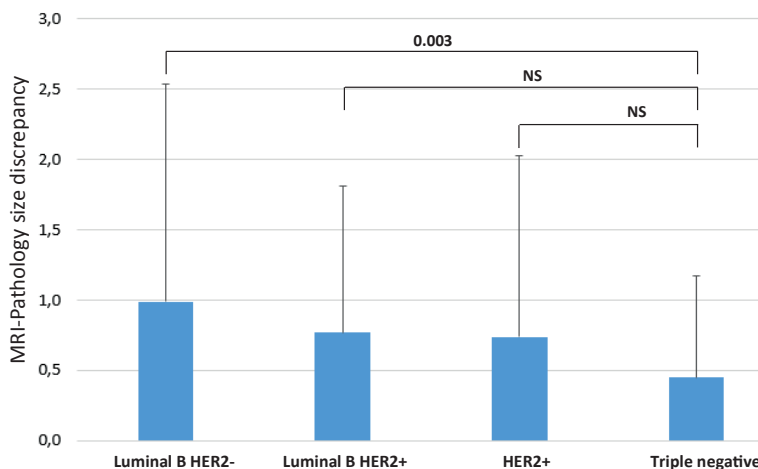


FIGURE 1. Diagnostic accuracy of MRI. Size discrepancy by tumor subtypes. Mean size discrepancy by tumor subtypes (cm): luminal B/HER2-: 0.98; luminal B/HER2+: 0.77; HER2+: 0.74; triple negative: 0.45.

TABLE 3. Factors affecting the MRI accuracy based on the discrepancy between MRI and pathologic residual tumor size. Univariate and multivariate analysis

Variable	n*	Mean size discrepancy (± SD)	p
Age (years)			0.668
≤45	88	0.72 (± 0.95)	
>45	115	0.79 (± 1.43)	
Baseline tumor size (cm)			0.045
≤5	167	0.62 (± 0.87)	
>5	36	1.39 (± 2.18)	
Histological type			0.347
IDC	195	0.71 (± 1.02)	
ILC	8	2.05 (± 3.75)	
Tumor grade			0.006
Low-medium	60	1.25 (± 1.82)	
high	139	0.55 (± 0.82)	
Hormonal receptor status			0.059
positive	121	0.90 (± 1.38)	
negative	82	0.56 (± 0.97)	
HER2 status			0.956
positive	74	0.75 (± 1.13)	
negative	129	0.76 (± 1.30)	

Variable	β	se	p	95% CI
Tumor grade	0.679	0.192	0.001	0.300–1.058
HR status	0.214	0.181	0.239	-0.143–0.570
BTS (MRI)	0.872	0.217	<0.001	0.443–1.301

*n (number of patients) = 203; β = regression coefficient; BTS = baseline tumor size; CI = confidence interval; HR = hormonal receptor; IDC = invasive ductal carcinoma; ILC = invasive lobular carcinoma; se = standard error; SD = standard deviation

Factors influencing the accuracy of MRI for predicting residual tumor size after PST

The mean discrepancy between residual tumor extent measured on MRI and pathology according to various clinicopathologic factors was determined in 203 patients (Table 3). Pathologic residual tumor size was not available in one case due to the presence of scattered residual multifocal disease in the surgical specimen. On univariable analysis, high tumor grade and baseline tumor size smaller than 5 cm were associated with a higher MRI accuracy. HR status showed marginal significance ($p = 0.059$), with lower mean discrepancy in HR-negative breast cancers. Age, histological type and HER2 status were not significantly associated with MRI/pathologic tumor size discrepancy. On multivariable analysis, tumor grade and baseline tumor size were significant and independent predictors of MRI accuracy.

Surgical treatment after PST

After PST, 166 patients (81.4%) underwent BCS and 38 patients (18.6%) underwent mastectomy. From the BCS subset, 19 patients (11.4%) required re-excision because of positive margins (3 of 19 patients required a salvage mastectomy). Of these 19 patients, 2 (10.5%) had residual invasive disease on the final pathology. The positive margins rate after BCS was higher in patients with HR-positive breast cancer (23.6% for luminal B-like (HER2-negative) and 13.5% for luminal B-like (HER2-positive)) than in patients with HER2 positive (non-luminal) or TNBC (5% and 2.4%, respectively).

Discussion

PST is an increasing used treatment strategy for the management of operable breast cancer patients, whose main role in the surgical planning is to increase the rate of BCS.

Breast MRI is superior to conventional mammography and sonography for assessing tumor response after PST due to its ability to differentiate chemotherapy-induced fibrosis from residual disease.¹⁸⁻²⁰

The accuracy of MRI for determining the presence and size of residual invasive disease should be considered when BCS is planned after PST. The underestimation of residual tumor size increases the rate of positive margins and the overestimation of residual tumor size may affect the cosmetic outcome if the tissue removal is very extensive. Our results demonstrate that the diagnostic accuracy of MRI is influenced by tumor subtype, being more effective in TNBC.

In the present study, the overall NPV of MRI was 60.9%. However, MRI for predicting pCR is generally more accurate in those tumor subtypes with better response. In our study, MRI accurately predicted pCR in HER2 positive (non-luminal) and TNBC patients (80.9% and 83.9%, respectively) compared with HR-positive breast cancer patients. In a previous study, McGuire *et al.*¹⁴ found that the diagnostic accuracy of breast MRI for predicting pCR was higher in HR-negative breast cancer patients than in HR-positive breast cancer patients (73.6% vs. 27.3%, respectively). De Los Santos *et al.*¹³ concluded in their study that MRI accuracy differed significantly among breast cancer subtypes, and the highest NPV was observed in HER2 positive (non-luminal) and TNBC (62% and 60%, respectively).

Fukuda *et al.*¹⁵ reported that MRI was more effective for predicting pCR in TNBC (NPV = 72%).

The MRI accuracy for assessing tumor response depends on several factors, such as the used chemotherapeutic agents or the tumor regression pattern.²¹ PST in HER2-positive breast cancer patients includes targeted anti-HER2 agents and, therefore, the rate of achieving pCR is higher. In neoadjuvant setting, TNBC usually shows a concentric tumor regression pattern that allows MRI to be more accurate.²²

Our findings showed that baseline tumor size and tumor grade are significant and independent factors that affect MRI accuracy in predicting residual tumor extent after PST. In general, MRI accuracy is greater in tumors with better response to chemotherapy, such as high nuclear grade and cT1-2 breast cancers.^{23,24} Furthermore, MRI tend to be less accurate in HR-positive breast cancers. MRI may underestimate residual disease presenting as scattered cells within a large fibrotic region.²⁵ This fragmented tumor regression pattern occurs more often in HR-positive breast cancers, leading to a higher rate of positive margins after BCS.

The present study showed that MRI was more accurate at predicting residual tumor size in TNBC patients, in whom the smallest MRI-pathology tumor size discrepancy (mean of 0.45 cm) was observed. In addition, the rate of positive margins after BCS in TNBC patients was the lowest (2.4%). The highest MRI-pathology tumor size discrepancy was observed in luminal B-like (HER2-negative) breast cancer patients (mean of 0.98 cm) and, as a consequence, 23.6% of these women had positive margins after BCS. Previous studies also reported a higher MRI accuracy for predicting the residual tumor extent after PST in TNBC.^{26,27}

These results indicate that it is necessary to consider tumor biology to optimize the planning of BCS based on MRI findings. When breast MRI describes a complete response in HER2 positive (non-luminal) and TN tumors, a minimal surgical resection of the tumor bed should be performed.

Novel breast imaging methods of evaluation of tumor response after PST are currently being studied. Contrast-enhanced spectral mammography is comparable to MRI in assessing residual disease after PST, but also has a limited accuracy to predict pCR.²⁸ Stereotactic vacuum-assisted core needle biopsy of tumor bed after PST could help identify breast cancer patients with pCR to be included in prospective trials evaluating the safety of omitting surgical treatment.²⁹

The strength of this study lies in the consideration of tumor subtypes in the analysis of MRI accuracy. Nonetheless, our study has several limitations. First, it is a retrospective study with a small number of HER2-positive (non-luminal) breast cancer patients ($n = 30$) compared to the number of patients presenting other tumor subtypes. During the study period, patients received different types of chemotherapy regimens, which may have affected the tumor response and, therefore, the MRI accuracy. Furthermore, the tumor response evaluation was performed using a 1.5-T MRI system, which seems to present lower diagnostic accuracy compared with 3-T MRI with a higher spatial resolution.³⁰ Finally, only the absence of invasive residual disease was included in the definition of pCR in the breast.

In conclusion, if tumor response after PST is assessed by MRI, tumor subtype should be considered when BCS is planned. The accuracy of MRI is highest in TNBC patients.

Acknowledgements

The authors thank the team of the Department of Biostatistics of Complejo Hospitalario A Coruña for their contribution in the statistical analysis, specially Teresa Seoane.

Abbreviations

BCS = breast-conserving surgery; **BTS** = baseline tumor size; **HR** = hormone receptor; **HER2** = human epidermal growth factor 2 receptor; **iCR** = imaging complete response; **IDC** = invasive ductal carcinoma; **ILC** = invasive lobular carcinoma; **MRI** = magnetic resonance imaging; **NPV** = negative predictive value; **pCR** = pathologic complete response; **PPV** = positive predictive value; **PST** = primary systemic therapy; **TNBC** = triple-negative breast cancer

References

- Rouzier R, Perou CM, Symmans WF, Ibrahim N, Cristofanilli M, Anderson K, et al. Breast cancer molecular subtypes respond differently to preoperative chemotherapy. *Clin Cancer Res* 2005; **11**: 5678-85. doi: 10.1158/1078-0432.CCR-04-2421
- Yersal O, Barutca S. Biological subtypes of breast cancer: prognostic and therapeutic implications. *World J Clin Oncol* 2014; **5**: 412-24. doi: 10.5306/wjco.v5.i3.412
- Wolmark N, Wang J, Mamounas E, Bryant J, Fisher B. Preoperative chemotherapy in patients with operable breast cancer: nine-year results from National Surgical Adjuvant Breast and Bowel Project B-18. *J Natl Cancer Inst Monogr* 2001; **30**: 96-102. PMID: 11773300
- Gianni L, Baselga J, Eiermann W, Porta VG, Semiglazov V, Lluch A, et al. Phase III trial evaluating the addition of paclitaxel to doxorubicin followed by cyclophosphamide, methotrexate, and fluorouracil, as adjuvant or primary systemic therapy: European Cooperative Trial in Operable Breast Cancer. *J Clin Oncol* 2009; **27**: 2474-81. doi: 10.1200/JCO.2008.19.2567
- Kong X, Moran MS, Zhang N, Haffty B, Yang Q. Meta-analysis confirms achieving pathological complete response after neoadjuvant chemotherapy predicts favourable prognosis for breast cancer patients. *Eur J Cancer* 2011; **47**: 2084-90. doi: 10.1016/j.ejca.2011.06.014
- Murphy BL, Day CN, Hoskin TL, Habermann EB, Boughey JC. Neoadjuvant chemotherapy use in breast cancer is greatest in excellent responders: triple-negative and HER2+ subtypes. *Ann Surg Oncol* 2018; **25**: 2241-8. doi: 10.1245/s10434-018-6531-5
- Boughey J, McCall L, Ballman K, Mittendorf EA, Ahrendt GM, Wilke LG, et al. Tumor biology correlates with rates of breast-conserving surgery and pathologic complete response after neoadjuvant chemotherapy for breast cancer. *Ann Surg* 2014; **260**: 608-16. doi: 10.1097/SLA.0000000000000924
- von Minckwitz G, Untch M, Blohmer JU, Costa SD, Eidtmann H, Fasching PA, et al. Definition and impact of pathologic complete response on prognosis after neoadjuvant chemotherapy in various intrinsic breast cancer subtypes. *J Clin Oncol* 2012; **30**: 1796-804. doi: 10.1200/JCO.2011.38.8595
- Cortazar P, Zhang L, Untch M, Mehta K, Costantino JP, Wolmark N, et al. Pathological complete response and long-term clinical benefit in breast cancer: the CTNeoBC pooled analysis. *Lancet* 2014; **384**: 164-72. doi: 10.1016/S0140-6736(13)62422-8
- Boughey JC, Ballman KV, McCall LM, Mittendorf EA, Symmans WF, Julian TB, et al. Tumor biology and response to chemotherapy impact breast cancer-specific survival in node-positive breast cancer patients treated with neoadjuvant chemotherapy: long-term follow-up from ACOSOG Z1071 (Alliance). *Ann Surg* 2017; **266**: 667-76. doi: 10.1097/SLA.0000000000002373
- Dialani V, Chadashvili T, Slanetz PJ. Role of imaging in neoadjuvant therapy for breast cancer. *Ann Surg Oncol* 2015; **22**: 1416-24. doi: 10.1245/s10434-015-4403-9
- Straver ME, Loo CE, Rutgers EJ, Oldenburg HS, Wesseling J, Vrancken Peeters MJ, et al. MRI model to guide the surgical treatment in breast cancer patients after neoadjuvant chemotherapy. *Ann Surg* 2010; **251**: 701-7. doi: 10.1097/SLA.0b013e3181c5dda3
- De los Santos J, Cantor A, Amos KD, Forero A, Golshan M, Horton JK, et al. Magnetic resonance imaging as a predictor of pathologic response in patients treated with neoadjuvant systemic treatment for operable breast cancer. Translational Breast Cancer Research Consortium trial 017. *Cancer* 2013; **119**: 1776-83. doi: 10.1002/cncr.27995
- McGuire KP, Toro-Burguete J, Dang H, Young J, Soran A, Zuley M, et al. MRI staging after neoadjuvant chemotherapy for breast cancer: does tumor biology affect accuracy? *Ann Surg Oncol* 2011; **18**: 3149-54. doi: 10.1245/s10434-011-1912-z
- Fukuda T, Horii R, Gomi N, Miyagi Y, Takahashi S, Ito Y, et al. Accuracy of magnetic resonance imaging for predicting pathological complete response of breast cancer after neoadjuvant chemotherapy: association with breast cancer subtype. *Springerplus* 2016; **5**: 152. doi: 10.1186/s40064-016-1800-x
- Bouzón A, Acea B, Soler R, Iglesias Á, Santiago P, Mosquera J, et al. Diagnostic accuracy of MRI to evaluate tumour response and residual tumour size after neoadjuvant chemotherapy in breast cancer patients. *Radiol Oncol* 2016; **50**: 73-9. doi: 10.1515/raon-2016-0007
- Goldhirsch A, Winer EP, Coates AS, Gelber RD, Piccart-Gebhart M, Thürlimann B, et al. Personalizing the treatment of women with early breast cancer: highlights of the St Gallen International Expert Consensus on the Primary Therapy of Early Breast Cancer 2013. *Ann Oncol* 2013; **24**: 2206-23. doi: 10.1093/annonc/mdt303
- Rosen EL, Blackwell KL, Baker JA, Soo MS, Bentley RC, Yu D, et al. Accuracy of MRI in the detection of residual breast cancer after neoadjuvant chemotherapy. *Am J Roentgenol* 2003; **181**: 1275-82. doi: 10.2214/ajr.181.5.1811275

19. Yeh E, Slanetz P, Kopans DB, Rafferty E, Georgian-Smith D, Moy L, et al. Prospective comparison of mammography, sonography, and MRI in patients undergoing neoadjuvant chemotherapy for palpable breast cancer. *Am J Roentgenol* 2005; **184**: 868-77. doi: 10.2214/ajr.184.3.01840868
20. Croshaw R, Shapiro-Wright H, Svensson E, Erb K, Julian T. Accuracy of clinical examination, digital mammogram, ultrasound, and MRI in determining postneoadjuvant pathologic tumor response in operable breast cancer patients. *Ann Surg Oncol* 2011; **18**: 3160-3. doi: 10.1245/s10434-011-1919-5
21. Orel S. Who should have breast magnetic resonance imaging evaluation? *J Clin Oncol* 2008; **26**: 703-11. doi: 10.1200/JCO.2007.14.3594
22. Eom HJ, Cha JH, Choi WJ, Chae EY, Shin HJ, Kim HH. Predictive clinicopathologic and dynamic contrast-enhanced MRI findings for tumor response to neoadjuvant chemotherapy in triple-negative breast cancer. *Am J Roentgenol* 2017; **208**: 225-30. doi: 10.2214/AJR.16.17125
23. Wang J, Buchholz TA, Middleton L, Allred DC, Tucker SL, Kuerer HM, et al. Assessment of histologic features and expression of biomarkers in predicting pathologic response to anthracycline-based neoadjuvant chemotherapy in patients with breast cancer. *Cancer* 2002; **94**: 3107-14. doi: 10.1002/cncr.10585
24. Goorts B, van Nijnatten TJ, de Munck L, Moosdorff M, Heuts EM, de Boer M, et al. Clinical tumor stage is the most important predictor of pathological complete response rate after neoadjuvant chemotherapy in breast cancer patients. *Breast Cancer Res Treat* 2017; **163**: 83-91. doi: 10.1007/s10549-017-4155-2
25. Bahri S, Chen JH, Mehta RS, Carpenter PM, Nie K, Kwon SY, et al. Residual breast cancer diagnosed by MRI in patients receiving neoadjuvant chemotherapy with and without bevacizumab. *Ann Surg Oncol* 2009; **16**: 1619-28. doi: 10.1245/s10434-009-0441-5
26. Ko ES, Han BK, Kim RB, Ko EY, Shin JH, Hahn SY, et al. Analysis of factors that influence the accuracy of magnetic resonance imaging for predicting response after neoadjuvant chemotherapy in locally advanced breast cancer. *Ann Surg Oncol* 2013; **20**: 2562-8. doi: 10.1245/s10434-013-2925-6
27. Moon H-G, Han W, Ahn SK, Cho N, Moon WK, Im SA, et al. Breast cancer molecular phenotype and the use of HER2-targeted agents influence the accuracy of breast MRI after neoadjuvant chemotherapy. *Ann Surg* 2013; **257**: 133-7. doi:10.1097/SLA.0b013e3182686bd9
28. Patel BK, Hilal T, Covington M, Zhang N, Kosiorek HE, Lobbes M, et al. Contrast-enhanced spectral mammography is comparable to MRI in the assessment of residual breast cancer following neoadjuvant systemic therapy. *Ann Surg Oncol* 2018; **25**: 1350-6. doi: 10.1245/s10434-018-6413-x
29. Rauch GM, Kuerer HM, Adrada B, Santiago L, Moseley T, Candelaria RP, et al. Biopsy feasibility trial for breast cancer pathologic complete response detection after neoadjuvant chemotherapy: imaging assessment and correlation endpoints. *Ann Surg Oncol* 2018; **25**: 1953-60. doi:10.1245/s10434-018-6481-y
30. Heldahl MG, Lundgren S, Jensen LR, Gribbestad IS, Bathen TF. Monitoring neoadjuvant chemotherapy in breast cancer patients: improved MR assessment at 3 T? *J Magn Reson Imaging* 2011; **34**: 547-56. doi: 10.1002/jmri.22642

Diagnostic accuracy of haemophilia early arthropathy detection with ultrasound (HEAD-US): a comparative magnetic resonance imaging (MRI) study

Domen Plut^{1,2}, Barbara Faganel Kotnik^{2,3}, Irena Preloznik Zupan^{2,4}, Damjana Kljucsevsek^{2,3}, Gaj Vidmar^{2,5}, Ziga Snoj^{1,2}, Carlo Martinoli⁶, Vladka Salapura^{1,2}

¹ Clinical Radiology Institute, University Medical Centre Ljubljana, Ljubljana, Slovenia

² Faculty of Medicine, University of Ljubljana, Ljubljana, Slovenia

³ Division of Paediatrics, University Medical Centre Ljubljana, Ljubljana, Slovenia

⁴ Division of Internal Medicine, University Medical Centre Ljubljana, Ljubljana, Slovenia

⁵ University Rehabilitation Institute Republic of Slovenia, Ljubljana, Slovenia

⁶ School of Medicine and Pharmacy, University of Genoa, Genoa, Italy

Radiol Oncol 2019; 53(2): 178-186.

Received 21 February 2019

Accepted 25 April 2019

Correspondence to: Assist. Prof. Vladka Salapura, M.D., Ph.D., Clinical Radiology Institute, University Medical Centre Ljubljana, Zaloška cesta 7, SI-1000 Ljubljana, Slovenia. Phone: +386 1 522 85 30; Fax: +386 1 522 24 97; E-mail: salapura@siol.net

Disclosure: No potential conflicts of interest were disclosed.

Background. Repeated haemarthroses affect approximately 90% of patients with severe haemophilia and lead to progressive arthropathy, which is the main cause of morbidity in these patients. Diagnostic imaging can detect even subclinical arthropathy changes and may impact prophylactic treatment. Magnetic resonance imaging (MRI) is generally the gold standard tool for precise evaluation of joints, but it is not easily feasible in regular follow-up of patients with haemophilia. The development of the standardized ultrasound (US) protocol for detection of early changes in haemophilic arthropathy (HEAD-US) opened new perspectives in the use of US in management of these patients. The HEAD-US protocol enables quick evaluation of the six mostly affected joints in a single study. The aim of this prospective study was to determine the diagnostic accuracy of the HEAD-US protocol for the detection and quantification of haemophilic arthropathy in comparison to the MRI.

Patients and methods. The study included 30 patients with severe haemophilia. We evaluated their elbows, ankles and knees (overall 168 joints) by US using the HEAD-US protocol and compared the results with the MRI using the International Prophylaxis Study Group (IPSG) MRI score.

Results. The results showed that the overall HEAD-US score correlated very highly with the overall IPSG MRI score ($r = 0.92$). Correlation was very high for the evaluation of the elbows and knees ($r \approx 0.95$), and slightly lower for the ankles ($r \approx 0.85$).

Conclusions. HEAD-US protocol proved to be a quick, reliable and accurate method for the detection and quantification of haemophilic arthropathy.

Key words: haemophilia; haemophilic arthropathy; HEAD-US; ultrasound; magnetic resonance imaging

Introduction

Intra-articular joint bleeds (haemarthroses) affect approximately 90% of patients with severe haemophilia.¹ The most frequently involved joints are the ankles, knees, and elbows.² Repeated episodes of intra-articular bleeding lead to progressive ar-

thropathy, which is the main cause of morbidity in these patients.³ The prevention of the occurrence of haemarthrosis is therefore important for the prevention of the arthropathy.

Small intra-articular bleeds may be unnoticed at physical examination and the detection of early signs of osteochondral damage is difficult by

clinical evaluation. It is known that osteochondral damage can be present in the joints that are asymptomatic and in which none or just a few bleeding episodes were previously recognized.^{4,5} These subtle articular changes of the subclinical disease can be detected by diagnostic imaging. Consequently, based on the diagnostic findings, appropriate treatment can be introduced or modified to prevent further disease progression and disability.⁶⁻¹¹

Magnetic resonance imaging (MRI) is the modality of choice to evaluate the musculoskeletal system because of its excellent spatial and contrast resolution. By MRI, it is possible to detect disease specific findings and give an accurate visualization of early arthropathy changes. However, MRI is a modality of high cost, its time of examining is long, it is usually poorly accessible and as such, it is not suitable for multi-joint screening. Additionally, it requires sedation in young children.¹²

Ultrasound (US), with the advent of last generation equipment, has excellent spatial resolution for the superficial structures. By US, it is now possible to depict the small, superficial structures of the musculoskeletal system as present in the early stages of haemophilic arthropathy. Contrary to MRI, US has a low cost, the time of examining is short and it is widely accessible. The drawbacks for the use of US in musculoskeletal radiology are poor visualization of inner joint structures and lack of standardized evaluation and reporting. In the field of haemophilic arthropathy, the development of the standardized US protocol for the detection of early changes in haemophilic arthropathy (HEAD-US) by Martinoli *et al.* in 2013 opened new perspectives in the use of US in management of patients with haemophilia. The HEAD-US protocol and scoring method are rapid to perform and enable full screening of the six joints in a single study.⁶

The aim of the present study was to determine the diagnostic accuracy of the HEAD-US protocol and scoring method for the detection and quantification of haemophilic arthropathy in patients with haemophilia in comparison to MRI using the International Prophylaxis Study Group (IPSG) MRI scoring scale.

Patients and methods

Patients

All patients were recruited at the Slovenian National Haemophilia Comprehensive Care Centre at the University Medical Centre Ljubljana. The inclusion criteria were age over 16 years, diagnosis

of a severe haemophilia A or B and prophylactic treatment with factor concentrates. Exclusion criteria were non-cooperation and contraindications for the MRI examination. Patients with prosthetic joints were allowed to participate in the study, but the prosthetic joint was not evaluated. The study group included a total of 30 patients (age range 16 to 49, mean age 33) who were willing to participate and met the aforementioned criteria. In 23 patients, six joints (elbows, knees and ankles) were systematically examined by US and MRI according to the protocols. One out of six joints was not examined in six patients due to a prosthetic implant. Two joints were excluded from the evaluation in the patient who had left lower limb amputation. The elbows were excluded in two patients because MRI could not be performed due to patient discomfort. Overall, 168 joints were examined in this study: 59 elbows, 53 knees and 56 ankles. The clinical evaluation of the joints according to the haemophilia joint health score HJHS 2.1 was obtained by a trained haemathologist on the day of the imaging examinations.

This prospective observational study was performed at a single tertiary center from June 2016 to March 2017. Research was conducted following the Helsinki Declaration. All patients included in the study provided a written informed consent for study participation. The National Medical Ethics Committee approved the study (Project number 70/11/15, approved on 11/21/2015).

Diagnostic imaging

In each patient, the US and MRI examinations were performed on the same day.

Ultrasound

US examinations were performed using a 13–5 MHz electronic linear-array transducer on a ProSound F75 scanner (Hitachi Aloka Medical, Ltd. Tokyo, Japan) by an experienced radiologist using the HEAD-US protocol and scoring method described elsewhere.⁶ The total scanning time per patient for all six joints combined was approximately 20 minutes. A series of images from 10 US examinations were reviewed and scored by another radiologist to determine the inter-rater reliability. This latter reviewer was blinded from the original scores of the examinations.

Magnetic resonance imaging

MRI was performed on a 3 Tesla unit (Achieva, Philips Healthcare, Eindhoven, The Netherlands).

TABLE 1. Baseline characteristics of the study population

Age: median; range (years)	33; 16–49					
Age of start of prophylaxis: mean (years)	17.4					
age group: 0–9 (patient count)	7					
age group: 10–19 (patient count)	14					
age group: 20+ (patient count)	9					
Duration of prophylaxis: mean (years)	15.4					
	Ankles		Knees		Elbows	
	Right	Left	Right	Left	Right	Left
No. of joints	30	29	25	28	28	28
No. of lifetime joint bleeds:						
0–5 (joint count)	5	5	12	15	14	13
6–20 (joint count)	12	11	7	10	4	2
> 20 (joint count)	13	12	5	3	9	12
Unknown (joint count)	0	1	1	0	1	1
HJHS 2.1 score: mean; max*	3.3; 12	2.6; 11	1.4; 7	1.2; 8	1.9; 9	1.9; 8

* Minimum was 0 for all the scores

An 8 elements phased array SENSE knee coil was used for the knee imaging, an 8 elements phased-array SENSE foot-ankle coil for the ankle imaging, and two 2 elements phase-array SENSE flex coils for the elbow imaging. The protocol included 3D T2*-weighted water selective gradient echo sequence (FOV, 160×160×108mm; voxel size, 0.58×0.58×0.50mm; flip angle: 15°; TE, 9.2/6.1ms; TR, 26ms), and 3D proton density (PD) weighted turbo spin echo sequence (FOV, 160×160×161mm; voxel size: 0.52×0.52×0.52mm; TE, 33ms; TR, 1000ms). The total scanning time was approximately 15 minutes per joint. In each patient, all joints were scanned in a single session for a total examination time extending up to two hours. After examining each joint, the patient was encouraged to stretch the body while the coils for the imaging of the next joint were setup. As mentioned, two MRI examinations were incomplete due to patient discomfort. All the MRI examinations were scored according to the International Prophylaxis Study Group (IPSG) MRI scale described elsewhere.¹³ The scoring was performed by an experienced musculoskeletal radiologist who was blinded regarding the results of the HEAD-US examinations. Additionally, the datasets of 10 MRI examinations were reviewed and scored by another experienced musculoskeletal radiologist to determine the inter-rater reliability. This latter reader was blinded from the original IPSG scores of the MRI examinations and from the HEAD-US scores.

Statistical analysis

Descriptive statistics were obtained to describe characteristics of the study group. We checked the inter-rater reliability of HEAD-US and MRI for the total scores using intra-class correlation (two-way mixed model, ICC(2,1)) and for all the sub-scores using Cohen's kappa statistics (with quadratic weights). We analyzed the agreement between HEAD-US and MRI using the Pearson correlation coefficient (r) for the total score and separately for the hypertrophic synovium, cartilage degradation, and bone changes (we could not use agreement coefficients because all those scores derive from different scales for HEAD-US and MRI). Regarding the agreement between HEAD-US and MRI for the cartilage degradation, we used Cohen's Kappa (with quadratic weights), because both scores are based on the same (0–4) scale. Agreement was illustrated using the concordance bubble plots.¹⁴

Results

Baseline characteristics of the study group are shown in Table 1. In our series, all patients underwent prophylactic treatment for haemophilia: 7 patients started therapy before the age of 10 years, 14 patients between 10 and 19 years, and 9 patients after the age of 20 years. The mean age at which prophylactic treatment was started was 17.4 years and the mean duration of the prophylaxis was 15.4 years.

In our series, the disease presentation was quite variable with a mean HJHS 2.1 score of 2.3 (range 0–12). HJHS scores were the highest in the ankle and the lowest in the knee, and correlated well with the lifetime number of joint bleeding episodes. The ankles were the joints with the most often recorded history of prior bleeds: 42% of examined ankles had >20 prior lifetime bleeds recorded. The knees were the least affected joints, with 51% of the examined knees having <5 prior lifetime bleeds recorded.

Inter-rater reliability

The inter-rater reliability of the interpretation was excellent for the US examinations (ICC values 0.960–0.996 for total score, median κ across sub-scores 1.000) and for the MRI (ICC values 0.957–0.990 for total score, median κ across sub-scores 0.815).

Diagnostic accuracy of ultrasound

HEAD-US scores were correlated with the IPSG MRI scores; results are shown in Table 2. A high overall correlation was found between the scores ($r \approx 0.92$). Correlation for the overall scores at the joint level was nearly perfect in the elbows and knees ($r \approx 0.95$) and slightly lower, but still very high in the ankles ($r \approx 0.85$). Separate evaluation of each parameter of the joint (synovial hypertrophy, cartilage degradation, bone changes) showed a medium-high to high agreement for all the parameters. The correlation between the HEAD-US and MRI scores was the lowest for the evaluation of the synovium hypertrophy and cartilage degradation at the ankle level ($r \approx 0.55$). All other parameters showed a high agreement between the methods ($r > 0.70$).

Concordance bubble plot for agreement between the HEAD-US and MRI scores at all three joint levels is shown in Figure 1. The distribution of circles within the plots demonstrates the variable degree of haemophilic arthropathy presentation in our study group at all joint levels. The plots also explicitly demonstrate the high overall correlation between the HEAD-US and MRI scores. The biggest deviation from the perfect line is shown at the ankle level, in the ankles with higher degree of haemophilic arthropathy.

In our series there were 42 joints with no haemophilic arthropathy, that are the joints scored with 0 by the IPSG MRI scoring system: 19 elbows, 20 knees and 3 ankles. In 35 of those joints the HEAD-US score was also 0. An example of a perfect concordance between the US and MRI examination for a knee with no haemophilic arthropathy is shown in Figure 2. In 7 joints with the IPSG MRI score 0 the HEAD-US score was 1. These HEAD-US examinations are false positives for the presence of

TABLE 2. Correlation between the HEAD-US and IPSG MRI scores

	Elbows	Knees	Ankles	All joints
Overall score (r)	0.949	0.941	0.838	0.921
Detailed scores:				
Synovial hypertrophy (r)	0.840	0.710	0.561	
Cartilage degradation (r)	0.734	0.812	0.537	
Bone changes (r)	0.883	0.741	0.725	

Notes: all the reported correlations are statistically significant ($p < 0.001$); the values for the elbows, knees and ankles are the averages over the right and left side values (the differences between them were negligible); the correlations are averaged using Fisher-z transformation.

haemophilic arthropathy. The false positive rate was 16.7%, which means specificity of HEAD-US to diagnose haemophilic arthropathy in our study was 83.3%. Detailed evaluation of the false positive examinations reveals that the findings diagnosed by US and not confirmed by MRI were: mild synovium hypertrophy in one elbow and two knees, small cartilage defect in two elbows and one ankle, and a small osteophyte in one knee.

Conversely, there were 6 joints that were scored with 0 by HEAD-US and scored positive by the IPSG MRI scoring. These HEAD-US examinations are the false negatives for the presence of haemophilic arthropathy. The false negative rate was 4.8%, which means the sensitivity of HEAD-US to diagnose haemophilic arthropathy in our study was 95.2%. Detailed evaluation of the false negative examinations reveals that the findings missed by US were: a cartilage defect at the tibial side of the talocrural joint (Figure 3), a small synovium hypertrophy in the posterior recess in another ankle, two small cartilage defects at the ulnar side of the joint in elbows, and two small osteochondral lesions at the ulnar side of the joint in another two

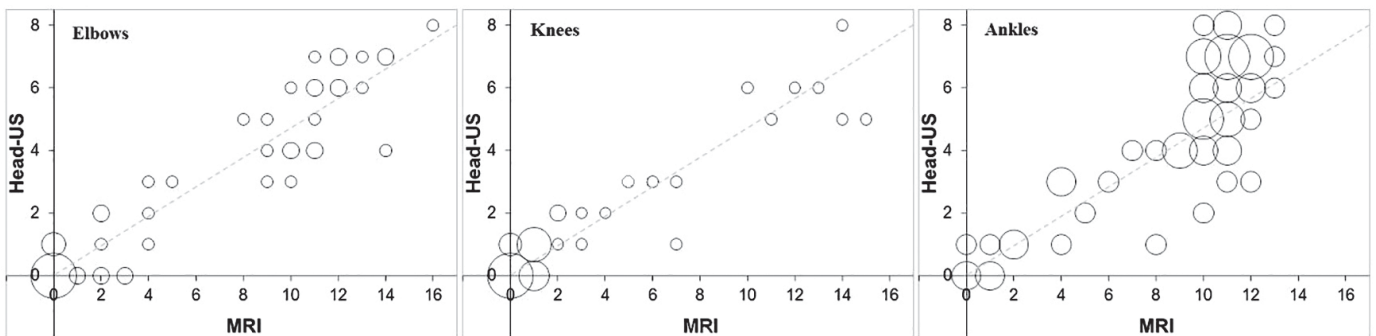


FIGURE 1. Concordance bubble-plot for depicting agreement between HEAD-US and MRI score for all three joints. The circles are centered at the observed combinations of the HEAD-US and MRI scores; their size is proportional to the number of the patients with a given combination. Dashed line represents a perfect agreement.

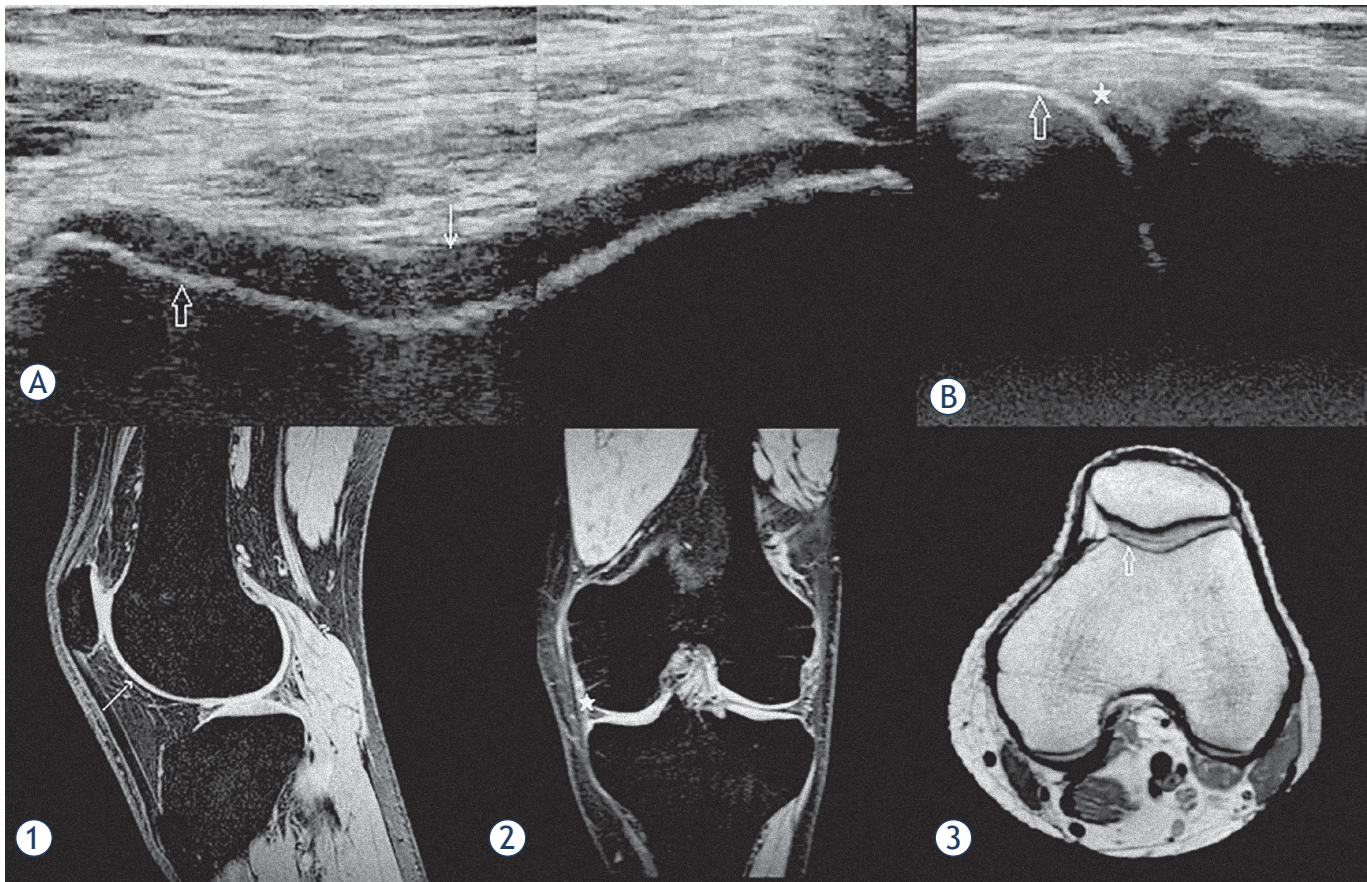


FIGURE 2. An example of a good concordance between HEAD-US and MRI. US images of the femoral trochlea in the transverse plane (**A**) and the medial femorotibial space in the coronal plane (**B**) are shown. T2* weighted MR images in the sagittal (**1**) and coronal (**2**) planes and a PD weighted MR image in the transverse plane (**3**) of the same knee are shown for comparison of the corresponding structures. The smooth surface, normal thickness and homogenous structure of the trochlear joint cartilage are shown in the US image (**A**) (white arrow); the corresponding intact cartilage is shown on MR image (**1**). The intact cortical bone of the medial femoral condyle (hollow arrow) is shown by US in the images (**A**) and (**B**); the corresponding cortical bone is depicted by MRI in the image (**3**). No signs of synovium hypertrophy are shown by US in the medial femorotibial recess (white star) in the image B; the corresponding recess confirming no synovium hypertrophy is shown by MRI in the image (**2**). On MRI, there were also no arthropathic changes in the parts of the joint not visualized by US. The images show a perfect concordance between US and MRI findings in this knee with no signs of haemophilic arthropathy.

elbows (images not shown). All the described osteochondral pathologic changes of haemophilic arthropathy were outside the area of visualization by US.

The positive predictive value for the presence of haemophilic arthropathy by HEAD-US in our study was 94.5% and the negative predictive value 85.4%.

Discussion

The aim of the study was to evaluate the diagnostic accuracy of US for the detection and quantification of haemophilic arthropathy using the HEAD-US protocol and scoring method in comparison to MRI using the IPSPG MRI scoring scale. We evalu-

ated the three most commonly affected joints in patients with severe haemophilia: the elbows, knees and ankles. Overall, we evaluated 168 joints: 59 elbows, 53 knees and 56 ankles. The sensitivity of HEAD-US to detect the signs of haemophilic arthropathy in our study was 95.2%; the specificity was 83.3%. The results of the correlation analysis showed a very high correlation for the quantification of haemophilic arthropathy between US using the HEAD-US protocol and scoring method and MRI using the IPSPG MRI score ($r = 0.921$, $p < 0.001$). The correlation was nearly perfect for the elbows and knees ($r \approx 0.95$), and very high for the ankles ($r \approx 0.85$). Excellent inter-rater reliability in our study for both MRI and US further support the validity of both scales (ICC values 0.960–0.996 for US, and ICC values 0.957–0.990 for MRI).

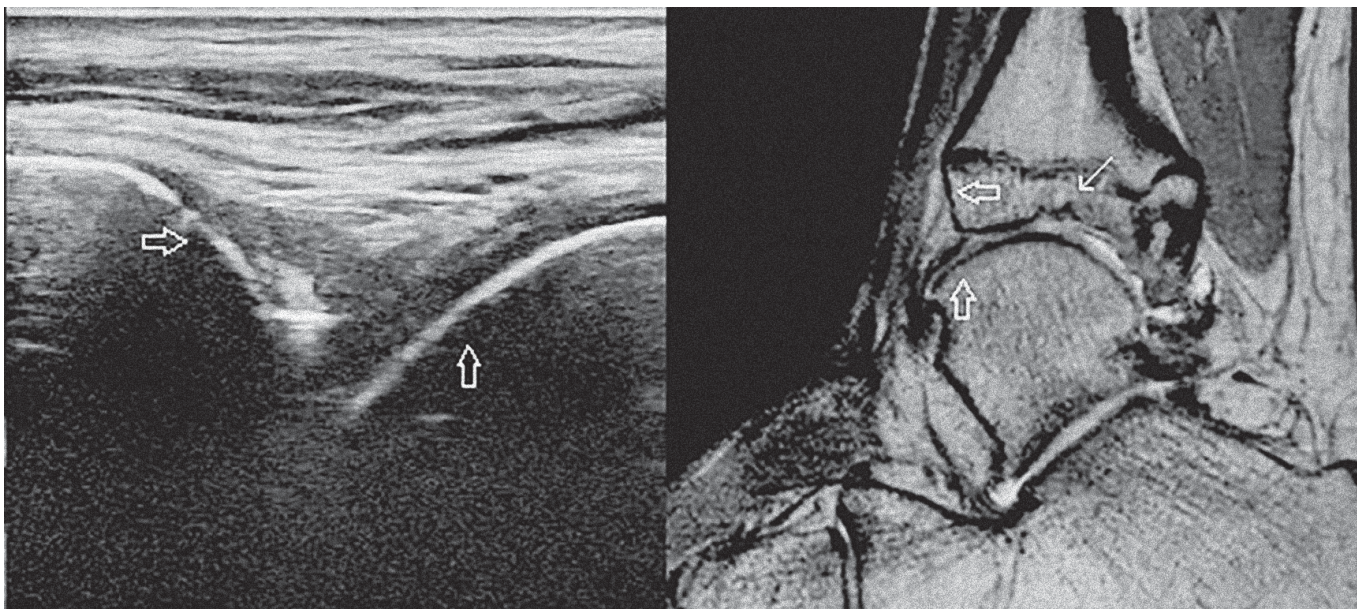


FIGURE 3. An example of a discordance between US and MRI. An US image of the tibiotalar joint in the sagittal plane is shown on the left, a PD weighted MR image of the same ankle in the sagittal plane is shown on the right for comparison of the corresponding structures. In both images, the smooth surface of the tibial cortical bone is marked by the horizontal hollow arrow and the smooth surface of the talar cortical bone is marked by the vertical hollow arrow. MRI demonstrates an osteochondral defect at the tibial side of the talocrural joint (white arrow), which is outside of the visualization area of US.

These results show that the HEAD-US method is highly accurate and reliable in comparison to MRI for detection and quantification of haemophilic arthropathy changes. High sensitivity and specificity verify the method is a dependable tool for the recognition of presence of arthropathy changes. High correlation proves a great value of the method for evaluation of pathology at any different stage of the disease. Our results indicate that HEAD-US is equally applicable for all evaluated joints. However, we noticed some differences in evaluation of specific parameters in the ankle joint. The agreement between the methods for the evaluation of the ankles in comparison to the other joints was lower for the osteochondral changes (especially cartilage degradation, $r = 0.54$ for the ankles, 0.81 for knees, and 0.73 for elbows) and for the synovium hypertrophy ($r = 0.56$ for the ankles, 0.71 for knees and 0.84 for elbows). The lower agreement for the osteochondral changes in the ankles is likely due to the limited visualization of the weight-bearing part of the osteochondral surface of the ankle joint by US. By US, only a part of the osteochondral surface of the talar dome is accessible for the evaluation, whereas MRI enables optimal visualization of the whole osteochondral surfaces of the talocrural and talocalcaneal joints. The lower agreement for the synovium hypertro-

phy in the ankles between US and MRI could be because of the ability of MRI to depict haemosiderin deposits in the synovia that appear due to the susceptibility artifact. This artifact allows great visualization of the synovia with haemosiderin deposits on MRI even when the synovia is not extensively hypertrophied. The ankles were in average the most affected joints in our study (HJHS average score of 8.9 , compared to 5.5 for the elbows and 2.7 for the knees); consequently, this fact may have the biggest impact in the ankles. Another reason for the lower agreement for the synovial hypertrophy is probably in the scoring scales: minimal hypertrophy of the synovium is scored 0 by the HEAD-US scoring scale, while it is scored 1 on the IPSG MRI scale.

In the literature, some studies investigated the diagnostic accuracy of US in the assessment of haemophilic arthropathy in comparison with MRI.^{5,15-18} These studies showed promising results for US and stressed the importance of further research in this field.^{5,19} In comparison to these studies, our study included a larger cohort of 168 joints and included all three mostly involved joints with a wide range of haemophilic arthropathy presentation. These characteristics make our study the biggest and most comprehensive study for the evaluation of diagnostic accuracy of US for detection and quanti-

fication of haemophilic arthropathy in comparison to MRI to date.

In a recent study published in May 2018 by Foppen *et al.*, the HEAD-US system was compared with MRI using the IPSPG MRI scoring scale. Their study evaluated knees and ankles of 24 patients with haemophilia with no or minimal arthropathy. The study demonstrated a strong correlation between the HEAD-US score and the IPSPG MRI score for the evaluation of the synovium hypertrophy ($r = 0.90$, $p < 0.01$), cartilage degradation ($r = 0.73$, $p < 0.01$) and bone changes ($r = 0.88$, $p < 0.01$).¹⁵ Comparing their results to the results of our study, the biggest discrepancy is in the correlation between the methods for the evaluation of the synovium hypertrophy. In their study, the correlation between US and MRI was the highest for the evaluation of synovium hypertrophy of all evaluated parameters of the joint, whereas in our study, the correlation between US and MRI was the lowest for the evaluation of synovium hypertrophy in comparison to other joint parameters, especially at the ankle level. We believe the key for the differences in the results between our studies is in the evaluation of the synovium hypertrophy by MRI. The assessment of the degree of synovium hypertrophy is not clearly defined in the IPSPG MRI scoring scale; it is defined as no, small, moderate, or large hypertrophy, with no objective measurements to define the different degrees. In their study, the authors determined the lower cut-off values for the synovium measurements to define the presence/absence of synovium hypertrophy on MRI.¹⁵ In our study, any impression of synovium hypertrophy, due to a focal increase in thickness or loss of signal due to the susceptibility artifact was evaluated as synovium hypertrophy by the MRI reviewers. Consequently, in our study some more minimal synovium hypertrophy was scored 1 by the IPSPG MRI scale, which was not scored by the HEAD-US. As already mentioned earlier, minimal synovial hypertrophy is scored 0 by the HEAD-US scoring scale. Nevertheless, the results of both studies prove that the HEAD-US method is a reliable tool for the detection and quantification of haemophilic arthropathy with significant correlation to the evaluation by MRI.

The other comparable studies also presented a high correlation between US and MRI, with some differences in the methodology used. Doria *et al.* evaluated 34 ankles and 25 knees in two centers, using IPSPG MRI scale as a reference standard. Their US examination was comprehensive with an US scoring scale corresponding to the items evalu-

ated in the IPSPG MRI scale. Their results showed that when data was acquired by radiologists, US was highly reliable for assessing soft-tissue changes (ICC 0.98 for ankles and 0.97 for knees) and substantially to highly reliable for assessing osteochondral changes (ICC 0.61 for ankles and 0.89 for knees).¹⁶ Sierra Aisa *et al.* evaluated 30 joints (knees and ankles), comparing findings detected by a comprehensive US exam to findings found on MRI. The parameters used for MRI analysis were the same as analyzed by US. Their results showed a good positive correlation between US and MRI in detecting synovial hypertrophy ($\kappa = 0.839$ – 1.000) and erosions ($\kappa = 0.850$ – 1.000). They showed lower correlation between the methods for detecting bone cysts ($\kappa = 0.643$ – 0.552) and cartilage loss ($\kappa = 0.643$ – 0.462).¹⁷ Di Minno *et al.* evaluated 40 clinically asymptomatic joints (knees, elbows and ankles) in patients with haemophilia, evaluating ability of US to detect early haemophilic arthropathy. A comprehensive US examination with Doppler was performed for joint evaluation, progressive and additive MRI scales were used as a reference standard. Their results showed significant correlation between US and MRI ($r = 0.732$ for the additive MRI scale, $r = 0.598$ for the progressive MRI scale).⁵ Acharya *et al.* compared power Doppler and grey-scale US findings with dynamic contrast enhanced MRI in 33 joints (elbows, knees and ankles). Their results showed a strong correlation between US and MRI in assessment of synovial hypertrophy ($r = 0.70$) and vascularity ($r = 0.73$).¹⁸

All the aforementioned studies were based on comprehensive US protocols that were very complex, with only trained readers potentially able to get an acceptable reproducibility. In the present paper, we used a simplified HEAD-US scanning protocol and scoring method which was developed for non-imaging specialists to enable them to analyze the joints at the time and place of patient care (point-of-care). The HEAD-US system includes systematic evaluation of the recesses of the elbow, knee, and ankle for the detection of synovium hypertrophy and evaluation of a single osteochondral surface in the elbow (anterior aspect of the distal humeral epiphysis), knee (femoral trochlea) and ankle (the anterior aspect of the talar dome) for the detection of osteochondral damage. The rationale of selecting one reference surface is based on the evidence that the diffuse establishment of osteochondral damage in haemophilic arthropathy may warrant the policy of considering one surface representative of the overall status of the joint without significantly reducing the sensitivity of the meth-

od. This keeps the HEAD-US method easy and fast to perform, thus enabling the examiner to screen the six joints of interest in a single study.⁶ In our study, the HEAD-US was performed by an experienced radiologist. The results of our study prove, that even this simplified US examination is reliable and accurate for the detection and quantification of haemophilic arthropathy.

Regarding the inter-rater reliability of US and MRI scores, an excellent agreement between readers was noted in our study, a finding that is supported by previous studies with US^{15,20} and MRI.^{13,15}

Generally speaking, MRI is still the only widely validated gold standard tool for precise evaluation of joints. MRI scoring scales have been widely used and approved as reference standards in haemophilic arthropathy trials, although barely applied in clinical practice for diagnosis and outcome, because of their complexity, time commitment and cost. In our study, the protocol used for MR imaging was optimized for the detection of early haemophilic arthropathy. It achieved good visualization of the cortical bone, articular cartilage and synovium hypertrophy, including haemosiderin deposits, while keeping the examination time as short as possible. Despite keeping the examination time very short, we encountered the typical problems related to this modality. One patient was claustrophobic, so imaging of all joints was not possible on MRI. In several patients, immobilization was uncomfortable, caused pain and the process of image acquisition was impaired by motion artifact and imaging had to be repeated. On the contrary, US due to its great availability, low cost and feasibility is a great method for diagnostic evaluation and regular follow-up of patients with haemophilia. The development of the standardized and simplified HEAD-US protocol and scoring method made a crucial step towards wider clinical application with ability to perform it quickly and with high reproducibility. Regarding the evaluation by HEAD-US, the joints affected by severe arthropathy with prominent osteophytes and narrowed joint space were somewhat more demanding to evaluate. However, the interpretation that the joint status was severely compromised was straightforward. Our study results prove that this fast and simplified protocol is diagnostically accurate and reliable. For this reason we believe that HEAD-US is the most appropriate method for regular screening and patient follow-up. We implemented this method into our regular clinical practice during yearly follow-up of pediatric patients with haemophilia in 2017. Since then we managed to include all pediatric patients with

haemophilia in our country into the regular screening program.

Although, our study group included all patients with severe haemophilia in Slovenia aged 16–50 years, we had a relatively small number of patients with an early haemophilic arthropathy. This gave us only a limited insight into depiction of early arthropathy changes.

Conclusions

In our study, the HEAD-US protocol and scoring method proved to be a quick, reliable and accurate method for the detection and quantification of haemophilic arthropathy in comparison to MRI. HEAD-US shows great promise in diagnostics and regular follow-up of patients with haemophilia, possibly influencing prophylactic treatment to prevent occurrence of haemophilic arthropathy, especially in children, or prevent disease progression. Further long-term studies are needed to evaluate the role of US in modification of prophylactic therapy and prevention of haemophilic arthropathy or its progression.

References

- Hilgartner MW. Current treatment of hemophilic arthropathy. *Curr Opin Pediatr* 2002; **14**: 46-9. PMID: 11880733
- Dalyan M, Tuncer S, Kemahli S. Hemophilic arthropathy: evaluation of clinical and radiological characteristics and disability. *Turk J Pediatr* 2000; **42**: 205-9. PMID: 11105618
- Roosendaal G, Lafeber FP. Pathogenesis of haemophilic arthropathy. *Haemophilia* 2006; **12**: 117-21. doi: 10.1111/j.1365-2516.2006.01268.x
- Manco-Johnson MJ, Abshire TC, Schapiro AD, Riske B, Hacker MR, Kilcoyne R, et al. Prophylaxis versus episodic treatment to prevent joint disease in boys with severe hemophilia. *N Engl J Med* 2007; **357**: 535-44. doi: 10.1056/NEJMoa067659
- Di Minno MND, Iervolino S, Soscia E, Tosetto A, Coppola A, Schiavulli M et al. Magnetic resonance imaging and ultrasound evaluation of "healthy" joints in young subjects with severe haemophilia A. *Haemophilia* 2013; **19**: e167-73. doi: 10.1111/hae.12107
- Martinoli C, Della Casa Alberighi O, Di Minno G, Graziano E, Molinari AC, Pasta G, et al. Development and definition of a simplified scanning procedure and scoring method for haemophilia early arthropathy detection with ultrasound (HEAD-US). *J Thromb Haemost* 2013; **109**: 1170-9. doi: 10.1160/th12-11-0874
- Berntorp E, Boulyjenkov V, Brettler D, Chandy M, Jones P, Lee C, et al. Modern treatment of haemophilia. *Bull World Health Organ* 1995; **73**: 691-701. PMID: 8846496
- Ljung R. Paediatric care of the child with haemophilia. *Haemophilia* 2002; **8**: 178-82. doi: 10.1046/j.1365-2516.2002.00631.x
- Nilsson IM, Berntorp E, Lofqvist T, Pettersson H. Twenty-five years' experience of prophylactic treatment in severe haemophilia A and B. *J Intern Med* 1992; **232**: 25-32. doi: 10.1111/j.1365-2796.1992.tb00546.x
- Rosendaal FR, Smit C, Varekamp I, Brocker-Vriends AH, van Dijk H, Suurmeijer TP, et al. Modern haemophilia treatment: medical improvements and quality of life. *J Intern Med* 1990; **228**: 633-40. doi: 10.1111/j.1365-2796.1990.tb00291.x

11. Berntorp E. Joint outcomes in patients with haemophilia: the importance of adherence to preventive regimens. *Haemophilia* 2009; **15**: 1219-27. doi: 10.1111/j.1365-2516.2009.02077.x
12. Kilcoyne RF, Nuss R. Radiological assessment of haemophilic arthropathy with emphasis on MRI findings. *Haemophilia* 2003; **9**: 57-63. doi: 10.1046/j.1365-2516.9.s1.11.x
13. Lundin B, Manco-Johnson ML, Ignas DM, Moineddin R, Blanchette VS, Dunn AL, et al; International Prophylaxis Study Group. An MRI scale for assessment of haemophilic arthropathy from the International Prophylaxis Study Group. *Haemophilia* 2012; **18**: 962-70. doi: 10.1111/j.1365-2516.2012.02883.x
14. Vidmar G, Rode N. Visualizing concordance. *Comput Stat* 2007; **22**: 499-509. doi: 10.1007/s00180-007-0057-9
15. Foppen W, der Schaaf ICV, Beek FJA, Mali WPTM, Fischer K. Diagnostic accuracy of point-of-care ultrasound for evaluation of early blood-induced joint changes: comparison with MRI. *Haemophilia*; **24**: 971-9. doi: 10.1111/hae.13524
16. Doria AS, Keshava SN, Mohanta A, Jarrin J, Blanchette V, Srivastava A, et al. Diagnostic accuracy of ultrasound for assessment of hemophilic arthropathy: MRI correlation. *Am J Roentgenol* 2015; **204**: W336-47. doi: 10.2214/AJR.14.12501
17. Sierra Aisa C, Lucía Cuesta JF, Rubio Martínez A, Fernández Mosteirín N, Iborra Muñoz A, Abío Calvete M, et al. Comparison of ultrasound and magnetic resonance imaging for diagnosis and follow-up of joint lesions in patients with haemophilia. *Haemophilia* 2014; **20**: e51-7. doi: 10.1111/hae.12268
18. Acharya SS, Schloss R, Dyke JP, Mintz DN, Christos P, Dimichele DM, et al. Power Doppler sonography in the diagnosis of hemophilic synovitis - a promising tool. *J Thromb Haemost* 2008; **6**: 2055-61. doi: 10.1111/j.1538-7836.2008.03160.x
19. Ligocki CC, Abadeh A, Wang KC, Adams-Webber T, Blanchette VS, Doria AS. A systematic review of ultrasound imaging as a tool for evaluating haemophilic arthropathy in children and adults. *Haemophilia* 2017; **23**: 598-612. doi: 10.1111/hae.13163
20. Stephensen D, Classey S, Harbidge H, Patel V, Taylor S, Wells A. Physiotherapist inter-rater reliability of the haemophilia early arthropathy detection with ultrasound protocol. *Haemophilia* 2018; **24**: 471-6. doi: 10.1111/hae.13440

Efficacy and durability of radiopaque gelified ethanol in management of herniated discs

Dimitrij Kuhelj¹, Anita Dobrovec², Igor Jozef Kocijancic¹

¹ Clinical Radiology Institute, University Medical Centre Ljubljana, 1000 Ljubljana, Slovenia

² Celje General Hospital, Department of Radiology, 3000 Celje, Slovenia

Radiol Oncol 2019; 53(2): 187-193.

Received 21 February 2019

Accepted 25 April 2019

Correspondence to: Assist. Prof. Dimitrij Kuhelj, M.D., Ph.D., Councilor, Clinical Radiology Institute, University Medical Centre Ljubljana, Zaloška cesta 7, SI-1000 Ljubljana, Slovenia. Phone: + 386 41 882 991; Fax: +386 1 522 24 97; E-mail: dimitrij.kuhelj@guest.arnes.si

Disclosure: No potential conflicts of interest were disclosed.

Background. Percutaneous image-guided intradiscal injection of gelified ethanol was introduced to treat herniated disc disease lately. The aim of the study was to assess clinical efficacy and durability over a 36 months' period.

Patients and methods. Eighty-three patients (47 males, 36 females, mean age 48.9 years (18–79 years) were treated between May 2014 and December 2015 for 16 cervical and 67 lumbar chronic contained disc herniations. For pain assessment evaluation, the visual analog scale (VAS) was used. Physical activity, the use of analgesics, patients' satisfaction with the treatment results and patient's willingness to repeat the treatment were also evaluated.

Results. Fifty-nine patients responded to questionnaire. 89.8% had significant reduction in VAS after 1 month ($p < 0.001$); 76.9% of patients with cervical symptoms and 93.5% of patients with lumbar symptoms. In cervical group it remained stable, while in lumbar group VAS decreased even more during 36 months ($p = 0.012$). Single patient had spinal surgery. Moderate and severe physical disability prior to treatment (96.6%) was reduced to less than 30% after 12 months. The majority of active patients returned to their regular job (71.1%); 78% needed less analgesics. Only 5.1% patients were not satisfied with the treatment and 10.2% would not repeat the treatment if needed.

Conclusions. Percutaneous image-guided intradiscal injection of gelified ethanol is safe, effective and durable therapy for chronic contained cervical and lumbar herniations. Due to minimal invasiveness and long-lasting benefits, this kind of treatment should be proposed to designated group of patients as first-line therapy.

Key words: herniated discs; intradiscal injection; gelified ethanol

Introduction

Number of adults burdened by acute and chronic back pain is rising in prevalence in the industrialized Western societies lately.¹ Disability with physical and cognitive consequences of the back pain usually leads to long-lasting treatment span, along with the cost of lost productivity, resulting in a substantial societal cost. Deterioration of the intervertebral disk quality with decrease in disc hydration and height reduction with eventual disk bulging, which further affects spatial relationship of the surrounding anatomic structures, primarily muscles and ligaments. Consequently, it may, later in life, lead to severe health issues related to spi-

nal stenosis. The corresponding pain is caused by injury of the nociceptive nerve receptors that get injured and exposed to inflammatory substances in the course of disc degeneration. Hence, the main purpose of the treatment is to lower the intra-discal pressure.² Discogenic brachialgia and sciatica can be, from the pathophysiological point of view, characterized as a combination of mechanical nerve disruption, inflammation and up regulated immune response.³

Treatment armamentarium for the intervertebral discogenic pain ranges from conservative treatment, minimally invasive interventional treatments up to the total surgical disc excisions and arthrodesis. Surgical treatment is still considered

to be the main treatment choice after failure of conservative therapy. It however results in significant range or readmissions (up to 14.7%) within 30 days.⁴ Also, spinal surgery shows no long-term difference when compared with the conservative treatment.⁵ Suboptimal surgical outcomes resulted in development of a wide range of minimally invasive image-guided techniques, all of which are based on percutaneous introduction of trocar into the fibrous ring through which chemical, thermal or ablative devices are introduced. All these techniques target reduction of intra-discal pressure. Chemonucleolysis was introduced in 1963 by Smith⁶ and was the treatment of choice for more than 2 decades, primarily based on intradiscal injection of chymopapain, achieving high level of treatment success rate, ranging between 80–90% in cervical and lumbar hernias.^{7–11} This substance was removed from the market due to safety concerns, mainly anaphylaxis issues.¹² Ethanol substituted chymopapaine as the chemical basis of the interventional chemonucleolysis procedures lately.^{13–15} On the contrary to the chymopapaine, pure alcohol did not cause allergic reactions. There were however significant drawbacks linked to the ethanol utilization with uncontrolled leaks of highly liquid non-radio opaque chemical.¹² DiscoGel[®] substance, an ethanol based derivate with ethyl

cellulose (Gelscom[®], France), used in our study, replaced pure alcohol by adding ethyl cellulose to increase viscosity and Tungsten powder making DiscoGel[®] diffusion visible on fluoroscopy. This results in slower and controlled substance diffusion, without loosing hydrophilic properties of alcohol. Migration of the water from the periphery towards the center of the disc leads to disc decompression and reduction of intradiscal pressure.

Patients and methods

Patient selection

Eighty-three consecutive patients, treated by a single interventional neuroradiologist in University Medical Centre Ljubljana and General Hospital Murska Sobota between May 2014 and Dec 2015 were included in the study.

There were 47 male and 36 female patients, age 18–79, mean age 48.9 years treated for persistent pain, present for more than 6 months and not responding to conservative management. Sixteen patients were treated for refractory neck pain and/or brachialgia, while refractory lower back pain and/or sciatica was a primary complaint of 67 patients.

Magnetic resonance imaging (MRI) performed before the procedure confirmed a contained disc rupture and disc degeneration in all included patients (Figure 1). Contained disc rupture was defined as herniated disc bulging into the spinal canal that is still contained by posterior longitudinal ligament; without discal extrusion or sequestration.¹⁶ Additionally, physical examination by the operator was performed prior to the therapy.

The study protocol was approved by National Ethical Committee (KME 44/06/16); all patients signed informed consent and Helsinki Declaration was followed. Data gathering was performed by questioners, sent to patients 1, 6, 12, 24 and 36 months after the treatment. The data collection was concluded on September 30th 2018.

Treatment planning and delivery

The treatment was performed on fixed angiographic systems, with low frame rate fluoroscopic imaging guidance and under the strict aseptic conditions. All procedures were performed in local anesthesia. Patients with lower back involvement were treated in comfortable lateral decubitus position on their symptomatic side; patients with cervical symptoms were positioned supine. The access was lateral oblique to the disc, 22 Gauge needle

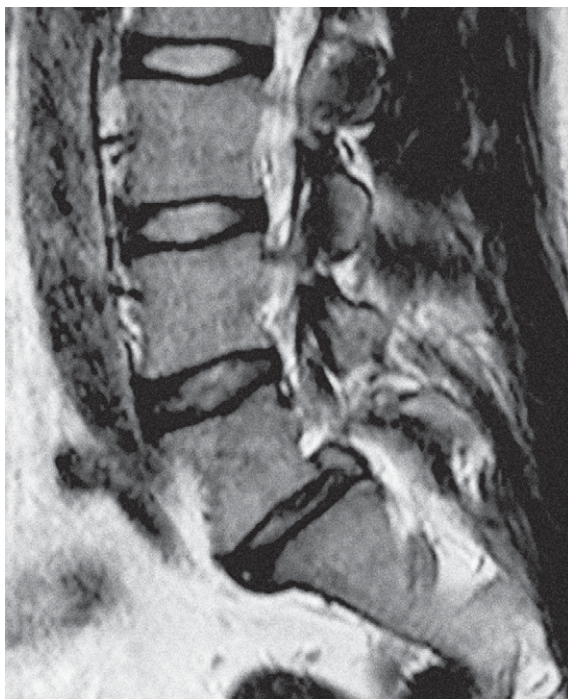


FIGURE 1. MR of lumbosacral spine showing herniation on level L5–S1.

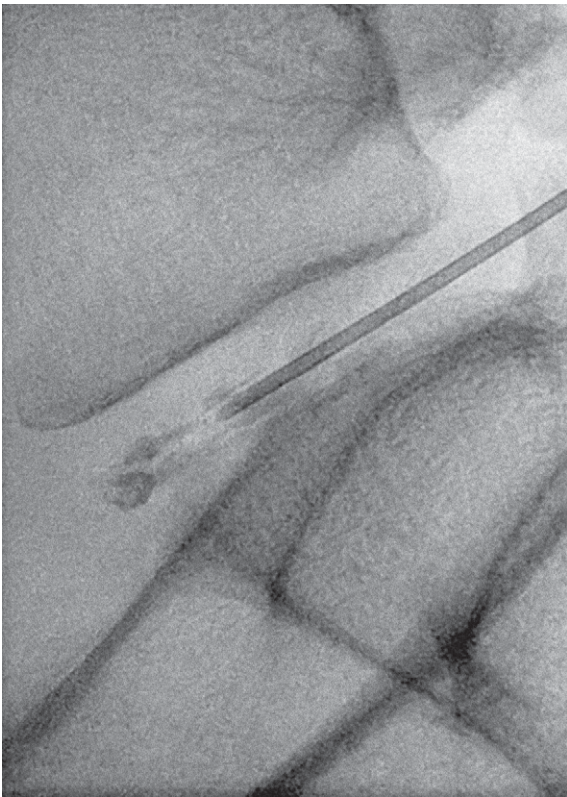


FIGURE 2. Fluoroscopic image during DiscoGel® application on level L5–S1.

was used for tract infiltration with 1% Lidocaine® (skin, tract and facet joints). Then 18 Gauge needle was inserted into median and posterior part of the disc and antibiotic prophylaxis with 40 mg of Gentamycin was applied. DiscoGel® was injected slowly and fractionally (0.1 ml during 30 s period) (Figure 2). The expected dosage of DiscoGel® for lumbar spine was 0.6–0.8 ml and up to 0.3 ml for cervical spine. Control of early leakage outside the disc was achieved by fluoroscopic monitoring. The needle was left in place for 2 minutes after the application to prevent late leakage. Patients were hospitalized up to 24 hours.

Patients' assessment and follow up

Pain intensity was recorded by Visual Analogue Scale (VAS), 0 representing no pain and 10 representing the worst pain imaginable. Pain reduction, expressed as the mean VAS value of all patients was measured prior to the treatment and monitored over 36 months with 5 assessment points: after 1 month, 6 months, 12, 24, and 36 months, respectively. Physical activity of patients was evaluated

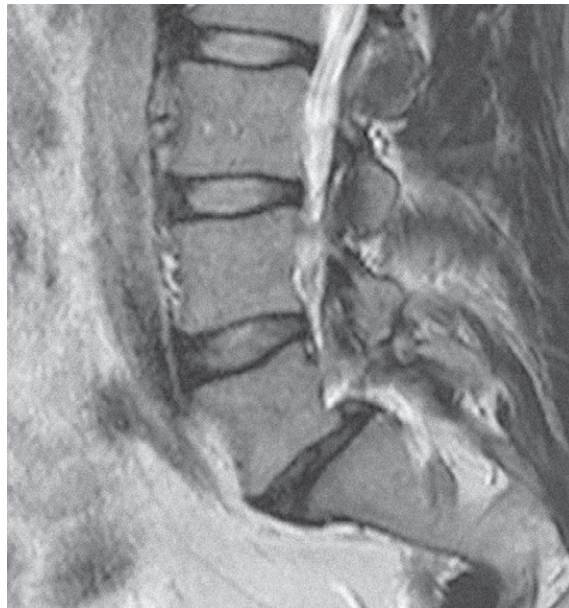


FIGURE 3. MR control 27 months after application of DiscoGel® showing marked reduction of herniation on level L5–S1.

over 12 months' period. It was distributed in 4 different categories: serious limitations (chair-bound or bed-bound), moderate limitations (seated work with very little option to move around), mild limitations (light work) and no limitations (strenuous work). The use of analgesics was assessed, as was return to fully productive life. Patients' satisfaction with treatment and willingness to repeat the treatment were also recorded. CT and/or MRI follow-up scans were performed only in cases of failure and in certain patients on their or referring physicians' request (Figure 3).

Statistical analysis

Analysis was performed on the data collected before the treatment and in five designated periods for VAS and up to 12 months for mean physical activity. Descriptive statistics such as mean and range were calculated and displayed.

Statistical significance of VAS reduction 1, 6 and 36 months after the treatment were evaluated by pooled variance t-test. P values < 0.05 were considered as significant.

Results

Out of 83 patients, included in the study (47 male and 36 female patients, age 18–79, mean age 48.9

TABLE 1. The No. of levels treated in patients with herniated discs

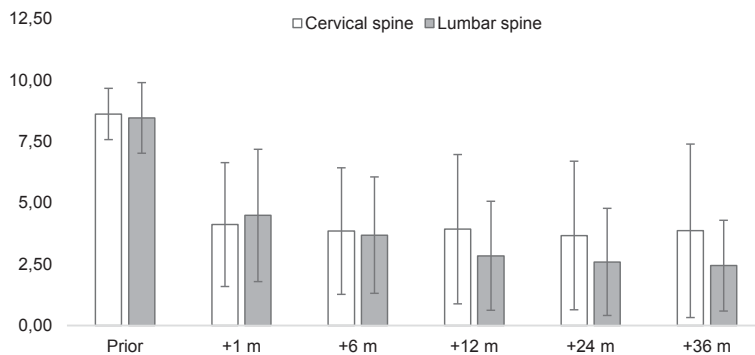
Single level	Two levels	Three levels	Four levels
46 pts (55.5%) (C -10 pts/ L-36 pts)	27 pts (32.5%) (C- 3 pts/ L-24 pts)	9 pts (10.8%) (C- 3 pts/ L-6 pts)	1 pt (1.2%) (L- 1 pt)

C = cervical spine; L = lumbar spine; pt = patient; ptc = patients

TABLE 2. The distribution of most commonly affected spine segments

Lumbar spine	L4–L5 (45 pts; 67.2%)	L5–S1 (30 pts, 44.8%)
Cervical spine	C5–C6 (11 pts, 69%)	C3–C4/ C6–C7 (5 pts, 31%)

C = cervical spine; L = lumbar spine; ptc = patients

**FIGURE 4.** Reduction of VAS score during observational period- the difference is statistically significant already 1 month after treatment ($p < 0,001$).

m = month(s).

years), majority was treated on a single level and less than 1/3 of patients were treated on two levels. Only 12% of patients were treated on three or four levels (Table 1). Some patients were treated on a single or on a multiple sessions, due to patients' disposition. The distribution of most common affected segments of the spine is presented in Table 2.

All-together 59 patients (71.1%) responded to questioners, 21 patients with lumbar pathology and 3 with cervical pathology were not accessible to follow up.

TABLE 3. Mean VAS reduction (radicular pain in parenthesis)

	CERVICAL SPINE	LUMBAR SPINE
Prior to therapy	8.6 (8,0)	8,5 (8,0)
After 1 month	4.1 (no data)	4,5 (3,7)
After 6 months	3,8 (6,3)	3,7 (3,3)
After 1 year	3,9 (7,3)	2,8 (2,6)
After 2 years	3,7 (6,8)	2,6 (2,4)
After 3 years	3,9 (7,3)	2,4 (2,1)

VAS = visual analog scale

Pain reduction was noted in 53 patients (89.8%), while it persisted in 6 patients. In cervical group the pain was reduced in 10/13 patients (76.9%) while in lower back group the pain was reduced in 43/46 pts (93.5%). The reduction was significant in all patients already after 1 month ($p < 0,001$). VAS reduction remained stable in cervical group for the whole observational period, while additional VAS reduction was observed in patients with lower back pathology ($p = 0,012$) (Figure 4).

The only patient operated from the group was a patient with cervical involvement, operated two years after percutaneous treatment.

Mean reduction of VAS is represented in Table 3. The mean VAS was reduced in cervical involvement for 4.7 points after 6 months, remaining constant until 36 months. In patients with lower back involvement the mean VAS decreased for 5.7 points in 6 months and for 6.7 in 36 months. Similar results were recorded in radicular pain group where mean VAS decreased for 5.4 points in 12 months and 5.9 points in 36 months. Less remarkable results were recorded in cervical radicular pain, where mean VAS lowered for 0.7 points after a year and remaining fairly constant during 36 months.

Evaluation of physical activity, presented in Table 4 showed that 96.6% of patients were seriously to moderately disabled prior to treatment and this reduced post-procedurally to approximately 42 % in 6 months' time, further reducing to less than 30 % one year after the procedure.

TABLE 4. Mean physical activity

	Serious limitations	Moderate limitations	Mild limitations	No limitations
Prior to therapy	38/59 (64.4%)	19/59 (32.2%)	2/59 (3.4%)	0
6 months after	3/59 (5.1%)	22/59 (37.3%)	26/59 (44.1%)	8/59 (13.5%)
After 1 year	2/59 (3.4%)	15/59 (25.4%)	32/59 (54.2%)	10/59 (16.9%)

Apart from retired patients (14 pts, 23.7%), the majority of patients returned to their regular job (32 pts, 71.1% of working population), while 6 patients (13.3%) were retired and 7 patients (15.6%) required easier job assignments.

In the post-treatment period more than 3/4 of patients reduced the amount of analgesics as presented in Table 5, while only about 5% needed higher doses. The same percentage of patients treated was also not satisfied with the treatment, as shown in Table 6.

More than 3/4 of the patient population expressed willingness to repeat the treatment if and when deemed needed and about 10% were unwilling to repeat the treatment again (Table 7). The willingness for treatment repetition was lower in patients with cervical pathology (Table 8).

The only postprocedural complication reported was postpunctional syndrome with intracranial hygroma in one patient. It was resolved by surgical drainage. There was no collection locally at the site of the puncture and patient had history of trauma, so the connection with the procedure is difficult to be established.

Discussion

In the most Western societies low back and neck pain are the leading cause of disability, increasing more than 17% in 10 years' time.¹⁷ Lumbar and cervical disc herniations with radiculitis are considered as one of the most prevalent conditions of back pain. Many minimally invasive therapeutic options were proposed as alternative to surgical management, that is not ideal. Our data confirmed efficacy of percutaneous treatment with Radiopaque Gelified Ethanol in management of herniated discs, resulting in almost 90% of patients treated benefited from such minimally invasive treatment with minimal number of complications. The results proved durable, since benefit extended into a third year after our minimally invasive therapy.

The distribution of discs affected in our patients was similar to other reports; L5/S1 and L4/L5 being the most commonly affected in lower back, while C6/C6 being the most affected in cervical spine.^{18,19}

Our results are comparable to results reported by Theron initially¹⁹ (82–91.4% success rate) and confirmed by numerous reports lately.²⁰⁻²⁴ We recorded better data in lumbar region (pain was reduced in 93.5% of patients), since in cervical area the pain was reduced in 76.9% of patients. No relevant pain relief in 10.2% of our patients is also

TABLE 5. The use of analgesics after the treatment

Lesser usage	Equal usage	More usage
46/59 (78%)	10/59 (16.9%)	3/59 (5.1%)

TABLE 6. Satisfaction with the treatment

Extremely satisfied	Very satisfied	Moderately satisfied	Not satisfied
35/59 (59.3%)	16/59 (27.1%)	5/59 (8.5%)	3/59 (5.1%)

TABLE 7. Willingness to repeat the treatment in all patients

Very willing	Potentially willing	Not willing
45/59 (76.3%)	8/59 (13.5%)	6/59 (10.2%)

TABLE 8. Willingness to repeat the treatment- cervical

Very willing	Potentially willing	Not willing
9/13 (69.2%)	1/13 (7.7%)	3/13 (23.1%)

similar to reports from majority of studies except report by Leglise²⁵, reporting treatment failure rate of 64%, requiring secondary treatment in a cohort of 25 patients. High failure rate reported by Leglise was not confirmed by other authors and neither by our data. However, this report proves that percutaneous treatment with DiscoGel[®] does not interfere with secondary procedures in cases of failure seen also in a single operated patient from our series.

Physical disability is extremely important for patients' quality of life. Our data showed that serious and moderate physical impairment prior to treatment (almost 97% of patients) was converted into mild impairment in more than half of patients after 12 months and even in additional 16.9% of patients presenting no physical limitations at all after the treatment. It is noteworthy mentioning that none of the patients from our cohort was able to perform physical activity without limitations and only a few were able to perform moderate activity prior to treatment. This was converted to more than 70% of patients performing activity without or with only moderate limitations already 12 months after therapy. The practical application of these data resulted in majority of patients (more than 70% of working population) returning to their

previous work. In addition, the use of analgesics was reduced in almost 80% of patients, lowering the costs and reducing potential complications of such therapy. Active life has also an important economic impact on society, reducing disability and raising productivity, since majority of our patients were active population (mean age 48.9 years).

Based on good results and minimal invasiveness of the treatment, our data showed that vast majority of our patients would be willing to repeat the treatment. Since the results are poorer in patients with cervical pathology, especially radicular, less patients from this group were willing to repeat the treatment.

Complications were minimal, one patient had postpunctional syndrome not necessarily attributed to the procedure itself since there was previous history of trauma. No infections or bleedings were reported, only one patient required surgical therapy after the procedure.

Most of the studies published so far focused on immediate or short-term follow-up, reporting results up to 1 year.^{18,20,21,23,24,26} Longer follow-up was reported in Croatian multicentric study²⁷, however the patients' cohort was smaller than in our study and there were only four patients followed longer than 24 months. Since discal degeneration is a chronic, progressive disease that permanently disables patients and negatively influences their quality of life, long-term results of the treatment are extremely important. In terms of durability, pain reduction was extended into second and third year after the treatment, in patients with lumbar symptoms the pain was further reduced after 36 months. Beneficial long-term effects in both groups showed VAS reduction in patients with lower back pathology around 70% after 3 years and in patients with cervical symptoms the reduction was about 50%. Least marked results were detected in patients with cervical radicular involvement, since overall VAS reduction was about 10%. There were only three patients in this cohort so it is hard to draw firm conclusions. Further studies will have to confirm these biases.

The vast majority of patients treated experienced significant improvement in the post-treatment period; excellent results were achieved in lumbar region, while in cervical region, especially in patients with radicular involvement, pain reduction was less marked. Intra-procedural patient compliance was very high due to minimally invasive percutaneous approach, non-traumatic lesion access, very good procedural cosmetic and virtually no infection or blood loss. The hospitalization time

was minimized to 24h post-procedural monitoring, short recovery time and return to full productive life proved patient-friendly. Also, our results showed long-term durability of the procedure in all patients, especially in those with lower-back symptoms, improving even after 12 months.

The major drawback of our study is that the number of patients included, especially in cervical group is relatively low. Larger cohort might show different results. More than 1/4 of patients did not respond to questioner, so we were able to follow up only 59 patients for the designated period. Observational character of the study could also not exclude additional external parameters (such as different techniques for pain reduction including physical activity, exercises, additional or alternative analgetics, acupuncture etc.) possibly influencing results, especially long-term VAS reduction. A large double-blinded randomized study would be helpful in confirming our data.

Conclusions

Minimally invasive percutaneous treatment with DiscoGel® in our patient cohort showed very good clinical outcome. The procedure can be considered as a relatively economic, providing a good option for patients with small and medium sized cervical and lumbar herniations that could avoid primary open surgical approach.

Acknowledgment

The study was not founded by the third party. Authors would like to express their gratitude to Urban Zdešar, M.Sc., physicist for his help in statistical analysis and Draženko Babić, M.D. for his contribute in manuscript.

References

1. Institute of Medicine. Committee on Advancing Pain Research. *Relieving pain in America: a blueprint for transforming prevention, care, education, and research*. Washington, DC: The National Academies Press; 2011. doi: 10.17226/13172
2. Ray PP. Intervertebral disc: anatomy-physiology-pathophysiology-treatment. *Pain Pract* 2008; **8**: 18-44. doi: 10.1111/j.1533-2500.2007.00171
3. Russell WHJ, Perry AB. Treatment of disk disease of lumbar spine. In: Winn HR, editor. *Youmans neurological surgery*. 5th edition. Philadelphia (PA): WB Saunders; 2004. p. 4513-20.
4. Cusimano MD, Pshonyak I, Lee MY, Ilie G. Causes of 30-day readmission after neurosurgery of the spine. *J Neurosurg Spine* 2016; **24**: 281-90. doi: 10.3171/2015.4.SPINE15445.

5. Weinstein JN, Lurie JD, Tosteson TD, Skinner JS, Hanscom B, Tosteson AN, et al. Surgical vs nonoperative treatment for lumbar disk herniation: the Spine Patient Outcomes Research Trial (SPORT) observational cohort. *JAMA* 2006; **296**: 2451-9. doi: 10.1001/jama.296.20.2451
6. Smith L. Enzyme dissolution of the nucleus pulposus in humans. *JAMA* 1964; **187**: 137-40. doi: 10.1001/jama.1964.03060150061016
7. Theron J, Blais M, Casasco A, Courtheoux P, Adam Y, Derlon JM, et al. Therapeutic radiology of the lumbar spine. Disk chemonucleolysis, infiltration and coagulation of posterior articulations. *J Neuroradiol* 1983; **10**: 209-30. PMID: 6355403
8. Krause D, Drape JL, Jambon F, de Souza-Lima A, Tongio J, Maitrot D, et al. Cervical nucleolysis: indications, technique, results. 190 patients. *J Neuroradiol* 1993; **20**: 42-59. PMID: 8492175
9. Gogan WJ, Fraser RD. Chymopapain: a 10-year, double-blind study. *Spine (Phila Pa 1976)* 1992; **17**: 388-94. PMID: 1579872
10. Smith L. Chemonucleolysis. Personal history, trials, and tribulations. *Clin Orthop Relat Res* 1993; **287**: 117-24. PMID: 8448928
11. Smith L. Enzyme dissolution of the nucleus pulposus in humans. *JAMA* 1964; **187**: 137-40. doi: 10.1001/jama.1964.03060150061016
12. Knezevic NN, Mandalia S, Raasch J, Knezevic I, Candido KD. Treatment of chronic low back pain - new approaches on the horizon. *J Pain Res* 2017; **10**: 1111-23. doi: 10.2147/JPR.S132769
13. Riquelme C, Musacchio M, Mont'Alverne F, Tournade A. Chemonucleolysis of lumbar discs herniation with ethanol. *J Neuroradiol* 2001; **28**: 219-29. PMID: 11924136
14. Bennedbak FN, Nielsen L, Hegedüs L. Effect of percutaneous ethanol injection therapy versus suppressive doses of L-thyroxine on benign solitary solid cold thyroid nodules; a randomized trial. *J Clin Endocrinol Metab* 1998; **83**: 830-35. doi: 10.1210/jcem.83.3.4673
15. Doppman JL, Oldfield EH, Heiss JD. Symptomatic vertebral hemangiomas: treatment by means of direct intralésional injection of ethanol. *Radiology* 2000; **214**: 341-48. doi: 10.1148/radiology.214.2.r00fe46341
16. Silber JS, McGraw KJ and Lippert JA. Section II: Treatment of discogenic back pain. In: McGraw KJ, editor. *Interventional radiology of the spine: image-guided pain therapy*. New York: Springer; 2004. p. 167-80. doi: 10.1007/978-1-59259-418-4
17. GBD 2015 Disease and Injury Incidence and prevalence Collaborators. Global, regional, and national incidence, prevalence, and years lived with disability for 310 diseases and injuries, 1990-2015; a system analysis for the Global Burden of Disease Study 2015. *Lancet* 2016; **388**: 1545-602. doi: 10.1016/S0140-6736(16)31678-6
18. Gangi A, Tsoumakidou G, Buy X, Cabral JF, Garnon J. Percutaneous techniques for cervical pain of discal origin. *Semin Musculoskelet Radiol* 2011; **15**: 172-80. doi: 10.1055/s-0031-1275601
19. Touraine S, Damiano J, Tran O, Laredo JD. Cohort study of lumbar percutaneous chemonucleolysis using ethanol gel in sciatica refractory to conservative treatment. *Eur Radiol* 2015; **25**: 3390-7. doi: 10.1007/s00330-015-3740-1
20. Stagni S, de Santis F, Cirillo L, Dall'Olio M, Princiotta C, Simonetti L, et al. A minimally invasive treatment for lumbar disc herniation: DiscoGel® chemonucleolysis in patients unresponsive to chemonucleolysis with oxygen-ozone. *Interv Neuroradiol* 2012; **18**: 97-104. doi: 10.1177/159101991201800113
21. de Seze M, Saliba L, Mazaux JM. Percutaneous treatment of sciatica caused by a herniated disc: an exploratory study on the use of gaseous discography and DiscoGel® in 79 patients. *Ann Phys Rehabil Med* 2013; **56**: 143-54. doi: 10.1016/j.rehab.2013.01.006
22. Guarnieri G, De Dominicis G, Muto M. Intradiscal and intramuscular injection of DiscoGel®: radiopaque gelified ethanol - pathological evaluation. *Neuroradiology J* 2010; **23**: 249-52. doi: 10.1177/197140091002300216
23. Bellini M, Romano DG, Leonini S, Grazzini I, Tabano C, Ferrara M, et al. Percutaneous injection of radiopaque gelified ethanol for the treatment of lumbar and cervical intervertebral disk herniations: experience and clinical outcomes in 80 patients. *AJNR Am J Neuroradiol* 2015; **36**: 600-5. doi: 10.3174/ajnr.A4166
24. Sayhan H, Bayaz SG, Ulgen AM, Yuca MF, Taomak Y. Long-term clinical effects of DiscoGel for cervical disc herniation. *Pain Physician* 2018; **21**: E71-8. PMID: 29357343
25. Leglise A, Lombard J, Moufid A. Discogel in patients with discal lumboscoliosis. Retrospective results in 25 consecutive patients. *Orthop Traumatol Surg Res* 2015; **101**: 623-6. doi: 10.1016/j.otsr.2015.05.007
26. Theron J, Guimaraens L, Casasco A, Sola T, Cuellar H: Percutaneous treatment of lumbar intervertebral disk hernias with radiopaque gelified ethanol: a preliminary study. *J Spinal Dis Tech* 2007; **20**: 526-32. doi: 10.1097/BSD.0b013e318033e860
27. Houra K, Perovic D, Rados I, Kvesic D. Radiopaque gelified ethanol application in lumbar intervertebral soft disc herniations: Croatian Multicentric Study. *Pain Med* 2018; **19**: 1550-8. doi: 10.1093/pm/pnx270

The use of high-frequency short bipolar pulses in cisplatin electrochemotherapy *in vitro*

Maria Scuderi¹, Matej Rebersek², Damijan Miklavcic², Janja Dermol-Cerne²

¹ University of Padua, Department of Information Engineering, Padua, Italy

² University of Ljubljana, Faculty of Electrical Engineering, Ljubljana, Slovenia

Radiol Oncol 2019; 53(2): 194-205.

Received 4 February 2019

Accepted 23 April 2019

Correspondence to: Janja Dermol-Černe, Ph.D., University of Ljubljana, Faculty of Electrical Engineering, Tržaška cesta 25, SI-1000 Ljubljana, Slovenia. E-mail: Janja.dermol-cerne@fe.uni-lj.si

Disclosure: No potential conflicts of interest were disclosed.

Background. In electrochemotherapy (ECT), chemotherapeutics are first administered, followed by short 100 μ s monopolar pulses. However, these pulses cause pain and muscle contractions. It is thus necessary to administer muscle relaxants, general anesthesia and synchronize pulses with the heart rhythm of the patient, which makes the treatment more complex. It was suggested in ablation with irreversible electroporation, that bursts of short high-frequency bipolar pulses could alleviate these problems. Therefore, we designed our study to verify if it is possible to use high-frequency bipolar pulses (HF-EP pulses) in electrochemotherapy.

Materials and methods. We performed *in vitro* experiments on mouse skin melanoma (B16-F1) cells by adding 1–330 μ M cisplatin and delivering either (a) eight 100 μ s long monopolar pulses, 0.4–1.2 kV/cm, 1 Hz (ECT pulses) or (b) eight bursts at 1 Hz, consisting of 50 bipolar pulses. One bipolar pulse consisted of a series of 1 μ s long positive and 1 μ s long negative pulse (0.5–5 kV/cm) with a 1 μ s delay in-between.

Results. With both types of pulses, the combination of electric pulses and cisplatin was more efficient in killing cells than cisplatin or electric pulses only. However, we needed to apply a higher electric field in HF-EP (3 kV/cm) than in ECT (1.2 kV/cm) to obtain comparable cytotoxicity.

Conclusions. It is possible to use HF-EP in electrochemotherapy; however, at the expense of applying higher electric fields than in classical ECT. The results obtained, nevertheless, offer an evidence that HF-EP could be used in electrochemotherapy with potentially alleviated muscle contractions and pain.

Key words: electroporation; electrochemotherapy; high-frequency bipolar pulses; cisplatin; cell survival; drug uptake

Introduction

When a cell is exposed to a sufficiently high electric field, the permeability of the cell membrane rapidly increases due to membrane electroporation. This transiently increased membrane permeability allows for the exchange of ions and molecules between inside and outside of the cells.¹⁻⁴ If cells recover and survive, electroporation is called reversible. If the damage is too extensive, resealing too slow, cells cannot restore the homeostasis, and they die, electroporation is called irreversible. Electroporation depends on the characteristics of the cells (shape, size, cytoskeleton structure, membrane composition) and the electrical param-

eters (amplitude, duration, number of electrical pulses and repetition frequency). Electroporation is used in medicine⁵⁻¹⁰ (electrochemotherapy, gene therapy, irreversible electroporation as an ablation technique and transdermal drug delivery), in biotechnology^{11,12}, (inactivation of microorganisms, extraction of biomolecules from microorganisms and plants, genetic transformation of microorganisms) and food processing.^{13,14}

Electrochemotherapy (ECT) is used in clinics to treat patients with various types of cancer (*e.g.*, melanoma, head-neck tumors, breast, liver, intestinal tract, brain cancer).¹⁵ The standard operating procedures for electrochemotherapy include intratumoral or intravenous delivery of the chemother-

apeutic drug, followed by the application of high-voltage 100 μ s long monopolar pulses to the tumor area.^{16–19} Two chemotherapeutics are currently used in clinics - bleomycin^{20,21} and cisplatin (cis-diaminodichloroplatin (II), CDDP).^{22,23} The cytotoxicity of the chemotherapeutic drugs is increased as the delivered pulses increase cell membrane permeability, and facilitate the influx of drugs into the tumor cells.^{24,25} Drawbacks of the application of 100 μ s long monopolar, high-voltage electric pulses at repetition frequency 1 Hz are pain, muscle contractions^{26–28}, the need to use muscle relaxants and general anesthesia²⁹ and to synchronize pulses with the heart rhythm.^{30,31} These problems can be alleviated for example by applying pulses at higher frequency²⁶, by using special designs of electrodes^{32,33}, or, as it was recently demonstrated, by delivering bursts of short high-frequency bipolar pulses, *i.e.*, the so-called high-frequency irreversible electroporation (H-FIRE) pulses.^{33–37} Treatment with H-FIRE pulses, however, comes at the expense of delivering pulses of considerably higher amplitudes.³⁸

Mostly, H-FIRE pulses have been used to achieve irreversible electroporation. However, they can also be used to increase the uptake of molecules into cells³⁸ which could be applied in achieving reversible electroporation to treat tumors with electrochemotherapy. Thus, this study aimed to determine whether H-FIRE pulses could also be used in electrochemotherapy which we call high-frequency electroporation (HF-EP).

We delivered 8 bursts of 50 bipolar pulses, each consisting of 1 μ s long positive and negative pulse, with a 1 μ s delay between them with electric field from 0.5–5 kV/cm. We compared HF-EP to classic eight monopolar 100 μ s long pulses, delivered at frequency 1 Hz, with electric field from 0.4–1.2 kV/cm. Cisplatin concentration was from 1 μ M to 330 μ M. We showed that HF-EP pulses indeed cause higher cytotoxicity of cisplatin *in vitro*; however, in comparison to the standard 100 μ s long monopolar pulses, higher voltage pulses must be delivered to obtain comparable effect.

Materials and methods

Cell preparation

Mouse skin melanoma cell line B16-F1, obtained from the European Collection of Authenticated Cell Cultures (ECACC, cat. no. 92101203, Sigma Aldrich, Germany, mycoplasma free), was grown 2–4 days in 75 cm² cell culture flasks (TPP, Austria) until 80% confluency in Dulbecco's Modified Eagle's Medium

(DMEM, cat. no. D5671, Sigma Aldrich, Germany) in an incubator (Kambič, Slovenia) at 37°C and humidified 5% CO₂. DMEM, used in this composition for all *in vitro* experiments, was supplemented with 10% fetal bovine serum (cat. no. F7524, Sigma Aldrich, Germany), 2 mM L-glutamine (cat. no. G7513, Sigma Aldrich, Germany) and antibiotics, 50 μ g/ml gentamycin (cat. no. G1397, Sigma Aldrich, Germany), 1 U/ml penicillin-streptomycin (cat. no. P11-010, PAA, Austria).

Cell suspension was prepared by detaching the cells in the exponential phase of growth with 10x trypsin-EDTA (cat. no. T4174, Sigma Aldrich, Germany), diluted 1:9 in Hank's basal salt solution (cat. no. H4641, Sigma Aldrich, Germany). After no more than 3 minutes, trypsin was inactivated by adding DMEM, and cells were transferred to a 50 ml centrifuge tube. Then, the cells were centrifuged (5 min, 180 g, 21°C) and re-suspended in DMEM at concentration 5x10⁶ cells/ml (experiments to measure the optimal parameters of electroporation and resealing rate of cells), 5x10⁴ cells/ml (experiments to measure the cytotoxicity of cisplatin without electroporation) or 2.2x10⁷ cells/ml (experiments to measure the cytotoxicity of cisplatin with electroporation). We performed experiments with different cell densities due to different requirements for cell number and sensitivities of the chosen assays. Even at the highest concentration (2.2x10⁷ cells/ml) we were still well below the concentration where shielding of the electric field and decreased uptake were observed.³⁹

Electroporation setup

Two types of pulses were applied – 100 μ s long monopolar pulses (*i.e.* classical electrochemotherapy) and bursts of short bipolar pulses (HF-EP pulses). They were applied between plate stainless-steel electrodes with 2 mm distance.⁴⁰ Between pulses, electrodes were cleaned in potassium-phosphate buffer (KPB, 10 mM KH₂PO₄/K₂HPO₄ in ratio 40.5:9.5, 1 mM MgCl₂, 250 mM sucrose) and dried with sterile gauze. 100 μ s long monopolar pulses (8 pulses, delivered at repetition frequency 1 Hz, Figure 1A) of different voltages (80, 120, 160, 200, 240 V) were delivered by the commercially available BetaTech pulse generator (Electro cell B10, BetaTech, France) or BTX Gemini X2 pulse generator (Harvard Apparatus, USA). Short bipolar pulses of different voltages (HF-EP protocol, 100 V to 1000 V with a step of 100 V, Figure 1B) were delivered by a laboratory prototype pulse generator (University of Ljubljana) based on H-bridge digital

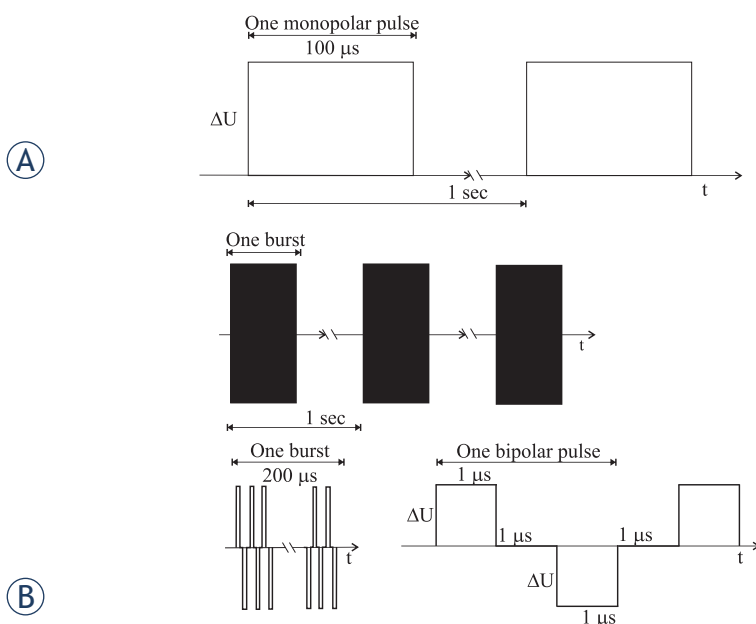


FIGURE 1. Scheme of the applied pulses. **(A)** 100 μs long monopolar pulses of amplitude ΔU (80 V – 240 V in a step of 40 V) were applied with a repetition frequency of 1 Hz. **(B)** Short bipolar pulses (HF-EP). Above: 8 bursts were applied with a repetition frequency of 1 Hz. Down left: One burst was 200 μs long and consisted of 50 bipolar pulses. Below right: One bipolar pulse of amplitude ΔU (100 V – 1000 V in a step of 100 V) consisted of 1 μs long positive pulse, 1 μs long negative pulse (both of voltage ΔU) with a 1 μs long delay between pulses.

amplifier with 1 kV MOSFETs (DE275-102N06A, IXYS, USA).^{38,41} Short bipolar pulses were delivered in 8 bursts at repetition frequency 1 Hz, each containing 50 short bipolar pulses of 1 μs positive and 1 μs negative pulse. The delay between short bipolar pulses and between positive and negative pulse was 1 μs . The on-time (the time when the voltage was different from zero) of the HF-EP pulses was 800 μs , equivalent to the duration of the eight 100 μs long monopolar pulses. The duration of one short bipolar pulse was chosen as it successfully permeabilized cell membranes as previously demonstrated by an increased uptake of a fluorescent dye.³⁸ The voltage and the current were monitored in all experiments with an oscilloscope Wavesurfer 422, 200 MHz, a differential voltage probe ADP305 and a current probe CP030 or AP015, all from LeCroy, USA to ensure that delivered voltage and current were consistent at the same settings even if delivered with different generators.

Determination of permeability and resealing

In permeability experiments, just before pulse application, 60 μl of cell suspension was mixed with

6 μl of 1.5 mM propidium iodide (PI) (136 μM final concentration). In resealing experiments, PI was not added before pulse application but after electroporation. 60 μl of the cell suspension was electroporated, and 50 μl of the treated sample was transferred to a 1.5 ml centrifuge tube. In resealing experiments, 5 μl of PI (136 μM final concentration) was added to 50 μl of the treated sample 2 min, 5 min, 10 min or 20 min after pulse delivery. Two minutes after electroporation (permeability experiments) or PI addition (resealing experiments), the samples were diluted in 100 μl of KPB, and vortexed. The uptake of propidium was measured on the flow cytometer (Attune NxT; Life Technologies, Carlsbad, CA, USA). Cells were excited with a blue laser at 488 nm, and the emitted fluorescence was detected through a 574/26 nm band-pass filter. The measurement was finished when 10,000 events were acquired. Single cells were separated from all events by gating. Obtained data were analyzed using the Attune NxT software. The percentage of permeabilized cells was determined from the histogram of PI fluorescence.

Cell survival following electroporation only

60 μl of the cell suspension was electroporated, 50 μl was transferred to a 15 ml centrifuge tube, and two minutes after pulses delivery, the samples were diluted in 450 μl of DMEM and mixed with a pipette. When all the samples were finished, 5×10^4 cells were transferred in each well on a 96-well plate in three technical repetitions. After 24 h of incubation at 37°C and humidified 5% CO_2 , the survival assay was performed. 20 μl of MTS (CellTiter 96® Aqueous One Solution Cell Proliferation Assay (MTS), Promega, USA) was added per well according to manufacturer's instructions and left in an incubator for 2h. MTS assay was used to quantify the number of viable cells evaluating their metabolic activity by measuring the formazan absorbance at 490 nm. After 2 h, the absorbance was measured on a spectrofluorometer (Tecan Infinite 200; Tecan, Grödig, Austria). Cell survival was calculated by first subtracting the background (only DMEM and MTS) from all measurements and then normalizing the absorbance of the treated samples to the absorbance of the control samples.

Cytotoxicity of cisplatin without electroporation

On the first day, 5×10^3 B16-F1 cells were seeded per well on a 96-well plate and left for one day in an in-

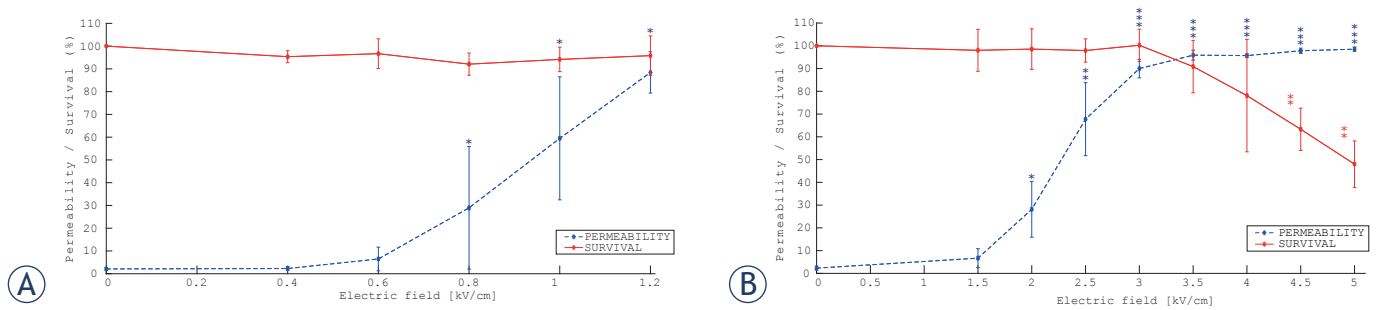


FIGURE 2. Cell membrane permeability and cell survival as a function of electric field for **(A)** $8 \times 100 \mu\text{s}$ long monopolar pulses, delivered at repetition frequency 1 Hz; **(B)** 8 bursts of short bipolar pulses (HF-EP) of 1-1-1-1 μs , delivered at repetition frequency 1 Hz. Each data point was repeated 3–4 times (mean \pm standard deviation). In the control sample, no pulses were applied. Note different scales on the x-axes. On **(A)**, the threshold of electroporation was at 0.8 kV/cm ($P = 0.029$, t-test) and survival did not decrease in comparison with control (one-sample t-test). On **(B)** the threshold of electroporation was at 2 kV/cm ($P = 0.022$, t-test), while the survival decreased at 4.5 kV/cm ($P = 0.004$, one-sample t-test). In Figure 2B, blue asterisks refer to permeability curve and red asterisks to the survival curve.

cubator (Kambič, Slovenia) at 37°C and humidified 5% CO₂. On the second day (24 h after cell seeding), the 3.3 mM stock cisplatin (Accord HealthCare, Poland) was diluted in 0.9% NaCl (physiological solution) to obtain the 10x higher concentration of cisplatin than desired with the cells (1, 10, 100, 330 μM). Diluted cisplatin was then mixed with the DMEM in ratio 1:9 and cells were incubated in DMEM with cisplatin for 10 min, 1 h, 24 h or 48 h. After the indicated time, DMEM with cisplatin was substituted with DMEM only. On the fourth day (72 h after cell seeding), the MTS survival assay was performed as described in the subsection *Cell survival following electroporation only*.

Electroporation with cisplatin

We performed two types of experiments. We applied: 1) different electric fields at fixed cisplatin concentration (100 μM) to evaluate the effect of electric field on cell death; 2) fixed electric field (optimal value – long monopolar pulses $E = 1.2 \text{ kV/cm}$ and short bipolar (HF-EP) pulses $E = 3 \text{ kV/cm}$) with different cisplatin concentrations to evaluate the effect of cisplatin concentration on cell survival. Optimal parameters of electroporation were determined with experiments described in the subsections *Determination of permeability and resealing*, and *Cell survival following electroporation only* and were chosen as those where the highest uptake of propidium iodide (*i.e.*, highest cell membrane permeability) and the highest cell survival were obtained.

The 3.3 mM stock cisplatin was diluted in 0.9% NaCl to obtain the desired concentrations of cisplatin with the cells (1, 10, 100, 330 μM) in both experiments. The drug was prepared fresh for each experiment. Right before experiments, 120 μl of

cell suspension was mixed with 13.3 μl of cisplatin. 60 μl of the cell suspension with added cisplatin was transferred between the electrodes, and long monopolar or short bipolar (HF-EP) pulses were delivered (electroporation+cisplatin). The remaining 60 μl was used as a control and was transferred between the electrodes, but no pulses were delivered (only cisplatin). 50 μl of the treated and control sample were transferred in a 15 ml centrifuge tube. 10 minutes after pulse delivery, the samples were diluted 40x in full DMEM and vortexed. 5.5×10^3 cells were transferred in each well on a 96-well plate in triplicates. The survival assay was performed as described in the subsection *Cell Survival* after 72 hours as previously suggested.⁴²

Statistical analysis

Statistical analysis was performed using the software SigmaPlot v11 (Systat Software, San Jose, CA). We performed the t-test or one sample t-test when comparing two groups or one group towards normalized control. We performed the 1-way or 2-way ANOVA if the normality test was passed or the ANOVA on ranks if the normality test failed with the post-hoc Tukey test. The details on the performed test and the obtained P-value are written in respective figure captions in the Results section. On figures, one asterisk (*) signifies $P < 0.05$, two (**) $P < 0.01$ and three (***) $P < 0.001$.

Results

Electroporation with propidium iodide

First, we performed experiments to determine the optimal parameters of electroporation to be later

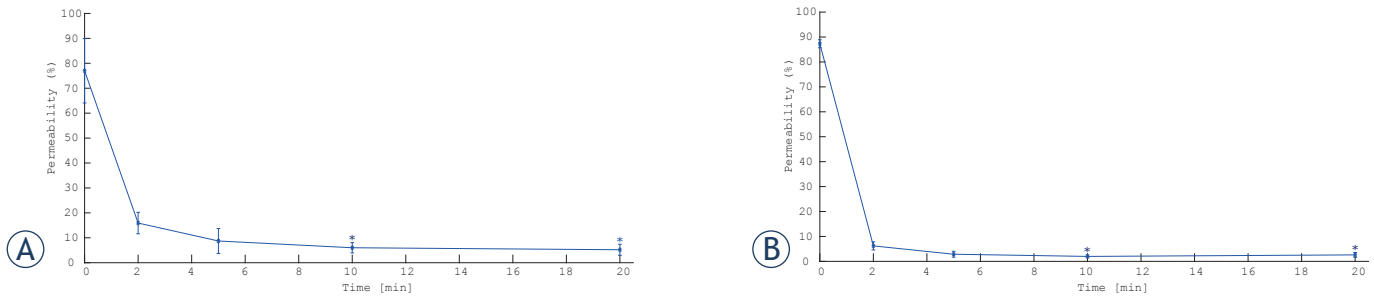


FIGURE 3. Cell membrane permeability as a function of different time of propidium iodide administration after electroporation for **(A)** 8 x 100 μ s long monopolar pulses, delivered at a repetition frequency 1 Hz; **(B)** 8 bursts of short bipolar pulses (HF-EP) of 1-1-1 μ s, delivered at repetition frequency 1 Hz. Each data point was repeated 4 times (mean \pm standard deviation). We performed a 1-way ANOVA on ranks. For both types of pulses, there was a significant difference between 0 min vs 10 min and 20 min ($P < 0.05$), other pairwise comparisons were not significant.

used in the experiments with cisplatin. As optimal parameters of electroporation were considered those where the highest cell membrane permeability and the highest cell survival were achieved. In Figure 2 we can observe the permeability curves (blue dashed line) and the survival curves (red solid line) as a function of electric field amplitude for (A) 100 μ s long monopolar pulses and (B) bursts of short bipolar (HF-EP) pulses. In Figure 2A we can see that the threshold of electroporation was at 0.8 kV/cm and highest uptake and survival were achieved at 1.2 kV/cm which was considered as the optimal point of electroporation. In Figure 2B we can see that the threshold of electroporation was at 2 kV/cm, the threshold for irreversible electroporation at 4.5 kV/cm and the highest uptake and survival for HF-EP pulses were obtained at 3 kV/cm which was chosen as the optimal point of electroporation with short bipolar pulses. Electric pulses of 1.2 kV/cm with 100 μ s monopolar pulses and 3 kV/cm in HF-EP protocol were thus considered to be equivalent and were used in further experiments.

With the optimal parameters of electroporation, we measured the resealing of cell membranes after electroporation. Figure 3 shows the permeability curves obtained as a function of different time of exposure to propidium iodide after electroporation delivering (A) long monopolar pulses at $E = 1.2$ kV/cm and (B) HF-EP pulses at $E = 3$ kV/cm. Figure 3A and Figure 3B show a peak of permeability at 0 min, *i.e.*, right after the pulses are applied. Then, we can see a decrease in permeability that reaches a plateau after 10 min. We chose 10 min as the time after which cell membranes resealed. Accordingly, in the subsequent experiments, electroporated samples with cisplatin were diluted after 10 minutes.

Cytotoxicity of cisplatin without electroporation

We measured the cytotoxicity of cisplatin without electroporation at different cisplatin concentrations and incubation times on attached confluent cell monolayers (Figure 4). Cells were more affected if they were exposed to cisplatin for a longer time (24 h and 48 h incubation caused significantly higher cell death than 10 min and 1 h incubation). There was no difference if cells were incubated for 10 min vs 1 h and 24 h vs 48 h. There was no difference between 1 μ M and 10 μ M, but in general, cytotoxicity increased with higher cisplatin concentrations. After 10 min and 1 h of incubation (red solid and green dashed curve, respectively) there was a decrease in cell survival with increasing cisplatin concentration and at the highest tested concentration

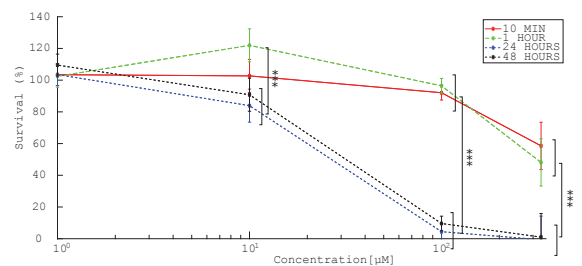


FIGURE 4. Cytotoxicity of cisplatin without electroporation at different concentrations and time of incubation. Each data point was repeated 4 times (mean \pm standard deviation) and is normalized to the control sample in which cisplatin was substituted by 0.9% NaCl. A 2-way ANOVA was performed. 10 min or 1 h of incubation was different from 24 h or 48 h ($P < 0.001$) while there was no difference between 10 min vs 1 h and 24 h vs 48 h. 330 μ M cisplatin was more cytotoxic than other tested concentrations ($P < 0.001$). There was no significant difference between 1 μ M and 10 μ M cisplatin; all other comparisons were significantly different ($P < 0.001$).

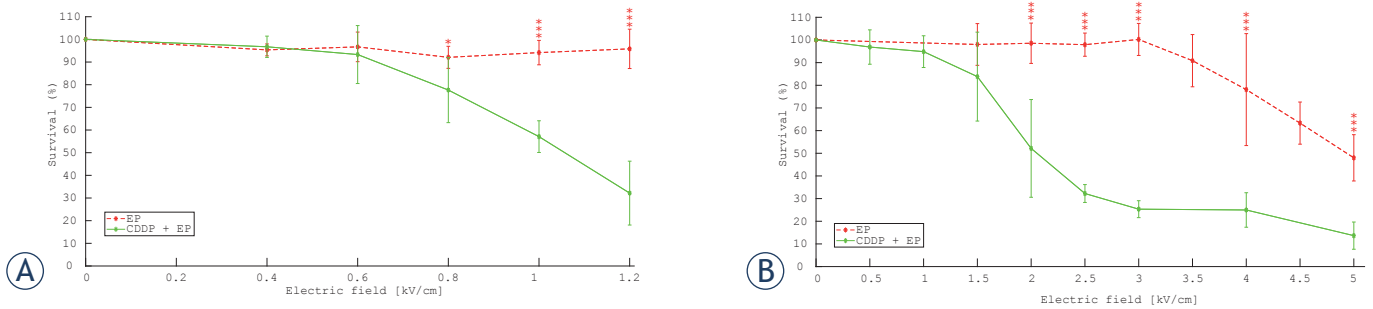


FIGURE 5. Cytotoxicity of cisplatin in combination with electroporation (EP) at fixed value of cisplatin (CDDP) 100 μ M as a function of electric field: **(A)** 8 x 100 μ s long monopolar pulses (ECT) were delivered at repetition frequency 1 Hz; **(B)** 8 bursts of short bipolar pulses (HF-EP) of 1-1-1-1 μ s were delivered at repetition frequency 1 Hz. Each data point was repeated 3–6 times (mean \pm standard deviation). Results are normalized to the control sample without an electric field and with 100 μ M cisplatin. We performed a **(A)** 2-way ANOVA or **(B)** 2-way ANOVA on ranks. **(A)** At 0.8 kV/cm ($P = 0.036$) and 1 kV/cm and 1.2 kV/cm ($P < 0.001$) EP samples were significantly different from CDDP+EP samples. **(B)** At electric fields equal to or higher than 2 kV/cm EP samples were significantly different from CDDP+EP samples ($P < 0.001$).

(330 μ M) we obtained 58.55% \pm 14.90% and 48.12% \pm 14.01% survival for 10 min and 1 h, respectively. After 24 h and 48 h (blue dotted and black dash-dot curve, respectively) of incubation, cell survival decreased rapidly to less than 10% already with 100 μ M of cisplatin.

Cytotoxicity of cisplatin with electroporation - electrochemotherapy

First, we measured the cytotoxicity of cisplatin with electroporation at different electric fields and selected cisplatin (CDDP) concentration of 100 μ M. In Figure 5, we can observe cell survival as a function of applied electric field, on Figure 5A for long monopolar pulses and Figure 5B for HF-EP pulses. The solid green line shows cell survival after electroporation with cisplatin and red dashed line survival after only electroporation without cisplatin. The red dashed curves of Figure 5A and B are already shown in Figure 2A and B. We can see in both Figure 5A and B that the combination of electric pulses and cisplatin is more efficient in achieving cell death than applying only electric pulses or only cisplatin (100% survival at 100 μ M cisplatin and 10 min incubation time, Figure 4) and that cytotoxicity of cisplatin increases with increasing electric field, starting at 0.8 kV/cm for 100 μ s long monopolar pulses and 2 kV/cm for short bipolar pulses, which coincides with the thresholds for reversible electroporation (Figure 2). In Figure 5A we can see that at $E = 1.2$ kV/cm with cisplatin 32.16% \pm 14.08% of cells survive while when we apply only electric pulses, all cells survive. Similarly, in Figure 5B at $E = 3$ kV/cm 25.33% \pm 3.73% of cells survive electroporation with cisplatin opposed to 100% when only electric pulses are applied.

Then, we measured cytotoxicity of cisplatin with electroporation at a fixed electric field (optimal point of electroporation with the highest cell membrane permeability and lowest survival - long monopolar pulses at $E = 1.2$ kV/cm and HF-EP pulses at $E = 3$ kV/cm) and different cisplatin concentrations. In Figure 6 we can see two cell survival curves obtained by applying 1) only cisplatin (red dashed curve) and 2) cisplatin in combination with electroporation (solid green curve). From the red dashed curve in Figure 6A and B we can see that cell survival does not decrease with increasing cisplatin concentration due to short incubation time (see also Figure 4). From the solid green curve in Figure 6A and B we can see that the cytotoxicity of cisplatin increases when electric pulses are applied with increasing cisplatin concentration. A similar trend in survival is observed for both types of pulses.

Discussion

We aimed to determine whether it is possible to use bursts of short bipolar pulses (HF-EP) in *in vitro* electrochemotherapy (ECT) treatments instead of standard long monopolar pulses (classical ECT). We thus performed *in vitro* experiments on mouse skin melanoma cells, as melanoma is one of the cancers successfully treated with electrochemotherapy.⁴³

Optimal treatment parameters

First, we determined the cytotoxic effects of cisplatin on a confluent monolayer of cells, because survival after longer exposure time was not possi-

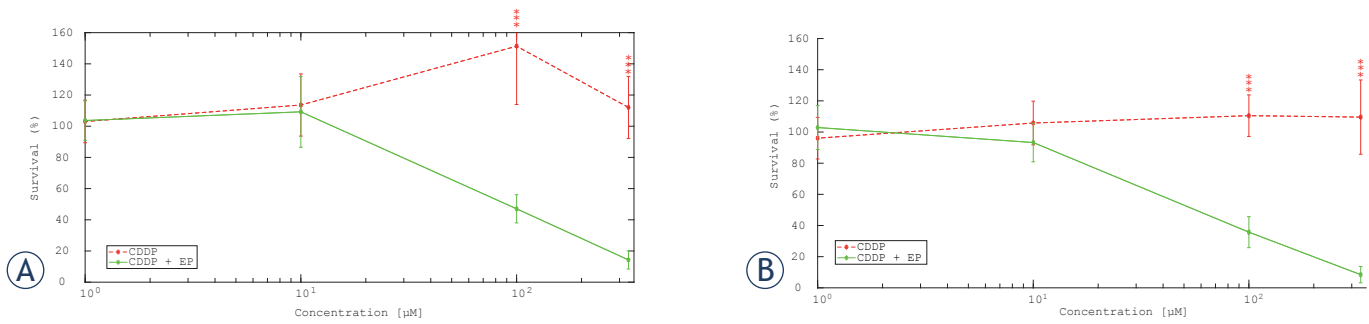


FIGURE 6. Cytotoxicity of cisplatin at different concentration of cisplatin (CDDP) and electroporation (EP) at a fixed value of electric field **(A)** 1.2 kV/cm, 8x100 μ s long monopolar pulses, delivered at repetition frequency 1 Hz; **(B)** 3 kV/cm, 8 bursts of short bipolar pulses (HF-EP) of 1-1-1-1 μ s, delivered at repetition frequency 1 Hz. Each data point was repeated 3-7 times (mean \pm standard deviation). Each data was normalized to the control sample electroporated and with 0.9% NaCl instead of cisplatin. We performed a 2-way ANOVA. For both types of pulses, at 100 μ M and 330 μ M the CDDP samples were significantly different from the CDDP+EP samples ($P < 0.001$).

ble to evaluate on cell suspension (Figure 4). At 100 μ M, short exposure (1 hour or less) did not affect survival. We decided to perform experiments with electroporation at 100 μ M cisplatin in order to see possible potentiation of the cytotoxic effect of cisplatin after electroporation. Namely, using higher concentration could already decrease survival without applying electric pulses and we could not assess, if electroporation increases cytotoxicity. In the experiments assessing survival after incubation with cisplatin as determined by the MTS assay, 24 h and 48 h time points were not different one from another and we assumed that also 72 h exposure (which was used in the electroporation experiments) would yield similar results. However, we did not make experiments also at 72 h exposure time.

We determined the optimal parameters for experiments with cisplatin and electric pulses, *i.e.*, the optimal voltage of electric pulses, incubation time with cisplatin after pulse application and cisplatin concentration with a) 100 μ s long monopolar pulses (ECT) and b) short bipolar pulses (HF-EP). In experiments with 8x100 μ s monopolar pulses, the optimal electric field (highest uptake of propidium and the highest cell survival) was 1.2 kV/cm (Figure 2A) which is in agreement with other studies⁴⁴ and corroborates our existing data where cell permeabilization was detected via intracellular platinum measurements.⁴⁵ Unfortunately, we could not apply voltages higher than 240 V (1.2 kV/cm) due to the current limitations of the pulse generator. We determined that the optimal electric field with HF-EP pulses was 3 kV/cm (Figure 2B). With bipolar pulses, we had to apply 2.5-times higher electric field than with monopolar pulses to obtain comparable effect, which is in agreement

with the results reported by Sweeney *et al.* for propidium uptake³⁸ and with the *in vitro* data on irreversible electroporation, where irreversible electroporation threshold increased 2.1-times, when 1 μ s long pulses were applied in bursts instead as 100 μ s long pulses.⁴⁶

With the selected parameters of electroporation, we measured the resealing rate of cells after electroporation. We determined that after 10 min cell membrane is mostly resealed (Figure 3) and did all subsequent cisplatin experiments with 10 min incubation. Dilution of cells with permeable membranes would namely reduce or stop the influx too early or even cause efflux of cisplatin due to dilution and potential reversal of the direction of the concentration gradient.⁴⁷ This time range is in agreement with the existing *in vitro* studies, where the incubation time ranges from 5 minutes²³ to 60 minutes⁴⁸ as well as with the *in vivo* standard operating procedures where the pulses are applied between 8 and 28 minutes after intravenous drug injection.¹⁹ With propidium iodide (PI) we could use shorter incubation times (2 minutes) as PI binds soon after entering the cell⁴⁹, but with cisplatin, we do not know how fast it binds, and we have to wait until cell membranes are completely resealed before the dilution is made. PI was used as a model for cisplatin as its molecular weight is in the same range as of cisplatin (668 g/mol and 300 g/mol for PI and cisplatin, respectively). The similarity in the shape of the permeabilization curve (Figure 2) and cell death due to cisplatin uptake (Figure 5) is another indicator that PI is an appropriate molecule to assess the uptake of cisplatin. Also, experiments with PI and flow cytometry are fast and easy to perform, enable screening of a wide range of parameters quicker than assessing cell survival or plati-

num uptake via mass spectrometry and are thus usually used to determine optimal parameters of electric pulses for electrochemotherapy *in vitro*.⁵⁰⁻⁵²

100 μM cisplatin concentration was chosen as we could (1) test several pulse parameters without reaching the limitations of the survival assay, (2) it is in a similar range as used in other *in vitro* studies.^{23,45,48,53,54} Other tested concentrations (1, 10, 100, 330 μM) were chosen as they were already used in previous *in vitro* experiments.^{23,45} (3) The IC50 value of cisplatin pooled together from several studies in⁵³ was determined to be between 0.83 μM and 1000 μM without electroporation and 0.083 μM and 106 μM with electroporation. As we determined graphically from Figure 6, the IC50 value was in our study 85 μM for monopolar, and 45 μM for bipolar pulses, which is in agreement with the literature and close to the 100 μM .

In our study, different cell densities were used due to different requirements for cell number and sensitivities of the chosen assays. However, even at the highest concentration (2.2×10^7 cells/ml) we were still well below the concentration where shielding of the electric field and decreased uptake were observed.³⁹ 72 h growth time after electrochemotherapy was chosen as it was shown that results of metabolic assays are highly dependent on evaluation time point and they correspond to the results of clonogenic assay better at later time points.⁴²

Cytotoxicity of cisplatin with electroporation

We measured the cytotoxicity of cisplatin with electroporation at fixed cisplatin concentration of 100 μM and different electric fields (Figure 5). We were interested in the effect of electric field intensity on cisplatin cytotoxicity, as usually when treating tumors *in vivo*, the electric field distribution is inhomogeneous due to different dielectric properties of different tissues and various electrode configurations.^{55,56} A similar tendency of cell survival as a function of the electric field was observed with monopolar as well as HF-EP pulses - we achieved greater cell death by applying cisplatin in combination with electric pulses than by only applying electric pulses. Survival decreased with increasing electric field. In Figure 5A, comparing the red curve with the green one, we can see that at $E = 1.2$ kV/cm cells die because of the cisplatin uptake and not due to irreversible electroporation. The survival after applying 1.2 kV/cm was still 100%, the survival with electric pulses and cisplatin dropped to $32.16\% \pm 14.08\%$. Similarly as with monopolar

pulses, when applying bipolar pulses of $E = 3$ kV/cm, cells die due to the cisplatin uptake and not due to irreversible electroporation (Figure 5B). At $E > 3$ kV/cm cell death is due to the cytotoxic effect of cisplatin as well as irreversible electroporation. As expected and in accordance with previously published results for propidium iodide, we needed to deliver 2.5-times higher electric field with the HF-EP pulses to achieve a comparable effect.³⁸

Interestingly, the shape of the permeabilization curve to propidium (Figure 2) corresponds perfectly to the shape of the survival curve after electrochemotherapy (Figure 5). The onset of membrane permeabilization is at 0.8 kV/cm for long monopolar pulses (Figure 2A) and at 2 kV/cm for HF-EP pulses (Figure 2B), which corresponds to the onset of the decrease in survival after electrochemotherapy (Figure 5). The plateau of membrane permeabilization for HF-EP pulses is reached at 3–3.5 kV/cm (Figure 2B) which corresponds to the reached plateau of survival (Figure 5B). Thus at our specific conditions, membrane permeability to propidium is a good indicator of cytotoxicity of cisplatin.

In Figure 6, we measured cytotoxicity of cisplatin with electroporation at a fixed electric field (monopolar pulses $E = 1.2$ kV/cm and short bipolar pulses $E = 3$ kV/cm) and different cisplatin concentrations. Namely, in tissues, inhomogeneous cisplatin concentration is expected, also initial cisplatin concentration is usually inhomogeneous after intratumoral injection.⁴⁵ Both (A) monopolar pulses at $E = 1.2$ kV/cm and (B) HF-EP pulses at $E = 3$ kV/cm show a similar behavior. In both Figures 6 A and B, the cytotoxicity of cisplatin increases more with cisplatin in combination with electric pulses than using only cisplatin.^{23,25} Indeed, without electric pulses application, a high dose of cisplatin and/or longer incubation times need to be used to achieve a decrease in cell survival (Figure 4). However, applying 330 μM cisplatin with long monopolar pulses only $14.28\% \pm 5.84\%$ of cell survived and with short bipolar pulses (HF-EP) only $8.45\% \pm 5.22\%$ of cell survived. We must keep in mind, that with short bipolar pulses, 2.5-times higher electric field was applied to achieve a similar effect. From the red dashed curve in Figure 6A and B we can see that cell survival did not decrease with increasing cisplatin concentration. This result should be the same as in Figure 4 considering only the 10 min curve, but in Figure 4 cell survival slightly decreases with increasing cisplatin concentration. The reasons for this discrepancy could be the differences in the protocols: attached cell monolayers to measure the cytotoxicity of cisplatin without

electroporation and cells in suspension to measure the cytotoxicity of cisplatin in combination with electroporation. Also, the attached cells were diluted much less with fresh DMEM after exposure to cisplatin than cells in suspension. Besides, cell survival was measured after 48h for the attached cell and after 72 h for the cell in suspension.

Outlooks for using high-frequency electroporation in the clinics

HF-IRE pulses were reported to reduce muscle contractions in comparison with classic 100 μ s pulses which was observed in several studies *in vivo*. For example, muscle contractions with HF-IRE pulses were much less noticeable than with 100 μ s long monopolar pulses in experiments on rabbit liver.^{33,57,58} Even in the absence of cardiac synchronization and paralytics, only minor muscle twitch was recorded in one out of 24 cases^{59,60} when treating porcine liver. Sano *et al.* observed that HF-IRE waveforms reduced the intensity of muscle contractions in comparison with traditional IRE pulses on *ex-vivo* porcine model³⁴ and in *in vivo* murine tumor.⁴⁶ Arena *et al.* observed that HF-IRE pulses eliminated muscle contractions when electric pulses were applied to the brain of rats³⁷ and achieved blood-brain-barrier disruption without inducing local or distal muscle contractions.⁶¹ Latouche *et al.* observed no evidence of muscle or nerve excitation or cardiac arrhythmia during any pulse delivery when treating intracranial meningioma in dogs.³⁵ In a first human study on high-frequency irreversible electroporation of prostate cancer, only a small amount of muscle relaxant was needed, and there were no visible muscle contractions during the pulse delivery process.³⁶ Additionally, the histological analysis in *in vivo* porcine experiments indicates that with HF-IRE rapid and reproducible ablation in the liver can be achieved, while preserving gross vascular/biliary architecture.⁶⁰ The mechanism for decreased muscle contractions is still unknown. However, different possible explanations were offered. It was suggested that (1) stimulation threshold raises faster than the threshold for irreversible electroporation with decreasing pulse length⁶² which is a consequence of geometrical differences between nerve fibers and tumor cells.⁶³ (2) At around 1 μ s there is an overlap of the depolarization threshold and electroporation threshold on the strength-intensity curve.⁴¹ (3) The short negative pulse delivered after a positive pulse accelerated the passive repolarization and swamped the regenerative response, thus abolishing the action

potential.⁶⁴ The pain was not yet evaluated, but promising results regarding muscle contractions indicate that we can expect less pain with HF-EP than with classical 100 μ s pulses.

Before transfer to the clinical setting, more experiments *in vitro* as well *in vivo* need to be performed. In the scope of the current study, experiments with bleomycin are not feasible due to organizational reasons. However, we are planning to perform, in the future, experiments using bleomycin with HF-EP, as bleomycin is frequently used for ECT in the clinics. So, cytotoxicity of bleomycin and HF-EP needs to be assessed, and experiments determining intratumoral cisplatin/bleomycin concentration should be performed. The electric field needed to achieve cell death is with HF-EP higher than in classical EP, and thus the effect of high voltage on important structures in the vicinity of the tumors should be investigated, similarly as in⁶⁰ for hepatic veins. Also, temperature increase due to Joule heating has to be minimized for example by introducing a delay between bursts^{36,59}, limiting electric current or number of bursts^{36,46,61} and avoiding increased temperature by optimizing treatment parameters.^{35,37,58,61} The influence of HF-EP on muscle contractions, pain and heart rhythm should also be studied, as is being done for high-frequency irreversible electroporation. Currently, pulses in the published studies are being applied with laboratory prototypes - a clinical generator of bipolar pulses needs to be designed and certified before clinical use. However, electrode geometry could be the same as those used with the longer monopolar pulses, but electrical isolation of the wiring and stray capacitance should be re-evaluated.

Applying HF-EP pulses comes at the expense of delivering considerably higher pulse amplitude. However, we need to take into account that in our study, we focused on eight bursts in total on-time of 800 μ s to enable comparison with the standard ECT protocol and be consistent with previous studies.³⁸ To obtain a good effect while keeping the applied voltage low, we could apply more bursts, longer pulses than 1 μ s or asymmetrical bipolar pulses^{34,65}, although it was indicated that muscle contractions are increased with the asymmetrical waveforms. Also of importance is that with pulses in the range of a few microseconds, we are already in the range of the so-called cancellation effect which could be partially responsible for decreased effect of shorter pulses in comparison to longer pulses.^{38,66} We can nevertheless conclude that HF-EP pulses can be successfully used in electrochemotherapy treat-

ments *in vitro*, however, at the expense of delivering electric pulses of higher amplitudes.³⁸

Although still at the *in vitro* testing stage, we believe that the use of HF-EP pulses for electrochemotherapy in the clinics could potentially decrease the discomfort connected with muscle contractions and pain, simplifying the treatment procedure by lowering dose of muscle relaxants and anesthesia, and avoid synchronization with the electrocardiogram, while potentially achieving more homogeneous electric field distribution⁶⁷ and reducing the electrolytic contamination.⁶⁸

Conclusions

In conclusion, with long monopolar and short bipolar pulses (HF-EP), we achieved similar efficiency of electrochemotherapy with cisplatin *in vitro*, however, with short bipolar pulses, we had to apply a much higher electric field for the same effect. Nevertheless, we believe that HF-EP pulses could eventually be translated into the clinical setting to be used in electrochemotherapy treatments to alleviate pain, reduce muscle contractions, decrease the needed dose of anesthetics and muscle relaxants while maintaining high treatment efficacy. Further studies of the HF-EP pulses for electrochemotherapy with bleomycin *in vitro* and *in vivo* are needed.

Acknowledgments

This work was supported by the Slovenian Research Agency (ARRS) [research core funding No. P2-0249 and IP-0510]. The research was conducted within the scope of the electroporation in Biology and Medicine (EBAM) European Associated Laboratory (LEA). Authors would like to thank L. Vukanović and D. Hodžić for their help in the cell culture laboratory and dr. T. Jarm for his help with the statistical analysis and M. Bernik for the linguistic revision of Slovenian abstract. M.S. would like to thank dr. E. Sieni for her help and acknowledge the Erasmus+ grant.

References

- Kotnik T, Kramar P, Pucihar G, Miklavcic D, Tarek M. Cell membrane electroporation-part 1: the phenomenon. *IEEE Electr Insul Mag* 2012; **28**: 14-23. doi: 10.1109/MEI.2012.6268438
- Weaver JC. Electroporation: a general phenomenon for manipulating cells and tissues. *J Cell Biochem* 1993; **51**: 426-35. doi: 10.1002/jcb.2400510407
- Tsong TY. Electroporation of cell membranes. *Biophys J* 1991; **60**: 297-306. doi: 10.1016/S0006-3495(91)82054-9
- Kotnik T, Rems L, Tarek M, Miklavcic D. Membrane electroporation and electroporabilization: mechanisms and models. *Annu Rev Biophys* 2019; **48**. doi: 10.1146/annurev-biophys-052118-115451
- Yarmush ML, Golberg A, Serša G, Kotnik T, Miklavcic D. Electroporation-based technologies for medicine: principles, applications, and challenges. *Annu Rev Biomed Eng* 2014; **16**: 295-320. doi: 10.1146/annurev-bioeng-071813-104622
- Jiang C, Davalos RV, Bischof JC. A review of basic to clinical studies of irreversible electroporation therapy. *IEEE Trans Biomed Eng* 2015; **62**: 4-20. doi: 10.1109/TBME.2014.2367543
- Scheffer HJ, Nielsen K, de Jong MC, van Tilborg AA, Vieveen JM, Bouwman AR, et al. Irreversible electroporation for nonthermal tumor Ablation in the clinical setting: a systematic review of safety and efficacy. *J Vasc Interv Radiol* 2014; **25**: 997-1011. doi: 10.1016/j.jvir.2014.01.028
- Mali B, Jarm T, Snoj M, Serša G, Miklavcic D. Antitumor effectiveness of electrochemotherapy: a systematic review and meta-analysis. *Eur J Surg Oncol* 2013; **39**: 4-16. doi: 10.1016/j.ejso.2012.08.016
- Haberl S, Miklavcic D, Serša G, Frey W, Rubinsky B. Cell membrane electroporation – part 2: the applications. *Electr Insul Mag IEEE* 2013; **29**: 29-37. doi: 10.1109/MEI.2013.6410537
- Cadossi R, Ronchetti M, Cadossi M. Locally enhanced chemotherapy by electroporation: clinical experiences and perspective of use of electrochemotherapy. *Future Oncol* 2014; **10**: 877-90. doi: 10.2217/fon.13.235
- Kotnik T, Frey W, Sack M, Meglič SH, Peterka M, Miklavcic D. Electroporation-based applications in biotechnology. *Trends Biotechnol* 2015; **33**: 480-8. doi: 10.1016/j.tibtech.2015.06.002
- Golberg A, Sack M, Teissie J, Pataro G, Pliquett U, Saulis G, et al. Energy-efficient biomass processing with pulsed electric fields for bioeconomy and sustainable development. *Biotechnol Biofuels* 2016; **9**: 94. doi: 10.1186/s13068-016-0508-z
- Toepfl S, Siemer C, Saldaña-Navarro G, Heinz V. Overview of pulsed electric fields processing for food. In: Sun DW, editor. *Emerging technologies for food processing*. Second edition. Amsterdam: Academic press; Elsevier; 2014. p. 93-114. doi: 10.1016/B978-0-12-411479-1.00006-1
- Mahnich-Kalamiza S, Vorobiev E, Miklavcic D. Electroporation in food processing and biorefinery. *J Membr Biol* 2014; **247**: 1279-304. doi: 10.1007/s00232-014-9737-x
- Campana LG, Edhemović I, Soden D, Perrone AM, Scarpa M, Campanacci L, et al. Electrochemotherapy - emerging applications technical advances, new indications, combined approaches, and multi-institutional collaboration. *Eur J Surg Oncol* 2019; **45**: 92-102. doi: 10.1016/j.ejso.2018.11.023
- Miklavcic D, Mali B, Kos B, Heller R, Serša G. Electrochemotherapy: from the drawing board into medical practice. *Biomed Eng OnLine* 2014; **13**: 29. doi: 10.1186/1475-925X-13-29
- Mir LM, Gehl J, Serša G, Collins CG, Garbay J-R, Billard V, et al. Standard operating procedures of the electrochemotherapy: instructions for the use of bleomycin or cisplatin administered either systemically or locally and electric pulses delivered by the Cliniporator™ by means of invasive or non-invasive electrodes. *Eur J Cancer Suppl* 2006; **4**: 14-25. doi: 10.1016/j.ejcsup.2006.08.003
- Gehl J, Serša G, Matthiessen LW, Muir T, Soden D, Occhini A, et al. Updated standard operating procedures for electrochemotherapy of cutaneous tumours and skin metastases. *Acta Oncol Stockh Swed* 2018; **57**: 874-82. doi: 10.1080/0284186X.2018.1454602
- Marty M, Serša G, Garbay JR, Gehl J, Collins CG, Snoj M, et al. Electrochemotherapy – An easy, highly effective and safe treatment of cutaneous and subcutaneous metastases: results of ESOP (European Standard Operating Procedures of Electrochemotherapy) study. *Eur J Cancer Suppl* 2006; **4**: 3-13. doi: 10.1016/j.ejcsup.2006.08.002
- Mir LM, Tounekti O, Orłowski S. Bleomycin: revival of an old drug. *Gen Pharmacol* 1996; **27**: 745-8. doi: 10.1016/0306-3623(95)02101-9
- Tounekti O, Pron G, Belehradek J, Mir LM. Bleomycin, an apoptosis-mimetic drug that induces two types of cell death depending on the number of molecules internalized. *Cancer Res* 1993; **53**: 5462-9. PMID: 7693342

22. Spreckelmeyer S, Orvíg C, Casini A. Cellular transport mechanisms of cytotoxic metallo drugs: an overview beyond cisplatin. *Molecules* 2014; **19**: 15584-610. doi: 10.3390/molecules191015584
23. Serša G, Čemažar M, Miklavčič D. Antitumor effectiveness of electrochemotherapy with cis-diamminedichloroplatinum(II) in mice. *Cancer Res* 1995; **55**: 3450-5. PMID: 7614485
24. Tozon N, Serša G, Čemažar M. Electrochemotherapy: potentiation of local antitumor effectiveness of cisplatin in dogs and cats. *Anticancer Res* 2001; **21**: 2483-8. PMID: 11724311
25. Jaroszeski MJ, Dang V, Pottinger C, Hickey J, Gilbert R, Heller R. Toxicity of anticancer agents mediated by electroporation in vitro. *Anticancer Drugs* 2000; **11**: 201-8. PMID: 10831279
26. Županič A, Ribarič S, Miklavčič D. Increasing the repetition frequency of electric pulse delivery reduces unpleasant sensations that occur in electrochemotherapy. *Neoplasma* 2007; **54**: 246-50. PMID: 17447858
27. Miklavčič D, Pucihar G, Pavlovec M, Ribarič S, Mali M, Maček-Lebar A, et al. The effect of high frequency electric pulses on muscle contractions and antitumor efficiency in vivo for a potential use in clinical electrochemotherapy. *Bioelectrochemistry* 2005; **65**: 121-8. doi: 10.1016/j.bioelechem.2004.07.004
28. Arena CB, Davalos RV. Advances in therapeutic electroporation to mitigate muscle contractions. *J Membr Sci Technol* 2012; **2**: 1-3. doi: 10.4172/2155-9589.1000e102
29. Ball C, Thomson KR, Kavvounias H. Irreversible electroporation: a new challenge in "Out of Operating Theater" anesthesia. *Anesth Analg* 2010; **110**: 1305-9. doi: 10.1213/ANE.0b013e3181d27b30
30. Mali B, Jarm T, Čorović S, Paulin-Kosir MS, Čemažar M, Serša G, et al. The effect of electroporation pulses on functioning of the heart. *Med Biol Eng Comput* 2008; **46**: 745-57. doi: 10.1007/s11517-008-0346-7
31. Deodhar A, Dickfeld T, Single GW, Hamilton WC, Thornton RH, Sofocleous CT, et al. Irreversible electroporation near the heart: ventricular arrhythmias can be prevented with ECG synchronization. *AJR Am J Roentgenol* 2011; **196**: W330-5. doi: 10.2214/AJR.10.4490
32. Golberg A, Rubinsky B. Towards electroporation based treatment planning considering electric field induced muscle contractions. *Technol Cancer Res Treat* 2012; **11**: 189-201. doi: 10.7785/tcrt.2012.500249
33. Yao C, Dong S, Zhao Y, Lv Y, Liu H, Gong L, et al. Bipolar microsecond pulses and insulated needle electrodes for reducing muscle contractions during irreversible electroporation. *IEEE Trans Biomed Eng* 2017; **64**: 2924-37. doi: 10.1109/TBME.2017.2690624
34. Sano MB, Fan RE, Cheng K, Saenz Y, Sonn GA, Hwang GL, et al. Reduction of muscle contractions during irreversible electroporation therapy using high-frequency bursts of alternating polarity pulses: a laboratory investigation in an ex vivo swine model. *J Vasc Interv Radiol JVIR* 2018; **29**: 893-8.e4. doi: 10.1016/j.jvir.2017.12.019
35. Latouche EL, Arena CB, Ivey JW, Garcia PA, Pancotto TE, Pavlisko N, et al. High-frequency irreversible electroporation for intracranial meningioma: A feasibility study in a spontaneous canine tumor model. *Technol Cancer Res Treat* 2018; **17**: 1-10. doi: 10.1177/1533033818785285
36. Dong S, Wang H, Zhao Y, Sun Y, Yao C. First human trial of high-frequency irreversible electroporation therapy for prostate cancer. *Technol Cancer Res Treat* 2018; **17**: 1-9. doi: 10.1177/1533033818789692
37. Arena CB, Sano MB, Rossmel JH, Caldwell JL, Garcia PA, Rylander M, et al. High-frequency irreversible electroporation (H-FIRE) for non-thermal ablation without muscle contraction. *Biomed Eng OnLine* 2011; **10**: 102. doi: 10.1186/1475-925X-10-102
38. Sweeney DC, Reberšek M, Dermol J, Rems L, Miklavčič D, Davalos RV. Quantification of cell membrane permeability induced by monopolar and high-frequency bipolar bursts of electrical pulses. *Biochim Biophys Acta BBA - Biomembr* 2016; **1858**: 2689-98. doi: 10.1016/j.bbame.2016.06.024
39. Pucihar G, Kotnik T, Teissié J, Miklavčič D. Electroporation of dense cell suspensions. *Eur Biophys J* 2007; **36**: 173-85. doi: 10.1007/s00249-006-0115-1
40. Dermol J, Miklavčič D. Mathematical models describing chinese hamster ovary cell death due to electroporation in vitro. *J Membr Biol* 2015; **248**: 865-81. doi: 10.1007/s00232-015-9825-6
41. Dermol-Černe J, Miklavčič D, Reberšek M, Mekuč P, Bardet SM, Burke R, et al. Plasma membrane depolarization and permeabilization due to electric pulses in cell lines of different excitability. *Bioelectrochemistry* 2018; **122**: 103-14. doi: 10.1016/j.bioelechem.2018.03.011
42. Jakštys B, Ruzgys P, Tamošiūnas M, Šatkauskas S. Different cell viability assays reveal inconsistent results after bleomycin electrotransfer in vitro. *J Membr Biol* 2015; **248**: 857-63. doi: 10.1007/s00232-015-9813-x
43. Serša G, Štabuc B, Čemažar M, Miklavčič D, Rudolf Z. Electrochemotherapy with cisplatin: clinical experience in malignant melanoma patients. *Clin Cancer Res* 2000; **6**: 863-7. PMID: 10741708
44. Čemažar M, Jarm T, Miklavčič D, Maček Lebar A, Ihan A, Kopitar NA, et al. Effect of electric-field intensity on electroporation and electro-sensitivity of various tumor-cell lines in vitro. *Electro-Magnetobiology* 1998; **17**: 263-72. doi.org/10.3109/15368379809022571
45. Dermol-Černe J, Vidmar J, Ščančar J, Uršič K, Serša G, Miklavčič D. Connecting the in vitro and in vivo experiments in electrochemotherapy - a feasibility study modeling cisplatin transport in mouse melanoma using the dual-porosity model. *J Control Release* 2018; **286**: 33-45. doi: 10.1016/j.jconrel.2018.07.021
46. Sano MB, Arena CB, Bittleman KR, DeWitt MR, Cho HJ, Szot CS, et al. Bursts of Bipolar Microsecond Pulses Inhibit Tumor Growth. *Sci Rep* 2015; **5**: 14999. doi: 10.1038/srep14999
47. Puc M, Kotnik T, Mir LM, Miklavčič D. Quantitative model of small molecules uptake after in vitro cell electroporation. *Bioelectrochemistry Amst Neth* 2003; **60**: 1-10. doi: 10.1016/S1567-5394(03)00021-5
48. Gehl J, Skovsgaard T, Mir LM. Enhancement of cytotoxicity by electroporation: an improved method for screening drugs. *Anticancer Drugs* 1998; **9**: 319-25. PMID: 9635922
49. Pucihar G, Kotnik T, Miklavčič D, Teissié J. Kinetics of transmembrane transport of small molecules into electroporated cells. *Biophys J* 2008; **95**: 2837-48. doi: 10.1529/biophysj.108.135541
50. Čemažar M, Serša G, Miklavčič D. Electrochemotherapy with cisplatin in the treatment of tumor cells resistant to cisplatin. *Anticancer Res* 1998; **18**: 463-6. PMID: 9891510
51. Saczko J, Kamińska I, Kotulska M, Bar J, Choromańska A, Rembiałkowska N, et al. Combination of therapy with 5-fluorouracil and cisplatin with electroporation in human ovarian carcinoma model in vitro. *Biomed Pharmacother* 2014; **68**: 573-80. doi: 10.1016/j.biopha.2014.05.005
52. Žakelj M, Prevc A, Kranjc S, Čemažar M, Todorovič V, Savarin M, et al. Electrochemotherapy of radioresistant head and neck squamous cell carcinoma cells and tumor xenografts. *Oncol Rep* 2019; **41**: 1658-68. doi: 10.3892/or.2019.6960
53. Todorovič V, Serša G, Flisar K, Čemažar M. Enhanced cytotoxicity of bleomycin and cisplatin after electroporation in murine colorectal carcinoma cells. *Radiol Oncol* 2009; **43**: 264-73. doi: 10.2478/v10019-009-0037-5
54. Vásquez JL, Ibsen P, Lindberg H, Gehl J. In vitro and in vivo experiments on electrochemotherapy for bladder cancer. *J Urol* 2015; **193**: 1009-15. doi: 10.1016/j.juro.2014.09.039
55. Kranjc M, Markelc B, Bajd F, Čemažar M, Serša I, Blagus T, et al. In situ monitoring of electric field distribution in mouse tumor during electroporation. *Radiology* 2015; **274**: 115-23. doi: 10.1148/radiol.14140311
56. Čorović S, Pavlin M, Miklavčič D. Analytical and numerical quantification and comparison of the local electric field in the tissue for different electrode configurations. *Biomed Eng OnLine* 2007; **6**: 37. doi: 10.1186/1475-925X-6-37
57. Dong S, Yao C, Zhao Y, Lv Y, Liu H. Parameters optimization of bipolar high frequency pulses on tissue ablation and inhibiting muscle contraction. *IEEE Trans Dielectr Electr Insul* 2018; **25**: 207-16. doi: 10.1109/TDEI.2018.006303
58. Zhao Y, Bhonsle S, Dong S, Lv Y, Liu H, Safaai-Jazi A, et al. Characterization of conductivity changes during high-frequency irreversible electroporation for treatment planning. *IEEE Trans Biomed Eng* 2018; **65**: 1810-9. doi: 10.1109/TBME.2017.2778101
59. Siddiqui IA, Latouche EL, DeWitt MR, Swet JH, Kirks RC, Baker EH, et al. Induction of rapid, reproducible hepatic ablations using next-generation, high frequency irreversible electroporation (H-FIRE) in vivo. *HPB* 2016; **18**: 726-34. doi: 10.1016/j.hpb.2016.06.015

60. Siddiqui IA, Kirks RC, Latouche EL, DeWitt MR, Swet JH, Baker EH, et al. High-frequency irreversible electroporation: Safety and efficacy of next-generation irreversible electroporation adjacent to critical hepatic structures. *Surg Innov* 2017; **24**: 276-83. doi: 10.1177/1553350617692202
61. Arena CB, Garcia PA, Sano MB, Olson JD, Rogers-Cotrone T, Rossmeis JH, et al. Focal blood-brain-barrier disruption with high-frequency pulsed electric fields. *Technology* 2014; **2**: 206-13. doi: 10.1142/S2339547814500186
62. Rogers WR, Merritt JH, Comeaux JA, Kuhnel CT, Moreland DF, Teltschik DG, et al. Strength-duration curve for an electrically excitable tissue extended down to near 1 nanosecond. *IEEE Trans Plasma Sci* 2004; **32**: 1587-99. doi: 10.1109/TPS.2004.831758
63. Mercadal B, Arena CB, Davalos RV, Ivorra A. Avoiding nerve stimulation in irreversible electroporation: a numerical modeling study. *Phys Med Biol* 2017; **62**: 8060-79. doi: 10.1088/1361-6560/aa8c53
64. van den Honert C, Mortimer JT. The response of the myelinated nerve fiber to short duration biphasic stimulating currents. *Ann Biomed Eng* 1979; **7**: 117-25. doi: 10.1007/BF02363130.
65. Sano MB, Fan RE, Xing L. Asymmetric waveforms decrease lethal thresholds in high frequency irreversible electroporation therapies. *Sci Rep* 2017; **7**: 40747. doi: 10.1038/srep40747
66. Valdez CM, Barnes R, Roth CC, Moen E, Ibey B. The interphase interval within a bipolar nanosecond electric pulse modulates bipolar cancellation. *Bioelectromagnetics* 2018; **39**: 441-50. doi: 10.1002/bem.22134
67. Bhonsle SP, Arena CB, Sweeney DC, Davalos RV. Mitigation of impedance changes due to electroporation therapy using bursts of high-frequency bipolar pulses. *Biomed Eng Online* 2015; **14(Suppl 3)**: S3. doi: 10.1186/1475-925X-14-S3-S3
68. Kotnik T, Miklavčič D, Mir LM. Cell membrane electropermeabilization by symmetrical bipolar rectangular pulses. Part II. Reduced electrolytic contamination. *Bioelectrochemistry* 2001; **54**: 91-5. doi: 10.1016/S1567-5394(01)00115-3

The influence of genetic variability of DNA repair mechanisms on the risk of malignant mesothelioma

Kristina Levpuscek¹, Katja Goricar², Viljem Kovac³, Vita Dolzan², Alenka Franko⁴

¹ Faculty of Medicine, University of Ljubljana, Ljubljana, Slovenia

² Pharmacogenetics Laboratory, Institute of Biochemistry, Faculty of Medicine, University of Ljubljana, Ljubljana, Slovenia

³ Institute of Oncology Ljubljana, Ljubljana, Slovenia

⁴ Clinical Institute of Occupational Medicine, University Medical Center Ljubljana, Ljubljana, Slovenia

Radiol Oncol 2019; 53(2): 206-212.

Received 6 February 2019

Accepted 25 February 2019

Correspondence to: Assoc. Prof. Alenka Franko, M.D., Ph.D., Clinical Institute of Occupational Medicine, University Medical Center Ljubljana, Poljanski nasip 58, Ljubljana, Slovenia. Phone: +386 1 522 2119; Fax: +386 1 522 2478; Email: alenka.franko@siol.net

Disclosure: No potential conflicts of interest were disclosed.

Background. Malignant mesothelioma (MM) is a rare aggressive tumour of mesothelium caused by asbestos exposure. It has been suggested that the genetic variability of proteins involved in DNA repair mechanisms affects the risk of MM. This study investigated the influence of functional polymorphisms in *ERCC1* and *XRCC1* genes, the interactions between these polymorphisms as well as the interactions between these polymorphisms and asbestos exposure on MM risk.

Patients and methods. In total, 237 cases with MM and 193 controls with no asbestos-related disease were genotyped for *ERCC1* and *XRCC1* polymorphisms.

Results. *ERCC1* rs3212986 polymorphism was significantly associated with a decreased risk of MM (odds ratio [OR] = 0.61; 95% confidence interval [CI] = 0.41–0.91; $p = 0.014$). No associations were observed between other genetic polymorphisms and MM risk. Interactions between polymorphisms did not significantly influence MM risk. Interaction between *ERCC1* rs11615 and asbestos exposure significantly influenced MM risk (OR = 3.61; 95% CI = 1.12–11.66; $p = 0.032$). Carriers of polymorphic *ERCC1* rs11615 allele who were exposed to low level of asbestos had a decreased risk of MM (OR = 0.40; 95% CI = 0.19–0.84; $p = 0.016$). Interactions between other polymorphisms and asbestos exposure did not significantly influence MM risk.

Conclusions. Our findings suggest that the genetic variability of DNA repair mechanisms could contribute to the risk of developing MM.

Key words: malignant mesothelioma; DNA repair mechanisms; *ERCC1*; *XRCC1*; genetic polymorphism

Introduction

Malignant mesothelioma (MM) is a rare and aggressive tumour of the serosal membranes with poor prognosis. It is mainly localized to the pleura, but could also arise in the peritoneum, pericardium and tunica vaginalis.¹⁻³ MM is more commonly found in men than in women. It occurs mainly in adults, 75% of patients are older than 65 years.⁴ The majority of MM cases could be attributed to occupational or environmental exposure to asbestos.^{3,5-7}

The global incidence is expected to continue to increase due to a long latency period, which could range from 15 to 60 years.⁸ Although the association between asbestos exposure and occurrence of MM is well established, the mechanism of carcinogenesis is not fully explained.^{9,10} Nevertheless, some studies reported genotoxic effects of asbestos.¹¹⁻¹³ It has been suggested that the DNA damage may be caused by the direct influence of asbestos fibres that interfere with mitosis or by the indirect effect caused by the release of reactive oxygen

species (ROS) and reactive nitrogen species (RNS) from macrophages. It is well established, that oxidative stress triggers DNA repair mechanisms, however, their role in the development of MM has not been fully studied yet.^{12,13} It has been suggested that the genetic variability of proteins involved in DNA repair mechanisms affects the risk of MM. In particular, excision repair cross-complementing group 1 (ERCC1) and X-ray repair cross-complementing protein 1 (XRCC1) may be involved and genes coding for these proteins are known to be polymorphic.^{14,15}

ERCC1 is a protein involved in the repair of DNA by nucleotide excision repair (NER). Together with the Xeroderma pigmentosum F it forms an endonuclease, which also participates in homologous recombination and base excision repair (BER).¹⁶ The ERCC1 protein plays crucial role in NER, so some studies suggested that *ERCC1* polymorphisms could attribute to increased risk of several malignant diseases.^{17,18} The gene for the ERCC1 protein is located on the chromosome 19q13.32 and consists of 10 exons.¹⁹ Numerous polymorphisms of *ERCC1* gene have been described, rs11615 and rs3212986 being the most commonly studied ones. Single nucleotide polymorphism (SNP) *ERCC1* rs11615 results in the replacement of cytosine (C) with thymine (T) without amino acid substitution. Studies have shown that carriers of this SNP have an increased risk of head and neck squamous cell carcinomas, breast cancer and a reduced risk of ovarian cancer.^{18,20,21} The SNP *ERCC1* rs3212986 causes the replacement of T with guanine (G) in the 3' untranslated region. It has been associated with an increased risk of colorectal cancer and a reduced risk of hepatocellular carcinoma.^{22,23}

XRCC1 is an important protein involved in BER and the repair of DNA single-strand breaks (SSBR). It does not have enzymatic activity, but acts as a scaffolding protein that interacts with repair enzymes.²⁴ The *XRCC1* gene is located on chromosome 19q13.2 and consists of 17 exons. Recent studies have been investigating association between *XRCC1* polymorphisms and the development of various types of cancer. More than 60 polymorphisms of this gene are known. The most common are rs25487, rs25489 and rs1799782.²⁵ SNP *XRCC1* rs25487 causes the replacement of G with adenine (A), causing the substitution of glycine (Gln) with arginine (Arg) in codon 399 (p.399Gln>Arg).²⁶ This polymorphism has been associated with an increased risk of developing thyroid and lung cancer.^{27,28} Other common *XRCC1* polymorphism is rs1799782, which causes the replacement of C with

T and consequently the replacement of Arg with tryptophan (Trp) at position 194 (p.194Arg> Trp). A Chinese study described that the SNP *XRCC1* rs1799782 is associated with an increased risk of lung cancer.²⁸

So far only two studies investigated the influence of the genetic variability of proteins involved in DNA repair mechanisms on the development of MM. The first study investigated the influence of *XRCC1* rs25487 and rs1799782, and *XRCC3* rs861539 and rs861535 polymorphisms on the development of MM and found that carriers of polymorphic allele *XRCC1* rs25487 have an increased risk on the development of this cancer.¹⁴ The second study investigated the influence of *ERCC1* rs11615, rs2298881, rs3212948 and rs3212965, and *XRCC1* rs25487, rs3213245, rs1799782, rs3213247, rs12973352, rs2854496, rs2307174, rs2023614, rs1799778, rs3213356, rs3213371 and rs3213403 polymorphisms on the risk of MM. It has been reported that carriers of polymorphic alleles *ERCC1* rs11615 and *XRCC1* rs25487 have an increased risk of MM. The interaction between these polymorphisms also contributed to an increased risk of developing MM.¹⁵

According to our knowledge and available literature the influence of the *ERCC1* rs3212986 polymorphism as well as the impact of interactions between polymorphisms of proteins involved in DNA repair mechanisms and asbestos exposure on the risk of developing MM has not been studied yet.

The aim of this study was to investigate whether functional polymorphisms in *ERCC1* and *XRCC1* genes influence the risk of MM, to study the influence of the interactions between *ERCC1* and *XRCC1* polymorphisms on MM risk as well as to investigate the effect of the interactions between these polymorphisms and asbestos exposure on MM risk.

Patients and methods

Patients

A retrospective case-control study included 237 patients with pleural or peritoneal MM treated at the Institute of Oncology Ljubljana between November 2001 and October 2016, along with 193 controls who worked and were occupationally exposed to asbestos in the asbestos cement factory of Salonit Anhovo, Slovenia. The controls were evaluated at the State Board for the Recognition of Occupational Asbestos Diseases between January

1999 and December 2003 and did not have any asbestos-related disease.

The study was approved by the Slovenian Ethics Committee for Research in Medicine and was carried out according to the Declaration of Helsinki.

Methods

Patients with pleural MM were diagnosed by ultrasound-guided biopsy or thoracoscopy and patients with peritoneal MM were diagnosed by laparoscopy. The diagnosis was confirmed by a histopathological examination by an experienced pathologist.⁵

The asbestos exposure was determined by semi-quantitative method. For all controls and some patients with MM, the data on cumulative asbestos exposure in fibres/cm³-years were available. On the basis of this data, the subjects were divided into three groups: low (< 11 fibres/cm³-years), medium (11–20 fibres/cm³-years) and high (> 20 fibres/cm³-years) asbestos exposure. For those patients with MM where cumulative asbestos exposure data were not available, a precise work history was obtained and their asbestos exposure was deduced from comparison to a group of subjects with known cumulative asbestos exposure at a given working place. Also in this case the exposure was divided into three groups: low, medium and high asbestos exposure. A personal interview with each of the subjects was performed to obtain

the data on smoking using a standardized questionnaire.^{5,29}

DNA of the MM patients and some controls without asbestos-related diseases was available from our previous studies.⁵ DNA from the rest of the controls was isolated from capillary blood collected on Whatman FTA cards during this study using MagMax™ DNA Multi-Sample Kit (Applied Biosystems, Foster City, California, USA). Competitive allele-specific and real-time polymerase chain reaction (PCR) based KASP and TaqMan assays were used for the analysis of *ERCC1* rs11615, rs3212986 and *XRCC1* rs1799782, rs25487 polymorphisms as recommended by the manufacturer (KBioscience, Hoddesdon, Herts, UK and Thermo Fisher Scientific, USA). Amplification was not successful in 19 subjects for *ERCC1* rs11615, in 17 for *ERCC1* rs3212986, in 12 for *XRCC1* rs1799782 and in 20 subjects for *XRCC1* rs25487 polymorphism due to limited DNA samples.

Statistical methods

Standard descriptive statistics were first performed. To determine the differences in age between the cases and controls the non-parametric Mann-Whitney (U) test was performed.

The dominant genetic models were used for all the comparisons. To analyse the association between genotypes, cumulative asbestos exposure, and standard confounders (age, gender) and MM,

TABLE 1. Characteristics of malignant mesothelioma (MM) patients, controls and the influence of these characteristics on MM risk

	MM patients (n = 237)	Controls (n = 193)	Test	OR (95% CI)	p
Gender					
Male n (%)	175 (73.8%)	128 (66.3%)	$\chi^2 = 2.889$	0.70 (0.46–1.06)	0.089
Female n (%)	62 (26.2%)	65 (33.7%)			
Age					
Years; median (25–75%)	66 (58–72)	56.2 (49.3–65.0)	U = 32583	1.08 (0.46–1.06)	< 0.001
Cumulative asbestos exposure¹					
Low	36 (44.4%)	149 (77.2%)	$\chi^2 = 31.933$		< 0.001
Medium	24 (29.6%)	15 (7.8%)			
High	21 (25.9%)	29 (15.0%)			
Low Medium and high	36 (44.4%) 45 (55.6)	149 (77.2%) 44 (22.8%)	$\chi^2 = 27.916$	4.23 ³ (2.44–7.36)	< 0.001
Smoking²					
No	122 (53.0%)	106 (54.9%)	$\chi^2 = 0.149$	1.08 (0.74–1.58)	0.699
Yes	108 (47.0%)	87 (45.1%)			

¹ data available for 81 MM patients, ² data missing for 7 MM patients, ³ medium and high exposure in comparison to low exposure

univariate logistic regression was first used, followed by multivariate logistic regression modeling. The interactions were calculated by logistic regression models using dummy variables.

Results

The patients' and controls' characteristics are shown in Table 1. There was no statistical difference in gender ($p = 0.089$) and smoking ($p = 0.699$)

between the two groups. Groups differed significantly by age ($p < 0.001$) and cumulative asbestos exposure ($p < 0.001$). The median age was 66.0 years for patients and 56.2 years for controls. In univariate logistic regression analysis age, gender and smoking did not affect the risk of MM. The results showed that medium and high level of asbestos exposure increased the risk of MM 4-fold (odds ratio [OR] = 4.23; 95% confidence interval [CI] = 2.44–7.36; $p < 0.001$) in comparison to a low level of asbestos exposure (Table 1).

TABLE 2. The influence of polymorphisms on MM risk

Polymorphism	Genotype	MM patients	Controls	Unadjusted risk		Adjusted risk by gender and age	
		N (%)	N (%)	OR (95% CI)	p	OR (95% CI)	p
ERCC1 rs11615	TT	97 (41.8) ¹	64 (35.8) ²				
	TC	94 (40.5)	87 (48.6)				
	CC	41 (17.7)	28 (15.6)	0.78 (0.52–1.16)	0.213	0.69 (0.45–1.06)	0.091
ERCC1 rs3212986	GG	142 (59.9)	84 (47.7) ³				
	GT	77 (32.5)	75 (42.6)				
	TT	18 (7.6)	17 (9.7)	0.61 (0.41–0.91)	0.014	0.52 (0.34–0.80)	0.003
XRCC1 rs1799782	CC	196 (86.0) ⁴	171 (90.0) ⁵				
	CT	32 (14.0)	19 (10.0)	1.47 (0.80–2.69)	0.211	1.12 (0.58–2.16)	0.728
XRCC1 rs25487	CC	90 (38.0)	74 (42.8) ⁶				
	CT	125 (52.7)	79 (45.7)				
	TT	22 (9.3)	20 (11.6)	1.22 (0.82–1.82)	0.327	1.03 (0.67–1.59)	0.890

For determining MM risk, carriers of at least one polymorphic allele were compared to non-carriers

¹missing data for 5 patients; ²missing data for 14 patients; ³missing data for 17 patients; ⁴missing data for 9 patients; ⁵missing data for 3 patients; ⁶missing data for 20 patients

TABLE 3. The influence of interactions between investigated genetic polymorphisms on MM risk

Gene 1	Gene 2			Interaction			
Genotypes	OR (95% CI)	p	Genotypes	OR (95% CI)	p	OR (95% CI)	p
ERCC1 rs 11615 TC + CC vs. TT	0.78 (0.52–1.16)	0.213	ERCC1 rs3212986 GT + TT vs. GG	0.61 (0.41–0.91)	0.014	1.97 ¹ (0.42–9.17)	0.75
ERCC1 rs 11615 TC + CC vs. TT	0.78 (0.52–1.16)	0.213	XRCC1 rs1799782 CT vs. CC	1.47 (0.80–2.69)	0.211	1.30 ² (0.37–4.52)	0.680
ERCC1 rs 11615 TC + CC vs. TT	0.78 (0.52–1.16)	0.213	XRCC1 rs25487 CT + TT vs. CC	1.22 (0.82–1.82)	0.327	0.79 ³ (0.34–1.86)	0.592
ERCC1 rs3212986 GT + TT vs. GG	0.61 (0.41–0.91)	0.014	XRCC1 rs1799782 CT vs. CC	1.47 (0.80–2.69)	0.211	1.49 ⁴ (0.42–5.21)	0.537
ERCC1 rs3212986 GT + TT vs. GG	0.61 (0.41–0.91)	0.014	XRCC1 rs25487 CT + TT vs. CC	1.22 (0.82–1.82)	0.327	0.65 ⁵ (0.29–1.47)	0.302
XRCC1 rs1799782 CT vs. CC	1.47 (0.80–2.69)	0.211	XRCC1 rs25487 CT + TT vs. CC	1.22 (0.82–1.82)	0.327	2.41 ⁶ (0.66–8.80)	0.182

¹ rs 11615 ERCC1 TC + CC vs. TT * rs3212986 ERCC1 GT + TT vs. GG; ² rs 11615 ERCC1 TC + CC vs. TT * rs1799782 XRCC1 CT vs. CC; ³ rs 11615 ERCC1 TC + CC vs. TT * rs25487 XRCC1 CT + TT vs. CC; ⁴ rs3212986 ERCC1 GT + TT vs. GG * rs1799782 XRCC1 CT vs. CC; ⁵ rs3212986 ERCC1 GT + TT vs. GG * rs25487 XRCC1 CT + TT vs. CC; ⁶ rs1799782 XRCC1 CT vs. CC * rs25487 XRCC1 CT + TT vs. CC

The frequency distribution of the studied genetic polymorphisms is shown in Table 2. Minor allele frequencies were 39.9% for *ERCC1* rs11615, 31.0% for *ERCC1* rs3212986, 5.0% for *XRCC1* rs1799782 and 34.5% for *XRCC1* rs25487 in the control group. All SNPs were in Hardy-Weinberg equilibrium in controls (all $p > 0.05$). Analysing the association between MM and the investigated genetic polymorphisms, the risk of MM was statistically significantly influenced only by *ERCC1* rs3212986 polymorphism (OR = 0.61; 95% CI = 0.41–0.91; $p = 0.014$). Carriers of at least one polymorphic *ERCC1* rs3212986 genotype GT or TT had a decreased risk of MM even when adjusting for age and gender. No association was observed between MM and other genetic polymorphisms (Table 2).

In further logistic regression modelling the interactions between *ERCC1* rs11615 and rs3212986 and *XRCC1* rs1799782 and rs25487 polymorphisms did not significantly influence the risk of MM (Table 3).

Analysing the influence of interactions between the *ERCC1* and *XRCC1* polymorphisms and the asbestos exposure on the risk of MM, the interaction between *ERCC1* rs11615 polymorphism and asbestos exposure statistically significantly increased the risk of MM (OR = 3.61, 95% CI = 1.12–11.66, $p = 0.032$). Other interactions between polymorphisms and asbestos exposure did not statistically significantly affect the risk of MM (Table 4).

Finally, we analysed the interaction between *ERCC1* rs11615 polymorphism and asbestos exposure in more detail. Table 5 shows that carriers of at least one polymorphic *ERCC1* rs11615 allele that have been exposed to low level of asbestos had a statistically significant decreased risk of MM (OR = 0.40; 95% CI = 0.19–0.84; $p = 0.016$). If their exposure was medium or high, the risk of MM was statistically significantly increased (OR = 3.00; 95% CI = 1.42–6.34; $p = 0.004$).

TABLE 4. The influence of interactions between the investigated polymorphisms and asbestos exposure on MM risk

Polymorphism	OR	95% CI	p
<i>ERCC1</i> rs11615	3.61	1.12–11.66	0.032
<i>ERCC1</i> rs3212986	1.93	0.61–6.10	0.262
<i>XRCC1</i> rs1799782	1.85	0.33–10.48	0.489
<i>XRCC1</i> rs25487	2.80	0.89–8.79	0.078

Discussion

The relationship between MM and asbestos exposure was first described in 1960, but relatively little has been known about the mechanisms of carcinogenesis and the influence of genetic factors on the development of this malignant disease.³⁰ In the current study we investigated the influence of *ERCC1* and *XRCC1* polymorphisms, interactions between studied polymorphisms, and interactions between these polymorphisms and asbestos exposure on the risk of MM.

In this study, the majority of patients with MM were older than 58 years. This is consistent with the findings of previous studies showing that this tumour occurs primarily in the elderly, which could be contributed by the long latency period.^{3,4,8}

Our study did not detect any association between smoking and the risk of MM, which is in agreement with the findings of some previous studies.^{31,32} On the contrary, a previous Slovenian study showed that smoking increased the risk of MM.³ The relation between smoking and the risk of MM development has to be further investigated.

An important finding of our study is that the medium and higher levels of asbestos exposure is associated with a 4-fold higher risk of developing

TABLE 5. The influence of interaction between *ERCC1* rs11615 polymorphism and asbestos exposure on MM risk

	Asbestos exposure								OR for asbestos exposure inside category <i>ERCC1</i>	
	Low				Medium and high				OR (95% CI)	p
<i>ERCC1</i> rs11615	MM (N)	Controls (N)	OR (95% CI)	p	MM (N)	Controls (N)	OR (95% CI)	p	OR (95% CI)	p
TT	20	48	1	Ref.	14	16	2.10 (0.87–5.10)	0.101	2.10 (0.87–5.10)	0.101
TC+CC	15	91	0.40 (0.19–0.84)	0.016	30	24	3.00 (1.42–6.34)	0.004	7.58 (3.53–16.31)	< 0.001
OR for <i>ERCC1</i> inside category asbestos exposure			0.40 (0.19–0.84)	0.016			1.43 (0.58–4.50)	0.435		

MM compared to low level of exposure. Although it is assumed that there is no threshold dose for developing MM,¹⁰ some studies have proven that the occurrence of MM is associated with the level of asbestos exposure at the beginning of employment and the length of exposure.^{33,34}

A key finding of our study is that the carriers of at least one polymorphic *ERCC1* allele rs3212986 had a decreased risk of MM. According to our knowledge, the association between the *ERCC1* rs3212986 polymorphism and the MM has not been studied yet. The protective effect of the above mentioned polymorphism could be explained by the fact that the *ERCC1* protein is involved in the NER, which removes the oxidatively induced DNA damage caused by ROS and RNS that are released from the inflammatory cells as a consequence of contact with asbestos. In accordance with the described cell defence mechanism against genomic instability and hence against carcinogenesis, the result obtained could be understood as biologically plausible.

Other investigated polymorphisms did not have a statistically significant effect on the risk of MM. Our results differ from the previous two Italian studies, which found an increased risk for MM in the carriers of polymorphic allele *ERCC1* rs11615 and *XRCC1* rs25487,^{14,15} therefore additional research is needed to clarify these associations.

In this study, the interactions between studied polymorphisms did not have a statistically significant effect on the risk of MM. In contrast, the former Italian study indicated the effect of interactions between *ERCC1* rs11615 and *XRCC1* rs25487 polymorphisms on the increased risk of MM.¹⁵

According to our knowledge the influence of interactions between the studied polymorphisms and the asbestos exposure on the risk of MM have not been investigated so far. An important finding of our study is that the interaction between *ERCC1* rs11615 polymorphism and asbestos exposure affects the risk of MM, although we have not found an independent association between this polymorphism and MM. The analysis showed that the *ERCC1* rs11615 polymorphism modifies the influence of asbestos exposure on the development of MM. Carriers of the polymorphic alleles that had been exposed to low level of asbestos had a decreased risk of MM in comparison with carriers of a normal allele. If the carriers of the polymorphic *ERCC1* rs11615 alleles were exposed to medium or high level of asbestos, they had an increased risk of MM. The observed protective effect of the *ERCC1* rs11615 polymorphism could be explained by the

fact that there may be fewer asbestos fibers in the lungs at low levels of asbestos exposure than in medium or high levels of exposure. Consequently less ROS and RNS may be released and the NER would be able to repair the damage despite reduced function, thereby preventing the development of MM. Thus, the protective effect of *ERCC1* rs11615 could be considered as biologically plausible. In medium or high level of asbestos exposure, the level of DNA damage could be higher and consequently NER may not be able to repair it optimally, which could lead to genomic instability and carcinogenesis of MM. The interactions between other genetic polymorphisms and the exposure did not influence the risk of MM.

A limitation of our study is that the information on smoking and asbestos exposure was not available for all subjects. Therefore some of the analyses were performed only on the subgroup of MM patients. The next drawback is that we failed to determine the genotype in some subjects due to the insufficient amount and the degraded DNA in samples isolated from Whatman FTA cards and contamination.

In conclusion, our study showed the protective effect of the *ERCC1* rs3212986 polymorphism on the risk of MM and the impact of the interaction between the *ERCC1* rs11615 polymorphism and asbestos exposure on the risk of developing this aggressive tumour. The results of this research could facilitate our understanding of carcinogenesis of MM.

References

1. Carbone M, Ly BH, Dodson RF, Pagano I, Morris PT, Dogan UA, et al. Malignant mesothelioma: facts, myths, and hypotheses. *J Cell Physiol* 2012; **227**: 44-58. doi: 10.1002/jcp.22724
2. Linton A, Vardy J, Clarke S, van Zandwijk N. The ticking time-bomb of asbestos: its insidious role in the development of malignant mesothelioma. *Crit Rev Oncol Hematol* 2012; **84**: 200-12. doi: 10.1016/j.critrevonc.2012.03.001
3. Franko A, Kotnik N, Goricar K, Kovac V, Dodic-Fikfak M, Dolzan V. The influence of genetic variability on the risk of developing malignant mesothelioma. *Radiol Oncol* 2018; **52**: 105-11. doi: 10.2478/raon-2018-0004
4. Remon J, Lianes P, Martinez S, Velasco M, Querol R, Zanui M. Malignant mesothelioma: new insights into a rare disease. *Cancer Treat Rev* 2013; **39**: 584-91. doi: 10.1016/j.ctrv.2012.12.005
5. Franko A, Dolzan V, Kovac V, Arneric N, Dodic-Fikfak M. Soluble mesothelin-related peptides levels in patients with malignant mesothelioma. *Dia Markers* 2012; **32**: 123-31. doi: 10.3233/DMA-2011-0866
6. Weiner SJ, Neragi-Miandoab S. Pathogenesis of malignant pleural mesothelioma and the role of environmental and genetic factors. *J Cancer Res Clin Oncol* 2009; **135**: 15-27. doi: 10.1007/s00432-008-0444-9
7. Zellos L, Christiani DC. Epidemiology, biologic behavior, and natural history of mesothelioma. *Thorac Surg Clin* 2004; **14**: 469-77, viii. doi: 10.1016/j.thorsurg.2004.06.011

8. Sen D. Working with asbestos and the possible health risks. *Occup Med (Lond)* 2015; **65**: 6-14. doi: 10.1093/occmed/kqu175
9. Bianchi C, Bianchi T. Malignant mesothelioma: global incidence and relationship with asbestos. *Ind Health* 2007; **45**: 379-87. doi: 10.2486/indhealth.45.379
10. Case BW, Abraham JL, Meeker G, Pooley FD, Pinkerton KE. Applying definitions of "asbestos" to environmental and "low-dose" exposure levels and health effects, particularly malignant mesothelioma. *J Toxicol Environ Health B Crit Rev* 2011; **14**: 3-39. doi: 10.1080/10937404.2011.556045
11. Toyokuni S. Mechanisms of asbestos-induced carcinogenesis. *Nagoya J Med Sci* 2009; **71**: 1-10. doi: 10.1265/jjh.66.562
12. Upadhyay D, Kamp DW. Asbestos-induced pulmonary toxicity: role of DNA damage and apoptosis. *Exp Biol Med (Maywood)* 2003; **228**: 650-9. doi: 10.1177/153537020322800602
13. Manning CB, Vallyathan V, Mossman BT. Diseases caused by asbestos: mechanisms of injury and disease development. *Int Immunopharmacol* 2002; **2**: 191-200. doi: 10.1016/S1567-5769(01)00172-2
14. Dianzani I, Gibello L, Biava A, Giordano M, Bertolotti M, Betti M, et al. Polymorphisms in DNA repair genes as risk factors for asbestos-related malignant mesothelioma in a general population study. *Mutat Res* 2006; **599**: 124-34. doi: 10.1016/j.mrfmmm.2006.02.005
15. Betti M, Ferrante D, Padoan M, Guarrera S, Giordano M, Aspesi A, et al. XRCC1 and ERCC1 variants modify malignant mesothelioma risk: a case-control study. *Mutat Res* 2011; **708**: 11-20. doi: 10.1016/j.mrfmmm.2011.01.001
16. Spivak G. Nucleotide excision repair in humans. *DNA Repair (Amst)* 2015; **36**: 13-8. doi: 10.1016/j.dnarep.2015.09.003
17. Zhang L, Wang J, Xu L, Zhou J, Guan X, Jiang F, et al. Nucleotide excision repair gene ERCC1 polymorphisms contribute to cancer susceptibility: a meta-analysis. *Mutagenesis* 2012; **27**: 67-76. doi: 10.1093/mutage/ger062
18. Zhao Z, Zhang A, Zhao Y, Xiang J, Yu D, Liang Z, et al. The association of polymorphisms in nucleotide excision repair genes with ovarian cancer susceptibility. *Biosci Rep* 2018; **38**(3): BSR20180114. doi: 10.1042/BSR20180114
19. Manandhar M, Boulware KS, Wood RD. The ERCC1 and ERCC4 (XPF) genes and gene products. *Gene* 2015; **569**: 153-61. doi: 10.1016/j.gene.2015.06.026
20. Ding YW, Gao X, Ye DX, Liu W, Wu L, Sun HY. Association of ERCC1 polymorphisms (rs3212986 and rs11615) with the risk of head and neck carcinomas based on case-control studies. *Clin Transl Oncol* 2015; **17**: 710-9. doi: 10.1007/s12094-015-1298-7
21. Li B, Shi X, Yuan Y, Peng M, Jin H, Qin D. ERCC1 rs11615 polymorphism increases susceptibility to breast cancer: a meta-analysis of 4547 individuals. *Biosci Rep* 2018; **38**(3): BSR20180440. doi: 10.1042/BSR20180440
22. Chen J, Sun N, Hu G, Chen X, Jiang J, Wu H, et al. Association of ERCC1 polymorphisms with the risk of colorectal cancer: a meta-analysis. *Crit Rev Eukaryot Gene Expr* 2017; **27**(3): 267-75. doi: 10.1615/CritRevEukaryotGeneExpr.2017019713
23. De Mattia E, Cecchin E, Polese J, Bignucolo A, Roncato R, Lupo F, et al. Genetic biomarkers for hepatocellular cancer risk in a caucasian population. *World J Gastroenterol* 2017; **23**: 6674-84. doi: 10.3748/wjg.v23.i36.6674
24. London RE. The structural basis of XRCC1-mediated DNA repair. *DNA Repair* 2015; **30**: 90-103. doi: 10.1016/j.dnarep.2015.02.005
25. Wang Y, Spitz MR, Zhu Y, Dong Q, Shete S, Wu X. From genotype to phenotype: correlating XRCC1 polymorphisms with mutagen sensitivity. *DNA Repair (Amst)* 2003; **2**: 901-8. doi: 10.1016/S1568-7864(03)00085-5
26. Srivastava A, Srivastava K, Pandey SN, Choudhuri G, Mittal B. Single-nucleotide polymorphisms of DNA repair genes OGG1 and XRCC1: association with gallbladder cancer in North Indian population. *Ann Surg Oncol* 2009; **16**: 1695-703. doi: 10.1245/s10434-009-0354-3
27. Jafari Nedooshan J, Forat Yazdi M, Neamatzadeh H, Zare Shehneh M, Kargar S, Seddighi N. Genetic association of XRCC1 gene rs1799782, rs25487 and rs25489 polymorphisms with risk of thyroid cancer: a systematic review and meta-analysis. *Asian Pac J Cancer Prev* 2017; **18**: 263-70. doi: 10.22034/APJCP.2017.18.1.263
28. Zhu DQ, Zou Q, Hu CH, Su JL, Zhou GH, Liu P. XRCC1 genetic polymorphism acts a potential biomarker for lung cancer. *Tumour Biol* 2015; **36**: 3745-50. doi: 10.1007/s13277-014-3014-6
29. Dodic Fikak M, Kriebel D, Quinn MM, Eisen EA, Wegman DH. A case control study of lung cancer and exposure to chrysotile and amphibole at a slovenian asbestos-cement plant. *Ann Occup Hyg* 2007; **51**: 261-8. doi: 10.1093/annhyg/mem003
30. Wagner JC, Sleggs CA, Marchand P. Diffuse pleural mesothelioma and asbestos exposure in the North Western Cape Province. *Br J Ind Med* 1960; **17**: 260-71.
31. Muscat JE, Wynder EL. Cigarette smoking, asbestos exposure, and malignant mesothelioma. *Cancer Res* 1991; **51**: 2263-7.
32. Berry G, Newhouse ML, Antonis P. Combined effect of asbestos and smoking on mortality from lung cancer and mesothelioma in factory workers. *Br J Ind Med* 1985; **42**: 12-8.
33. Lacourt A, Leveque E, Guichard E, Gilg Soit Ilg A, Sylvestre MP, Leffondre K. Dose-time-response association between occupational asbestos exposure and pleural mesothelioma. *Occup Environ Med* 2017; **74**: 691-7. doi: 10.1136/oemed-2016-104133
34. Ulvestad B, Kjaerheim K, Martinsen JI, Damberg G, Wannag A, Mowe G, et al. Cancer incidence among workers in the asbestos-cement producing industry in Norway. *Scand J Work Environ Health* 2002; **28**: 411-7. doi: 10.5271/sjweh.693

Radiological and clinical patterns of myeloid sarcoma

Hans-Jonas Meyer¹, Maximilian Beimler¹, Gudrun Borte¹, Wolfram Pönisch², Alexey Surov¹

¹ Department of Diagnostic and Interventional Radiology, University Hospital Leipzig, Leipzig, Germany

² Department of Hematology and Oncology, University Hospital Leipzig, Leipzig, Germany

Radiol Oncol 2019; 53(2): 213-218.

Received 18 October 2018

Accepted 17 February 2019

Correspondence to: Hans-Jonas Meyer, M.D., Department of Diagnostic and Interventional Radiology, University Leipzig, Liebigstraße 20, 04103 Leipzig, Germany. Phone: +49 341 9717100; E-mail: hans-jonas.meyer@medizin.uni-leipzig.de

Disclosure: No potential conflicts of interest were disclosed.

Background. Myeloid sarcoma (MS), also known as granulocytic sarcoma or chloroma, is a solid tumor of extramedullary localization composed of malignant primitive myeloid cells. The purpose of the study was to identify clinical and imaging features in a large patient sample.

Patients and methods. Overall, 71 cases (34 females (47.9%) and 37 males (52.1%) with a median age of 56 (\pm 16 years) of histopathologically confirmed myeloid sarcoma were included into this study. The underlying hematological disease, occurrence, localizations and clinical symptoms as well as imaging features on computed tomography and magnetic resonance imaging were investigated.

Results. In 4 cases (5.63%) the manifestation of MS preceded the systemic hematological disease by a mean value of 3.8 ± 2.1 months. In 13 cases, first presentation of MS occurred simultaneously with the initial diagnosis of leukemia, and 51 patients presented MS after the initial diagnosis of the underlying malignancy with a mean latency of 39.8 ± 44.9 SD months. The visceral soft tissue was affected in 26 cases, followed by the cutis/subcutis was affected in 21 cases. Further localizations were bones ($n = 13$), central nervous system ($n = 9$), lymph nodes ($n = 4$) and visceral organs ($n = 9$).

Conclusions. MS is a rare complication of several hematological malignancies, predominantly of acute myeloid leukemia, which can affect any part of the body. In most cases it occurs after the diagnosis of the underlying malignancy, and affects frequently the cutis and subcutis.

Key words: myeloid sarcoma, granulocytic sarcoma, chloroma, acute myeloid leukaemia

Introduction

Myeloid sarcoma (MS), also known as granulocytic sarcoma or chloroma, is a solid tumor of extramedullary localization composed of malignant primitive myeloid cells.¹ A first mention of the pathology was found in 1811 by Burns and later called chloroma on account of its typical green appearance caused by the presence of the enzyme myeloperoxidase in the granules of the immature granulocytic precursors.^{2,3} Its occurrence is linked with leukemic diseases of the myeloid cell line, primarily in patients with acute myeloid leukemia (AML) and less commonly in those with its chronic

form (CML), myelodysplastic syndrome (MDS) or other myeloproliferative disorders.⁴ It may develop concurrently with mentioned primary diseases or be the initial manifestation of relapse in an already treated case.⁴ Especially, after allogeneic bone marrow transplantation an increased incidence has been described.⁵ Very rarely, MS can occur in the absence of a systemic disease and predate onset of an underlying hematologic malignancy by months to years.⁶ Treatment options, including radiation and chemotherapy are based upon an early and accurate diagnosis is crucial.⁷ However, particularly inapparent bulks pose a diagnostic challenge lacking indicative laboratory findings. Moreover, MS

can possibly involve any organ system.^{4,5,8} There are only a few systematic evaluations of radiologic findings with small patient populations, mainly limited to case reports.⁹⁻¹³

Therefore, the purpose of this study was to evaluate imaging characteristics of MS in a large patient sample and to establish possible correlations between imaging and clinical data, assess growth patterns and typically imaging features.

Patients and methods

Patients

The study was conducted in accordance with the Declaration of Helsinki and the protocol was approved by the Ethic Committee of the University of Leipzig. For this retrospective study, the Institutional Ethic Committee waived the need for informed consent (Committee of the University of Leipzig, Study codes Nr. 027/2002 and 162/2004). Patient records of the local oncology and hematology department from October 1992 to February 2016 were screened for myeloid sarcoma. Overall, 71 cases of histopathologically confirmed MS were identified and included into this study. There were 34 females (47.9%) and 37 males (52.1%) with a median age of 56 ± 16 years (range 14–85 years). For 43 (60.6%) patients, imaging studies were available for evaluation.

Clinical features

All patient records were reviewed by one of the authors. The underlying hematological disease was categorized in following subgroups: acute myeloid leukemia (AML), chronic myeloid leukemia (CML), myeloproliferative syndrome (MPS), myelodysplastic syndrome (MDS), myelofibrosis, biphenotypic leukemia and chronic myelomonocytic leukemia (CMML). Number and type of bone marrow transplantation (autologous vs. allogeneic related donor vs. allogeneic non-related donor) were obtained. The time between the initial diagnosis of the primary disease together with a potential treatment by use of bone marrow transplantation and appearance of the granulocytic sarcoma was calculated. Finally, the kind of the first clinical manifestation was identified and sorted as followed: neurological failures; incidental by imaging; pain; skin-related color changes or swelling; Organ-specific dysfunction. If there was a combination of symptoms, the leading one was determined.

Image analysis

Three and forty patients with myeloid sarcoma underwent imaging with computed tomography (CT) ($n = 13$; 30.2%); magnetic resonance imaging (MRI) ($n = 27$; 62.8%); CT and MRI ($n = 1$; 2.3%). Imaging protocols varied due to the different body region. Two radiologists (MB and AS) with 3 and 15 years of radiological experience, respectively, analyzed the images in consensus and in awareness of the pathologically proven diagnosis. Following features were noted: type of modality (CT, MRI), maximum size (largest diameter in mm), number of lesions, type of affected site (osseous; soft tissue; central nervous system; visceral organ; (sub-)cutis; lymph nodes); application of contrast agent, imaging appearance (hypodense/hypointense, isodense/isointense, hyperdense/hyperintense) and type of enhancement (no enhancement; homogenous or inhomogenous enhancement).

Statistical analysis

Collected data were analyzed by means of descriptive statistics (absolute and relative frequencies) with SPSS (SPSS 17.0, SPSS Inc., Chicago IL, USA). Continuous variables were expressed as means \pm standard deviation (SD), and categorical variables as percentages.

Results

Clinical findings

Overall, 57 (80.3%) suffered from AML, 7 (9.9%) from CML, 3 (4.2%) from MDS, 2 (2.8%) from MPS (2.8%) and 2 (2.8%) from CMML.

In 4 cases (5.6%) the manifestation of MS preceded the systemic hematological disease by a mean value of 3.8 ± 2.1 months. In 13 (18.3%) cases first presentation of MS occurred simultaneously with the initial diagnosis of leukemia, and 51 (71.8%) patients presented MS after the initial diagnosis of the underlying malignancy with a mean latency of 39.8 ± 44.9 SD months.

Clinically, swelling ($n = 30$; 46.2%) was the most common finding, followed by pain ($n = 14$; 21.5%), neurological deficit ($n = 11$; 16.9%) and dysfunction of the affected organ ($n = 8$; 12.3%). In 8 patients (11.3%) the diagnosis was made incidentally by imaging.

TABLE 1. The affected body regions of the patients

Region	N	%
Visceral soft tissue	26	29.9
Cutis	21	24.1
Bones	13	14.9
Central nervous system	9	10.3
Lymph nodes	4	4.6
Stomach	3	3.4
Pancreas	3	3.4
Heart	2	2.3
Enteric	2	2.3
Testis	1	1.2
Breast	1	1.2
Bladder	1	1.2
Kidney	1	1.2
All	87	100

Number, size, and localizations of MS

In 30 patients (42.3%) one MS lesion occurred, in 41 cases (57.7%) 2 or more lesions. The size of all localized tumors varied from 7 mm to 150 mm with a mean value of 44.9 ± 27.8 mm.

In 58 patients (77.5%) MS was limited to one localization, 10 patients (14.1%) showed two different localizations, and in 3 (4.2%) patients three or four several localizations of were identified.

Overall, the visceral soft tissue was affected in 26 cases (29.9%), followed by the cutis/subcutis was affected in 21 cases (24.1%). Further localizations were bones ($n = 13$; 14.9%), central nervous system ($n = 9$; 10.3%), lymph nodes ($n = 4$; 4.6%) and visceral organs ($n = 9$; 10.3%). Table 1 displays the affected localizations.

Imaging findings

CT

14 patients with 23 lesions were investigated with CT. All lesions were isodense compared to musculature (Figure 1). Every lesion showed a moderate enhancement of intravenous contrast medium. The enhancement was homogenous in 15 cases (65.2%), and inhomogenous in 8 cases (34.8%). Figure 2 and 4 display CT findings of two cases.

MRI

Overall, 28 patients were investigated by MRI. On T2-weighted (T2w) images, in most cases ($n = 23$;

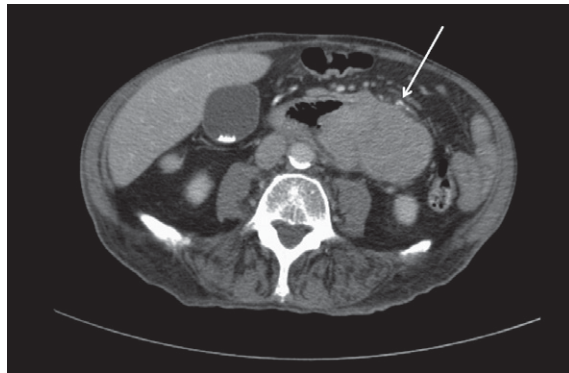


FIGURE 1. Computed tomography in a 89-years old patient with chronic myeloid leukemia showing a large abdominal mass (arrow) affecting the small bowel. Histological examination (not shown) after surgical biopsy confirms an extramedullary relapse of the known leukemia.

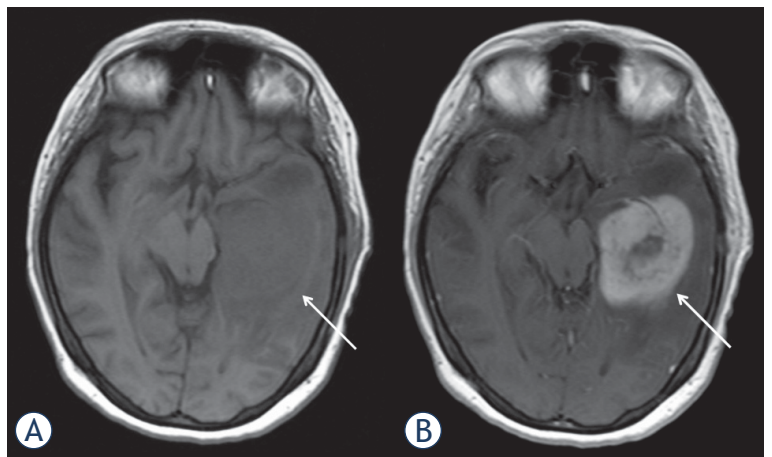


FIGURE 2. Magnetic resonance imaging findings in a 32-years old patient with known history of acute myeloid leukemia. Clinical presentation with headache. MRI documenting a large lesion in the left temporal lobe (arrows). On T1 weighted image it is slightly hypointense (A). After intravenous application of contrast medium, the lesion shows an inhomogenous enhancement (B). Histological examination (not shown) after surgical biopsy confirms an extramedullary relapse of the known leukemia.

82.1%) MS was hyperintense, and in 5 cases (17.9%) isointense in comparison to the musculature. On T1-weighted (T1w) images, MS was hypointense in 11 cases (39.3%) and isointense in 17 cases (60.7%) (Figure 2).

In 22 cases (78.6%) intravenous contrast media was applied. In most cases ($n = 21$; 95.4%), a moderate homogenous enhancement was found and one lesion showed no enhancement (4.6%).

Diffusion weighted imaging (DWI) was available for 5 patients. The mean apparent diffusion coefficient (ADC) value was $0.57 \times 10^{-3} \text{ mm}^2/\text{s}$

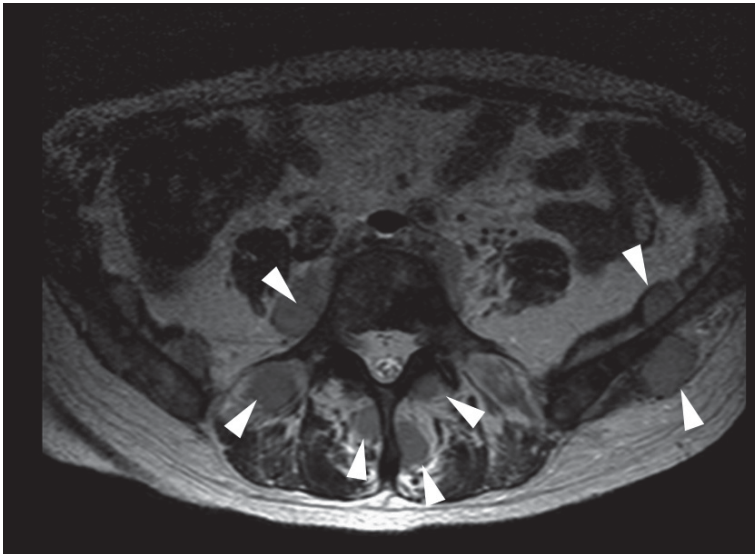


FIGURE 3. Axial T2 weighted image of the pelvis documenting multiple slightly hyperintense intramuscular lesions (arrows) in a 59-years old patient with known history of acute myeloid leukemia.

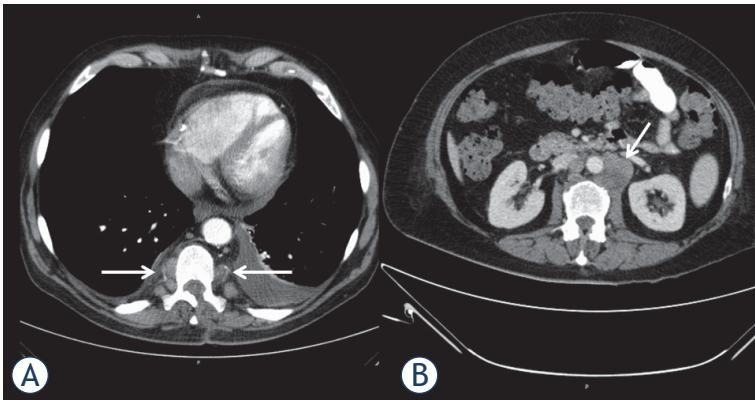


FIGURE 4. Computed tomography of the thorax (A) and abdomen in portal venous phase (B) in a 54-years old patient with acute myeloid leukemia documenting multiple paravertebral and retroperitoneal enhancing masses (arrows). Additionally, pleural and pericardial effusions are seen.

± 0.18 , median $0.50 \times 10^{-3} \text{mm}^2/\text{s}$, range $0.36\text{--}0.84 \times 10^{-3} \text{mm}^2/\text{s}$. Figure 3 and 4 display typically findings.

Discussion

The present study provides clinical and imaging findings of MS in a large patient sample. The diagnosis of MS might be challenging, even for the pathologist, and thus, typically clinical features are of importance for the radiologist and oncologist to establish the proper diagnosis. Furthermore, the

occurrence of MS is associated with an overall poor survival with 15.9 months.^{6,8,14}

According to the literature, the prevalence of MS varied from 2.5% to 9% in AML patients.^{9,15,16} However, due to its rare incidence, systemic data is still lacking to date. Additionally, the incidence of MS in myelodysplastic syndrome is even lower.¹⁶ Concordantly, only 2 patients with myelodysplastic syndrome and 2 patients with myeloproliferative disorders were identified in our patient sample.

As reported previously, MS can occur in three different situations. Firstly, it can occur prior to marrow/blood leukemia. In such cases systemic leukemia generally develops within one or two years after diagnosis of extramedullary relapse.^{6,8,9}

Secondly, MS can occur in systemic disease, either at the time of diagnosis of leukemia or subsequent to diagnosis.^{6,8,9} Thirdly, MS can manifest itself as a relapse after therapy or stem cell transplantation.^{6,8,9} Most frequently, MS occurred in up to 50% after onset of AML, in 15–35% contemporaneous with the leukemic manifestation and, less frequently, before the diagnosis of the underlying malignancy.¹⁶

In the present study, in 71.30% of cases MS occurred with a mean of 40 months after the primary diagnosis. Overall, these results are in good agreement with the literature. Interestingly, the time between occurrence of MS and the initial onset of disease was longer than in a recent study by Kaur *et al.*, in which it was only 8.8 months.⁶ Clearly, the diagnosis of MS is easier in cases with known AML. However, 18.3% of our patients developed MS simultaneous and even in 5.6% before the onset of a hematological disease. In these cases, the diagnosis may be very challenging to make due to several possible differential diagnoses. It has been reported that misdiagnosis rates in cases with MS varied from 25% to 47%.¹⁵ Frequently, Hodgkin-Lymphomas, MALT lymphoma, or Ewing's sarcoma were diagnosed instead of MS.¹⁵ Furthermore, infectious diseases like abscesses have to be considered as a diagnosis because these occur very frequently in leukemic patients with immunosuppression, either due to chemotherapy or due to the malignancy itself.⁹

The clinical presentation largely depends on the affected site of MS, and, thus, MS can be presented with a lot of different symptoms.¹⁵ Regarding localizations, MS affects most frequently cutis, subcutis and visceral soft tissue.^{6,9} In an older study investigated 50 patients, 21 patients had a lesion in the soft tissue, 15 patients had lymph nodal lesions,

and skin lesions in 13 patients.¹⁷ Only one patient had a brain lesion and 4 had gastrointestinal lesions.¹⁷ However, in a recent study analyzed 23 patients, skin and subcutaneous tissue was affected the most cases (69.5%).⁶ Furthermore, according to Neiman *et al.*, in most cases, MS presented with one lesion, and 16% had two and more lesions.¹⁷

In the present study, MS was isolated to one body area in up to 80% of the cases. However, 42.3% of patients had more than 3 lesions, especially found in patients with subcutaneous involvement. This finding might be beneficial to rule out possible differential diagnosis like solid tumors, which only presents with a single lesion.

Concordantly to the literature, a preference for subcutaneous involvement was also identified, followed by osseous and affection of the central nervous system. Affection of visceral organs and lymph nodes were rarer in the present patient sample than in the previous studies.

Clearly, every unknown lesion no matter the localization in a patient with known AML, should be indicative for MS.

Clinically, myeloid sarcoma was apparent in half of the cases with swelling and skin discoloration, which underlines the importance of a good physical examination in oncologic patients. Furthermore, in 29.2% neurological and organ dysfunctions were found and in 21.5% pain was the main symptom. Notably, 11.3% of the MS cases were detected incidentally by imaging studies. For example, these included one patient with a cardiac manifestation. Due to increasing performance of imaging studies in oncologic patients, we hypothesize that the amount of incidentally detected MS will increase concordantly. Therefore, the radiologist and oncologist need to be aware of the entity of MS.

Shinagare *et al.* described MRI features of 25 patients with 41 different MS localizations.¹⁸ The authors identified lesions with a mean size of 5.6 cm (range 1–20 cm), which is good comparable with our data. Regarding signal intensities, 75.6% were isointense and 24.4% were hypointense on T1-weighted images. Moreover, on T2-weighted images, 95.1% were hyperintense and 4.9% were isointense.¹⁸ These results are also in good agreement with the present study, however, we detected more hypointense lesions on T1-weighted images, and more isointense lesions on T2-weighted images. Furthermore, Oii *et al.* investigated 11 patients with MS with similar imaging characteristics.¹³ MS lesions were concordantly isodense in the present study on CT. Regarding contrast media enhancement, every lesion showed a moderate contrast

media enhancement with more lesions with a homogenous enhancement than heterogenous.

However, it should be acknowledged that neither the behavior of the signal intensity on MRI and CT nor the contrast enhancement is specific for MS lesions. For example, inflammatory lesions, such as abscess formations or other neoplastic lesions, such as lymphomas can show similar imaging findings.⁹

Chaundhry *et al.* reported a diffusion restriction in 96% of patients with cerebral myeloid sarcoma on diffusion weighted images (DWI).¹² In our study, the apparent diffusion coefficients of the lesions ranged from 0.36 to 0.84 mm²/s. This finding might be caused by high cellularity in these lesions as it was shown in several other malignancies.¹⁹ Our results are in good agreement with those of Chaundhry *et al.* Therefore, DWI might be a useful diagnostic tool for myeloid sarcoma evaluation. However, other cell rich tumors and tumor-like lesions, such as lymphomas, poorly differentiated carcinomas, and abscesses can also show restricted diffusion.

According to the literature, another beneficial imaging modality is PET/CT, which has better accuracy than CT alone in diagnosing MS.²⁰ As reported, MS lesions show elevated FDG uptake and the uptake changes under therapy, which also correlates with clinical outcome.²⁰

Our study has several limitations. First, it is a retrospective study with potential confounding factors. Second, the patient sample is relatively small, mainly caused by the rare incidence of myeloid sarcoma. However, the present study sample is one of the largest to date. Furthermore, prospective studies are lacking to this date due to low incidence. Third, some previously identified localizations like involvement of the lung was not identified in the present study sample.

Conclusions

Myeloid sarcoma is a rare occurrence of several hematological malignancies, predominantly of AML, which can affect any part of the body. In most cases it occurs after the diagnosis of the underlying malignancy, and affects frequently the cutis and subcutis. This study provides typical clinical and imaging findings in a large patient sample. However, the imaging findings are not specific for myeloid sarcoma and other differential diagnoses, such as inflammatory lesions or other neoplastic lesions have to be considered.

References

1. Liu PI, Ishimaru T, McGregor DH, Okada H, Steer AI. Autopsy study of granulocytic sarcoma (chloroma) in patients with myelogenous leukemia, Hiroshima-Nagasaki 1949-1969. *Cancer* 1973; **31**: 948-55.
2. Burns A. *Observations of surgical anatomy in head and neck*. London: Royce; 1811. p. 364.
3. King A. A case of chloroma. *Monthly J Med* 1853; **17**: 17
4. Campidelli C, Agostinelli C, Stitson R, Pileri SA. Myeloid sarcoma: extramedullary manifestation of myeloid disorders. *Am J Clin Pathol* 2009; **132**: 426-37. doi: 10.1309/AJCP1ZA7HYZKAZHS
5. Mortimer J, Blinder MA, Schulman S, Appelbaum FR, Buckner CD, Clift RA, et al. Relapse of acute leukemia after marrow transplantation: natural history and results of subsequent therapy. *J Clin Oncol* 1989; **7**: 50-7. doi: 10.1200/JCO.1989.7.1.50
6. Kaur V, Swami A, Alapat D, Abdallah AO, Motwani P, Hutchins LF, et al. Clinical characteristics, molecular profile and outcomes of myeloid sarcoma: a single institution experience over 13 years. *Hematology* 2017; **23**: 17-24. doi: 10.1080/10245332.2017.1333275
7. Fleming DR, Greenwood ME, Garrison J, Geil JD, Romond EH. Lymphocyte infusion for delayed extramedullary relapse of acute leukemia following bone marrow transplantation. *Leuk Lymphoma* 1996; **21**: 525-8. doi: 10.3109/10428199609093456
8. Pileri SA, Ascani S, Cox MC, Campidelli C, Bacci F, Piccioli M, et al. Myeloid sarcoma: clinico-pathologic, phenotypic and cytogenetic analysis of 92 adult patients. *Leukemia* 2007; **21**: 340-50. doi: 10.1038/sj.leu.2404491
9. Singh A, Kumar P, Chandrashekhara SH, Kumar A. Unravelling chloroma: review of imaging findings. *Br J Radiol* 2017; **90**: 20160710. doi: 10.1259/bjr.20160710
10. Choi EK, Ha HK, Park SH, Lee SJ, Jung SE, Kim KW, et al. Granulocytic sarcoma of bowel: CT findings. *Radiology* 2007; **243**: 752-9. doi: 10.1148/radiol.2433060747
11. Seok JH, Park J, Kim SK, Choi JE, Kim CC. Granulocytic sarcoma of the spine: MRI and clinical review. *AJR Am J Roentgenol* 2010; **194**: 485-9. doi: 10.2214/AJR.09.3086
12. Chaudhry AA, Gul M, Chaudhry AA, Dunkin J. Qualitative assessment of diffusion weighted imaging and susceptibility weighted imaging of myeloid sarcoma involving the brain. *J Comput Assist Tomogr* 2016; **40**: 61-6. doi: 10.1097/RCT.0000000000000337
13. Ooi GC, Chim CS, Khong PL, Au WY, Lie AK, Tsang KW, et al. Radiologic manifestations of granulocytic sarcoma in adult leukemia. *AJR Am J Roentgenol* 2011; **176**: 1427-31. doi: 10.2214/ajr.176.6.1761427
14. Lazzarotto D, Candoni A, Fili C, Forghieri F, Pagano L, Busca A, et al. Clinical outcome of myeloid sarcoma in adult patients and effect of allogeneic stem cell transplantation. Results from a multicenter survey. *Leuk Res* 2017; **53**: 74-81. doi: 10.1016/j.leukres.2016.12.003
15. Almond LM, Charalampakis M, Ford SJ, Gourevitch D, Desai A. Myeloid sarcoma: presentation, diagnosis, and treatment. *Clin Lymphoma Myeloma Leuk* 2017; **17**: 263-7. doi: 10.1016/j.clml.2017.02.027
16. Avni B, Koren-Michowitz M. Myeloid sarcoma: current approach and therapeutic options. *Ther Adv Hematol* 2011; **2**: 309-16. doi: 10.1177/2040620711410774
17. Neiman RS, Barcos M, Berard C, Bonner H, Mann R, Rydell RE, et al. Granulocytic sarcoma: a clinicopathologic study of 61 biopsied cases. *Cancer* 1981; **48**: 1426-37
18. Shinagare AB, Krajewski KM, Hornick JL, Zukotynski K, Kurra V, Jagannathan JP, et al. MRI for evaluation of myeloid sarcoma in adults: a single-institution 10-year experience. *AJR Am J Roentgenol* 2012; **199**: 1193-8. doi: 10.2214/AJR.12.9057
19. Surov A, Meyer HJ, Wienke A. Correlation between apparent diffusion coefficient (ADC) and cellularity is different in several tumors: a meta-analysis. *Oncotarget* 2017; **8**: 59492-9. doi: 10.18632/oncotarget.17752
20. Aschoff P, Häntschel M, Oksüz M, Werner MK, Lichy M, Vogel W, et al. Integrated FDG-PET/CT for detection, therapy monitoring and follow-up of granulocytic sarcoma. Initial results. *Nuklearmedizin* 2009; **48**: 185-91. doi: 10.3413/nukmed-0236

A new instrument for predicting survival of patients with cerebral metastases from breast cancer developed in a homogeneously treated cohort

Stefan Janssen^{1,2}, Heinke C. Hansen¹, Liesa Dziggel¹, Steven E. Schild³, Dirk Rades¹

¹ Department of Radiation Oncology, University Hospital Lubeck, Lubeck, Germany

² Medical Practice for Radiotherapy and Radiation Oncology, Hannover, Germany

³ Department of Radiation Oncology, Mayo Clinic Scottsdale, Arizona, U.S.A.

Radiol Oncol 2019; 53(2): 219-224.

Received 12 February 2019

Accepted 27 March 2019

Correspondence to: Dirk Rades, M.D., Chair of the Department of Radiation Oncology, University of Lübeck, Ratzeburger Allee 160, 23562 Lubeck, Germany. Phone: +49-451-500-45401; Fax: +49-451-500-45404; E-mail: dirk.rades@uksh.de

Disclosure: No potential conflicts of interest were disclosed.

Background. Previous survival scores for breast cancer patients with cerebral metastases were developed in cohorts receiving heterogeneous treatments, which could have introduced selection biases. A new instrument (WBRT-30-BC) was created from 170 patients receiving whole-brain radiotherapy (WBRT) alone with 30 Gy in 10 fractions.

Methods. Characteristics showing significant associations ($p < 0.05$) with overall survival (OS) or a trend ($p < 0.08$) on multivariate analysis were used for the WBRT-30-BC. For each characteristic, 6-month OS rates were divided by 10. These scoring points were added for each patient (patient scores). The WBRT-30-BC was compared to the diagnosis-specific graded prognostic assessment (DS-GPA) classification and Rades-Score for breast cancer regarding positive predictive values (PPVs) to identify patients dying within 6 months and patients surviving at least 6 months following WBRT.

Results. On multivariate analysis, Karnofsky performance score (KPS) was significant (risk ratio [RR]: 2.45, $p < 0.001$). In addition, extra-cerebral metastatic disease (RR: 1.52, $p = 0.071$) and time between breast cancer diagnosis and WBRT (RR: 1.37, $p = 0.070$) showed a trend. Based on these three characteristics, four predictive groups were designed: 7–9, 10–12, 13–15 and 16 points. Six-month OS rates were 8%, 41%, 68% and 100% ($p < 0.001$). PPVs to identify patients dying within 6 months were 92% (WBRT-30-BC), 84% (DS-GPA) and 92% (Rades-Score). PPVs to identify patients surviving for at least 6 months were 100% (WBRT-30-BC), 74% (DS-GPA) and 68% (Rades-Score).

Conclusions. The WBRT-30-BC appeared very accurate in predicting death ≤ 6 months and survival ≥ 6 months of breast cancer patients receiving WBRT. It was superior to previous instruments in predicting survival ≥ 6 months.

Key words: breast cancer; cerebral metastases; whole-brain radiotherapy; overall survival time; diagnosis-specific predictive tool

Introduction

Breast cancer patients account for about 25% of patients developing cerebral metastases.^{1,2} A considerable proportion of these patients present with multiple lesions when the cerebral lesions are detected or a low performance score. These patients often receive whole-brain radiotherapy (WBRT)

alone. Common WBRT-regimens include 20.0 Gy in 5 fractions (duration = one week), 30.0 Gy in 10 fractions (two weeks), 35.0–37.5 Gy in 14–15 fractions (three weeks) and 40.0 Gy in 20 fractions (four weeks).¹ In general, patients with a short expected overall survival (OS) time should receive a 20 Gy in 5 fractions, since this regimen was not inferior to 30 Gy in 10 fractions with respect to OS, local

(= intracerebral) control and feasibility.³ For selected patients with a very poor prognosis, WBRT may be omitted, and supportive care alone can be administered instead.⁴ On the contrary, for patients with more favorable OS prognoses, *i.e.* a median OS time of longer than one year, improved outcomes were found for 40 Gy in 20 fractions when compared to 30 Gy in 10 fractions.⁵ Moreover, since patients of the latter group will likely live long enough to experience WBRT-associated late toxicities including neuro-cognitive impairment, WBRT should be given with doses per fraction of less than 3.0 Gy.⁶ In addition, hippocampal sparing and administration of memantine are helpful in preserving cognition.^{7,8}

Thus, it is important to be able to judge an individual patient's OS prognosis to select the optimal WBRT-regimen. Several scoring systems were developed for patients to be treated for cerebral metastases. To go one step further and allow for even better personalization of treatment, separate scoring tools were created for single tumor entities spreading to the brain.⁹ This is an important approach, because the tumor entities vary considerably with respect to biological behaviour and prognoses. Such diagnosis-specific tools were already developed also for patients treated with WBRT for cerebral metastases from breast cancer.^{9,10} However, these tools were designed from patients who had received heterogeneous treatment-regimens, including different WBRT-regimens with one or two daily fractions and the addition of chemotherapy, a

radio-sensitizer or radiosurgery. This heterogeneity might have resulted in hidden biases. Therefore, this study was conducted and another scoring tool, the WBRT-30-BC, was created specifically for patients with cerebral metastases from breast cancer assigned to receive WBRT. In this study, all patients were homogeneously treated with 30 Gy in 10 fractions of WBRT alone. The new WBRT-30-BC was compared to two previous scoring tools that were also developed for estimating the OS of breast cancer patients with cerebral metastases.

Patients and methods

The data of 170 breast cancer patients receiving 30 Gy in 10 fractions of WBRT alone for cerebral metastases between 1994 and 2017 were retrospectively evaluated. The study was approved by the ethics committee of the University of Lübeck. Seven clinical pre-treatment characteristics were investigated for potential correlations with OS including age at WBRT (≤ 61 vs. ≥ 62 years, median age: 61.5 years), Karnofsky performance score (KPS) ($< 70\%$ vs. 70% vs. $> 70\%$), time between first diagnosis of breast cancer and WBRT (≤ 33 vs. ≥ 34 months, median time: 33.5 months), systemic treatment prior to WBRT (no vs. yes), number of cerebral lesions (1-3 vs. ≥ 4), controlled primary tumor (no vs. yes) and presence of extra-cerebral metastatic disease (no vs. yes) (Table 1).

For all seven characteristics, univariate analyses were performed using the Kaplan-Meier method and the log-rank test.¹¹ Characteristics with a p-value of < 0.20 on log-rank test, were additionally included in a multivariate analysis (Cox regression model). Those characteristics that showed a significant ($p < 0.05$) association with OS or a trend ($p < 0.08$) in the multivariate analysis were taken to create the new WBRT-30-BC score. For the development of the WBRT-30-BC, the same method was used as for the general WBRT-30 which was created from patients with different primary tumor types.¹² For each characteristic included in the score, the 6-month OS rate (in %) was divided by 10 to get the scoring points. The corresponding scoring points were added for each patient, and the patient scores were received. Based on the 6-month OS rates of the patient scores, prognostic groups were formed to estimate the 6-month OS probability of individual patients.

The new WBRT-30-BC was compared to two other diagnosis-specific tools that were developed for patients with cerebral metastases from breast

TABLE 1. Distribution of the patient characteristics

Characteristic	Number of patients	Proportion (%)
Age		
≤61 years	85	50
≥62 years	85	50
Karnofsky performance score		
<70%	76	45
70%	41	24
>70%	53	31
Time between first diagnosis of breast cancer and WBRT		
≤33 months	85	50
≥34 months	85	50
Systemic treatment prior to WBRT		
No	22	13
Yes	148	87
Number of cerebral lesions		
1-3	52	31
≥4	118	69
Controlled primary tumor		
No	12	7
Yes	158	93
Extra-cerebral metastatic disease		
No	38	22
Yes	132	78

TABLE 2. Univariate analyses of overall survival (OS); p-values were received from the Wilcoxon test.

Characteristic	OS at 3 months (%)	OS at 6 months (%)	OS at 9 months (%)	OS at 12 months (%)	P-value
Age					
≤61 years	58	39	30	24	0.076
≥62 years	47	28	22	15	
Karnofsky performance score					
<70%	26	8	5	5	<0.001
70%	54	32	19	0	
>70%	89	72	60	51	
Time between first diagnosis of breast cancer and WBRT					
≤33 months	46	29	22	18	0.062
≥34 months	59	38	29	21	
Systemic treatment prior to WBRT					
No	45	23	11	11	0.27
Yes	53	35	28	21	
Number of cerebral lesions					
1-3	46	35	27	18	0.43
≥4	55	33	36	20	
Controlled primary tumor					
No	33	25	25	25	0.18
Yes	54	34	26	19	
Extra-cerebral metastatic disease					
No	76	53	43	36	0.001
Yes	45	28	21	15	
Entire cohort	52	34	26	20	

cancer. These tools included the diagnosis-specific graded prognostic assessment (DS-GPA) classification for breast cancer and the Rades-Score for brain metastases from breast cancer.^{9,10} The DS-GPA consisted of four prognostic groups based on the KPS. These groups were 0.0–1.0 points (KPS ≤ 70%), 1.5–2.5 (KPS 80%), 3.0 (KPS 90%) and 3.5–4.0 (KPS 100%).⁹ The Rades-Score was based on KPS (< 70%: 1 point, ≥ 70%: 6 points) and extra-cerebral metastases (yes: 3 points, no: 6 points) and included three prognostic groups (4–7 points, 9 points and 12 points).¹⁰

The WBRT-30-BC and the other two scores were compared regarding the positive predictive values (PPVs) for identification of patients dying within 6 months (poor prognosis groups) and of patients surviving at least 6 months (favorable prognosis groups) following WBRT. Both PPVs were calculated by dividing the number of true positives by (number of true positives + number of false positives).

Results

On univariate analyses (Table 2), better OS was significantly associated with KPS > 70% ($p < 0.001$) and absence of extra-cerebral metastases ($p = 0.006$). In addition, for age ≤ 61 years ($p = 0.097$), time between first diagnosis of breast cancer and

WBRT ≥ 34 months ($p = 0.19$) and systemic treatment prior to WBRT ($p = 0.17$), p -values < 0.20 were found. These five characteristics were included in the Cox regression analysis, in which KPS was significant (risk ratio [RR]: 2.45; 95%-confidence interval [CI]: 1.93–3.13; $p < 0.001$). In addition, the time between diagnosis of breast cancer and WBRT (RR: 1.37; 95% CI: 0.97–1.94; $p = 0.070$) and extra-cerebral metastatic disease (RR: 1.52; 95% CI: 0.97–2.48; $p = 0.071$) showed a trend. Age (RR: 1.19; 95% CI: 0.84–1.67; $p = 0.33$) and systemic treatment prior to WBRT (RR: 1.32; 95% CI: 0.77–2.15; $p = 0.31$) were not significantly associated with OS on multivariate analysis.

TABLE 3. Six-month overall survival rates (OS) of the characteristics included in the WBRT-30-BC and the related scoring points

Characteristic	6-month OS rate (%)	Scoring points
Karnofsky performance score		
<70%	8	1
70%	32	3
>70%	72	7
Time between first diagnosis of breast cancer and WBRT		
≤33 months	29	3
≥34 months	38	4
Extra-cerebral metastatic disease		
No	53	5
Yes	28	3

WBRT = whole-brain radiotherapy

TABLE 4. Overall survival (OS) rates of the four prognostic groups at 3, 6, 9 and 12 months following WBRT; the p-value was received from the Wilcoxon test

Prognostic group	OS at 3 months (%)	OS at 6 months (%)	OS at 9 months (%)	OS at 12 months (%)	P-value
6-9 points	25	8	5	2	<0.001
10-12 points	69	41	25	0	
13-15 points	87	68	54	47	
16 points	100	100	100	83	

Thus, the three characteristics KPS, time between first diagnosis of breast cancer and WBRT and extra-cerebral metastatic disease were used to create the WBRT-30-BC. The 6-months OS rates and the related scoring points are shown in Table 3. The sum of the scoring points for each patient resulted in patient scores ranging between 7 and 16 points. The 6-month OS rates of the patient scores are illustrated in Figure 1. These OS rates led to the following prognostic groups: 7–9 points (n = 88), 10–12 points (n = 29), 13–15 points (n = 47) and 16 points (n = 6). The 6-month OS rates of these groups were 8%, 41%, 68% and 100% (p < 0.001, Table 4).

When using the WBRT-30-BC, the PPV of the 7–9 points (= poor prognosis) group to correctly identify patients dying within 6 months following WBRT was 92% compared to 84% for a DS-GPA score of 0.0–1.0 points and 92% for 4–7 points in the previous Rades-Score.^{9,10} The PPV of the 16 points (= most favorable prognosis) group of the WBRT-30-BC to correctly identify patients surviving for at least 6 months following WBRT was 100% compared to 74% for a DS-GPA score of ≥ 3.0 points and 68% for 12 points in the previous Rades-Score.^{9,10} For the DS-GPA, ≥ 3.0 points were used, since only one patient had a DS-GPA score of > 3.0. This patient died four months after WBRT.

Discussion

Cerebral metastases are quite common in breast cancer patients.^{1,2} A considerable number of these patients have relatively favorable survival prognoses and will live long enough to experience late treatment-related toxicity including neuro-cognitive decline.¹ Therefore, in comparison to several other primary tumors more patients with a limited number of cerebral lesions receive treatment with a local therapy alone such as neurosurgical resection and radiosurgery. However, many patients with cerebral metastases from breast cancer are still assigned to WBRT alone, particularly those with

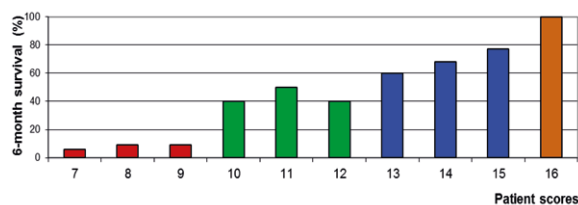


FIGURE 1. The 6-month overall survival rates related to the scoring points that range from 7 to 16 points.

more than five lesions, poor general condition and high co-morbidity index.¹

In patients with a longer expected survival, WBRT with total doses exceeding 30 Gy in 10 fractions and doses per fraction of less than 3 Gy are recommended.^{5,6} According to the findings of a retrospective study of 186 patients with a median OS time of 15 months, 40 Gy in 20 fractions resulted in significantly (p = 0.007) better OS than 30 Gy in 10 fractions at 1 year (61% versus 50%).⁵ Cerebral control rates were 44% versus 28%, respectively (p = 0.064). Since the risk of developing neuro-cognitive deficits increases with lifetime, longer-term surviving patients should not be treated with doses per fraction of 3 Gy or higher.⁶ The risk of neuro-cognitive decline may also be reduced with sparing of the hippocampal neural stem-cell compartment and administration of memantine.^{7,8}

In contrast to longer-term survivors, patients with a very short remaining lifespan should receive WBRT with a short overall treatment time to avoid that they spend more time than necessary on a radiation oncology ward or with transports to the radiation oncology department.¹ 20 Gy in 5 fractions appears a reasonable option, since it was not inferior to 30 Gy in 10 fractions in a previous study with more than three cerebral lesions.³ For selected patients with a very short expected lifespan, best supportive care (BSC) alone can be considered, since in a randomized trial of poor prognosis non-small lung cancer patients with brain metastases, BSC alone was not significantly inferior to BSC plus 20 Gy in 5 fractions with respect to quality-adjusted life-years.⁴

Thus, to select the optimal WBRT regimen, estimation of the patient's OS prognosis appears crucial. Several instruments were developed in cohorts of patients receiving WBRT including the recursive partitioning analysis (RPA) classification, the graded prognostic assessment (GPA) classification and the WBRT-30.^{12,14,15} Patients used to develop the RPA and GPA classifications had received various treatments such as different WBRT-regimens

including hyperfractionation, WBRT plus misonidazole and WBRT plus chemotherapy.^{14,15} For the development of the GPA classification, additionally patients treated with WBRT plus radiosurgery boost were included.¹⁵ Thus, the creation of both RPA and GPA classification might have been influenced by treatment-related biases. The WBRT-30 score was created in a homogeneously treated cohort; all patients received WBRT alone with 30 Gy in 10 fractions.¹² This may have led to the fact that the WBRT-30 score demonstrated the highest accuracy of the three tools for correctly predicting death within 6 months (PPV of 97% versus 92% and 85%) and survival for at least 6 months (PPV of 96% versus 75% and 64%) following treatment.¹²

The next step to provide optimal personalization for patients with cerebral metastases is the creation of specific survival scores for single tumor entities. For breast cancer patients, such tools already exist.^{9,10} However, like most previous scores they were developed in heterogeneously treated series of patients. Considering the high accuracy of the general WBRT-30 score in predicting death within 6 months and survival for at least 6 months, we developed a WBRT-30 score particularly for breast cancer patients (WBRT-30-BC) in this study.¹⁵ The WBRT-30-BC included four predictive groups with significantly different 6-month OS rates. When compared to the DS-GPA and the Rades-Score, the PPV of the WBRT-30-BC to identify patients who will die within 6 months after WBRT of 92% was higher than for the DS-GPA (84%) and the same as for the Rades-Score (92%).^{9,10} Regarding the PPV to identify patients who will live 6 months or longer after WBRT, the WBRT-30-BC (100%) was superior to both DS-GPA (74%) and Rades-Score (68%).

Thus, the WBRT-30-BC appears preferable to the other two instruments. However, when using the WBRT-30-BC, one should be aware that the data used to create it were retrospective in nature. Patients of the 7–9 points group had a very poor OS and, therefore, should be treated with 20 Gy in 5 fractions plus BSC or, in selected cases, with BSC alone.^{3,4} The OS prognoses of the 10–12 points group can be considered intermediate, and WBRT with 30 Gy in 10 fractions might be a reasonable option. Of the patients of the 13–15 points group 68% survived for at least 6 months and 47% for at least 12 months (Table 4). Considering this relatively favorable prognosis, these patients appear good candidates for longer-course WBRT with lower doses per fraction and may even benefit from total doses >30 Gy.^{5,6} Patients of the 16 points group had very favorable OS prognoses with 6-month

and 12-months OS probabilities of 100% and 83%, respectively. If assigned to WBRT, these patients should be treated with 40 Gy in 20 fractions of 2 Gy.⁵ Moreover, patients of the latter two groups (13–15 points and 16 points) should be considered for hippocampal sparing WBRT and treatment with memantine during WBRT to optimally decrease the risk of neuro-cognitive decline.^{7,8}

In summary, the new WBRT-30-BC appeared very accurate in predicting death within 6 months and survival for at least 6 months of breast cancer patients receiving WBRT. The new score was superior to previous instruments in predicting survival for at least 6 months following WBRT. It can contribute to the development of personalized treatments and may be valuable for clinical trials (stratification) in the future.

References

1. Tsao MN, Rades D, Wirth A, Lo SS, Danielson BL, Gaspar LE, et al. Radiotherapeutic and surgical management for newly diagnosed brain metastasis(es): an American Society for Radiation Oncology evidence-based guideline. *Pract Radiat Oncol* 2012; **2**: 210-25. doi: 10.1016/j.clon.2012.03.008
2. Siegel RL, Miller KD, Jemal A. Cancer statistics, 2019. *CA Cancer J Clin* 2019; **69**: 7-34. doi: 10.3322/caac.21551
3. Rades D, Kieckebusch S, Lohynska R, Veninga T, Stalpers LJ, Dunst J, et al. Reduction of overall treatment time in patients irradiated for more than three brain metastases. *Int J Radiat Oncol Biol Phys* 2007; **69**: 1509-13.
4. Mulvenna P, Nankivell M, Barton R, Faivre-Finn C, Wilson P, McColl E, et al. Dexamethasone and supportive care with or without whole brain radiotherapy in treating patients with non-small cell lung cancer with brain metastases unsuitable for resection or stereotactic radiotherapy (QUARTZ): results from a phase 3, non-inferiority, randomised trial. *Lancet* 2016; **388**: 2004-14. doi: 10.1016/S0140-6736(16)30825-X
5. Rades D, Panzner A, Dziggel L, Haatanen T, Lohynska R, Schild SE. Dose-escalation of whole-brain radiotherapy for brain metastasis in patients with a favorable survival prognosis. *Cancer* 2012; **118**: 3853-9. doi: 10.1002/ncr.26680
6. DeAngelis LM, Delattre JY, Posner JB. Radiation-induced dementia in patients cured of brain metastases. *Neurology* 1989; **39**: 789-96.
7. Gondi V, Pugh SL, Tome WA, Caine C, Corn B, Kanner A, et al. Preservation of memory with conformal avoidance of the hippocampal neural stem-cell compartment during whole-brain radiotherapy for brain metastases (RTOG 0933): a phase II multi-institutional trial. *J Clin Oncol* 2014; **32**: 3810-6. doi: 10.1200/JCO.2014.57.2909
8. Brown PD, Pugh S, Laack N, Wefel JS, Khuntia D, Meyers C, et al.; Radiation Therapy Oncology Group (RTOG): Memantine for the prevention of cognitive dysfunction in patients receiving whole-brain radiotherapy: a randomized, double-blind, placebo-controlled trial. *Neuro Oncol* 2013; **15**: 1429-37. doi: 10.1093/neuonc/not114
9. Sperduto PW, Chao ST, Sneed PK, Luo X, Suh J, Roberge D, et al. Diagnosis-specific prognostic factors, indexes, and treatment outcomes for patients with newly diagnosed brain metastases: a multi-institutional analysis of 4,259 patients. *Int J Radiat Oncol Biol Phys* 2010; **77**: 655-61. doi: 10.1016/j.ijrobp.2009.08.025
10. Rades D, Dziggel L, Segedin B, Oblak I, Nagy V, Marita A, et al. A simple survival score for patients with brain metastases from breast cancer. *Strahlenther Onkol* 2013; **189**: 664-7. doi: 10.1007/s00066-013-0367-5
11. Kaplan EL, Meier P. Non parametric estimation from incomplete observations. *J Am Stat Assoc* 1958; **53**: 457-81.

12. Rades D, Dziggel L, Nagy V, Segedin B, Lohynska R, Veninga T, et al. A new survival score for patients with brain metastases who received whole-brain radiotherapy (WBRT) alone. *Radiother Oncol* 2013; **108**: 123-7. doi: 10.1016/j.radonc.2013.06.009
13. Mehta MP, Rodrigus P, Terhaard CH, Rao A, Suh J, Roa W, et al. Survival and neurologic outcomes in a randomized trial of motexafin gadolinium and whole-brain radiation therapy in brain metastases. *J Clin Oncol* 2003; **21**: 2529-36. doi: 10.1200/JCO.2003.12.122
14. Gaspar L, Scott C, Rotman M, Asbell S, Phillips T, Wasserman T, et al. Recursive partitioning analysis (RPA) of prognostic factors in three Radiation Therapy Oncology Group (RTOG) brain metastases trials. *Int J Radiat Oncol Biol Phys* 1997; **37**: 745-51.
15. Sperduto PW, Berkey B, Gaspar LE, Mehta M, Curran W. A new prognostic index and comparison to three other indices for patients with brain metastases: an analysis of 1,960 patients in the RTOG database. *Int J Radiat Oncol Biol Phys* 2008; **70**: 510-4. doi: 10.1016/j.ijrobp.2007.06.074

Swallowing disorders after treatment for head and neck cancer

Martina Pezdirec¹, Primož Strojan², Irena Hocevar Boltezar^{1,3}

¹ Faculty of Medicine, University of Ljubljana, Ljubljana, Slovenia

² Institute of Oncology, Ljubljana, Slovenia

³ University Department of Otorhinolaryngology and Cervicofacial Surgery, University Medical Center, Ljubljana, Slovenia

Radiol Oncol 2019; 53(2): 225-230.

Received 04 February 2019

Accepted 23 April 2019

Correspondence to: Irena Hočevnar Boltežar, M.D., Ph.D., University Department of Otorhinolaryngology and Cervicofacial Surgery, University Medical Centre, Zaloška cesta 2, 1000 Ljubljana, Slovenia. Phone: +386 41 958 336; Fax: +386 1 522 41 08; E-mail: boltezar.irena@gmail.com or irena.hocevar-boltezar@mf.uni-lj.si

Disclosure: No potential conflicts of interest were disclosed.

Background. Dysphagia is a common consequence of treatment for head and neck cancer (HNC). The purpose of the study was to evaluate the prevalence of dysphagia in a group of patients treated for HNC in Slovenia, and to identify factors contributing to the development of dysphagia.

Patients and methods. One-hundred-nine consecutive patients treated for HNC at two tertiary centers were recruited during their follow-up visits. They fulfilled EORTC QLQ-H&N35 and "Swallowing Disorders after Head and Neck Cancer Treatment questionnaire" questionnaires. Patients with dysphagia were compared to those without it.

Results. Problems with swallowing were identified in 41.3% of the patients. Dysphagia affected their social life (in 75.6%), especially eating in public (in 80%). Dysphagia was found the most often in the patients with oral cavity and/or oropharyngeal cancer (in 57.6%) and in those treated less than 2 years ago ($p = 0.014$). In univariate analysis, a significant relationship was observed between dysphagia prevalence and some of the consequences of anti-cancer treatment (impaired mouth opening, sticky saliva, loss of smell, impaired taste, oral and throat pain, persistent cough, and hoarseness), radiotherapy ($p = 0.003$), and symptoms of gastroesophageal reflux ($p = 0.027$). After multiple regression modelling only persistent cough remained.

Conclusions. In order to improve swallowing abilities and, consequently, quality of life of the patients with HNC a systematic rehabilitation of swallowing should be organized. A special emphasis should be given to gastroesophageal reflux treatment before, during and after therapy for HNC.

Key words: head and neck cancer; swallowing disorders; symptoms; questionnaire; quality of life

Introduction

In 2015, head and neck cancer (HNC) represented 3.5% of all cancer cases in Slovenia. It was the 7th most common type of cancer in the population and with the share of 5.2% the 5th most common cancer in males. Among 459 new HNC cases in Slovenia in 2015, there were 144 oral cavity primaries, 122 oropharyngeal, 70 hypopharyngeal, and 90 laryngeal primary tumors. Locally advanced disease stages (UICC TNM stages III or IVA-B) were diagnosed in 32%, 92%, 90% and 53% of patients with oral cavi-

ty, oropharyngeal, hypopharyngeal, and laryngeal primaries, respectively.¹

Due to its invasive growth with destruction of neighboring anatomical structures, HNC has an adverse effect on important functions, including swallowing, breathing, coughing and speech. Thus, it can profoundly influence quality of life of the patient. Treatment of the tumor may significantly deteriorate these functions. Treatment modalities, including surgery, irradiation and systemic therapy, either alone or combined, can result in tissue defects, excessive scarring, and changed anatomi-

cal setting and function of the involved organs.²⁻⁶ The treatment options in late sequelae of different therapies are limited and of variable benefit.⁷

Dysphagia is an important cause of malnutrition, dehydration, weight loss, chronic aspiration and aspiration pneumonia. All these complications can lead to not only serious health issues and even death, but may also result in depression and social isolation.⁸⁻¹⁵ In addition, late dysphagia, even of a mild grade, is one of the most important factors adversely influencing quality of life of HNC patients, with feeding-tube dependency having the most negative impact.⁹

In the present cross-sectional study, we investigated the most common dysphagia-related factors and problems in a group of survivors who were treated for HNC in the last decade at two tertiary centers. The primary aim was to identify factors that participate to the development of dysphagia in studied cohort of HNC patients.

Patients and methods

Patient's selection

The study cohort consisted of 109 patients who have been successfully treated for HNC in the past decade with either primary surgery or (chemo) radiotherapy. The consecutive patients who came for their regular follow-up visits to the Outpatient Clinics of the Institute of Oncology Ljubljana (IOL) or the University Department of Otorhinolaryngology and Cervicofacial Surgery (ORL), University Medical Center Ljubljana during the period October – December 2017 and were willing to participate were included in the study.

Questionnaires

The patients completed Slovenian translation of the EORTC QLQ-H&N35 questionnaire, and the "Swallowing Disorders after Head and Neck Cancer Treatment" questionnaire. The first one evaluates the impact of head and neck cancer and its treatment on quality of patient's life.¹⁶ It comprises of 35 items, which can be condensed into seven multi-item and eleven single-item symptom scales. Only those 23 questions related to swallowing and to organs involved were considered for the further analyses. The second questionnaire was specifically designed for the purpose of present study to determine the patients' age, gender, details concerning cancer treatment, swallowing problems, and associated diseases that may be re-

lated to dysphagia (i.e. gastroesophageal reflux, stroke, recurrent pneumonia). The patients were asked to complete both questionnaires at the clinic while waiting for scheduled follow-up visit. If purposely agreed, the detailed information on their disease was collected from their medical documentation (i.e. primary tumor site, TNM stage).

Statistical analysis

Data was analyzed with SPSS version 22 (SPSS Inc., Chicago; USA) software package. Depending on whether swallowing problems were consistently reported in both questionnaires, the patients were divided into two groups, i.e. dysphagia group (DG) and to those without swallowing problems (OTH). Groups were compared by using the χ^2 -test for trend or Fischer's exact test, and the t-test. Only those parameters which were found related to dysphagia were included into the multiple regression model. Non-significant variables were removed using backward stepwise selection. The level of statistical significance was set at 0.05 and all statistical tests were two-sided.

The study was conducted according to the Helsinki declaration and was approved by the National Medical Ethics Committee of the Republic of Slovenia (No. 0120-204/2017-3). All patients included in the study signed an informed consent confirming their voluntary participation in the study and agreement with analysis of data for the study purposes.

Results

Patients' characteristics

The study group consisted of 109 patients: 50 patients were recruited at the IO, and 59 patients at the ORL. Their age ranged from 43 to 91 years (mean 65.4 years, standard deviation [SD] 10.6 years). There were 31 female (43 to 91 years, mean 68 years, SD 12 years) and 78 male (46 to 87 years, mean 64.5 years, SD 10 years) patients with no significant difference in age profile between the two ($p = 0.141$).

The primary tumor sites were paranasal sinuses, nasal cavity or nasopharynx in altogether 10 patients (9.2%), oral cavity or oropharynx in 33 (30.3%), hypopharynx or larynx in 51 (46.8%), and neck metastasis of unknown primary tumor in 15 patients (13.8%).

Twenty-two patients (20.2%) were treated only with surgery, 10 patients (9.2%) only with radio-

therapy, and 16 patients (14.7%) with concurrent chemoradiotherapy. In 41 patients (37.6%) surgery was followed by radiotherapy, and in 20 patients (18.3%) surgery was followed by chemoradiotherapy.

The time interval between treatment completion and inclusion into the study ranged from 0.2 to 10 years (mean 3.13 years, SD 2.84 years). Sixty patients (55%) finished therapy less than 2 years ago, and in 49 patients (45%) treatment was completed more than 2 years before.

Results of the questionnaires

All 109 patients fulfilled both questionnaires. Eleven patients (10.1%) did not give their permission to obtain data on their cancer and its treatment from medical documentation.

According to pre-defined criteria, 45 patients (41.3%) were found to experience various swallowing difficulties, both in a week before the interview (EORTC QLQ-H&N35 questionnaire) and generally (“Swallowing Disorders after Head and Neck Cancer Treatment” questionnaire), and were sorted into the DG group. Other 64 patients (58.7%) who did not report problems with swallowing at all or only at one questionnaire formed the OTH group.

Dysphagia was reported in 2 (20%) patients treated for cancer of the nasal cavity, paranasal sinuses or nasopharynx, 19 (57.6%) patients treated for cancer of the oral cavity or oropharynx, 20 (39.2%) patients treated for cancer of the hypopharynx or larynx, and in 4 (26.7%) patients treated for neck metastasis of unknown primary tumor.

Twenty-seven out of 45 patients (60%) with dysphagia finished their treatment less than 2 years before the study and four patients (8.9%) from the DG group were feeding-tube-dependent.

In DG, impaired swallowing of liquids, soft food, and solid food was reported in 25 (55.6%), 26 (57.8%), and 42 cases (93.3%), respectively. Problems with sticking food in the oral cavity or pharynx, and cough during or immediately after swallowing were present in 32 (71.1%), and 33 (73.3%) patients, respectively.

Results of comparison of different clinical and swallowing-related parameters between the DG and OTH are shown in Table 1. Only the significant results are presented. In 11 patients who did not give their consent to collect details on their disease from the medical documentation, information on the primary tumor site as provided by the themselves was used. (Table 1).

TABLE 1. Comparison of the patients with dysphagia and the patients without dysphagia after head and neck treatment. Only the significant results are presented

Parameter	No Dysphagia N = 64	Dysphagia N = 45	P-Value
Swallowing vs. non-swallowing area			
Oral cavity, oropharynx, hypopharynx, larynx (N= 84)	45 (70.3%)	39 (86.7%)	0.046
Nasal cavity, paranasal sinuses, nasopharynx, metastases (N = 25)	19 (29.7%)	6 (13.3%)	
TNM stage*			
Stages I-III	41 (64.1%)	17 (37.8%)	0.005
Stages IV	17 (26.6%)	23 (51.1%)	
Treatment modalities			
Surgery	19 (29.7%)	3 (6.7%)	
RT or concurrent RT-CT	15 (23.4%)	11 (24.4%)	
Surgery + RT or RT-CT	30 (46.9%)	31 (57.4%)	0.010
Role of RT			
RT included in treatment	45 (70.3%)	42 (93.3%)	0.002
Therapy completed			
Less than 2 years ago	15 (23.4%)	21 (46.7%)	0.014
Two years or more ago	49 (76.6%)	24 (53.3%)	
Oral problems			
Mucosa irritability	23 (35.9%)	28 (62.2%)	0.007
Mouth wide opening	5 (7.8%)	15 (33.3%)	0.001
Thick and sticky saliva	35 (54.7%)	38 (84.4%)	0.001
Problems with chewing	4 (6.3%)	16 (35.6%)	0.000
Problems with			
Feeding	5 (7.8%)	35 (77.8%)	0.000
Feeding in the presence of family	3 (4.7%)	28 (62.2%)	0.000
Feeding in the public	7 (10.9%)	36 (80%)	0.000
Enjoying food	3 (4.7%)	17 (37.7%)	0.000
Avoiding public areas			
	18 (28.1%)	34 (75.6%)	0.020
Loss of smell			
	7 (10.9%)	15 (33.3%)	0.004
Impaired taste			
	18 (28.1%)	34 (75.6%)	0.000
Acid reflux and heartburn			
	18 (28.1%)	22 (48.9%)	0.027
Pain			
Oral pain	4 (6.3%)	14 (31.1%)	0.001
Throat pain	12 (18.8%)	18 (40%)	0.014
Persistent coughing			
	30 (46.9%)	38 (84.4%)	0.000
History of recurrent pneumonia			
	2 (3.1%)	7 (15.6%)	0.031
Presence of hoarseness			
	25 (39.1%)	28 (62.2%)	0.017
Loss of weight			
	17 (26.6%)	24 (53.3%)	0.005
Use of nutritional supplements			
	6 (9.3%)	16 (35.6%)	0.001

*The data on tumor stage was accessible only for 95 patients; CT = chemotherapy; RT = radiotherapy; SD = standard deviation

After exclusion of all dysphagia-derived parameters (i.e. problems with feeding, avoiding public areas, enjoying food, loss of weight, use of nutritional supplements), the remaining, dysphagia-generating variables that appeared statistically significant in univariate analysis were included into the multiple regression model for testing their impact to dysphagia formation. In the final model, only problems with persistent cough remained significant (coefficient 0.249; 95% confidential interval 0.035-0.472; p = 0.023).

Discussion

The management of locally advanced HNC still represents a challenge to the clinicians despite recent improvements in diagnostics and treatment. Excessive scarring secondary to aggressive surgery, intensive irradiation and systemic therapy may result in different degree of swallowing disorders.^{17,18} Malnutrition, the need for enteral tube feeding, social isolation and the feeling of hopelessness may significantly impair quality of patient's life.^{19,20} The results of our study confirmed these observations. Almost 40% of patients from the present study had problems with feeding out of their homes and almost half of the patients avoided going to public areas and thus had social life impaired. Majority of patients from the DG reported problems with feeding (77.8%), feeding in public (80%), and even feeding in the presence of the family (62.2%). In the OTH patients, these problems were recorded significantly less often. Discomfort when eating in presence of other people was probably one of the important reasons that 75.6% of the patients who reported difficulties with swallowing also reported avoiding public places, which makes dysphagia an important reason for their social isolation.

The prevalence of dysphagia in our study was 41.3%, which is less than in some other series.^{3,4,6,7} We assume that differences in studied populations of patients in regard to distribution of primary tumor sites and treatment modalities used as well as methods for dysphagia assessment are the reasons for this discrepancy.

As expected, among our patients a higher prevalence of dysphagia was significantly related to primaries originated in the swallowing-related areas of the head and neck and to more advanced disease stages, which is in line with other reports.⁷ In addition, radiation therapy also appeared to be a significant causative factor for dysphagia in univariate analysis. Among 45 patients with dysphagia, almost all (93.3%) were treated with radiation therapy, either as the sole therapy or in combination with surgery and/or chemotherapy. One of the reasons for more aggressive treatment scenario could be more advanced tumor stage that necessitates addition of radiotherapy to surgery or intensification of radiotherapy with concurrent chemotherapy. However, using multiple regression analysis with disease stage taking into account, radiotherapy did not remain in the final model. This result supports the observation of other authors who found no differences in the severity of dysphagia or aspiration according to type of treatment.^{7,15}

Pathophysiological mechanisms implicated in development of swallowing disorders after HNC treatment differ according to modality used. In case of surgery, tissue defect resulted from tumor removal adversely effects organ's function because its integrity is truncated. When organs crucial for swallowing are the site of primary tumor (e.g. tongue, velopharyngeal orifice, larynx, pharyngeal wall, and upper esophageal sphincter), dysphagia appears. With destruction of primary tumor, radiation therapy induces scarring at the site of its origin and fibrotic changes elsewhere in tissues inside irradiation field, which reduces their elasticity and flexibility. Thus, the dose-volume relationship in case of pharyngeal constrictor muscles appears to be the most important predictor of later swallowing disorders.²¹

Sensory impairment of the upper aerodigestive tract mucosa as a result of tissue loss or post-radiotherapy changes seems also to be an important causative mechanism of swallowing disorders and especially aspiration. Thus, both, surgical treatment and radiation therapy, can adversely influence laryngeal innervation and alter its functions, including its role in swallowing. In the present study, 62.2% of the patients with dysphagia reported hoarseness, and 84.4% of them reported persistent cough. In multiple regression modelling only persistent cough remained significant factor related to dysphagia. The cough can be a consequence of hyposensibility of the larynx after surgery or irradiation, leading to persistent micro aspiration in the trachea. When the secretions or food come in contact with intact tracheal mucosa with preserved sensibility, they induce protective coughing which successfully clears the airway.^{12,15} This cough can be the reason that in our series only 8.2% of the patients experienced pneumonia. The flexible endoscopic evaluation of swallowing could prove this hypothesis; however, no such examination was foreseen in the study protocol.

There are other symptoms which can cause dysphagia that appeared more often in the DG than in the OTH, i.e. oral pain (31.1% vs. 6.3%), throat pain (40% vs. 18.8%), oral mucosa irritability (62.2% vs. 35.9%), thick saliva (84.4% vs. 54.7%), impaired sense of taste (75.6% vs. 28.1%), change of smelling abilities (33.3% vs. 10.9%). The highest prevalence was reported for problems related to production of saliva and to impaired tasting abilities, which can be interconnected.⁵ However, in our analysis, none of these parameters demonstrated to be significantly related to dysphagia in multiple regression testing.

Dysphagia was repeatedly reported to be a chronic problem in HNC patients cured of their cancer. Nguyen *et al.* showed by means of repeated modified barium swallow that up to two years post-surgery dysphagia disappeared in 8% and decreased in its severity in 32% of the patients; in all others patients it worsened or remained unchanged.¹⁵ This observation confirms our finding that dysphagia was more often reported in patients with a less than 2 years of follow-up after treatment.

Other late sequel in patients treated for HNC is changed quality of mucus in the upper aerodigestive tract. Among our DG patients, thick and sticky mucus was reported in 84.4% of cases. We hypothesize that alterations in mucus quality are responsible for improper dissolution of taste molecules, which resulted in impaired sense of taste. The other cause of (partial) taste loss are postirradiation changes of the taste buds in oral cavity and oropharynx or loss of receptors because of surgical excision.²² However, a well-known interconnection between the sense of taste and the sense of smell could participate to decreased smelling ability which was reported in one third of our patients with dysphagia.²³

An interesting finding of the present study is a connection between dysphagia and the symptoms of gastroesophageal reflux. Reflux of gastric acid and pepsin is well-recognized etiologic factor in dysphagia even in subjects without cancer, simply by causing inflammation of the laryngeal and hypopharyngeal mucosa.^{24,25} Such inflammation can additionally aggravate pre-existing radiomucositis in irradiated patients, leading to scarring and impaired sensitivity of involved mucosa. Reflux to the level above the upper esophageal sphincter was found to impair the sensibility of the throat and hypopharynx in otherwise healthy subjects.²⁶

The only significant variable in multiple regression analysis was persistent cough. The gastroesophageal reflux to the level of laryngopharynx can also be the reason for persistent cough, induced by altered mucosal sensitivity and mobility impairment of the cilia of respiratory epithelium of the larynx.²⁷ Consequently, mucus accumulated at the laryngeal inlet causes throat clearing and persistent cough. The causative role of microaspiration and impaired mucosal sensitivity in persistent cough has already been mentioned.

The third association between the gastroesophageal reflux and persistent cough is managed through the neural reflexes. The vagus nerve-mediated reflex arc originates at distal esophagus

and can initiate a reflex coughing when the receptors in the esophageal wall are stimulated by the reflux.^{28,29} Therefore, in order to decrease the incidence of coughing in the patients after HNC treatment, pre-treatment identification and proper management of patients with gastroesophageal reflux symptoms is mandatory.

We acknowledge the limitations of our study. This is a questionnaire-based review of a small number of patients who might be too subjective in their answers. There is also a heterogeneity of population regarding the cancer location, stage of the disease, and treatment modalities used. The exact data from the medical documentation regarding anatomical details of cancer extension, treatment intensity and its complications and assessment of dysphagia with objective methods would add significantly to the quality of study.

In conclusion, in order to enable safe swallowing and to reduce the risk of aspiration in HNC patients, a systematic assessment and rehabilitation of swallowing should be organized before and after treatment. According to presented results, special emphasis should be put on gastroesophageal reflux screening and treatment before, during and after the therapy. Only with implementation of these interventions in the routine management algorithms used in HNC patients, a quality of life improvement can be expected.

References

1. Epidemiology and Cancer Registry, Cancer Registry of Republic of Slovenia, Institute of Oncology Ljubljana. *Cancer in Slovenia 2015*. Ljubljana: Institute of Oncology Ljubljana; 2018.
2. van der Molen L, van Rossum MA, Burkhead LM, Smeele LE, Hilgers FJM. Functional outcomes and rehabilitation strategies in patients treated with chemoradiotherapy for advanced head and neck cancer: a systematic review. *Eur Arch Otorhinolaryngol* 2009; **266**: 889-900. doi: 10.1007/s00405-008-0817-3
3. Hey C, Lange BP, Aere C, Zaretsky Y, Sader R, Stöver T, et al. Predictability of oral and laryngopharyngeal function for aspiration and limitation of oral intake in patients after surgery for head and neck cancer. *Anticancer Res* 2013; **33**: 3347-53. PMID: 23898102
4. Rinkel RN, Verdonck-Leeuw IM, van den Brakel N, de Bree R, Eerenstein SE, Aaronson N, et al. Patient-reported symptom questionnaires in laryngeal cancer: voice, speech and swallowing. *Oral Oncol* 2014; **50**: 759-64. doi: 10.1016/j.oraloncology.2014.05.009
5. Likhterov I, Ru M, Ganz C, Urken ML, Chai R, Okay D, et al. Objective and subjective hyposalivation after treatment for head and neck cancer: long-term outcomes. *Laryngoscope* 2018; **128**: 2732-9. doi: 10.1002/lary.27224
6. Patterson JM, McColl E, Carding PN, Wilson JA. Swallowing beyond six years post (chemo)radiotherapy for head and neck cancer; a cohort study. *Oral Oncol* 2018; **83**: 53-8. doi: 10.1016/j.oraloncology.2018.06.003
7. Strojanc P, Hutcheson KA, Eisbruch A, Beitler JJ, Langendijk JA, Lee AWM, et al. Treatment of late sequelae after radiotherapy for head and neck cancer. *Cancer Treat Rev* 2017; **59**: 79-92. doi: 10.1016/j.ctrv.2017.07.003

8. Carmignani I, Locatello G, Desideri I, Bonomo P, Olmetto E, Livi L, et al. Analysis of dysphagia in advanced-stage head-and-neck cancer patients: impact on quality of life and development of a preventive swallowing treatment. *Eur Arch Otorhinolaryngol* 2018; **275**: 2159-67. doi: 10.1007/s00405-018-5054-9
9. Nguyen NP, Frank C, Moltz CC, Vos P, Smith HJ, Karlsson U, et al. Impact of dysphagia on quality of life after treatment of head and neck cancer. *Int J Radiat Oncol Biol Phys* 2005; **61**: 772-8. doi: 10.1016/j.ijrobp.2004.06.017
10. Eisele DW, Koch DG, Tarazi AE, Jones B. Case report: aspiration from delayed radiation fibrosis of the neck. *Dysphagia* 1991; **6**: 120-2. PMID: 1935259
11. Smith RV, Kotz T, Beitler JJ, Wadler S. Long-term swallowing problems after organ preservation therapy with concomitant radiation therapy and intravenous hydroxyurea. *Arch Otolaryngol Head Neck Surg* 2000; **126**: 384-9. doi: 10.1001/archotol.126.3.384
12. Eisbruch A, Lyden T, Bradford CR, Dawson LA, Haxer MJ, Miller AE, et al. Objective assessment of swallowing dysfunction and aspiration after radiation concurrent with chemotherapy for head and neck cancer. *Int J Rad Oncol Biol Phys* 2002; **53**: 23-8. doi: 10.1016/S0360-3016(02)02712-8
13. Ward EC, Bishop B, Frisby J, Stevens RM. Swallowing outcomes following laryngectomy and pharyngolaryngectomy. *Arch Otolaryngol Head Neck Surg* 2002; **128**: 181-6. doi: 10.1001/archotol.128.2.181
14. Pauloski BR, Rademaker AW, Logemann JA, Colangelo LA. Speech and swallowing in irradiated and nonirradiated postsurgical oral cancer patients. *Otolaryngol Head Neck Surg* 1998; **118**: 616-24. doi: 10.1177/019459989811800509
15. Nguyen NP, Moltz CC, Frank C, Vos P, Smith HJ, Karlsson U, et al. Evolution of chronic dysphagia following treatment for head and neck cancer. *Oral Oncol* 2006; **42**: 374-80. doi: 10.1016/j.oraloncology.2005.09.003
16. Singer S, Arraras JL, Chie WC, Fisher SE, Galalae R, Hammerlid E, et al. Performance of the EORTC questionnaire for the assessment of quality of life in head and neck cancer patients EORTC QLQ-H&N35: a methodological review. *Qual Life Res* 2013; **22**: 1927-41. doi: 10.1007/s11136-012-0325-1
17. Nguyen NP, Moltz CC, Frank C, Vos P, Smith HJ, Karlsson U, et al. Long-term aspiration following treatment for head and neck cancer. *Oncology* 2008; **74**: 25-30. doi: 10.1159/000138976
18. Nguyen NP, Sallah S. Combined chemotherapy and radiation in the treatment of locally advanced head and neck cancers. *In Vivo* 2000; **14**: 35-9. PMID: 10757059
19. Al-Sarraf M. Treatment of locally advanced head and neck cancer, historical and critical review. *Cancer Control* 2002; **9**: 387-99. doi: 10.1177/107327480200900504
20. Lazarus CL, Husaini H, Hu K, Culliney B, Li Z, Urken M, et al. Functional outcome and quality of life after chemoradiotherapy: baseline and 3 and 6 months' post-treatment. *Dysphagia* 2014; **29**: 365-75. doi: 10.1007/s00455-014-9519-8
21. Duperz F, Madani I, De Potter B, Botenberg T, De Neve W. Systematic review of dose-volume correlates for structures related to late swallowing disturbances after radiotherapy for head and neck cancer. *Dysphagia* 2013; **28**: 337-49. doi: 10.1007/s00455-013-9452-2
22. Maes A, Huygh I, Weltens C, Vandeveldel G, Delaere P, Evers G, et al. De Gustibus: time scale of loss and recovery of tastes caused by radiotherapy. *Radiother Oncol* 2002; **63**: 195-201. doi: 10.1016/S0167-8140(02)00025-7
23. Czarnecki L, Fontanini A. Gustation and olfaction: the importance of place and time. *Curr Biol* 2019; **29**: R18-20. doi: 10.1016/j.cub.2018.11.038
24. Bulmer DM, Ali MS, Brownlee IA, Dettmar PW, Pearson JP. Laryngeal mucosa: its susceptibility to damage by acid and pepsin. *Laryngoscope* 2010; **120**: 777-82. doi: 10.1002/lary.20665
25. Johnston N, Wells CW, Samuels TL, Blumin JH. Pepsin in nonacidic refluxate can damage hypopharyngeal epithelial cells. *Ann Otol Rhinol Laryngol* 2009; **118**: 677-85. doi: 10.1177/000348940911800913
26. Phua SY, McGarvey L, Ngu M, Ing A. The differential effect of gastroesophageal reflux disease on mechanostimulation and chemostimulation of the laryngopharynx. *Chest* 2010; **138**: 1180-5. doi: 10.1378/chest.09-2387
27. Hawkshaw M, Pebdani P, Sataloff RT. Reflux laryngitis: an update, 2009–2012. *J Voice* 2013; **27**: 486-494. doi: 10.1016/j.jvoice.2013.03.001
28. Johnston N, Bulmer D, Gill GA, Panetti M, Ross PE, Pearson JP, et al. Cell biology of laryngeal defenses in health and disease: further studies. *Ann Otol Rhinol Laryngol* 2003; **112**: 481-91. doi: 10.1177/000348940311200601
29. Pauwels A, Blondeau K, Dupont L, Sifrim D. Cough and gastroesophageal reflux: from the gastroenterologist end. *Pulm Pharmacol Ther* 2009; **22**: 135-8. doi: 10.1016/j.pupt.2008.11.007

Health-related quality of life in Slovenian patients with colorectal cancer: a single tertiary care center study

Jan Grosek¹, Jerica Novak², Katja Kitek³, Alta Bajric³, Ana Majdic³, Jurij Ales Kosir¹, Ales Tomazic¹

¹ Department of Abdominal Surgery, Ljubljana University Medical Center, Ljubljana, Slovenia

² Department of Surgical Oncology, Ljubljana Institute of Oncology, Ljubljana, Slovenia.

³ Medical Faculty, University of Ljubljana, Ljubljana

Radiol Oncol 2019; 53(2): 231-237.

Received 12 December 2018

Accepted 02 February 2019

Correspondence to: Jan Grosek, M.D., Ph.D., Department of Abdominal Surgery, Ljubljana University Medical Center, Zaloška cesta 7, SI-1000 Ljubljana, Slovenia. Phone: +386 1 522 4788; Fax: +386 1 522 2209; E-mail: jan.grosek@kclj.si

Disclosure: No potential conflicts of interest were disclosed.

Background. The aim of this study was to evaluate the influence of the surgical treatment on Slovenian colorectal cancer patients' health-related quality of life and to compare the results to the health-related quality of life of the general Slovenian population.

Patients and methods. A total of 413 patients with colorectal cancer operated on at the Abdominal Surgery Department at the Ljubljana University Medical Center between January 1st, 2016 and December 31st, 2017 were sent two standardized and validated questionnaires: the EORTC QLQ-C30 version 3 and EORTC QLQ-CR29. The questionnaires were returned by 197 patients.

Results. Compared to the general population, poorer physical ($p < 0.001$), role ($p = 0.002$), cognitive ($p = 0.021$), and social functioning ($p < 0.001$) with higher frequency of constipation ($p < 0.001$), diarrhea ($p < 0.001$), and financial difficulties ($p < 0.001$) were reported by the colorectal patients. Female patients reported lower cognitive ($p = 0.034$) and emotional ($p = 0.008$) functioning, as well as higher frequency of bloating ($p = 0.049$) and hair loss ($p = 0.01$). Compared to the younger group of patients, lower physical functioning ($p < 0.001$) and higher urinary frequency ($p = 0.007$), urinary incontinence ($p = 0.007$), buttock pain ($p = 0.007$), and anxiety regarding body weight ($p = 0.031$) were detected among the older group of colorectal patients.

Conclusions. The global health status of colorectal patients in Slovenia is comparable to that of the general Slovenian population, but there is a significantly lower level in some of the quality-of-life scales.

Key words: health-related quality of life; colorectal cancer; colorectal surgery; Slovenia

Introduction

Colorectal cancer (CRC) is an important cause of death as well as decreased quality of life. Worldwide, CRC is the third most commonly diagnosed malignancy and the fourth most common cause of death.¹ The incidence of CRC is higher in the developed countries.² The 5-year and 10-year

survival rates of operable and localized colorectal cancer are 60% and 50%, respectively.³

In Slovenia, 11,269 patients (56% men, 44% women) with CRC were still alive at the end of 2015. CRC is the fourth most commonly diagnosed malignancy among Slovenian cancer patients.⁴ In 2015, 1,356 patients were diagnosed with CRC (58% men, 42% women). Colon cancer was found

most frequently (63%), followed by cancer of the rectum and rectosigmoid junction. (37%).⁴

Impaired health-related quality of life (QoL) in CRC patients may result from the disease itself and/or treatment.⁵ It can be described as psychophysical, functional, and emotional disruption or social impairment.^{6,7} Standardized questionnaires are used to evaluate QoL in cancer patients.⁸ The most commonly used questionnaire for evaluating QoL in oncology is the EORTC QLQ-C30 questionnaire, launched by the European Organisation for Research and Treatment of Cancer (EORTC).⁹ It has been translated into many languages, including Slovenian.¹⁰ The reference values of the EORTC QLQ-C30 questionnaire for the general Slovenian population have already been obtained and published.¹¹ Moreover, the EORTC developed the colorectal QoL module EORTC QLQ-CR29, which has been used as an addition to the EORTC QLQ-C30 to evaluate QoL in CRC patients.¹²

The aim of this study was to evaluate QoL in CRC patients after colorectal surgery and to compare the results with the reference data from the general Slovenian population.

Patients and methods

Patients

QoL was evaluated for patients with CRC, stages I–IV, with and without metastatic disease, operated on at the Abdominal Surgery Department of the Ljubljana University Medical Center from January 1st, 2016 to January 31st, 2017. Patients still alive on January 1st, 2018 were included. A patient chart review was performed. A total of 413 patients met the inclusion criteria and were sent the questionnaire; of these, 197 patients (116 male, 81 female) returned the questionnaire. Patients at least one year and no more than two years from the initial operation were included in the study.

Questionnaires

For the purpose of this study, the standardized questionnaires EORTC QLQ-C30 and QLQ-CR29 were utilized. The questionnaires were translated into Slovenian.

The EORTC QLQ-C30 questionnaire consists of three scoring scales that grade function, symptoms, and global health. The scales include one or more questions. Each question has four response options from 1 = not at all to 4 = very much. A higher score corresponds to a poorer result and more symptoms

present. On the other hand, global health status is categorized with seven-point scoring scale on which a higher score corresponds to greater well-being and higher quality of life.

The EORTC QLQ-CR29 questionnaire consists of two scoring scales that grade function and symptoms, and it has specifically been used to assess QoL in CRC patients. As for the EORTC QLQ-C30, the responses range from 1 to 4 and a higher score defines a poorer outcome, with exception of the response for sexual interest, for which a higher score correlates with a better result.

Statistical analysis

Because the scoring scales consist of one or more questions (anxiety on the EORTC QLQ-CR29 and cognitive functions on the EORTC-CR29), a raw score (RS) was calculated for each scoring scale. Linear transformation was used to standardize the RS and the transformed recorded answers into dimensions ranging from 0 to 100. Higher scores on functional scoring scales correlated with better functions in patients and, on the other hand, higher scores on symptom scoring scales correlated with poorer outcomes. For the linear transformation, the following formulas were applied:

- For functional scoring scales: $S =$;
- For symptom scoring scales: $S =$;
- For global health-status: $S =$.

The numerical variables were represented by means and standard deviations. The differences between numerical variables were tested using Student's *t*-test. For the purpose of the statistical analysis, patients were divided into two age groups according to the reported median age of 73 years. First group included patients from 39 to 73 years and the second group patients from 74 to 92 years. The association between age groups and sexes was tested using the Mann–Whitney test. A *p*-value < 0.05 was considered statistically significant. Statistical analyses were performed using SPSS software (IBM Corp., version 24.0 Armonk, NY).

Approval for the study was obtained from the Medical Ethics Committee of the Republic of Slovenia, the Protocol Review Board (MZ 0120-48/2018-6). Written consent from all patients included was provided prior to study enrollment.

Results

A total of 413 patients received the questionnaire, and the response rate was 47.7% (197 patients).

Characteristics of the study population are shown in Table 1.

EORTC QLQ-C3 Scoring scale

When the average scores of the EORTC QLQ-C30 in the general Slovenian population and in patients with CRC were compared, statistically significant differences in QoL were detected. Physical, role, cognitive, and social functioning scores were significantly lower in patients with CRC compared to the general population. Compared to the general population, CRC patients more often experienced symptoms as constipation and diarrhea. Moreover, compared to general population, financial difficulties were also more often reported by the CRC patients. No other statistically significant differences were detected between CRC patients and the general population (Table 2).¹¹

When comparing QoL among CRC patients, statistically significant lower scores for cognitive and emotional functioning were detected in females. No other statistically significant differences between the sexes were detected (Table 3).

When comparing the different age groups of the CRC patients (younger group 39–73 years, older group 74–92 years), statistically significant lower physical functioning scores were reported among the older patients. In addition, insomnia and dyspnea were more often reported among the older patients compared to the younger ones (Table 4).

EORTC QLQ-CR29 Scoring scale

Females more often reported bloating and hair loss. No other statistically significant differences in the rate of reporting other symptoms and in the scoring for mental health were found between the sexes (Table 5).

Compared to younger patients, older patients more often reported symptoms such as urinary frequency, urinary incontinence, and buttock pain. Older patients were also more concerned regarding their weight (Table 6).

Discussion

QoL is a substantial factor when outcomes and effects of the disease on CRC patients after multimodal treatment are evaluated.¹³ In Slovenia, the evaluation of QoL in CRC patients is not yet systematically used. To the best of our knowledge, this is the first study evaluating QoL in CRC pa-

TABLE 1. Characteristics of the study population

	Responders n 197	Non-responders n 216	p-value
Median age (IQR)	72 (62–79)	74 (65–81)	0.016
Sex			
Male (%)	116 (58.9)	133(61.5)	0.603
Female (%)	81 (41.1)	83 (38.5)	
Complications			
Not reported	175 (88.8)	150 (69.4)	<0.001
Severe* (%)	15 (7.6)	32 (14.8)	
Operation			
Right hemicolectomy	80 (40.6)	101 (46.8)	0.208
Extended right hemicolectomy	8(4.1)	17(7.9)	0.033
Left hemicolectomy	26 (13.2)	19 (8.8)	0.152
Hartmann's procedure	10 (5.1)	14 (6.5)	0.542
Rectosigmoid resection	4 (2)	8 (3.7)	0.312
Low anterior resection	13 (6.6)	8 (3.7)	0.181
Sigmoid resection	46 (23.4)	38 (17.6)	0.147
Subtotal colectomy	2 (1)	5 (2.3)	0.298
Total colectomy	5 (2.5)	3 (1.4)	0.396
Segmental resections of the colon	4(2)	2(0.9)	0.007
Other procedures	1 (0.5)	2 (0.9)	0.613

*Clavien–Dindo classification 3 to 5; IQR = interquartile range; n = number of patients

tients after surgery and comparing it with QoL for the general Slovenian population.

This study found no statistical differences in the reported global health score between CRC patients and the general Slovenian population. The results are comparable to other similar studies.^{6,14–17} On the other hand, compared to the general Slovenian population, our CRC patients reported poorer physical, cognitive, and social functioning. Moreover, they also more frequently reported symptoms such as constipation, diarrhea, and financial difficulties compared to the general Slovenian population. Similar results have been observed in other published studies.^{15,17} A comparable discovery was made by Rauch *et al.*, in which patients more frequently reported lower physical functioning but also had greater levels of pain than the general population.¹⁴

When comparing the responding and non-responding group of CRC patients, a higher rate of major postoperative complications was observed in the non-responding group. Postoperative complications that lead to reoperation, longer hospitalization, or stoma formation can greatly alter QoL in CRC patients. In our study, the reported satisfaction with QoL in the responding group may therefore be due to the lower rates of major postoperative complications. Nevertheless, patients in

TABLE 2. Comparison of the scores for all scales of the EORTC QLQ-C30 between CRC patients and the general Slovenian population

	Colorectal patients					General Slovenian population M (SD)	p-value
	Min	Max	M (SD)	Me (IQR)	n		
Functional scoring scale							
Physical functions	0	100	83 (20.2)	87 (80–100)	197	91.8 (14)	< 0.001
Role functions	0	100	82.7 (26.8)	100 (67–100)	196	88.7 (20.1)	0.002
Cognitive functions	0	100	87.2 (18.1)	100 (83–100)	197	90.2 (16)	0.021
Emotional functions	0	100	83.4 (16.2)	83 (75–100)	197	82 (18.5)	0.239
Social functions	0	100	82.1 (24)	100 (67–100)	197	90.9 (17.3)	< 0.001
Symptom scoring scale							
Dyspnea	0	100	6.2 (16.1)	0 (0–0)	197	5.3 (15.3)	0.928
Insomnia	0	100	22.4 (27.5)	0 (0–33)	197	19.8 (25.1)	0.182
Loss of appetite	0	100	5.6 (17.2)	0 (0–0)	195	5.3 (15.5)	0.791
Nausea and vomiting	0	50	2.9 (8.1)	0 (0–0)	195	3.3 (10.6)	0.524
Constipation	0	100	13.2 (22.5)	0 (0–33)	196	6.9 (16.9)	< 0.001
Diarrhea	0	100	12.6 (22.7)	0 (0–33)	196	4.2 (13.6)	< 0.001
Fatigue	0	100	22.2 (22.2)	22 (0–33)	197	19.8 (19.8)	0.126
Pain	0	100	13.8 (21.8)	0 (0–17)	195	14.5 (20.2)	0.633
Financial impact of disease	0	100	14.2 (26.6)	0 (0–33)	196	6.6 (17.5)	< 0.001
Global health status							
Global health status	17	100	68.3 (20.5)	67 (50–83)	197	71.1 (21.4)	0.058

IQR = interquartile range; Max = maximum value; Me = median; Min = minimal value; SD = standard deviation; n = number of patients

TABLE 3. Comparison of the scores for all the scales of the EORTC QLQ-C30 by sex.

	Male			Female			p-value
	M (SD)	Me (IQR)	n	M (SD)	Me (IQR)	n	
Functional scoring scale							
Physical functions	82.9 (19.1)	87 (80–100)	116	83.1 (21.8)	93 (80–100)	81	0.584
Role functions	84.1 (23.2)	100 (67–100)	115	80.7 (31.2)	100 (67–100)	81	0.982
Cognitive functions	89.8 (15.2)	100 (83–100)	116	83.5 (21)	83 (67–100)	81	0.034
Emotional functions	85.7 (14.9)	92 (75–100)	116	80 (17.5)	83 (75–92)	81	0.008
Social functions	81.5 (22.7)	83 (67–100)	116	82.9 (25.8)	100 (67–100)	81	0.329
Symptom scoring scale							
Dyspnea	6 (16.2)	0 (0–0)	116	6.5 (16.1)	0 (0–0)	81	0.570
Insomnia	21.2 (26.9)	0 (0–33)	116	24.2 (28.4)	33 (0–33)	81	0.450
Loss of appetite	4.3 (15.6)	0 (0–0)	115	7.5 (19.1)	0 (0–0)	80	0.115
Nausea and vomiting	3.1 (8.7)	0 (0–0)	115	2.7 (7.3)	0 (0–0)	80	0.934
Constipation	13.6 (22.9)	0 (0–33)	115	12.7 (22)	0 (0–33)	81	0.903
Diarrhea	12.8 (22)	0 (0–33)	115	12.3 (23.8)	0 (0–33)	81	0.641
Fatigue	19.9 (21)	11 (0–33)	116	25.5 (23.5)	22 (0–33)	81	0.110
Pain	12.3 (19.8)	0 (0–17)	114	15.8 (24.4)	0 (0–22)	81	0.338
Financial impact of disease	13.5 (26.7)	0 (0–33)	116	15.4 (26.5)	0 (0–33)	80	0.441
Global health status							
Global health status	68.1 (21.4)	67 (50–83)	116	68.6 (19.3)	67 (50–83)	81	0.903

IQR = interquartile range; M = mean; Me = median; n = number of patients SD = standard deviation

TABLE 4. Comparison of the scores for all the scales of the EORTC QLQ-C30 by age groups

	Age 39–73 years			Age 74–92 years			p-value
	M (SD)	Me (IQR)	n	M (SD)	Me (IQR)	n	
Functional scoring scale							
Physical functions	87.5 (16.3)	93 (80–100)	98	78.6 (22.7)	87 (67–93)	99	0.001
Role functions	82.2 (28.7)	100 (67–100)	97	83.2 (24.9)	100 (67–100)	99	0.724
Cognitive functions	89.3 (15)	100 (83–100)	98	85.1 (20.5)	100 (83–100)	99	0.268
Emotional functions	85 (14.7)	83 (75–100)	98	81.7 (17.5)	83 (75–92)	99	0.218
Social functions	84.7 (23.3)	100 (67–100)	98	79.5 (24.5)	83 (67–100)	99	0.069
Symptom scoring scale							
Dyspnea	3 (9.6)	0 (0–0)	98	9.4 (20.2)	0 (0–0)	99	0.014
Insomnia	16.6 (23.5)	0 (0–33)	98	28.2 (29.9)	33 (0–33)	99	0.004
Loss of appetite	6.4 (18.3)	0 (0–0)	98	4.8 (15.9)	0 (0–0)	97	0.511
Nausea and vomiting	2.9 (7.9)	0 (0–0)	98	2.9 (8.4)	0 (0–0)	97	0.993
Constipation	11.6 (22.6)	0 (0–33)	97	14.7 (22.4)	0 (0–33)	99	0.177
Diarrhea	10.8 (20.9)	0 (0–33)	97	14.4 (24.3)	0 (0–33)	99	0.286
Fatigue	20.9 (22.7)	22 (0–33)	98	23.6 (21.7)	22 (0–33)	99	0.228
Pain	11.5 (21.6)	0 (0–17)	98	16.1 (21.9)	0 (0–33)	97	0.061
Financial impact of disease	18.7 (29.9)	0 (0–33)	98	9.8 (22)	0 (0–0)	98	0.025
Global health status							
Global health status	69.8 (22.4)	75 (50–83)	98	66.8 (18.5)	67 (50–83)	99	0.132

IQR = interquartile range; M = mean; Me = median; SD = standard deviation; n = number of patients

TABLE 5. Comparison of the scores for all the scales of the EORTC QLQ-CR29 by sex

	Male			Female			p-value
	M (SD)	Me (IQR)	n	M (SD)	Me (IQR)	n	
Symptom scoring scale							
Urinary frequency	29.4 (2.8)	33 (0–50)	115	28.1 (24.4)	33 (17–33)	81	0.670
Urinary incontinence	9.1 (18.3)	0 (0–0)	116	9.1 (17.5)	0 (0–0)	80	0.941
Dysuria	4.6 (13.1)	0 (0–0)	115	2.4 (8.7)	0 (0–0)	81	0.266
Abdominal pain	10.5 (16.7)	0 (0–33)	116	12.7 (19.4)	0 (0–33)	81	0.548
Buttock pain	12.3 (22.2)	0 (0–33)	116	8.6 (20.3)	0 (0–0)	81	0.123
Bloating	18.9 (24.5)	0 (0–33)	116	25.4 (26)	33 (0–33)	81	0.049
Blood & mucus in stool	3.4 (11.7)	0 (0–0)	116	3.5 (11.1)	0 (0–0)	81	0.939
Dry mouth	21 (25.2)	16.5 (0–33)	116	24.7 (28.8)	0 (0–33)	81	0.503
Hair loss	1.4 (6.7)	0 (0–0)	116	5.7 (15.5)	0 (0–0)	81	0.010
Taste	6 (16.2)	0 (0–0)	116	11.6 (24.3)	0 (0–0)	80	0.090
No stoma							
Flatulence	25.7 (29.8)	33 (0–33)	88	27.1 (29.1)	33 (0–33)	70	0.651
Fecal incontinence	6.7 (18.2)	0 (0–0)	89	7.1 (16.8)	0 (0–0)	70	0.569
Sore skin	14 (22.4)	0 (0–33)	88	18.5 (25.1)	0 (0–33)	70	0.212
Stool frequency	11.8 (18.3)	0 (0–17)	89	11.6 (16.4)	0 (0–17)	71	0.772
Embarrassment	8.3 (18.3)	0 (0–0)	88	9.3 (20.6)	0 (0–0)	68	0.925
Mental health							
Anxiety	57.1 (29.1)	67 (33–67)	114	49.8 (26.6)	67 (33–67)	81	0.069
Weight	78.7 (28.1)	100 (67–100)	115	79.9 (29.2)	100 (67–100)	81	0.563
Body image	86.5 (20.2)	100 (78–100)	115	87.3 (21)	100 (78–100)	81	0.708

IQR = interquartile range; M = mean; Me = median; SD = standard deviation; n = number of patients

TABLE 6. Comparison of the scores for all the scales of the EORTC QLQ-CR29 by age groups

	Age 39–73 years			Age 74–92 years			p-value
	M (SD)	Me (IQR)	n	M (SD)	Me (IQR)	n	
Symptom scoring scale							
Urinary frequency	24.7 (25.2)	17 (0–33)	97	33 (23.3)	33 (17–50)	99	0.007
Urinary incontinence	5.9 (15.1)	0 (0–0)	98	12.4 (19.9)	0 (0–33)	98	0.007
Dysuria	3 (9.6)	0 (0–0)	98	4.4 (13.2)	0 (0–0)	98	0.607
Abdominal pain	8.8 (14.6)	0 (0–33)	98	14.1 (20.2)	0 (0–33)	99	0.087
Buttock pain	7.8 (20.2)	0 (0–0)	98	13.7 (22.3)	0 (0–33)	99	0.007
Bloating	19.6 (23.3)	0 (0–33)	98	23.5 (27.1)	33 (0–33)	99	0.404
Blood & mucus in stool	4.1 (14)	0 (0–0)	98	2.8 (8.2)	0 (0–0)	99	0.938
Dry mouth	18.7 (24.2)	0 (0–33)	98	26.2 (28.7)	33 (0–33)	99	0.069
Hair loss	4.4 (14)	0 (0–0)	98	2 (7.9)	0 (0–0)	99	0.193
Taste	7.1 (17.4)	0 (0–0)	98	9.5 (22.4)	0 (0–0)	98	0.648
No stoma							
Flatulence	22.2 (27.3)	3 (0–33)	81	30.7 (31)	33 (0–33)	77	0.068
Fecal incontinence	5.3 (14.4)	0 (0–0)	81	8.5 (20.4)	0 (0–0)	78	0.329
Sore skin	14.9 (23)	0 (0–33)	80	17 (24.4)	0 (0–33)	78	0.566
Stool frequency	12.3 (18.2)	0 (0–17)	82	11.2 (16.7)	0 (0–17)	78	0.860
Embarrassment	7.8 (17.7)	0 (0–0)	81	9.7 (21)	0 (0–0)	75	0.550
Mental health							
Anxiety	51.4 (30.1)	67 (33–67)	98	56.8 (26.1)	67 (33–67)	97	0.227
Weight	74.6 (30.8)	100 (67–100)	98	83.7 (25.4)	100 (67–100)	98	0.031
Body image	84.9 (22.8)	100 (78–100)	98	88.8 (17.7)	100 (78–100)	98	0.156

IQR = interquartile range; M = mean; Me = median; SD = standard deviation; n = number of patients

the responding group were also younger (median age 73 years, compared to 75.5 years in the non-responding group, respectively; $p = 0.016$), which can also be an important factor contributing to reported better QoL in this group of patients. As determined in a study by Velenik *et al.*, reported QoL in the general Slovenian population decreases with age.¹¹

In the general Slovenian population, a comparison of QoL between the sexes showed a statistically significant difference in reported physical functioning, which was poorer among females ($p < 0.000$). No other statistically significant differences in functioning were reported.¹¹ On the other hand, when comparing CRC patients by sex, female CRC patients more frequently reported lower cognitive and emotional functioning compared to males ($p = 0.034$ and 0.008 , respectively). Females also more frequently reported bloating and hair loss, and the difference was statistically significant ($p = 0.049$ and 0.01 , respectively). No other statistically significant differences were observed between the sexes. Similar to our study, Adams *et al.* discovered that female CRC patients, compared to males, more often reported lower cognitive and emotional functioning, and also lower physical and social functioning.¹⁸ As the results show, female patients may

need more emotional support following treatment. Therefore open discussion of the symptoms and suitable referrals for additional support or mental health treatments should be made during follow-ups.¹⁹

Reported QoL in the general Slovenian population is lower among the elderly.¹¹ This phenomenon has also been reported by other European researchers.^{20–22} Comparing QoL of different age groups shows lower physical functioning of older patients. ($p = 0.001$). Our results correlate with similar reports in the literature.^{23–25} Statistically significant differences between age groups were discovered when reporting the frequency of symptoms of urinary frequency, urinary incontinence, and buttock pain. On the other hand, Japanese and American studies discovered better QoL in elderly patients.^{26,27} One can conclude that society and environment significantly influence individual evaluations of QoL.

Our study has limitations. First of all, the response rate was low (47.7%). For optimal results, the respond rate should be above 85%. This could be achieved by systematically distributing the questionnaire to CRC patients at follow-ups. Therefore, not only the feedback but also immediately addressing patients' key issues with possible

additional referrals could be achieved. Another limitation is that the study was performed at a single tertiary center in Slovenia. For better results and optimal insight into QoL in CRC patients, a systematic multicenter study including all tertiary and regional centers in Slovenia should be carried out. The questionnaires should be given to CRC patients prior to surgery or neoadjuvant treatment, 1 month after surgery, and 1 and 5 years after treatment. In this way, comprehensive insight into QoL in CRC patients could be obtained, evaluating not only the influence of surgery but also the influence of neoadjuvant treatment on QoL in these patients.

Conclusions

This is the first Slovenian study comparing QoL in CRC patients with the general Slovenian population. The global health status of CRC patients in Slovenia is comparable to that of the general Slovenian population, but there is a significantly lower score on some of the QoL scales. For further research, a systematic multicenter study, including CRC patients from all Slovenian tertiary centers, should be performed with the aim of improving QoL for these patients with multidisciplinary follow-up treatment.

Acknowledgements

We wish to thank Ms. Vanja Erčulj, statistician who performed all necessary statistical calculations.

References

1. Ferlay J, Soerjomataram I, Ervik M, Dikshit R, Eser S, Mathers C, et al. Cancer incidence and mortality worldwide: sources, methods and major patterns in GLOBOCAN 2012. *Int J Cancer* 2015; **136**: E359-86. doi: 10.1002/ijc.29210
2. Arnold M, Sierra MS, Laversanne M, Soerjomataram I, Jemal A, Bray F. Global patterns and trends in colorectal cancer incidence and mortality. *Gut* 2017; **66**: 683-91. doi: 10.1136/gutjnl-2015-310912
3. van Gijn W, Marinjen CA, Nagtegaal ID, Kranenbarg EM, Putter H, Wiggers T, et al. Dutch Colorectal Cancer Group. Preoperative radiotherapy combined with total mesorectal excision for resectable rectal cancer: 12-year follow-up of the multicenter, randomized controlled TME trial. *Lancet Oncol* 2011; **12**: 575-82. doi: 10.1016/S1470-2045(11)70097-3
4. Zadnik V, Primc Zakej M, Lokar K, Jarm K, Ivanus U, Zagar T. Cancer burden in Slovenia with the time trends analysis. *Radiol Oncol* 2017; **51**: 47-55. doi: 10.1515/raon-2017-0008
5. Stiggelbout AM, Kunneman M, Baas-Thijssen MC, Neijenhuis PA, Loo AK, Jägers S, et al. The EORTC QLQ-CR29 quality of life questionnaire for colorectal cancer: validation of the Dutch version. *Qual Life Res* 2016; **25**: 1853-8. doi: 10.1007/s11136-015-1210-5
6. Marventano S, Forjaz MJ, Grosso G, Mistretta A, Giorgianni G, Platania A, et al. Health related quality of life in colorectal patients: state of the art. *BMC Surg* 2013; **13** (Suppl 2): S15. doi: 10.1186/1471-2482-13-S2-S15
7. Pucciarelli S, Bianco P, Toppan P, Serpentine S, Efficace F, Pasetto LM, et al. Health-related quality of life outcomes in disease-free survivors of mid-low rectal cancer after curative surgery. *Ann Surg Oncol* 2008; **15**: 1846-54. doi: 10.1245/s10434-008-9923-0
8. Lockett T, King MT, Butow PN, Oguchi M, Rankin N, Price MA, et al. Choosing between the EORTC QLQ-C30 and FACT-G for measuring health-related quality of life in cancer clinical research: issues, evidence and recommendations. *Ann Oncol* 2011; **22**: 2179-90. doi: 10.1093/annonc/mdq721
9. Aaronson NK, Ahmedzai S, Bergman B, Bullinger M, Cull A, Duez NJ, et al. The European Organisation for Research and Treatment of cancer QLQ-C30: a quality-of-life instruments for use in international clinical trials in oncology. *J Natl Cancer Inst* 1993; **85**: 365-76.
10. Life ESG qQo. EORTC QLQ-C30 (version 3.0) Slovenian. Brussels: EORTC; 1996.
11. Velenik V, Secerov-Ermenc A, But-Hadzic J, Zadnik V. Health-related quality of life assessed by the EORTC QLQ-C30 questionnaire in the general Slovenian population. *Radiol Oncol* 2017; **51**: 342-350. doi: 10.1515/raon-2017-0021
12. Gujral S, Conroy T, Fleissner C, Sezer O, King PM, Avery KN, et al. European Organisation for Research and Treatment of Cancer Quality of Life Group Assessing quality of life in patients with colorectal cancer: an update of the EORTC quality of life questionnaire. *Eur J Cancer* 2007; **43**: 1564-73. doi:10.1016/j.ejca.2007.04.005
13. Sahay TB, Gray RE, Fitch M. A qualitative study of patient perspectives on colorectal cancer. *Cancer Pract* 2000; **13**: 38-44. doi:10.1046/j.1523-5394.2000.81012.x
14. Rauch P, Miny J, Conroy T, Neyton L, Guillemin F. Quality of life among disease-free survivors of rectal cancer. *J Clin Oncol* 2004; **22**: 354-60. doi: 10.1200/jco.2004.03.137
15. Arnt V, Merx H, Stegmaier C, Ziegler H, Brenner H. Quality of life in patients with colorectal cancer 1 year after diagnosis compared with the general population: a population-based study. *J Clin Oncol* 2004; **22**: 4829-36. doi:10.1200/jco.2004.02.018
16. Jansen L, Koch L, Brenner H, Arndt V. Quality of life among long-term (≥ 5 years) colorectal cancer survivors - systematic review. *Eur J Cancer* 2010; **46**: 2879-88. doi: 10.1016/j.ejca.2010.06.010
17. Ramsey SD, Berry K, Moynour C, Giedzinska A, Andersen MR. Quality of life in long term survivors of colorectal cancer. *Am J Gastroenterol* 2002; **97**: 1228-34. doi: 10.1111/j.1572-0241.2002.05694.x
18. Adams SV, Ceballos R, Newcomb PA. Quality of life and mortality of long-term colorectal cancer survivors in the Seattle colorectal cancer family registry. *PLoS ONE* 2016; **11**: e0156534. doi:10.1371/journal.pone.0156534
19. Avery JC, Nishimoto PW. Psychosocial issues in colorectal cancer survivorship: the top ten questions patients may not be asking. *J Gastrointest Oncol* 2014; **5**: 395-400. doi: 10.3978/j.issn.2078-6891.2014.058
20. Juul T, Petersen MA, Holzner B, Laurberg S, Christensen P, Grønvald M. Danish population-based reference data for the EORTC QLQ-C30: associations with gender, age and morbidity. *Qual Life Res* 2014; **23**: 2183-93. doi: 10.1007/s11136-014-0675-y
21. Hjermstad MJ, Fayers P M, Bjordal K, Kaasa S. Health-related quality of life in the general Norwegian population assessed by the European Organization for Research and Treatment of Cancer Core Quality-of-Life Questionnaire: the QLQ=C30 (+ 3). *J Clin Oncol* 1998; **16**: 1188-96. doi:10.1200/jco.1998.16.3.1188
22. Derogar M, van der Schaaf M, Lagergren P. Reference values for the EORTC QLQ-C30 quality of life questionnaire in a random sample of the Swedish population. *Acta Oncol* 2012; **51**: 10-16. doi: 10.3109/0284186X.2011.614636
23. Schmidt CE, Bestmann B, Kuchler T, Longo WE, Kremer B. Impact of age on quality of life in patients with rectal cancer. *World J Surg* 2005; **29**: 190-97. doi:10.1007/s00268-004-7556-4
24. Sapp AL, Trentham-Dietz A, Newcomb PA, Hampton JM, Moynour CM, Remington PL. Social networks and quality of life among female long-term colorectal cancer survivors. *Cancer* 2003; **98**: 1749-58. doi:10.1002/cncr.11717
25. Trentham-Dietz A, Remington PL, Moynour CM, Hampton JM, Sapp AL, Newcomb PA. Health-related quality of life in female long-term colorectal cancer survivors. *The Oncologist* 2003; **8**: 342-49. doi: 10.1634/theoncologist.8-4-342
26. Hamashima C. Long-term quality of life of postoperative rectal cancer patients. *J Gastroenterol Hepatol* 2002; **17**: 571-76. doi: 10.1046/j.1440-1746.2002.02712.x
27. Klemm P, Miller M A, Fernsler J. Demands of illness in people treated for colorectal cancer *Oncol Nurs Forum* 2000; **27**: 633-39. PMID: 10833692

Long term survival in 200 patients with advanced stage of colorectal carcinoma and diabetes mellitus - a single institution experience

Nikola Besic¹, Milena Kerin Povsic²

¹ Department of Surgical Oncology, Institute of Oncology Ljubljana, Slovenia

² Department of Anesthesiology and Intensive Care, Institute of Oncology Ljubljana, Slovenia

Radiol Oncol 2019; 53(2): 238-244.

Received 31 January 2019

Accepted 7 April 2019

Correspondence to: Milena Kerin Povšič, M.D. Ph.D., Department of Anesthesiology and Intensive Care, Institute of Oncology Ljubljana, Zaloška 2, SI-1000 Ljubljana, Slovenia. Phone: +386 1 5879 916; Fax: +386 1 5879 400; E-mail: mkerin@onko-i.si

Disclosure: No potential conflicts of interest were disclosed.

Background. Diabetes mellitus (DM) and DM related comorbidities may initiate difficulties during cancer specific treatment and may have an impact on cancer management and outcome. The aim of our study was to find out if DM in patients with advanced colorectal carcinoma (CRC) is associated with cancer-specific or overall survival.

Patients and methods. This study included 200 consecutive patients (131 males, 69 females, mean age 63 years) with elective CRC surgery at the Institute of Oncology Ljubljana and DM was found in 39 (19.5%) of them. Even 64% of patients had Stage 3 or 4 disease, so neo-adjuvant chemotherapy (CTX) and/or radiotherapy (RT) were carried out in 59% of cases. Data about gender, age, body mass index, presence of DM, American Society of Anesthesiologists (ASA) physical status score, stage of disease and postoperative complications were collected prospectively. Cancer-specific survival and overall survival were compared by log-rank test.

Results. Patients with DM had a higher ASA score, BMI, the illness marker, rate of massive bleeding, blood transfusion and longer hospital stay than those without DM. The mean follow-up period was 4.75 years. All causes mortality in patients with DM and without DM was 23% and 27%, respectively. Three-year cancer-specific survival in patients with DM and without DM was 85% and 89%, respectively ($p = 0.68$). Three-year overall survival in patients with DM and without DM was 82% and 84%, respectively ($p = 0.63$).

Conclusions. The presence of DM was not associated with tumor stage, disease-specific survival or overall survival in patients with advanced CRC.

Key words: colorectal carcinoma, diabetes mellitus, surgery, survival

Introduction

Diabetes mellitus (DM) is known to be an independent risk factor for the development of colorectal cancer (CRC).^{1,2} The risk of colorectal cancer was estimated to be 27% higher in patients with type 2 DM than in non-diabetic controls.³ However, it is unclear if the presence of diabetes in patients with CRC is associated with the cancer-specific survival

of patients after cancer diagnosis.⁴ Some authors found that patients with CRC and diabetes are at greater risk of all-cause and cancer-specific mortality and have worse disease-free survival compared to those without diabetes.⁵ But other authors found that the presence of DM in patients with CRC was not associated with worse cancer-specific survival.⁴

Diabetes mellitus and DM related comorbidities may initiate difficulties during cancer specific

treatment and may have an impact on cancer management and outcome. Colorectal cancer surgery is often followed by postoperative complications which may impact survival. The aim of our study was to find out if DM in patients with advanced colorectal carcinoma is associated with cancer-specific or overall survival.

Patients and methods

This study included 200 consecutive patients (131 males, 69 females, mean age 63 years) with elective colorectal cancer surgery at the Institute of Oncology Ljubljana from September 2010 to March 2013. In 14 patients, curative resection of liver metastases was carried out during the same anesthesia. In all the patients, a laparotomy was performed. The exclusion criteria were preoperative infection, preoperative ileus and palliative surgical procedure.^{6,7} All 200 patients were prospectively included in the study about the usefulness of biomarker index CD64 for neutrophils (iCD64n) for early detection of postoperative infection.^{6,7} The study protocol was approved by the Republic of Slovenia National Medical Ethics Committee. Approval and written consent for the retrospective study of the long-term outcome of the patients was obtained from the Protocol Review Board (MZ 0120-28/2016-2, ERID-KSOPKR/20), and the Ethics Committee of the Institute of Oncology (ERID-KSOPKR/77, OIRIKE 0049).

Rectum, colon and both of them were affected by cancer in 68%, 30% and 2% of cases, respectively. Stage of tumor was evaluated clinically according to the nuclear magnetic resonance (NMR) investigation before the beginning of the treatment. The TNM classification was used for staging of colorectal cancer disease.⁸ Even 64% of patients had Stage 3 or 4 disease, so neo-adjuvant chemotherapy (CTX) and/or radiotherapy (RT) were carried out in 59% of cases. CTX and/or RT were carried out and finished six to eight weeks before surgery, as reported by Golo *et al.*⁹ Each patient was assessed preoperatively according to the American Society of Anesthesiologists (ASA) physical status classification, which accurately predicts morbidity and mortality.¹⁰ Bioelectric impedance analysis (BIA) measurement was performed on the day before the surgery using a portable bioelectrical impedance analyzer BodyStat QuadScan 4000 (Douglas, Great Britain), as already described by Kerin-Povsic *et al.*⁷ Phase angle is the ratio between the reactance and resistance.¹¹ The illness marker is the ratio between

the impedance measurement at 200kHz and 5kHz. A ratio closer to 1.00 indicates poor cellular health or extreme fluid overload.

DM was found in 39 (19.5%) of patients: 19 were treated only with metformin, 5 only with insulin, while 15 were treated with two or three different oral antidiabetics.

Data about gender, age, body mass index, presence of DM, American Society of Anesthesiologists (ASA) physical status score, stage of disease and postoperative complications were collected prospectively.

All patients had a follow-up at the Institute of Oncology Ljubljana. Cancer-specific survival was defined as the period from the first day of primary treatment (surgery, CTX or RT) to death from colorectal cancer, or the last follow-up. Overall survival was defined as the period from the first day of primary treatment (surgery, CTX or RT) to death from any cause, or the last follow-up. Disease-free survival was defined as the period from the first day of primary treatment to the radiologic or morphologic diagnosis of recurrence, or the last follow-up. The median duration of follow-up was 5.1 years (range 0.2–10.5 years).

The association between categorical variables was tested by the Pearson chi-square test or Fisher's exact test, as appropriate. Univariate analysis was used to identify factors associated with cancer-specific and overall survival. Cancer-specific survival and overall survival were compared by log-rank test. All comparisons were two-sided, and a *p*-value of <0.05 was considered statistically significant. Survival curves were calculated according to the Kaplan–Meier method. Statistical analyses were performed using the SPSS software (IBM Corp., version 22.0 Armonk, NY).

Results

Data about patient's characteristics, tumor, treatment and outcome are presented in Table 1. The mean age of patients with and without DM was 65 and 62 years, respectively. There was no statistically significant difference in the age of patients with and without DM (*p* = 0.13). However, patients with DM had a higher ASA score (*p* = 0.0001) and BMI (*p* = 0.003) than those without DM. Furthermore, before surgical procedure, the illness marker was higher in patients with DM in comparison to those without DM (*p* = 0.02). However, higher disease stages were not more common in patients with DM in comparison to those without DM. Stage 3 or 4

TABLE 1. Patient's characteristics, tumor, treatment and outcome

Characteristic		Without diabetes mellitus (N = 161)	With diabetes mellitus (N = 39)	p-value
Age (years) - mean		62.18 (SD ± 11.8)	65.26 (SD ± 8.9)	0.13
Gender	Male	106	25	0.84
	Female	55	14	
American Society of Anesthesiologists physical status classification score	I	14	0	0.0001
	II	95	10	
	III	47	29	
	IV	5	0	
Body mass index (kg/m ²) - mean		26.83 (SD ± 4.20)	29.06 (SD ± 4.1)	0.003
Treatment of diabetes	Insulin only	-	5	-
	Metformin only	-	19	
	2 or 3 oral antidiabetics	-	15	
Phase angle (°) - mean		5.47 (SD ± 1.0)	5.16 (SD ± 0.9)	0.11
Illness marker - mean		0.807 (SD ± 0.036)	0.825 (SD ± 0.049)	0.02
Dry lean body mass (kg) - mean		12.97 (SD ± 4.5)	12.65 (SD ± 4.6)	0.72
Tumor site	Rectum	113	24	0.09
	Colon	47	13	
	Rectum + Colon	1	2	
Stage TNM	0	3	0	0.50
	I	21	6	
	II	33	9	
	III	91	18	
	IV	13	6	
Preoperative radiotherapy	No	67	18	0.61
	Yes	94	21	
Preoperative chemotherapy	No	90	22	0.95
	Yes	71	17	
Surgical procedure	Low anterior resection	73	13	0.38
	Miles + Hartman	38	12	
	Colon resection	50	14	
Synchronous resection of liver metastases	No	151	35	0.48
	Yes	10	4	
Duration of surgery (min) - mean		175 (SD ± 66)	199 (SD ± 64)	0.034
Loss of blood (mL) - mean		584 (SD ± 497)	813 (SD ± 812)	0.027
Postoperative transfusion of packed red blood cells (mL) - mean		351 (SD ± 516)	603 (SD ± 665)	0.011
Postoperative infection (any site)	No	110	22	0.16
	Yes	51	17	
Re-operation	No	153	35	0.21
	Yes	8	4	
Hospital stay (days) - mean		14.4 (SD ± 7.6)	19.9 (SD ± 10.6)	0.028
Recurrence (N = 181)	No	111	28	0.63
	Locoregional	4	1	
	Distant	26	3	
	Locoregional + distant	7	1	
Outcome	Alive	117	30	0.74
	Dead of disease	34	7	
	Dead of other causes	9	1	
	Dead - Unknown cause	1	1	

disease was found in patients with DM and without DM in 62% and 65%, respectively ($p = 0.72$). So, also the proportion of patients treated with CTX and/or RT were not statistically different among patients with DM and without DM.

None of the patients had a laparoscopic procedure. A higher proportion of the patients with

DM had massive bleeding ($p = 0.027$) and received blood transfusion ($p = 0.011$) in comparison to patients without DM. Surgical procedure ($p = 0.034$) as well as hospital stay ($p = 0.028$) was longer in patients with DM in comparison to those without DM. None of patients died during the first month after a surgical procedure ($p < 0.0001$).

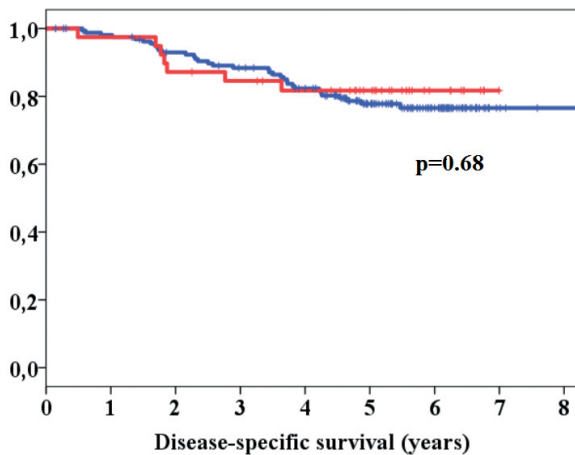


FIGURE 1. Cancer-specific survival of patients with and without Diabetes mellitus (DM).

red line = with DM; blue line = without DM

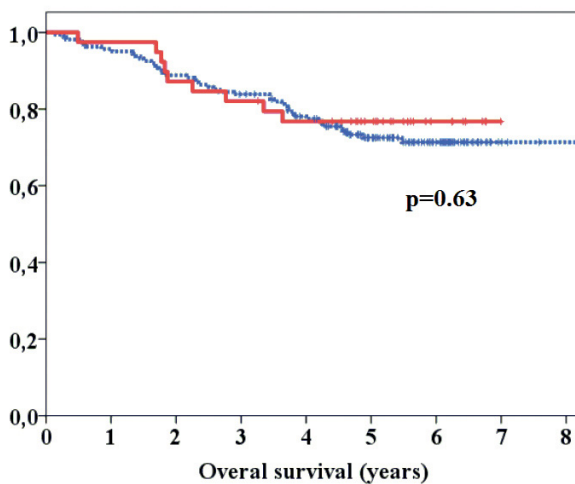


FIGURE 2. Overall survival of patients with and without Diabetes mellitus (DM).

red line = with DM; blue line = without DM

The mean follow-up period was 4.75 years. Recurrence was diagnosed in 23% of patients with DM and in 25% of patients without DM ($p = 0.63$). Locoregional recurrence was detected in 2/39 (5%) patients with DM and in 11/161 (6.8%) patients without DM. Distant metastases after surgical procedure were detected in 4 patients with DM and 33 patients without DM. Altogether, 41 patients died of cancer and 12 patients of other causes. Cause of death was not statistically different in patients with DM in comparison to those without DM ($p = 0.74$). Colorectal cancer was the cause of death in 18% and 21% of patients with and without DM, respectively. All causes mortality in patients with DM and without DM was 23% and 27%, respectively.

Three-year cancer-specific survival (Figure 1) in patients with DM and without DM was 85% and 89%, respectively ($p = 0.68$). Three-year overall survival (Figure 2) in patients with DM and without DM was 82% and 84%, respectively ($p = 0.63$). Patients with colon and rectal cancer had estimated median survival of 75 and 108 months ($p = 0.089$), respectively. All patients were included in our statistical analysis of survival because there was only small number of patients with low stage tumor, colon cancer and/or presence of DM which precluded adequate subgroup analysis.

Discussion

The aim of our study was to find out if DM in patients with advanced CRC was associated with cancer-specific and overall survival. In our 200 consecutive patients with elective surgical procedure for CRC, the presence of DM was not associated with cancer-specific or overall survival after the mean follow-up period of 4.75 years. Inversely, a meta-analysis of 26 observational studies on CRC has shown that patients with CRC and DM had a 17% increased risk of overall mortality and a 12% increased risk of cancer-specific mortality compared to those without DM.⁵ However, another meta-analysis has shown that persons with CRC and DM had a 32% increase in overall mortality compared to those without DM, but there were no associations between DM and risk of cancer-specific mortality.⁴ Bella *et al.* found that the presence of DM was significantly associated with decreased overall and cancer-specific survival.¹² They analyzed 1,039 CRC cases who were included in a EURO-CARE-5 high resolution study and were treated in Italy from 2003–2005.¹² Their patients with and without DM did not differ in terms of type of resection, elective versus emergency surgery, or number of lymph nodes examined. Their patients with DM were older in comparison to the patients without DM. Furthermore, diabetics were significantly less likely to receive adjuvant therapy than non-diabetics.¹² But our diabetics were not older than the non-diabetics ($p = 0.13$) and their overall and cancer-specific survival was not statistically different. A possible explanation is that the same proportion of patients from both groups had preoperative radiotherapy and/or chemotherapy, which might have influenced the survival of patients. Similarly to Bella *et al.*,¹² Van de Pol-Franse *et al.*¹³ also reported that patients with diabetes and CRC were treated less aggressively compared to those with-

out diabetes. Another possible explanation for the differences in survival among the reported studies is a selection bias between population based and single institution based cohorts of patients. Our patients were treated at a single cancer comprehensive center, while Bella *et al.* report data from seven Italian cancer registries, and Van de Pol-Franse *et al.* report data from the registration area of the Eindhoven Cancer Registry.^{12,13} Both of them also included patients treated in general hospitals.

A substantial proportion of deaths in older persons with colorectal cancer can be attributed to chronic heart failure, diabetes mellitus, and chronic obstructive pulmonary disease.¹⁴ Polednak *et al.*¹⁵, in a population-based statewide Connecticut cancer registry, found that the presence of DM was associated with a statistically significantly elevated risk of death from any cause. This finding was due to an elevated risk of death from causes other than CRC.¹⁵ Similarly, Ota *et al.*¹⁶ reported, in 1,216 patients with CRC, that overall survival was significantly inferior in the patients with DM than in those without, but there was no difference in cancer-specific survival between the two groups. Nevertheless, cancer-specific survival was worse in diabetics in stage IV cancer, but it remained unclear whether this has been attributed to differences in malignancy or in treatment.¹⁶ On the other hand, Rao Kondapally Seshasai *et al.*¹⁷ found that DM was moderately associated with deaths from CRC cancer from individual-participant data on 123,205 deaths among 820,900 people in 97 prospective studies. DM worsens prognosis because it is frequently associated with comorbidities such as cardiovascular disease because they are associated with increased risk of death.^{12,18,19} Certain comorbidities such as heart problems, alcohol abuse, liver disease, and deep vein thrombosis had an impact on prognosis.²⁰ Furthermore, the number of comorbid conditions was significant in predicting early mortality.²⁰ Multimorbidity is common, and exerts a substantial effect on CRC survival.¹⁴ Therefore, comorbidity increases the complexity of cancer management and affects survival duration.²⁰

Davila *et al.*²¹ studied 30-day mortality using National Veterans Administration administrative data, and found that patients who had received surgical resection more recently had a lower risk of 30-day mortality, compared with those resected in 1987–1988. Significant declines were observed in several postoperative disorders, including anesthesia complications and thromboembolism.²¹ Preoperative disorders associated with increased

mortality included chronic pulmonary disease, congestive heart failure, diabetes, hemiplegia/paraplegia, moderate/severe liver disease, and renal disease.²¹ Obviously, declining preoperative and postoperative disorders, as well as improvements in surgical care, could explain these findings.²¹ It is encouraging that none of our patients died during the first month after a surgical procedure. We believe that this reflects the high-quality postoperative care in our ICU and surgical wards. Similar observations were published by Jullumstro *et al.*²², who studied 1,194 patients treated for CRC at Levanger Hospital during a 25 year period. They found that the presence of DM was not associated with short-term survival or cancer specific survival.²² An important factor that might have contributed to the smoother postoperative course and low 30-day mortality in our center is our policy that all patients with malnutrition and/or cachexia had nutritional interventions and pharmacological therapy.^{23,24} It is well known that a low fat-free mass is associated with 28-day mortality after admission to the ICU.²⁵ In our patients with DM, the illness marker and BMI were higher in comparison to those without DM. Furthermore, diabetics had a higher ASA score, which reflects a worse general condition and concomitant diseases. Our patients did not differ in tumor stage, but a higher proportion of patients with DM had massive bleeding and received blood transfusion in comparison to patients without DM. Therefore, it was not surprising that surgical procedure as well as hospital stay was longer in patients with DM in comparison to those without DM.

Jeon *et al.*²⁶ observed that DM was significantly associated with worse overall survival and recurrence-free survival in colon cancer patients, while there was no association with the presence of DM and overall or disease-free survival in rectal cancer patients. This study in 4,131 patients with CRC suggests that DM negatively impacts survival outcomes of patients with colon cancer but not rectal cancer.²⁶ Similarly, in colon cancer patients, Meyerhardt *et al.*²⁷, in a large randomized adjuvant chemotherapy trial of 3,759 patients treated between 1988 and 1992, found that patients with DM experienced a significantly higher rate of overall mortality and cancer recurrence, and an increase in treatment-related diarrhea. Also Huang *et al.*²⁸ reported that DM was a poor prognostic factor for overall and cancer-specific survival in 2,762 consecutive patients diagnosed with colon cancer in Taipei Veterans General Hospital. However, Shonka *et al.*²⁹ found no significant relationship be-

tween stage of colon cancer or survival and presence of DM in 1,853 patients with colon cancer treated in a single institution during an 18-year period. On the other hand, Bella *et al.*¹² found that the presence of DM had a stronger adverse effect on rectal than colon cancer prognosis in 1,039 patients with CRC. Cancer-specific mortality was significantly higher among diabetics, while colon cancer-specific mortality was only non-significantly higher, even though overall mortality was significantly higher.¹² In our patients with colon and rectum cancer, overall and cancer-specific survival was not statistically different, but the number of patients was too small to allow any reliable conclusions about possible differences in prognosis.

A limitation of this study is that it is retrospective, and the follow-up period is relatively short. Furthermore, there were only a small number of diabetics, which precluded analysis of the association between diabetes, stage of disease, location of cancer (rectum versus colon) and survival. Other limitations are the lack of information about diabetes type and age of diabetes onset, as well as the type and duration of diabetic therapy. Because of the relatively small number of diabetics, we could not analyze the association between different diabetic therapies (metformin and insulin) on outcome of patients. On the other hand, an advantage of our study is that a large proportion of patients had an advanced stage of disease with a higher risk of recurrence or progression of disease. All our patients were followed at our institution, so our data on recurrence and cause of death are very reliable.

Conclusions

The presence of DM was not associated with tumor stage, disease-specific survival or overall survival in a group of patients with advanced colorectal carcinoma treated at a cancer comprehensive center.

Acknowledgements

The paper was supported by a research program, P3-0289, by the Ministry of Higher Education, Science and Sport of Slovenia.

References

- Berster JM, Göke B. Type 2 diabetes mellitus as risk factor for colorectal cancer. *Arch Physiol Biochem* 2008; **114**: 84-98. doi: 10.1080/13813450802008455

- Larsson SC, Orsini N, Wolk A. Diabetes mellitus and risk of colorectal cancer: a meta-analysis. *J Natl Cancer Inst* 2005; **22**: 1679-87. doi: 10.1093/jnci/dj375
- González N, Prieto I, Del Puerto-Nevado L, Portal-Nuñez S, Ardura JA, Corton M, et al. 2017 update on the relationship between diabetes and colorectal cancer: epidemiology, potential molecular mechanisms and therapeutic implications. *Oncotarget* 2017; **8**: 18456-85. doi: 10.18632/oncotarget.14472
- Stein KB, Snyder CF, Barone BB, Yeh HC, Peairs KS, Derr RL, et al. Colorectal cancer outcomes, recurrence, and complications in persons with and without diabetes mellitus: a systematic review and meta-analysis. *Dig Dis Sci* 2010; **7**:1839-51. doi: 10.1007/s10620-009-0944-8
- Mills KT, Bellows CF, Hoffman AE, Kelly TN, Gagliardi G. Diabetes mellitus and colorectal cancer prognosis: a meta-analysis. *Dis Colon Rectum* 2013; **11**: 1304-19. doi: 10.1097/DCR.0b013e3182a479f9
- Kerin Povsic M, Beovic B, Ihan A. Perioperative increase in neutrophil CD64 expression is an indicator for intra-abdominal infection after colorectal cancer surgery. *Radiol Oncol* 2016; **2**: 211-20. doi: 10.1515/raon-2016-0016
- Kerin Povsic M, Ihan A, Beović B. Post-Operative Infection is an independent risk factor for worse long-term survival after colorectal cancer surgery. *Surg Infect (Larchmt)* 2016; **6**: 700-12. doi: 10.1089/sur.2015.187
- International Union Against Cancer (UICC). *TNM classification of malignant tumors*, 7th edition. Sobin LH, Gospodarowicz MK, Wittekind Ch, editors. New York: Wiley; 2009.
- Golo D, But-Hadzic J, Anderluh F, Breclj E, Ehemovic I, Jeromen A, et al. Induction chemotherapy, chemoradiotherapy and consolidation chemotherapy in preoperative treatment of rectal cancer - long-term results of phase II OIGIT-01 Trial. *Radiol Oncol* 2018; **3**: 267-74. doi: 10.2478/raon-2018-0028
- Fitz-Henry J. The ASA classification and perioperative risk. *Ann R Coll Surg Engl* 2011; **93**: 185-7. doi: 10.1308/rcsann.2011.93.3.185a
- Gupta D, Lis CG, Dahlk SL, King J, Vashi PG, Grutsck JF, et al. The relationship between bioelectrical impedance phase angle and subjective global assessment in advanced colorectal cancer. *Nutr J* 2008; **7**: 19. doi: 10.1186/1475-2891-7-19
- Bella F, Minicozzi P, Giacomini A, Crocetti E, Federico M, Ponz de Leon M, et al. Impact of diabetes on overall and cancer-specific mortality in colorectal cancer patients. *J Cancer Res Clin Oncol* 2013; **8**: 1303-10. doi: 10.1007/s00432-013-1439-8
- Van de Poll-Franse LV, Houterman S, Janssen-Heijnen ML, Dercksen MW, Coebergh JW, Haak HR. Less aggressive treatment and worse overall survival in cancer patients with diabetes: a large population-based analysis. *Int J Cancer* 2007; **9**: 1986-92. doi: 10.1002/ijc.22532
- Gross CP, Guo Z, McAvay GJ, Allore HG, Young M, Tinetti ME. Multimorbidity and survival in older persons with colorectal cancer. *J Am Geriatr Soc* 2006; **12**: 1898-904. doi: 10.1111/j.1532-5415.2006.00973.x
- Polednak AP. Comorbid diabetes mellitus and risk of death after diagnosis of colorectal cancer: a population-based study. *Cancer Detect Prev* 2006; **5**: 466-72. doi: 10.1016/j.cdp.2006.07.003
- Ota Y, Ishihara S, Otani K, Yasuda K, Nishikawa T, Tanaka T, et al. Effect of nutrient starvation on proliferation and cytokine secretion of peripheral blood lymphocytes. *Mol Clin Oncol* 2016; **4**: 607-10. doi: 10.3892/mco.2016.763
- Rao Kondapally Seshasai S, Kaptoge S, Thompson A, Di Angelantonio E, Gao P, Sarwar N, et al. Diabetes mellitus, fasting glucose, and risk of cause-specific death. *N Engl J Med* 2011; **9**: 829-41. doi: 10.1056/NEJMoa1008862
- Woodward M, Zhang X, Barzi F, Pan W, Ueshima H, Rodgers A, et al. The effects of diabetes on the risks of major cardiovascular diseases and death in the Asia-Pacific region. *Diabetes Care* 2003; **26**: 360-6. doi: 10.2337/diacare.26.2.360
- Booth GL, Kapral MK, Fung K, Tu JV. Relation between age and cardiovascular disease in men and women with diabetes compared with non-diabetic people: a population-based retrospective cohort study. *Lancet* 2006; **368**: 29-36. doi: 10.1016/S0140-6736(06)68967-8
- Yancik R, Wesley MN, Ries LA, Havlik RJ, Long S, Edwards BK, et al. Comorbidity and age as predictors of risk for early mortality of male and female colon carcinoma patients: a population-based study. *Cancer* 1998; **11**: 2123-34. PMID: 9610691

21. Davila JA, Rabeneck L, Berger DH, El-Serag HB. Postoperative 30-day mortality following surgical resection for colorectal cancer in veterans: changes in the right direction. *Dig Dis Sci* 2005; **9**: 1722-8. doi: 10.1007/s10620-005-2925-x
22. Jullumstrø E, Kollind M, Lydersen S, Edna TH. Diabetes mellitus and outcomes of colorectal cancer. *Acta Oncol* 2009; **3**: 361-7. doi: 10.1080/02841860802637765
23. Gorenc M, Kozjek NR, Stojan P. Malnutrition and cachexia in patients with head and neck cancer treated with (chemo)radiotherapy. *Rep Pract Oncol Radiother* 2015; **4**: 249-58. doi: 10.1016/j.rpor.2015.03.001
24. Perpar A, Breclj E, Kozjek NR, Anderluh F, Oblak I, Vidmar MS, Velenik V. Mesenteric ischemia after capecitabine treatment in rectal cancer and resultant short bowel syndrome is not an absolute contraindication for radical oncological treatment. *Radiol Oncol* 2015; **2**: 181-4. doi: 10.2478/raon-2014-0024
25. Thibault R, Makhoul AM, Mulliez A, Cristina Gonzalez M, Kekstas G, Kozjek NR, et al. Fat-free mass at admission predicts 28-day mortality in intensive care unit patients: the international prospective observational study Phase Angle Project. *Intensive Care Med* 2016; **9**: 1445-53. doi: 10.1007/s00134-016-4468-3
26. Jeon JY, Jeong DH, Park MG, Lee JW, Chu SH, Park JH, et al. Impact of diabetes on oncologic outcome of colorectal cancer patients: colon vs. rectal cancer. *PLoS One* 2013; **2**: e55196. doi: 10.1371/journal.pone.0055196
27. Meyerhardt JA, Catalano PJ, Haller DG, Mayer RJ, Macdonald JS, Benson AB 3rd, et al. Impact of diabetes mellitus on outcomes in patients with colon cancer. *J Clin Oncol* 2003; **3**: 433-40. doi: 10.1200/JCO.2003.07.125
28. Huang YC, Lin JK, Chen WS, Lin TC, Yang SH, Jiang JK, et al. Diabetes mellitus negatively impacts survival of patients with colon cancer, particularly in stage II disease. *J Cancer Res Clin Oncol* 2011; **2**: 211-20. doi: 10.1007/s00432-010-0879-7
29. Shonka NA, Anderson JR, Panwalkar AW, Reed EC, Steen PD, Ganti AK. Effect of diabetes mellitus on the epidemiology and outcomes of colon cancer. *Med Oncol* 2006; **4**: 515-9. doi: 10.1385/MO:23:4:515

Impact of perioperative treatment on survival of resectable gastric cancer patients after D2 lymphadenectomy: a single European centre propensity score matching analysis

Tomaz Jagric¹, Bojan Iljavec¹, Vaneja Velenik², Janja Ocvirk², Stojan Potrc¹

¹ Department for Abdominal and General Surgery, University Clinical Centre Maribor, Maribor, Slovenia

² Institute of Oncology Ljubljana, Ljubljana, Slovenia

Radiol Oncol 2019; 53(2): 245-255.

Received 12 December 2018

Accepted 24 February 2019

Correspondence to: Tomaž Jagrič, M.D., Ph.D., Department for Abdominal and General Surgery, University Clinical Centre Maribor, Ljubljanska ulica 5, 2000 Maribor, Slovenia. Phone: +386-23211301; Fax: +386-23211262; E-mail: tomaz.jagric@gmail.com

Disclosure: No potential conflicts of interest were disclosed.

Background. To determine the effects of perioperative treatment of gastric cancer patients, we conducted an analysis with propensity score matched patient groups to determine the role of perioperative chemotherapy in patients after D2 lymphadenectomy.

Patients and methods. From our database of 1563 patients, 482 patients were selected with propensity score matching and divided into two balanced groups: 241 patients in the surgery only group and 241 patients in the perioperative group. The long-term results of treatment were compared between the two groups.

Results. Most of the included patients received radio-chemotherapy with capecitabine ($n = 111$; 46%) and perioperative chemotherapy with epirubicin, oxaliplatin and capecitabine ($n = 91$; 37.7%). 92.9% of the patients received a D2 lymph node dissection. Perioperative morbidity was similar between surgery only (18.3%) and perioperative treatment groups (20.7%) ($p = 0.537$). The perioperative mortality was not influenced by perioperative treatment. A pathological response was observed in 12.5% of patients. The overall 5-year and median survivals were significantly higher in the perioperative treatment group (50.5%; 51.7 months) compared to surgery only group (41.8%; 34.9 months; $p = 0.038$). The subgroup analysis revealed that only patients with the TNM stages T3 ($p = 0.028$), N2 ($p = 0.009$), N3b ($p = 0.043$), and UICC stages IIIb ($p = 0.003$) and IIIc ($p = 0.03$) significantly benefit from perioperative treatment.

Conclusions. Perioperative treatment in radically resected gastric cancer patients after D2 lymphadenectomy was beneficial in stages IIIb and IIIc. The effects of perioperative treatment in lower stages could be negated by the effects of the radical surgery in lower stages and in higher stages by the biology of the disease.

Key words: perioperative treatment; gastric cancer; D2 lymphadenectomy; propensity score matching

Introduction

Multimodal treatment has long been established as the only way to prolong the poor survival of patients with advanced gastric cancer.¹⁻¹³ With this therapy, long term survival has increased from 38% to 70%.¹⁻¹³ Chemotherapy is now a solid part of gastric cancer treatment guidelines, but there is still much debate on which regimen should be used, the time and duration of chemotherapy.^{1,2}

Before INT0116 trial, gastric cancer was supposed to be chemoresistant. The INT0116 trial was one of the first trials that established the adjuvant chemoradiotherapy.^{1,2,14} The study influenced the treatment in Northern America.^{1,2} Although it clearly demonstrated the effectiveness of the chemoradiotherapy in gastric cancer, the major concern was that it was carried out on patients with suboptimal lymphadenectomy.^{1,2} It is now accepted that this protocol improves survival in suboptimal oper-

ated patients.^{1,2} In the following years, the ACST-GC trial, and later the Sakato's trial conducted in Japan, proved beyond any doubt that adjuvant treatment can improve survival even in patients after adequate lymphadenectomy.⁶ But the results from FLAGS trial showed that the tolerance of S1 agent in Caucasian population was poor, and only a fraction of patients with esophago-gastric junction were included.² Meanwhile, in Europe the results of the MAGIC trial proved the efficiency of perioperative chemotherapy.³ Nonetheless, a sufficient lymph node dissection was performed only in 40% of patients and only 40% of patients could successfully end all postoperative cycles. In spite of the important results, there are still many trials that try to determine the best chemotherapy timing in adequate operated patients.³

In our institution, patients have been operated according to Japanese guidelines since 1992.¹⁵ We started to use the perioperative treatment in 2003. Theoretically, the study of patients from single institution where only five dedicated surgeons perform a standardised operation provides a homogenous group on which one could easily determine the beneficial effects of (perioperative and adjuvant) chemotherapy. Therefore, we conducted an analysis with propensity score matched patients to determine the role of perioperative and adjuvant chemotherapy in patients after D2 lymphadenectomy.

Patients and methods

Patients

Since 1991, 1563 patients were operated for gastric cancer in the department for Abdominal and General Surgery at the University Clinical Centre Maribor, Slovenia. The demographic characteristics of patients, the characteristics of the surgical procedures, and the pathological characteristics of tumours were prospectively stored on a computer database. The bone marrow, renal and hepatic functions are important determinants of chemotherapeutic treatment, those factors were not routinely stored in our database. Although this might have brought a certain bias into the analysis that is inherent to retrospective studies, we assumed that unfit patients would not have been operated in the first place. Since 1991 there have been several revisions of the The Union for International Cancer Control Tumour Node Metastases classification (UICC TNM) classification. We have therefore been regularly updating the TNM classification to con-

cur with the most current issue of the UICC TNM classification system. The survivals were annually updated with the data from the National Cancer Registry of Slovenia to obtain the most accurate survival data and to avoid losing any patient during follow-up. The perioperative treatment of gastric cancer patients was adopted based on the published results of the MAGIC trial from the year 2003.¹⁴ At first, patients were treated with the 5FU-LV (5-Fluorouracil-Leucovorin) protocol; but shortly after the results of the OE trial, this protocol was replaced with other chemotherapy regimens that are better tolerated by the patients.¹¹ Now, the most used chemotherapy regimens are epirubicin, oxaliplatin and capecitabine. More than half of patients in whom perioperative treatment was instituted received one of the formal chemotherapy regimens. To determine the efficiency of perioperative and adjuvant chemotherapy in patients from a European centre after formal D2 lymph node dissection, the prospectively stored data from our patients was used. For propensity score matching, only patients with histologically verified adenocarcinoma were included. Furthermore, only patients with a R0 resection were included in the study. Patients with a metastatic disease at presentation were excluded from the study. After exclusion, 1156 patients were used for propensity score matching. Age, tumour site, complication stage according to Dindo-Claviere classification, UICC stage and the TNM nodal stage were determined to be the significant covariates for perioperative and adjuvant chemotherapy with logistic regression. Based on these covariates, a propensity score was calculated for each patient. Patients were randomised and paired with the nearest score matching protocol. In the final group, 482 patients remained. These were used for further analysis.

The study was conducted according to the ethical directives of the Helsinki declaration. All of the patients gave their informed consent before treatment. All of the patient data was stored prospectively in the hospital database, and the study was approved by local Ethics Committee.

Treatment

The eligibility criteria for perioperative treatment were as follows: Resected gastric cancer stage IIA or higher and no distant metastases. Patients with IB gastric cancer were reviewed at tumour board for consideration of perioperative and adjuvant therapy. Further eligibility criteria were age 18 years or older, Eastern Cooperative Oncology

Group (ECOG) 0 to 1, and adequate hepatic, renal, marrow and cardiac function. Patients with a history of recent myocardial ischaemia, uncontrolled angina, hypertension, cardiac arrhythmias, congestive heart failure, or other serious medical illness were taken under review from the tumour board. The exclusion criteria for perioperative and adjuvant treatment were as follows: Stage IA or IB (T2aN0) disease, microscopically positive resection margins, and involvement of M1 lymph node or distant metastases. Severe renal impairment (calculated creatinine clearance less than 30 mL/min) suspected dihydropyrimidine dehydrogenase (DPD) deficiency.

Perioperative and adjuvant treatment was administered as described elsewhere.¹⁶ In brief; patients received one of the following perioperative protocols: capecitabine, EOX (epirubicin, oxaliplatin, capecitabine), XELOX (capecitabine, oxaliplatin). Patients subjected to EOX regimen received intravenous bolus of epirubicin at a dose of 50 mg per square meter, oxaliplatin at a dose of 130 mg per square meter and capecitabine at a dose of 1000 mg per square meter twice a day. Treatment was repeated every 3 weeks for maximum of six cycles. The XELOX regimen consisted of eight 3-week cycles of oral capecitabine 1000 mg per square meter twice a day on days 1 to 14 of each cycle and intravenous oxaliplatin 130 mg per square meter on day one of each cycle. Adjuvant treatment with capecitabine was initiated within 6–8 weeks after surgery and consisted of concomitantly applied chemo- and radiotherapy. Chemotherapy started with peroral capecitabine 1250 mg/m² twice a day (bid) on days 1–14, with a one-week break. Concurrently with irradiation, continuous capecitabine 825 mg/m² bid was administered, without weekend breaks. After the completion of radiotherapy with two-week break, the patients received three more cycles of capecitabine 1250 mg/m² bid on days 1–14, with a one-week break between each cycle. Patients were irradiated on linear accelerator with 15 MV photon beams for five days per week, at a daily dose of 1.8 Gy.¹⁶ A minority of patients received either 5-fluorouracil (5FU) and cisplatin or paclitaxel and docetaxel regimen. Patients received 75 to 1000 mg cisplatin per square meter as intravenous infusion on day one and 29 in the 5FU-CP (5-fluorouracil and cisplatin) group, and 750 to 1000 mg per square meter as continuous infusion over 24 hours on days one to 4 and 29 to 32 in the 5FU. Patients were irradiated on linear accelerator with 15 MV photon beams for five days per week, at a daily dose of 1.8 Gy.¹⁶ In the paclitaxel and docetaxel

group, patients received 135 to 250 mg paclitaxel per square meter as intravenous infusion every 21 days and 75 to 100 mg docetaxel per square meter as continuous infusion every 21 days.

Gastric cancer surgery in our institution is performed by five dedicated gastric cancer surgeons. These surgeons follow the Japanese Gastric Cancer guidelines (JGCC). In well differentiated cancers located in the distal third of the stomach, for the proximal border a two to three cm safety margin from the palpable tumour edge is used. In these patients, a distal subtotal gastrectomy is performed, with the distal margin at least 1.5 cm distal to pylorus. In moderately and poor differentiated tumours, a wider resection margin of four to six cm is used. In these patients, a total gastrectomy is usually performed. In patients with middle third gastric cancer, a total gastrectomy is performed. In proximal third tumours and tumours of the esophago-gastric junction Siewert II and Siewert III classification, a trans-hiatal extended total gastrectomy and distal esophagectomy or a proximal gastrectomy are performed. A pancreas preserving D2 lymphadenectomy is always performed. According to guidelines, the lymph node stations 1, 3, 4, 5, 6, 7, 8, 9, 11p and 12 are removed during a distal subtotal gastrectomy. During a total gastrectomy, the lymph node stations 1 to 12 and the left paraaortic lymph nodes are dissected. Additionally to formal lymph node stations, periesophageal lower and middle lymph nodes are dissected (lymph node stations 110 and 111) in transhiatally extended resections. The pancreatic tail is resected only if direct invasion from the tumour is present. Similarly, a splenectomy is performed only if direct invasion is present or if injury to the spleen should occur during the operation. It has been long established that splenectomy does not have an impact on long-term survival nor is splenectomy with gastrectomy considered multivisceral resection.¹⁷ These operations were therefore considered simple resections with D2 lymphadenectomy.

Propensity score matching

Patients in the surgery only and perioperative and adjuvant treatment groups were matched using the propensity score method as described by Rosenbaum and Rubin.^{18,19} First, the correlations between different covariates and the likelihood receiving perioperative and adjuvant treatment were analysed. The propensity score for an individual was calculated on the given covariates of preoperative serum haemoglobin levels, distal

resection border, lymphocyte infiltration and the TNM N stage using the multivariate logistic regression model. Because radically resected gastric cancer patients in whom D2 lymphadenectomy was performed were included in the study, lymph node dissection and resection margins were not considered as a covariates in the propensity score derivation model. Using the propensity scores, 241 surgery only patients were individually matched to 241 patients who received perioperative and adjuvant treatment using the technique of the nearest available score matching. This method consists of randomly ordering the case and control subjects, then selecting the first case subject and finding the control subject with the closest propensity score. Both subjects are then manually removed from the consideration for matching and the next case subject is selected.

Follow-up

Follow-up was carried out by surgeons and oncologists. Patients underwent regular clinical assessments and laboratory testing with tumour marker determination (CEA, Ca 19-9, and Ca 72-4 from the year 2012) and abdominal ultrasound every three months for the first two years, then every six months for three years, and yearly afterwards until death. After one year, every patient had a routine upper gastro-intestinal endoscopy and chest X-ray. In case of recurrence suspicion, additional computer tomography imaging or positron emission computer tomography was performed. Barium studies were performed in case of dysphagia.

The presence of a relapse was determined by means of imaging studies, including computer tomography, or in doubtful and inconclusive cases after negative computer tomography in patients with elevated tumour markers or high suspicion for recurrence, positron emission tomography or magnetic resonance imaging was performed. If a recurrence was detected, the patient was discussed on a tumour board to determine whether a palliative surgical procedure, palliative oncological treatment, or best supportive care should be recommended for the patient.

Outcomes

Primary end-point of the analysis was the 5-year overall survival and the median survival. Survival was defined as the time from the operation to the death from any cause. Secondary end-points of the study were the causes of death, prediction of

response, prediction of the effect of perioperative and adjuvant treatment on perioperative morbidity and mortality, and the analysis of the tumour recurrence sites. Other secondary end-points were the correlations between disease recurrence and tumour TNM stage.

Statistical analysis

Based on the results of the MAGIC trial, a 5-year survival in the perioperative and adjuvant chemotherapy group was expected to be 50% and 35% in the surgery only group. To achieve a statistical power of 80% to detect an effect at α level of 5%, at least 161 patients were needed in each group. Continuous variables were expressed as mean \pm SD and categorical variables as percentage. Continuous variables were compared with Student's t-test for normally distributed variables; nonparametric variables were tested with Mann-Whitney's U-test. Normality was tested with means of Q-Q plots. The correlations between variables were tested with Pearson's bivariate correlation test, Chi square test and Student's t-test. Variables above the threshold p value of 0.1 were included for multivariate analysis. The Cox regression model was used for primary analysis and included covariates that had a p value of more than 0.1 in univariate analysis. Estimates of treatment effect were expressed as hazard ratios with 95% confidence interval. Kaplan-Meier curves were constructed to determine time-to-event end-points. Differences in survivals between groups were determined with the Log-rank and Breslow tests. P value of > 0.05 was selected as the level of significance. All statistical analyses were performed on SPSS for Windows 10 v. 22 (IBM).

Results

Four hundred eighty-two patients operated between years 1991 and 2018 were included in the study. Half of the patients ($n = 241$) were treated with surgery only, while the other half of the included patients ($n = 241$) received perioperative radio-chemotherapy/chemotherapy and adjuvant chemotherapy. Patient demographic and tumour characteristics were well balanced between the two groups (Table 1).

Since 2003, when perioperative and adjuvant treatment became the standard for gastric cancer patients, different types of chemotherapy regimens were used. However, the main bulk of included

TABLE 1. Clinicopathological characteristics of the gastric cancer patients

Clinicopathological characteristic	All patients	Surgery only	Perioperative and adjuvant treatment	P
	(n = 482)	(n = 241)	(n = 241)	
Age [years ± SD]	62.2 ± 11.2	62.02 ± 12.3	62.35 ± 9.9	NS
Gender [n(%)]				NS
Male	322 (66.8)	153 (63.5)	169 (70.1)	
Female	160 (33.2)	88 (36.5)	72 (29.9)	
Type of chemotherapy [n (%)]*			Capecitabine 111(46) EOX 91(37.7) XELOX 16(6.6) 5FU/CP 19(7.9) 5FULV 3(1.2) Paclitaxel+CP 1(0.4)	
Tumor site				
Distal third	151 (31.3)	75 (31.1)	76 (31.5)	NS
Middle third	226 (46.9)	113 (46.9)	113 (46.9)	
Proximal third	85 (17.6)	38 (15.8)	47 (19.5)	
Whole stomach	11 (2.3)	7 (2.9)	4 (1.7)	
Stump	9 (1.9)	8 (3.3)	1 (0.4)	
ASA score [n (%)]				0.044
I	188 (39)	90 (37.3)	98 (40.7)	
II	239 (49.6)	113 (46.9)	126 (52.3)	
III	55 (11.4)	38 (15.8)	17 (7.1)	
T stage [n (%)]				NS
T0	6 (1.2)	2 (0.8)	4 (1.7)	
T1	62 (12.9)	36 (14.9)	26 (10.8)	
T2	75 (15.6)	35 (14.5)	40 (16.6)	
T3	266 (55.2)	138 (57.3)	128 (53.1)	
T4	73 (15.1)	30 (12.4)	43 (17.8)	
N stage [n (%)]				NS
N0	158 (32.8)	86 (35.7)	72 (29.9)	
N1	82 (17)	31 (12.9)	51 (21.2)	
N2	97 (20.1)	42 (17.4)	55 (22.8)	
N3a	89 (18.5)	53 (22)	36 (14.9)	
N3b	56 (11.6)	29 (12)	27 (11.2)	
UICC stage [n (%)]				
0	8 (8)	1 (0.4)	3 (1.2)	NS
Ia	54 (11.2)	35 (14.5)	19 (7.9)	
Ib	35 (7.3)	16 (6.6)	19 (7.9)	
IIa	73 (15.1)	36 (14.9)	37 (15.4)	
IIb	83 (17.2)	30 (12.4)	53 (22)	
IIc	2 (0.4)	2 (0.8)	0 (0)	
IIIa	94 (19.5)	44 (18.3)	50 (20.7)	
IIIb	79 (16.4)	47 (19.5)	32 (13.3)	
IIIc	57 (11.8)	30 (12.4)	27 (11.2)	
IV	1 (0.2)	0 (0)	1 (0.4)	
Clavien-Dindo classification [n (%)]				NS
0	388 (80.5)	197 (81.7)	191 (79.3)	
I	0 (0.0)	0 (0)	0 (0)	
II	44 (9.1)	14 (5.8)	30 (12.4)	
IIIa	10 (2.1)	3 (1.2)	7 (2.9)	
IIIb	27 (5.6)	16 (6.6)	11 (4.6)	
IV	0 (0)	0 (0)	0 (0)	
V	13 (2.7)	11 (4.6)	2 (0.8)	
Number of extracted LNs [n ± SD]	25.6 ± 13.1	24.9 ± 13.5	26.3 ± 12.6	NS
Number of positive LNs [n ± SD]	6.2 ± 9.3	6.8 ± 10.5	5.6 ± 8	NS
Tumour diameter [mm ± SD]	59.4 ± 35.8	61.4 ± 38.6	57.6 ± 33.3	NS
CEA [µg/l ± SD]	5 ± 14.5	4.25 ± 10.9	5.7 ± 16.9	NS
CA 19-9 [µU/l ± SD]	135.1 ± 799.5	66.8 ± 287.8	189.9 ± 1037.3	NS
Perioperative morbidity [%]	9 (33.3)	2 (28.6)	7 (35)	NS
Mortality [%]	0 (0)	0 (0)	0 (0)	NS

** = significance was not determined, because only one group received chemotherapy; ASA = American Society of Anesthesiologists; EOX = Epirubicin, Oxaliplatin, Capecitabine; LN = lymph nodes. NS = no significant difference between surgical procedures; UICC = The Union for International Cancer Control Tumour Node Metastases classification; XELOX = capecitabine, oxaliplatin; 5FU/CP = 5-fluorouracil and cisplatin; paclitaxel+CP = paclitaxel and cisplatin; 5FULV = 5-fluorouracil and leucovorin

patients received only two types of treatment: [i] radio-chemotherapy with capecitabine (n = 111; 46%); and [ii] perioperative chemotherapy with epirubicin, oxaliplatin and capecitabine (n = 91; 37.7%). The remaining types of chemotherapy or radio-chemotherapy regimens were applied only in less than 20% (Table 1). The perioperative treatment was completed in 71% of cases. Only 22.8% of perioperatively patients reported complications associated with their chemotherapy regimen. After preoperative treatment, 76.3% of patients proceeded to surgery and received adjuvant treatment. From these patients (n = 184), 93% completed the adjuvant treatment, with 7% patients who did not complete treatment because of location, size, depth of invasion, Lauren type, chemotherapy toxicity, poor general condition, tumour progression and noncompliance.

After preoperative chemotherapy/radio-chemotherapy, patients proceeded to surgery. A curative resection was achieved in all cases. The type of resection was dependant on the tumour; 46.9%), total gastrectomy was performed in the majority of patients (n = 331; 64.5%). The second most prominent tumour location was the distal third of the stomach (n = 151; 31.3%). From 85 patients (17.6%) with the tumour in the proximal third, a transhiatally extended total gastrectomy with resection of the distal esophagus had to be performed in 48 patients (10%). In our hospital, all patients, excluding those with early gastric cancer, are treated with extensive D2 lymphadenectomy with the preservation of the pancreatic tail and spleen. From the included patients in this study, 92.9% received a D2 lymph node dissection. Perioperative complications occurred in 94 patients (19.5%). According to Claviene-Dindo classification, 9.1% (n = 44) were grade II, 2.1% (n = 10) were grade IIIa, and 5.6% (n = 27) were grade IIIb. The cumulative perioperative mortality was 1.2%.

Perioperative morbidity was similar between surgery only (18.3%) and perioperative and adjuvant treatment group (20.7%) (p = 0.537). Although patients treated with perioperative radio-chemotherapy/chemotherapy had more grade II complications (12.4% in the perioperative and adjuvant group *vs.* 5.8% in the surgery group), and patients in the surgery only group had more grade IIIb complications (4.6% in the perioperative and adjuvant group *vs.* 6.6% in the surgery group), there was no significant difference in the distribution of the grade of complications between both groups (p = 0.537) (Table 1). Surgical and general complications were also equally distributed in both groups

(Table 1). The perioperative mortality in the surgery only group was 2.2% and 0.4% in the perioperative and adjuvant treatment group.

The pathological characteristics of the tumour were balanced between groups (Table 1). Most of the tumours were poorly differentiated (55.9% in surgery only *vs.* 53.2% in the perioperative and adjuvant treatment group; p = 0.696), intestinal type (44.9% surgery only *vs.* 51.6%; p = 0.644), without lymphocyte infiltration, vascular invasion, extranodal invasion and with perineural invasion (Table 1). The UICC and TNM stage distribution was similar between both groups (Table 1). Most of the patients had either IIb stage (13.2% in surgery only *vs.* 22% in perioperative and adjuvant group) or IIIb stage (18.3% in surgery only *vs.* 20.7% in perioperative and adjuvant treatment group; p = 0.954). The depth of invasion was mostly into subserosal layer in both groups (57.3% surgery only *vs.* 53.1% perioperative and adjuvant treatment group; p = 0.254), and only a third of the patients had a node negative disease (Table 1). Pathological response was estimated based on the number of patients with a complete response and patients with T1 tumours. Since patients with T1 tumours were not eligible for perioperative treatment, we assumed that higher stage tumours were downsized to T1 stage. A complete pathological response was observed in 1.7% of patients in the perioperative and adjuvant treatment group and 10.8% of patients had a partial response. Counted together, a downsizing was achieved in 12.5% of patients. The mean number of extracted lymph nodes per operation was balanced between groups (surgery only: 24.9±13.5 lymph nodes per operation *vs.* perioperative and adjuvant therapy group: 26.3±12.6 lymph nodes per operation; p = 0.252).

After a mean follow-up of 50.6 months (95% CI: 45.4–55.8), 55% (n = 132) of patients in the surgery only and 49.6% (n = 119) in the perioperative and adjuvant treatment group had died. In 23 (9.2% of the diseased patients) diseased patients, an autopsy was performed to determine the cause of death. Causes of death for these patients are listed in Table 1. The most common recurrence site in the autopsied patients was the peritoneal cavity (52%), followed by haematogenous spread (47%). The most common sites of hemathogenic recurrence were liver, lungs, adrenal glands and bone metastases listed in descending frequency (Table 2). Though the recurrence was determined only in 9.2% of diseased patients, we believe that the distribution of recurrence site in this group mirrors the actual recurrence sites in the 251 diseased patients.

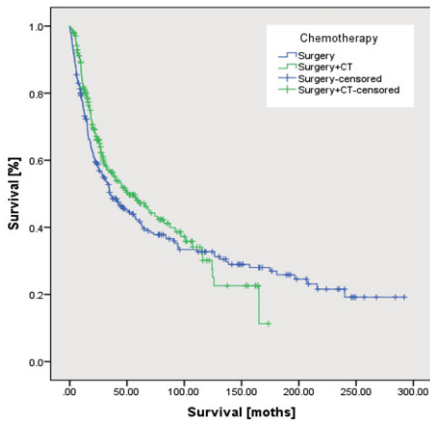


FIGURE 1. Overall survival of patients in Surgery compared to Surgery with chemotherapy group.

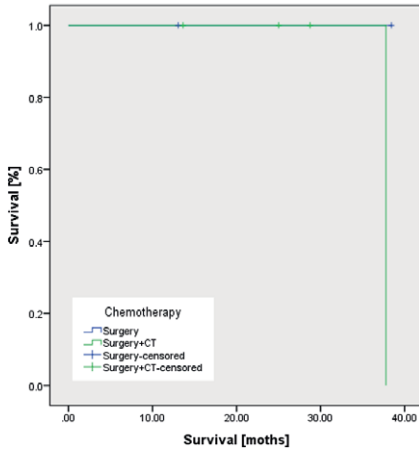
Surgery+CT = surgery with chemotherapy group

TABLE 2. Recorded recurrence patterns for T and N stage

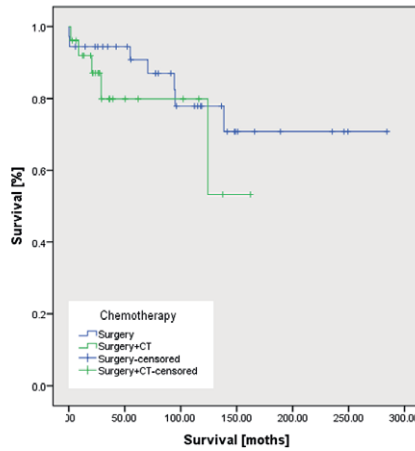
	Peritoneal carcinomatosis [n (%)]	Haemathogenous spread [n (%)]	P
T stage			
T1	0 (0)	0 (0)	0.019
T2	1 (8.3)	4 (36.4)	
T3	5 (41.7)	6 (54.5)	
T4	6 (50)	1 (9.1)	
N stage			
N0	2 (16.7)	1 (9.1)	NS
N1	1 (8.3)	2 (18.2)	
N2	3 (25)	6 (54.5)	
N3a	4 (33.3)	1 (9.1)	
N3b	2 (16.7)	1 (9.1)	

NS = non-significant

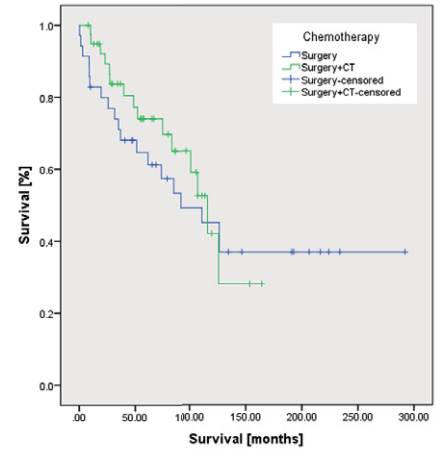
Stage pT0



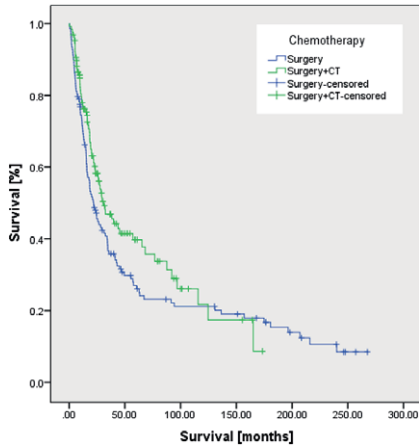
Stage pT1



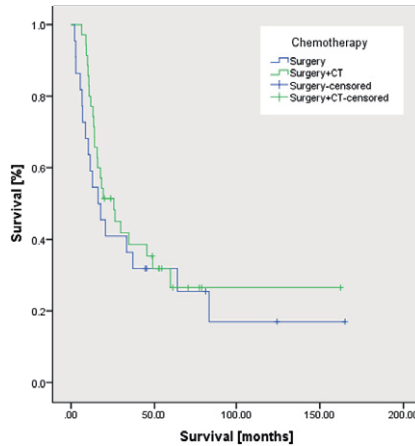
Stage pT2



Stage pT3



Stage pT4a



Stage pT4b

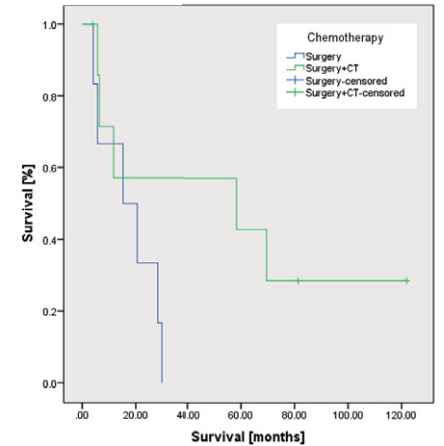


FIGURE 2. Overall survival of patients in Surgery compared to Surgery with chemotherapy group in different TNM T stages.

Surgery+CT: surgery with chemotherapy

TABLE 3. Predictors of survival

	Significance	HR	95.0% CI for HR	
			Lower	Upper
Age	0.000	1.024	1.011	1.037
CA 19-9	0.016	1.000	1.000	1.000
UICC stage	0.000	2.147	1.677	2.748
Positive lymph nodes	0.000	1.030	1.017	1.044
Perioperative therapy	0.032	0.741	0.563	0.975

HR = hazard ratio

The overall survival was significantly higher in the perioperative and adjuvant treatment group ($p = 0.038$) (Figure 1). The median survival in the surgery only group was 34.9 months compared to 51.7 months in the perioperative and adjuvant treatment group. The overall 5-year survival was 41.8% in the surgery only and 50.5% in the perioperative and adjuvant treatment group. The subgroup analysis

revealed that only patients with the TNM stages T3 ($p = 0.028$) (Figure 2), N2 ($p = 0.009$) (Figure 3), N3b ($p = 0.043$) significantly benefit from perioperative and adjuvant treatment (Figure 3). For UICC stages survival analysis revealed significance for IIIa ($p = 0.003$) and IIIc ($p = 0.03$) but not for IIIb.

The multivariate analysis identified age, tumour marker Ca 19-9, UICC stage, number of positive lymph nodes and perioperative and adjuvant treatment as significant predictors (Table 3). Patients who received perioperative and adjuvant treatment had HR 0.741 (95% CI: 0.563–0.975) compared to patients in the surgery only group.

Discussion

The long-term results of the Dutch trial and more recently the results of the prospective randomised Taipei trial clearly confirmed the benefits of D2 lymphadenectomy in gastric cancer treatment.^{20,21}

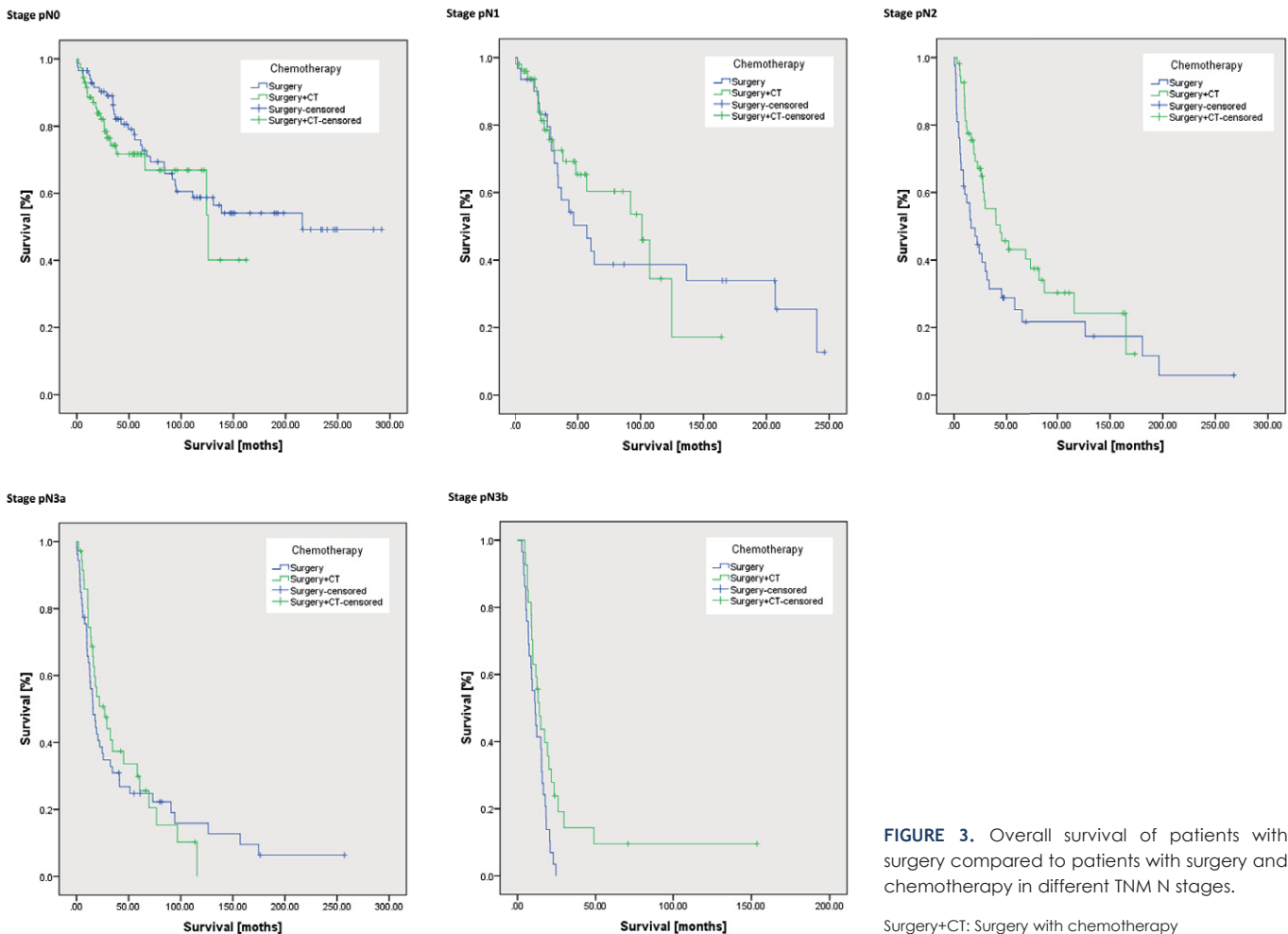


FIGURE 3. Overall survival of patients with surgery compared to patients with surgery and chemotherapy in different TNM N stages.

Surgery+CT: Surgery with chemotherapy

In order to evaluate the effects of any adjuvant treatment in an intention to treat cohort, the results should only be evaluated in the light of a standardised extensive surgery. In the present study, we compared the results of radically resected gastric cancer patients with a D2 lymphadenectomy from single European centre to their propensity score matched counterparts treated with perioperative radio-chemotherapy or chemotherapy.

In our centre, D2 lymphadenectomy is considered standard treatment. To ensure a high level of surgical quality, gastric cancer patients are treated by a group of five specialised surgeons. The included patients in the present study had a D2 lymphadenectomy performed in 92.9%, which is comparable to trials conducted in the East. The proportion of D2 lymphadenectomy resections in CLASSIC, ACTS-GS, ARTIST trials were 93% to 100%.^{6,13} The number of D2 lymphadenectomy procedures in our study was superior to the majority of Western studies. The proportion of D2 resection was less than 10% in the MacDonald trial, while less than 40% of patients in the MAGIC and FNCLCC study had a D2 lymphadenectomy.^{4,5,14} Even in a more recent European study ITACA-S, where the D2 lymph node dissection was the main goal of the study, a D2 lymphadenectomy was performed in 72%.¹²

The results in our analysis show the additional value of chemotherapy. The sufficient lymph node dissection allowed to evaluate the effect of multimodal treatment after D2 lymphadenectomy. Since 2003, when perioperative and adjuvant treatment was established for gastric cancer, many chemotherapy protocols were used; however, two types of perioperative and adjuvant treatment protocols dominated: perioperative radio-chemotherapy with capecitabine, and perioperative chemotherapy with epirubicin, oxaliplatin and capecitabine. While the latter protocols have recently been replaced by the FLOT (fluorouracil, leucovorin, oxaliplatin, docetaxel) protocol, the EOX and capecitabine protocols were applied in more than half of patients in the present study, with the remaining protocols being used in less than 10%. Therefore, the results mainly apply to EOX and capecitabine treatment. We could show that the tolerance to these two treatments was very high. From the patients that received neoadjuvant treatment, 76.3% proceeded to surgery. From the patients who received adjuvant treatment, 93% completed the therapy, while the remaining patients could not complete the treatment because of chemotherapy toxicity, poor general condition, tumour progres-

sion and noncompliance. Therefore, a dropout of only 29% was recorded due to treatment toxicity. These results compare favourably to other trials. MacDonald *et al.* reported a 36% rate of toxicity, while Sakuramoto *et al.* reported that only 65% of patients were able to finish the one-year adjuvant treatment with S1.^{6,14} Most of other studies also report a dropout of 30% to 40%.¹⁻¹² It seems that EOX and capecitabine stood out as excellently tolerated.

One of the rationales for perioperative treatment is the preoperative tumour downsizing and a higher R0 rate. In our study, a response was achieved in 12%. Al-Bosse *et al.* reported response rates of 16% in the FLOT4 trial.¹⁰ Anderson *et al.* reported complete response in 6% of patients, with a downsizing noted in 17% in the MRC OE05 trial.¹¹ In contrast to these studies where node negative patients were also counted as tumour downsizing, these patients were not included in our estimation of tumour downsizing. Hence, we believe that our estimation of tumour downsizing might be an underestimation. Nevertheless, these results are in concordance with other studies that used similar perioperative protocols to ours. These results confirmed that a downsizing of at least 12% can be expected with our perioperative treatment, further increasing the rates of resectability.

While the preoperative effects of radio-chemotherapy/chemotherapy might be undisputed, many opponents of preoperative treatment claim that preoperative treatment could increase perioperative morbidity and mortality due to chemo/radio therapy damaged microcirculation.⁹ In our study, the comparison of perioperative morbidity did not confirm any significant correlation to perioperative treatment. Patients in the perioperative treatment group did not suffer from more surgical complications, nor did they experience more general complications as a result of general fatigue after perioperative treatment. The perioperative mortality in the perioperative group was at 0.4%, even less than in surgery only group (2.2%). These results indicate that the fears from perioperative treatment causing greater morbidity and mortality might be unsubstantiated.

The median survival in the perioperative and adjuvant treatment group was significantly longer than in surgery only group (51.7 months *vs.* 34.9 months; $p = 0.038$). The overall 5-year survival was 50.5% in the perioperative group and 41.8% in the surgery only group. Most of the studies evaluating perioperative treatment similarly support that perioperative and adjuvant treatment prolongs overall and disease survival.¹⁻¹² Our study addi-

tionally confirms that perioperative and adjuvant treatment is beneficial after D2 lymphadenectomy. In the subgroup analysis, we detected a correlation between TNM stage and overall survival. However, the subgroup analysis only confirmed a survival benefit for perioperative and adjuvant treatment in stages T3, N2 and N3b. These results are not surprising, since they clearly point to the effects of D2 lymphadenectomy. Stages N0 to N1 can be completely cured with a radical lymph node dissection of the first and second tier; but once the lymph nodes have spread beyond the second tier, a systemic dissemination is highly likely. Therefore, patients with stages N2 and higher benefit from the addition of systemic treatment. Similar results were published by Zang *et al.* who showed that even the extension of lymphadenectomy beyond the second tier could not increase survival in patients with N3 disease.²² On the other hand, tumours that spread beyond the *serosal* layer (T4a and T4b) disseminate by direct shedding of tumour cells into peritoneal cavity. This is supported by the recurrence patterns in our autopsied patient cohort (Table 3). Patients with T1 to T3 tumours mainly recurred with haematogenous spread, while T4a and T4b predominantly recurred in the peritoneal cavity. The effects of perioperative treatment were negated by the higher rate of intraperitoneal recurrence in stages T4a and T4b. It has been shown in the ACTS-GS trial that capecitabine or epirubicin, oxaliplatin and capecitabine cannot prevent the intraperitoneal recurrence.² We have made the same observations that the regimens containing capecitabine or epirubicin, oxaliplatin and capecitabine are ineffective in patients with stages T4a and T4b where peritoneal recurrence is more prevalent.

The main limitation of our study is its retrospective nature. Although it was sufficiently powered and balanced with propensity score matching, we still must be cautious when interpreting the results. Although patients have been operated by the same group of experienced surgeons, and the surgical strategy and technique did not change since the beginning of the study period, comparison of patients from different time periods inevitably brings a certain bias to the analysis. Another drawback is the use of heterogenic perioperative regimens in our study. It is therefore difficult to determine which regimen has the best effect for D2 operated gastric cancer patients. Perhaps this question should be answered in a future study that will compare the effects of different subgroups of regimens to surgery only control group. Finally, the surgical procedures were performed in a highly specialized

gastric cancer centre with five dedicated surgeons. Therefore, questions could be raised about generalisation of study findings with an extension of these results to other centres with lower caseloads.

In conclusion, our study results support the use of perioperative and adjuvant treatment in radically resected gastric cancer patients after D2 lymphadenectomy in stages IIIa and IIIc. The effects of perioperative and adjuvant treatment could be negated by the effects of the radical surgery in lower stages and by the biology of the disease in higher stages.

References

- Cats A, Jansen EPM, Grieken NCT, Sikorska K, Lind P, Nordmark M, et al. Chemotherapy versus chemoradiotherapy after surgery and preoperative chemotherapy for resectable gastric cancer (CRITICS): an international, open-label, randomised phase 3 trial. *Lancet* 2018; **19**: 616-28. doi: 10.1016/S1470-2045(18)30132-3
- Noh SH, Park SR, Yang HK, Chung HC, Chung IJ, Kim SW, et al. Adjuvant capecitabine plus oxaliplatin for gastric cancer after D2 gastrectomy (CLASSIC): 5-year follow-up of an open-label, randomised phase 3 trial. *Lancet* 2014; **15**: 1389-96. doi: 10.1016/S1470-2045(14)70473-5
- Reece-Smith AM, Saunders JH, Soomro IN, Bowman CR, Duffy JP, Kaye PV, et al. Postoperative survival following perioperative MAGIC versus neoadjuvant OE02-type chemotherapy in oesophageal adenocarcinoma. *Ann R Coll Surg Engl* 2017; **99**: 378-84. doi: 10.1308/rcsann
- Cunningham D, Starling N, Rao S, Iveson T, Nicolson M, Coxon F, et al. Capecitabine and oxaliplatin for advanced esophagogastric cancer. *N Engl J Med* 2008; **358**: 36-46. doi: 10.1056/NEJMoa073149
- Yehou M, Boige V, Pignon JP, Conroy T, Bouche O, Lebreton G, et al. Perioperative chemotherapy compared with surgery alone for resectable gastroesophageal adenocarcinoma: An FNCLCC and FFCD multicentre phase III trial. *J Clin Oncol* 2011; **29**: 1715-21. doi: 10.1200/JCO.2010.33.0597
- Sakuramoto S, Sasako M, Yamaguchi T, Kinoshita T, Fujii M, Nashimoto A, et al. Adjuvant chemotherapy for gastric cancer with S-1, an oral fluoropyrimidine. *N Engl J Med* 2007; **357**: 1810-20. doi: 10.1056/NEJMoa0722
- Nakajima T, Fujii M. What make differences in the outcome in the outcome of adjuvant treatments for resected gastric cancer? *World J Gastroenterol* 2014; **20**: 11567-73. doi: 10.3748/wjg.v20.i33.11567
- Toneto MG, Viola L. Current status of the multidisciplinary treatment of gastric adenocarcinoma. [English, Portuguese]. *Arq Bras Cir Dig* 2018; **31**: 1-4. doi: 10.1590/0102-672020180001e1373
- Chuang J, Gong J, Klempner SJ, Woo Y, Chao J. Refining the management of resectable esophagogastric cancer: FLOT4, CRITICS, OE05, MAGIC-B and the promise of molecular classification. *J Gastrointest Oncol* 2018; **9**: 560-72. doi: 10.21037/jgo.2018.03.01
- Bose K, Franck C, Müller MN, Canbay A, Link A, Venerito M. Perioperative therapy of oesophagogastric adenocarcinoma and future directions. *Gastroenterol Res Pract* 2017; 1-6. doi: 10.1155/2017/5651903
- Alderson D, Cunningham D, Nankivell M, Blazeby JM, Griffin SM, Crellin A. Neoadjuvant cisplatin and fluorouracil versus epirubicin, cisplatin, and capecitabine followed by resection in patients with oesophageal adenocarcinoma (UK MRC OE05): an open-label, randomised phase 3 trial. *Lancet* 2017; **18**: 1249-60. doi: 10.1016/S1470-2045(17)30447-3
- Bajetta E, Floriani I, Di Bartolomeo M, Labianca R, Falcone A, DiCostanzo F, et al. Randomized trial on adjuvant treatment with FOLFIRI followed by docetaxel and cisplatin versus 5-fluorouracil and folinic acid for radically resected gastric cancer. *Ann Oncol* 2014; **25**: 1373-78. doi: 10.1093/annonc/mdl146

13. Park SH, Sohn TS, Lee J, Lim DH, Hong ME, Kim KM, et al. Phase III Trial to compare adjuvant chemotherapy with capecitabine and cisplatin versus concurrent chemoradiotherapy in gastric cancer: final report of the adjuvant chemoradiotherapy in stomach tumors trial, including survival and subset analyses. *J Clin Oncol* 2015; **33**: 3130-3136. doi: 10.1200/JCO.2014.58.3930
14. Macdonald JS, Smalley SR, Benedetti J, Hundahl SA, Estes NC, Stemmermann GN, et al. Chemoradiotherapy after surgery compared with surgery alone for adenocarcinoma of the stomach or gastroesophageal junction. *N Engl J Med* 2001; **345**: 725-30. doi: 10.1056/NEJMoa010187
15. Japanese Gastric Cancer Association. Japanese gastric cancer treatment guidelines 2010 (ver. 3). *Gastric Cancer* 2011; **14**: 113-23. doi: 10.1007/s10120-011-0042-4
16. Oblak I, Skoblar Vidmar M, Anderluh F, Velenik V, Jeromen A, But Hadzic J. Capecitabine in adjuvant radiochemotherapy for gastric adenocarcinoma. *Radiol Oncol* 2014; **48**: 189-96. doi: 10.2478/raon-2013-0065
17. Lee KY, Noh SH, Hyung WJ, Lee JH, Lah KH, Choi SH, et al. Impact of splenectomy for lymph node dissection on long-term outcome in gastric cancer. *Ann Surg Oncol* 2001; **8**: 402-6. PMID: 11407513
18. Rosenbaum PR, Rubin DB. The central role of the propensity score in observational studies for causal effects. *Biometrics* 1983; **70**: 41-55.
19. Li M. Using the propensity score method to estimate causal effects: a review and practical guide. *Organ Res Methods* 2012; **00**: 1-39. doi: 10.1177/1094428112447816
20. Hartgrink HH, van de Velde CJH, Putter H, Bonekamp JJ, Kranenbarg K, Songun I, et al. Extended lymph-node dissection for gastric cancer: who may benefit? Final results of the randomized Dutch Gastric Cancer Group trial. *J Clin Oncol* 2004; **22**: 2069-77. doi: 10.1200/JCO.2004.08.026
21. Wu CW, Hsiung CA, Lo SS, Hsieh MC, Chen JH, Li AFY, et al. Nodal dissection for patients with gastric cancer: a randomized control trial. *Lancet Oncol* 2006; **7**: 309-15. doi: 10.1016/S1470-2045(06)70623-4
22. Zhang Y, Tian S. Does D2 plus para-aortic nodal dissection surgery offer a better survival outcome compared to D2 surgery only for gastric cancer consistently? A definite result based on a hospital population of nearly two decades. *Scand J Surg* 2013; **102**: 251-7. doi: 10.1177/1457496913491343

Impact of body-mass factors on setup displacement during pelvic irradiation in patients with lower abdominal cancer

Wei-Chieh Wu¹, Yi-Ru Chang¹, Yo-Liang Lai¹, An-Cheng Shiau^{1,3,5}, Ji-An Liang^{1,2}, Chun-Ru Chien^{1,2}, Yu-Cheng Kuo¹, Shang-Wen Chen^{1,2,4}

¹ Department of Radiation Oncology, China Medical University Hospital, Taichung, Taiwan

² School of Medicine, College of Medicine, China Medical University, Taichung, Taiwan

³ Department of Biomedical Imaging and Radiological Sciences, China Medical University, Taichung, Taiwan

⁴ School of Medicine, College of Medicine, Taipei Medical University, Taipei, Taiwan

⁵ Department of Biomedical Imaging and Radiological Sciences, National Yang-Ming University, Taipei, Taiwan

Radiol Oncol 2019; 53(2): 256-264.

Received 4 September 2018

Accepted 3 March 2019

Correspondence to: Dr. Shang-Wen Chen, 2nd Yuh-Der Rd, North District, Taichung City, Taiwan. Phone: 886 4 22052121 7450; E-mail: vincent1680616@yahoo.com.tw and An-Cheng Shiau, PhD, Department of Radiation Oncology, China Medical University Hospital, Taichung, Taiwan. E-mail: shiau158@ms22.hinet.net

Disclosure: No potential conflicts of interest were disclosed.

Background. The aim of the study was investigate the impact of body-mass factors (BMF) on setup displacement during pelvic radiotherapy in patients with lower abdominal cancers.

Patients and methods. The clinical data of a training cohort composed of 60 patients with gynecological, rectal, or prostate cancer were analyzed. The daily alignment data from image-guided radiotherapy (IGRT) were retrieved. Setup errors for were assessed by systematic error (SE) and random error (RE) through the superior-inferior (SI), anterior-posterior (AP), and medial-lateral (ML) directions. Several BMFs and patient-related parameters were analyzed with binary logistic regression and receiver-operating characteristic curves. A scoring system was proposed to identify those with greater setup displacement during daily treatment. The results were validated by another cohort.

Results. A large hip lateral diameter correlated with a greater SI-SE and AP-SE, whereas a large umbilical AP diameter correlated with a greater ML-SE and ML-RE. A higher SI-RE was associated with a large hip circumference. The positive predictors for setup uncertainty were chosen to dichotomize patients into groups at high risk and low risk for setup displacement. Based on the scoring system, the adequate treatment margins for the SI direction in the high- and low-risk groups were 5.4 mm and 3.8 mm, whereas those for the ML direction were 8.2 mm and 4.2 mm, respectively. The validated cohort showed a similar trend.

Conclusions. Large BMFs including hip lateral diameter, hip circumference, and umbilical AP diameter are associated with greater setup uncertainty. Based on the scores, IGRT or required treatment margins can be adapted for patients with high risk features.

Key words: body-mass factors; setup displacement; image-guided radiotherapy; lower abdominal cancers

Introduction

Cancers in the lower abdomen, such as prostate, rectal, and gynecological cancers, are common malignancies worldwide.¹ Pelvic irradiation is frequently used in the treatment of these patients. However, acute or chronic gastrointestinal or genitourinary toxicities might jeopardize the treatment

compliance and quality of life in some patients. As a modern technique such as intensity-modulated radiation therapy (IMRT) is capable of dose painting and has been implemented to deliver tumoricidal doses to the target volume while sparing the adjacent normal tissues², setup accuracy is more critical to minimize deviation from the planned target. Currently, treatment alignment is carried out

by lining up skin markers with an equipped laser system. In some circumstances however, the effectiveness of skin alignment might be offset because the exact external position does not always match the internal anatomy accurately. The uncertainties, leading to inadequate dosage to the tumors or untoward toxicities, can be attributed to setup errors or organ motion.

Image-guided radiation therapy (IGRT) using kilo-voltage imaging, and cone beam computed tomography (CBCT) have been widely applied to quantify geometrical uncertainties for daily treatment setup^{3,4}; however, they are not feasible for widespread use due to the increasing treatment time, cost, and daily dose to the patients⁵, the technique and frequency of using IGRT should be adjusted based on the clinical conditions. In some developing countries, not all cancer patients requiring radiotherapy are able to receive adequate treatment.⁶ Particularly, patients who can undergo weekly or daily IGRT were limited even in some institutes where patient load was huge.⁷ In Europe, IGRT was available in only 49% of all linear accelerators.⁸ Therefore, tailored use of IGRT for patients with a high risk of setup displacement is an important issue, particularly in countries or institutions where IGRT resources are limited.

Many studies have reported that greater margins are required for obese patients due to higher setup uncertainties.^{3,4,9-11} However, most studies investigated only the relationship between body mass index (BMI) and the magnitude of setup errors. The impact of patient-related parameters or body-mass factors (BMF) on setup displacement in patients receiving pelvic irradiation remains to be clarified. We hypothesized that the uncertainties can be scored according to the BMFs. Therefore, this study investigated the effect of BMFs on the magnitude of setup displacement during pelvic radiotherapy. As a result, patients with high-risk features or those who requiring large margins between the planning target volume (PTV) and clinical target volume (CTV) can be determined.

Patients and methods

Patient

This study was approved by the local Institutional Review Board (CMUH106-REC3-119).

Patients were divided into two cohorts (60 for training, 30 for validation). In the training cohort, patients with gynecological (cervix or endometrium), rectal, or prostate cancer treated with pelvic

irradiation by daily IGRT between January 2012 and January 2015 at China Medical University Hospital were included. The sample size for gynecological, rectal, and prostate cancers was 20 each. The patient-related parameters and BMFs were retrieved. Staging was based on the staging system (7th edition, 2010).¹² Performance status was assessed according to the Eastern Cooperative Oncology Group criteria. The characteristics for the training cohort are listed in Table 1. Another 30 patients composed of 10 cases of each cancer type were labeled as the validation cohort.

Treatment planning

To minimize setup uncertainties as reported previously^{13,14}, patients were immobilized by a vacuum

TABLE 1. The patient-related parameters and body-mass factors of the training cohort

Parameters	Number	Median	Range
Age (y/o)		64.5	38-90
BW (kg)		61	45.4-99.3
BH (cm)		160.6	142.2-177.3
BMI (kg/m ²)		23.7	17.99-35.69
Umbilical circumference (UC, cm)		87.8	63.4-120.3
Umbilical AP diameter (UAPD, cm)		19.25	13.4-28.6
Umbilical lateral diameter (ULD, cm)		32.6	25-46.4
Hip circumference (HC, cm)		94.7	75-117.8
Hip AP diameter (HAPD, cm)		20.65	17.1-26.8
Hip Lateral diameter (HLD, cm)		35.45	30.6-46.4
CTV circumference (CTVC, cm)		93.45	72.8-118.3
CTV AP diameter (CTVAPD, cm)		20.45	15.1-27.9
CTV lateral diameter (CTVLD, cm)		35.45	27.2-46.5
Cancer	Rectum	20	
	Prostate	20	
	Gynecology	20	
Sex	Female	31	
	Male	29	
ECOG PS	0	29	
	1-2	31	
Surgery	-	46	
	+	14	
CCRT	-	25	
	+	35	

BH = body height; BMI = body mass index; BW = body weight; CCRT = concurrent chemoradiotherapy; CTV = clinical target volume; ECOG PS = Eastern Cooperative Oncology Group performance status;

bag (VacBag, Blessing Cathay Corporation) or alpha cradle (Blessing Cathay) from the chest to the lower pelvis to enhance the accuracy of the daily treatment position. All patients were suggested to defecate before simulation and daily treatment to reduce the organ motion of the rectum.¹³ In addition, patients with prostate cancer were requested to drink a fixed amount of water after emptying the bladder. Computed tomographic (CT) simulation was done with patients in the supine position using a CT scanner (HiSpeed NX/i, GE Healthcare, Florida, USA). The CT images were scanned from the T12 vertebral body to 2 cm below the ischial tuberosities using a slice thickness of 3 mm. External markers were made on the skin using setup lasers to facilitate an accurate daily position.

The CTV was contoured according to the radiotherapy guidelines for each cancer. Generally, the CTV was expanded by 0.7 to 1.5 cm to create the PTV for organ motion and setup errors. All patients underwent IMRT planning using 6 or 10 MV photons. All plans were calculated using a commercial radiation treatment planning system (Eclipse, Varian Medical Systems Inc, Palo Alto, California, USA).

Anthropometric measurements of body-mass factors

The studied BMFs included body weight (BW), body height (BH), BMI, umbilical circumference (UC), umbilical anterior-posterior diameter (UAPD), umbilical lateral diameter (ULD), hip circumference (HC), hip anterior-posterior diameter (HAPD), and hip lateral diameter (HLD). In addition, CTV circumference, CTV anterior-posterior diameter, and CTV lateral diameter were defined at the center of the CTV.

BW and BH were recorded from pretreatment evaluations. The BMI was calculated as the weight in kilograms divided by height in meters squared according to the definition of the World Health Organization.¹⁵ Circumferences and diameters were measured according to the CT images from the simulation. The UC, UAPD, and ULD were calculated at the level of the umbilicus. The HC, HAPD, and HLD were obtained at the top of the femoral head. Generally, BMFs of the hip measured at the top of the femoral head match the widest level of the hip. Representative images for definition of the BMFs are illustrated in Figure 1.

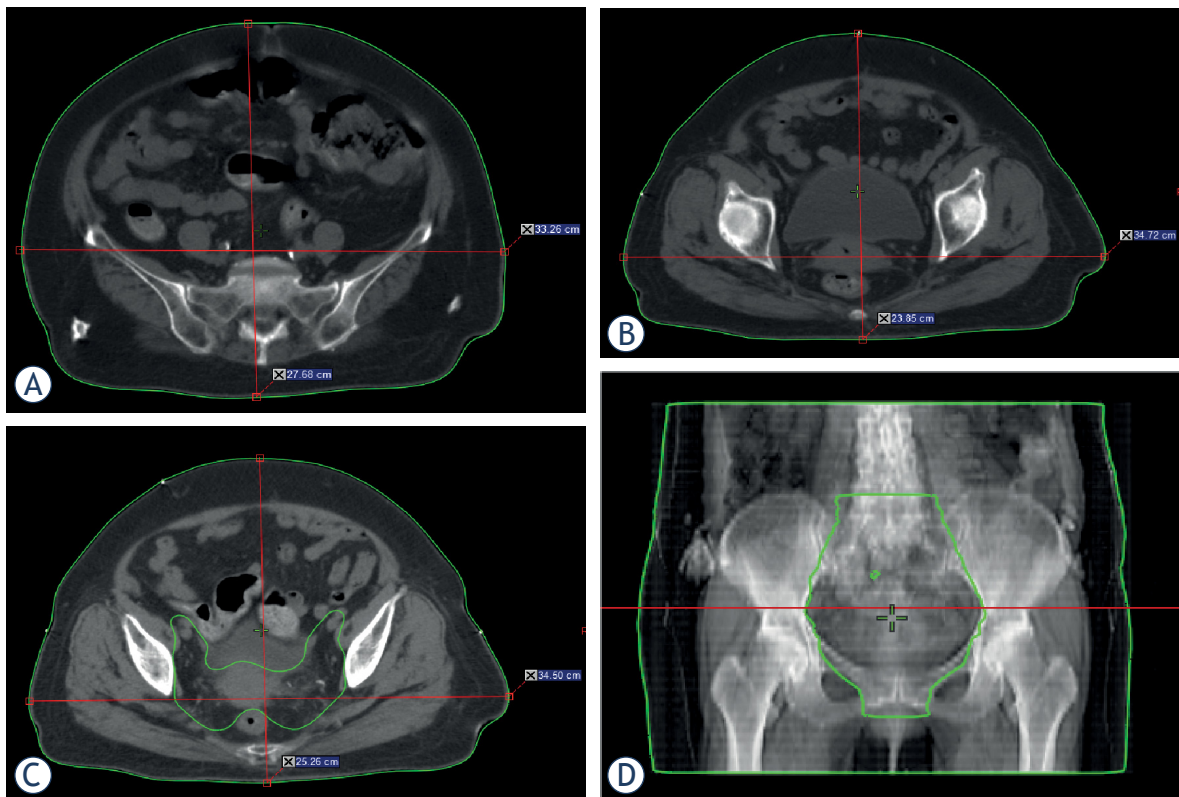


FIGURE 1. An example of body-mass factor measurement in a patient with rectal cancer. (A) umbilical circumference, umbilical anterior-posterior (AP) diameter, umbilical lateral diameter; (B) hip circumference, hip AP diameter, hip Lateral diameter; (C) clinical target volume (CTV) circumference, CTV AP diameter, CTV lateral diameter; (D) level of CTV center.

Daily treatment verification and setup displacement

All patients underwent pelvic radiotherapy with a daily dose of 1.8 Gy. The minimum prescribed dose was 45 Gy in 25 fractions. IGRT was carried out with a Varian Clinac iX linear accelerator (Varian Medical Systems) equipped with on-line on-board imaging (OBI) and CBCT function. Before daily treatment, patients were positioned on the couch according to the alignment markers drawn on the body during the simulation. On-line two-dimensional kilovoltage (kV) images were taken daily or three-dimensional kV CBCT images were obtained weekly to verify the setup accuracy. The images were registered to the digitally reconstructed radiographs from the treatment planning CT images and compared to the planning CT by aligning with the bony landmarks. As a result, the irradiated field could be adjusted by shifting the couch. The quantification of image correction was recorded in the superior-inferior (SI), anterior-posterior (AP), and medial-lateral (ML) directions, and couch rotation (CR). The on-line calibrated images were confirmed by physicians if the displacement of any translational direction was more than 3 mm.

As described previously^{13,16}, setup errors for each patient were assessed by systematic errors (SE) and random errors (RE) through the 4 directions. The mean and standard deviation (SD) of each translational displacement were documented for the individual. The population SE was calculated as the SD of the mean setup correction for each patient. The population RE was determined by calculating the root mean square of the SD of the setup displacement.^{17,18} The margins from the CTV to PTV were calculated via a formula described by Van Herk *et al.*^{19,20}, in which the suggested margin was $2.5 SE + 0.7 RE$ to ensure that the minimum dose to the CTV is 95% for 90% of patients.

Statistical analysis

The training cohort was stratified into low- and high- setup displacement groups according to the median values of the errors through the three translational directions. Pearson's correlation was performed to model the possibility of linear association between individual setup errors and BMFs. Because the dependent variable was dichotomous in this study, binary logistic regression was used to examine the effects of continuous or categorical variables across the patient-related parameters or BMFs associated with higher SEs or REs. Using the

optimal cutoffs of the parameters through receiver-operating characteristic curve analysis a scoring system was proposed according to the predictors identified from the results of binary logistic regression analysis. Accordingly, the patients were dichotomized to high- and low-risk groups and the required CTV-PTV margins were calculated for each group. To differentiate the risk groups, optimal cutoffs of the BMFs in predicting the setup errors were chosen through receiver-operating characteristic (ROC) curve analysis. To confirm the validity, the scoring system was applied to test the validation cohort. The magnitude of the setup displacement between groups was examined by the chi-square test. In this study, $P < .05$ was considered statistically significant. All statistical analyses were performed using IBM SPSS version 22.0 (IBM, Armonk, New York, USA).

Results

In the training cohort, a total of 1976 setup images including the CBCT or OBI were analyzed. As listed in Table 2, the population SE / REs were 1.1 / 2.6 mm, 1.1 / 2.0 mm, and 1.9 / 5.0 mm in the SI, AP and ML directions, respectively. The SEs and RE of CR were 0.23 and 0.44 degrees. According to Van Herk's formula^{19,20}, the suggested CTV- PTV margins for minimizing setup uncertainties were 4.5, 4.0 and 8.1 mm in the AP, ML and SI directions, respectively.

As shown in Figure 2, a linear relationship existed between the individual setup errors and certain BMFs, especially between ML-SE and umbilical AP diameter and between ML-RE and umbilical AP diameter (Coefficient: 0.536 and 0.604, respectively). Table 3 shows the results of univariate and multivariate analyses of the binary logistic regression in the training cohort. Female gender was associated with increasing uncertainties of ML-SE

TABLE 2. The population SE/RE and calculated PTV margins of training cohort

Direction	Population SE	Population RE	PTV margin (cm)
Superior-Inferior (cm)	0.11	0.26	0.45
Anterior-Posterior (cm)	0.11	0.20	0.40
Medial-Lateral (cm)	0.19	0.50	0.81
Couch rotation (degree)	0.23	0.44	

RE = random error; PPTV = phantom planning target volume; SE = systematic error

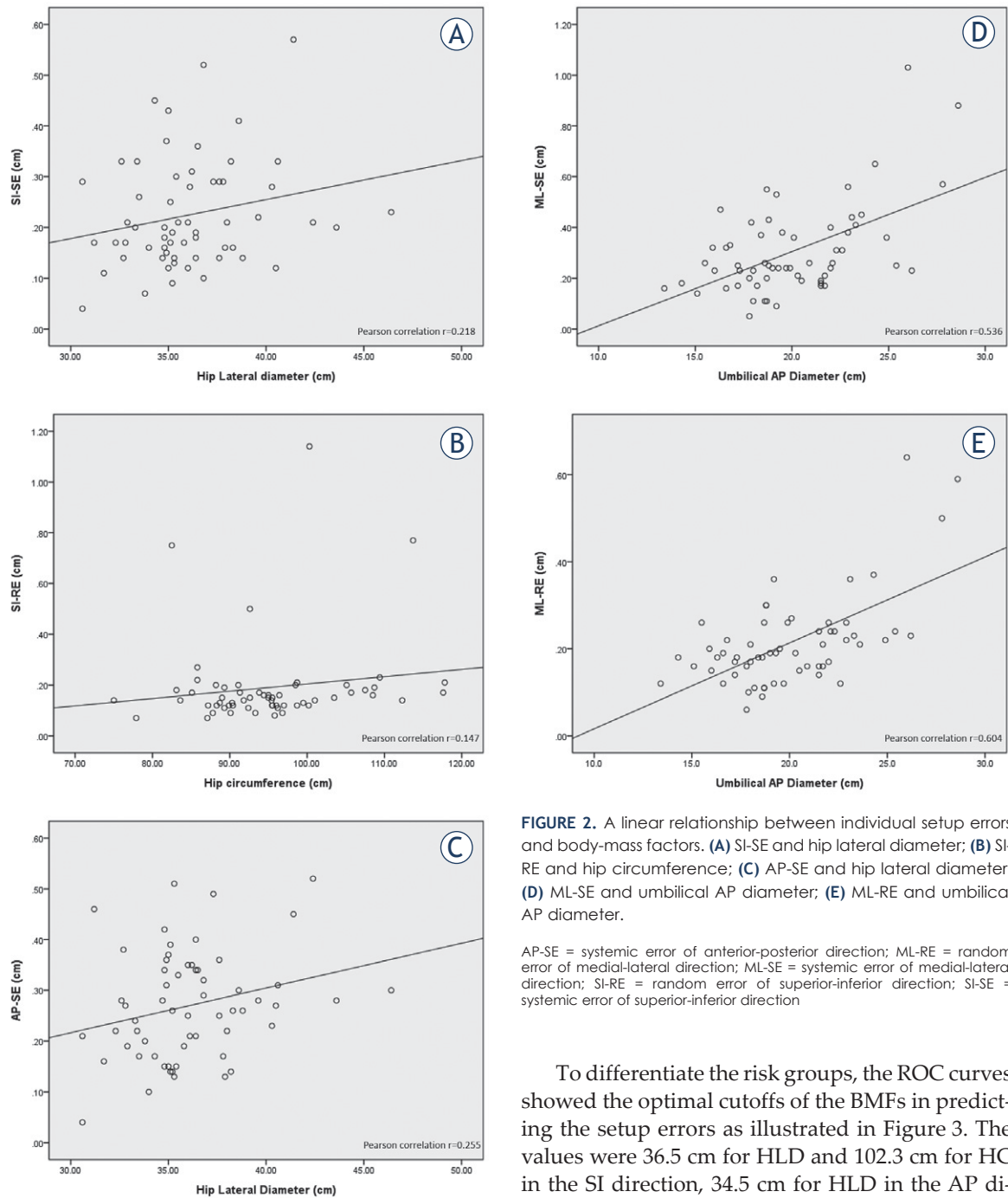


FIGURE 2. A linear relationship between individual setup errors and body-mass factors. **(A)** SI-SE and hip lateral diameter; **(B)** SI-RE and hip circumference; **(C)** AP-SE and hip lateral diameter; **(D)** ML-SE and umbilical AP diameter; **(E)** ML-RE and umbilical AP diameter.

AP-SE = systemic error of anterior-posterior direction; ML-RE = random error of medial-lateral direction; ML-SE = systemic error of medial-lateral direction; SI-RE = random error of superior-inferior direction; SI-SE = systemic error of superior-inferior direction

only in univariate analysis. We found that a large HLD correlated with a greater SI-SE and AP-SE ($P = 0.036$ and 0.044), whereas a large UAPD correlated with a greater ML-SE and ML-RE ($P = 0.021$ and 0.001). In addition, a higher SI-RE was associated with a large HC ($P = 0.008$). Furthermore, patients without previous surgery were vulnerable to a greater CR-RE ($P = 0.003$).

To differentiate the risk groups, the ROC curves showed the optimal cutoffs of the BMFs in predicting the setup errors as illustrated in Figure 3. The values were 36.5 cm for HLD and 102.3 cm for HC in the SI direction, 34.5 cm for HLD in the AP direction, and 22.1 cm for UAPD in the ML direction. A scoring system to stratify the risk groups was proposed according to the scores of these predictors. In the SI direction, the two BMFs (HLD and HC) were utilized to score the risk of setup errors. Each positive predictor scored one point and accordingly patients were dichotomized into groups at high risk and low risk (0 versus 1-2 points) for setup errors. In the AP and ML direction, patients were grouped according to the HLD and UAPD, respectively. Based on the scores, the required

TABLE 3. Univariate and multivariate of patient related parameters and BMFs for setup displacement

		SI-SE		SI-RE		AP-SE		AP-RE		ML-SE		ML-RE		CR-SE		CR-RE	
		UV	MV	UV	MV	UV	MV	UV	MV	UV	MV	UV	MV	UV	MV	UV	MV
BMFs																	
BW		0.284		0.748		0.698		0.734		0.027*		0.016*		0.911		0.85	
BH		0.477		0.13		0.141		0.514		0.168		0.527		0.43		0.914	
BMI		0.132		0.216		0.196		0.456		0.104		0.006*		0.752		0.909	
UC		0.257		0.216		0.447		0.499		0.043*		0.003*		0.129		0.45	
UAPD		0.397		0.437		0.908		0.876		0.019*	0.021*	0.001*	0.001*	0.176		0.819	
ULD		0.214		0.321		0.184		0.269		0.05		0.017*		0.467		0.348	
HC		0.066		0.041*	0.008*	0.171		0.298		0.044*		0.015*		0.594		0.374	
HAPD		0.066		0.122		0.326		0.334		0.042*		0.002*		0.351		0.746	
HLD		0.036*	0.036*	0.055		0.044*	0.044*	0.208		0.37		0.248		0.271		0.971	
CTVC		0.088		0.059		0.554		0.738		0.049*		0.013*		0.54		0.363	
CTVAPD		0.11		0.134		0.457		0.556		0.041*		0.002*		0.409		0.725	
CTVLD		0.237		0.22		0.075		0.164		0.047*		0.124		0.815		0.544	
Patient-related parameters																	
Cancer	Rectum																
	Prostate	0.749		0.749		0.344		0.749		0.508		0.744		0.752		1	
	Gynecology	0.114		0.114		0.344		0.209		0.061		0.209		1		0.209	
Age		0.039*		0.162		0.858		0.725		0.034*		0.446		0.157		0.785	
Sex		0.126		0.126		0.796		0.599		0.021*		0.586		0.782		0.192	
Married		0.599		0.524		0.561		0.524		0.999		0.453		0.999		0.488	
Education		0.448		0.782		0.605		0.782		0.629		0.024*		0.114		0.285	
ECOG PS		0.042*		0.042*		0.199		0.299		0.809		0.622		0.075		0.809	
Surgery		0.64		0.887		1.0		0.887		0.372		0.668		0.138		0.003*	0.003*
CCRT		0.129		0.129		0.793		0.965		0.383		0.895		0.223		0.485	
Cast		0.599		0.599		0.999		0.999		0.639		0.596		0.999		0.999	

AP = anterior-posterior; BH = body height; BMFs = body mass factors; BMI = body mass index; BW = body weight; CCRT = concurrent chemoradiotherapy; CR = couch rotation; CTVAPD = CTV anterior-posterior diameter; CTVC = CTV circumference; CTVLD = CTV lateral diameter; ECOG PS = Eastern Cooperative Oncology Group performance status; HAPD = hip anterior-posterior diameter; HC = hip circumference; HLD = hip lateral diameter; ML = medial-lateral; MV = multivariate; RE = random error; SE = systematic error; SI = superior-inferior; RE = random error; UAPD = umbilical anterior-posterior diameter; UC = umbilical circumference; ULD = umbilical lateral diameter; UV = univariate

PTV-CTV margin for the SI direction in the high- and low-risk groups were 5.4 mm and 3.8 mm, whereas those for the ML direction were 8.2 mm and 4.2 mm, respectively (Table 4).

In the validation cohort, a total of 959 setup images were retrieved. There was no difference between the training and validation cohorts regarding gender or BMI (gender 1:1, median BMI 25.3). The population SE / REs were 1.0 / 1.6 mm, 1.2 / 2.4 mm, and 1.6 / 2.8 mm in the SI, AP, and ML directions, respectively. As listed in Table 5, a similar trend of a greater population RE and required PTV-CTV margins could be found when using the same scoring criteria to classify the low- and high-risk groups.

Discussion

This is the first study to report the impact of image-derived BMFs and other patient-related parameters to score the magnitude of setup displacement during pelvic radiotherapy in patients with lower abdominal cancers. Our results disclosed that certain BMFs have a significant effect on setup errors in specific translational directions. The displacement in the SI direction was greater in patients with higher HC and HLD. A higher HLD and UAPD were associated with greater shifts in the AP and ML directions, respectively. Furthermore, a scoring system for the high-risk group was proposed and validated.

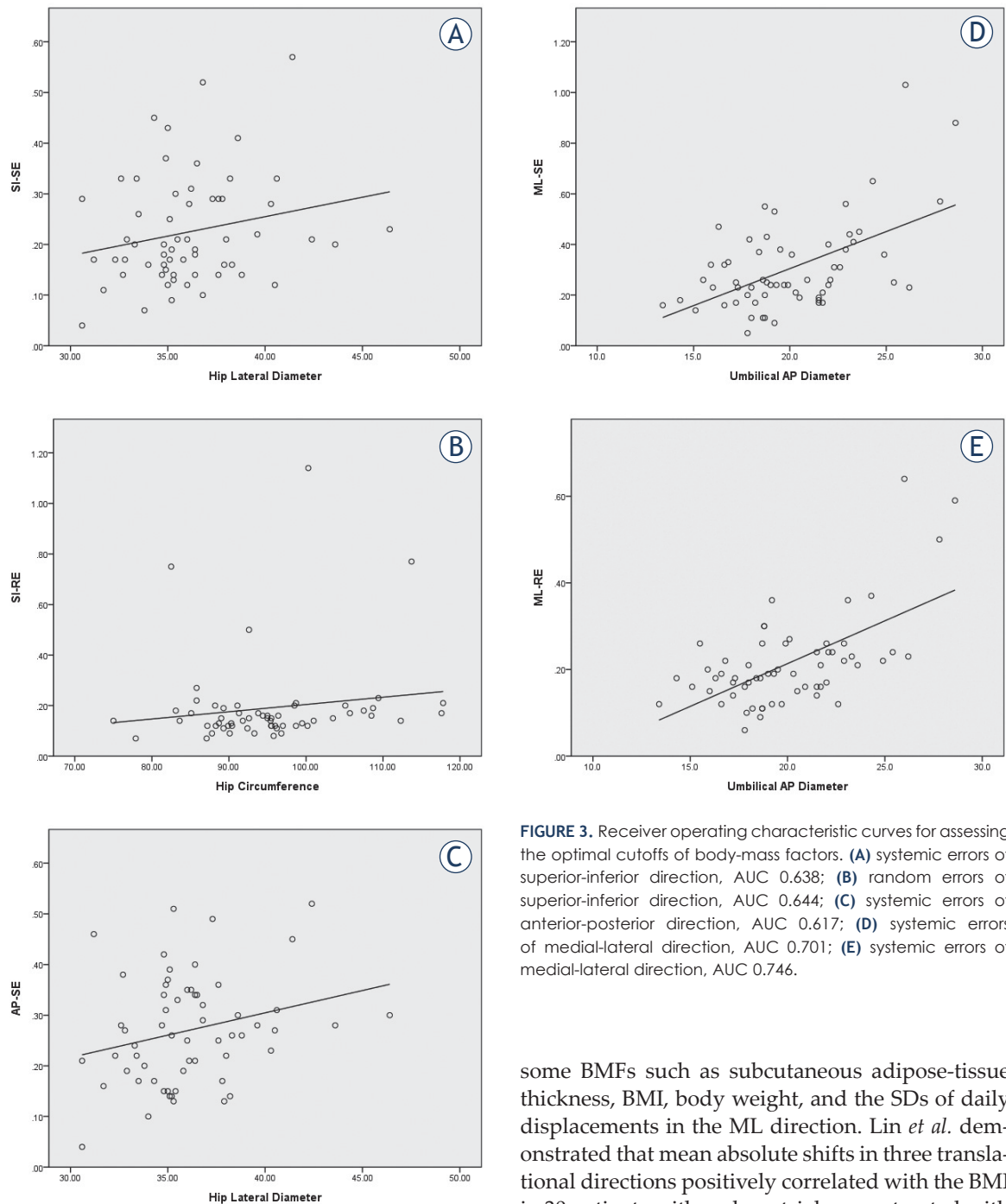


FIGURE 3. Receiver operating characteristic curves for assessing the optimal cutoffs of body-mass factors. **(A)** systemic errors of superior-inferior direction, AUC 0.638; **(B)** random errors of superior-inferior direction, AUC 0.644; **(C)** systemic errors of anterior-posterior direction, AUC 0.617; **(D)** systemic errors of medial-lateral direction, AUC 0.701; **(E)** systemic errors of medial-lateral direction, AUC 0.746.

Wong *et al.* investigated the correlation between BMI and daily setup deviation in 117 patients who received IGRT for prostate cancer.⁹ They reported that setup shifts greater than 10 mm in the ML direction increase significantly as the BMI increases, with a 1.3% shift for those with normal body weight to a 21.2% shift for those with severe obesity. Strong correlations were found between

some BMFs such as subcutaneous adipose-tissue thickness, BMI, body weight, and the SDs of daily displacements in the ML direction. Lin *et al.* demonstrated that mean absolute shifts in three translational directions positively correlated with the BMI in 30 patients with endometrial cancer treated with adjuvant pelvic IMRT¹⁰. Kim *et al.* revealed that the mean shifts in the ML direction were 0.9 mm for those with a BMI ≥ 30 and 0.1 mm for those with a BMI < 30 ($P = 0.02$)³. In addition, Bray *et al.* revealed that obese patients had larger mean displacements and REs in the ML direction.⁴ Undoubtedly, some BMFs have a great impact on setup uncertainties. However, a scoring system is required to identify high-risk patients for daily IGRT or to employ a large PVT-CTV margin.

In this study, the required CTV-PTV margins for all populations in the SI, AP, and ML directions were 4.5, 4.0 and 8.1 mm, respectively. The greatest setup uncertainties were present in the ML direction, similar to previous studies.^{3,4} Although daily IGRT could reduce setup variations in patients receiving pelvic irradiation^{3,4}, it is not always accessible due to limited facilities in some institutions as well as concerns about the increased daily dose to patients.⁸ Based on our scores, we could adapt the required PTV-CTV margins (5.4 mm for SI and 8.2 mm for ML) for patients with high risk features. Certainly, the clinical validity of the scoring system needs to be verified by external validation.

Laaksomaa *et al.*²¹ investigated the influence of gender on setup uncertainties in patients with pelvic cancers and found larger SEs and REs in women. As a result, women required greater PTV-CTV margins in the three translational directions. They also suggested that the difference in the amount of subcutaneous fat between sexes might contribute to this difference. In multivariate analysis in our study however, female gender did not impact the setup uncertainty. The discrepancy could be attributed to the fact that various distributions of accumulated adipose had been included in the BMF analyses, and consequently the impact of gender was diluted.

In several studies, the setup uncertainties were larger in obese patients despite the use of immobilization devices.^{3,4,9-11} Particularly, obesity has a negative influence on toxicity for prostate cancer patients treated with 3-dimensional radiotherapy without IGRT.²² Therefore, for prostate cancer patients who cannot be managed with IGRT or surgical treatment, a sophisticated guidance for PTV-CTV margin to reduce setup uncertainty during radiotherapy is required. Currently, obesity is usually determined by BMI alone. However, there are two kinds of obesity, the central and peripheral types, depending on the area of fat accumulation. The BMI is not able to distinguish entirely central obesity from the peripheral type.²³ Based on the external surface markers on the belly, the type of obesity might influence the setup errors because the skin folds would be more movable in central obesity. To overcome this limitation, this study retrieved the UC, HC, and diameters of in the AP and lateral directions from the simulation CT, which could include the effects of different types of obesity. Thus, our data evidenced that the abdominal or hip circumferences and diameters are more effective in predicting greater setup uncertainties compared with the BMI.

TABLE 4. Population SE/RE and adequate PTV margins according to scoring system by significant associated factors in three translational directions in training cohort

Direction		Population SE (cm)		Population RE (cm)		PTV margin (cm)
SI	High risk (1-2)	0.12	p=0.016*	0.33	p=0.016*	0.54
	Low risk (0)	0.09		0.20		0.38
AP	High risk	0.10	p=0.044*	0.20	p=0.236	0.40
	Low risk	0.10		0.18		0.38
ML	High risk	0.23	p=0.004*	0.34	p=0.005*	0.82
	Low risk	0.11		0.19		0.42

* = statistical significance

AP = anterior-posterior; ML = medial-lateral; PTV = planning target volume; RE = random error; SE = systematic error; SI = superior-inferior

TABLE 5. The Population SE/RE and adequate PTV margins according to scoring system in validation cohort

Direction		Population SE (cm)		Population RE (cm)		PTV margin (cm)
SI	High risk (1-2)	0.13	p=0.358	0.17	p=0.225	0.44
	Low risk (0)	0.07		0.14		0.27
AP	High risk	0.12	p=0.213	0.26	p=0.054	0.48
	Low risk	0.12		0.18		0.42
ML	High risk	0.23	p=0.195	0.45	p=0.004*	0.90
	Low risk	0.11		0.20		0.41

* = statistical significance

AP = anterior-posterior; ML = medial-lateral; PTV = planning target volume; RE = random error; SE = systematic error; SI = superior-inferior

This study was subject to several limitations. First, the circumferences and diameters of the patients were collected retrospectively from CT images instead of direct measurement of the girdle of the bodies. Although the mean deviation between the two methods was less than 5% according to a previous comparison test, the concordance of the two approaches should be assessed further. Second, the strength of the validation test was limited because of the small sample size. However, a trend of a greater RE in the high-risk group could be found among the three translational directions. Finally, organ motion or tumor regression may affect daily treatment accuracy, and the values across various cancers might be different. Our study did not explore the impact of these two factors through daily CBCT, as well as weekly dosimetric changes. Future studies should enroll patients prospectively and evaluate subsequent dosimetric changes according to evolution of the BMFs. Furthermore, external validation is needed to facilitate widespread utility of the scoring system.

Conclusions

Several BMFs including the HLD, HC, and UAPD are associated with greater setup uncertainties in patients receiving pelvic irradiation for lower abdominal cancers. Based on the scores, IGRT can be suggested for patients with high risk features, or required PTV margins could be adapted for patients who cannot be managed with IGRT.

Authors' contributions

WC Wu and SW Chen were responsible for design of the study, acquisition of data, analysis and interpretation of data, and drafting the article. YR Chang and YL Lai help to collect the clinical data. JA Liang, CR Chien, YC Kuo, and AC Shiau provided some intellectual content. SW Chen approved the version to be submitted.

Acknowledgements

We thank for the approval of Institutional Review Board of China Medical University Hospital.

References

- Jemal A, Siegel R, Ward E, Hao Y, Xu J, Thun MJ. Cancer statistics, 2009. *CA Cancer J Clin* 2009; **59**: 225-49. doi: 10.3322/caac.20006
- Hasselle MD, Rose BS, Kochanski JD, Nath SK, Bafana R, Yashar CM, et al. Clinical outcome of intensity-modulated pelvic radiation therapy for carcinoma of the cervix. *Int J Radiat Oncol Biol Phys* 2011; **80**: 1436-45. doi: 10.1016/j.ijrobp.2010.04.041
- Kim H, Beriwal S, Huq MS, Kannan N, Shukla G, Houser C: Evaluation of set-up uncertainties with daily kilovoltage image guidance in external beam radiation therapy for gynaecological cancers. *Clin Oncol (R Coll Radiol)* 2012; **24**: 39-45. doi: 10.1016/j.clon.2011.09.007
- Bray TS, Kaczynski A, Albuquerque K, Cozzi F, Roeske JC. Role of image guided radiation therapy in obese patients with gynecologic malignancies. *Pract Radiat Oncol* 2013; **3**: 249-55. doi: 10.1016/j.prro.2012.09.001
- Bujold A, Craig T, Jaffray D, Dawson LA. Image-guided radiotherapy: Has it influence patient outcomes? *Semin Radiat Oncol* 2012; **50**: 50-61. doi: 10.1016/j.semradonc.2011.09.001
- Zubizarreta EH, Fidarova E, Healy B, Rosenblatt E. Need for radiotherapy in low and middle income countries – the silent crisis continues. *Clin Oncol (R Coll Radiol)* 2015; **27**: 107-14. doi: 10.1016/j.clon.2014.10.006
- Deshpande S, Dhote DS, Kumar R, Naidu S, Sutar A, Kannan V. Use of image guided radiation therapy techniques and imaging dose measurement at Indian hospitals: A survey. *J Med Phys* 2015; **40**: 220-5. doi: 10.4103/0971-6203.170788
- Grau C, Defourny N, Malicki J, Dunscombe P, Borrás JM, Coffey M, et al. The impact of cancer incidence and stage on optimal utilization of radiotherapy: Methodology of a population based analysis by the ESTRO-HERO project. *Radiother Oncol* 2014; **112**: 155-64. doi: 10.1016/j.radonc.2014.08.029
- Wong JR, Gao Z, Merrick S, Wilson P, Uematsu M, Woo K, et al. Potential for higher treatment failure in obese patients: correlation of elevated body mass index and increased daily prostate deviations from the radiation beam isocenters in an analysis of 1,465 computed tomographic images. *Int J Radiat Oncol Biol Phys* 2009; **75**: 49-55. doi: 10.1016/j.ijrobp.2008.07.049
- Lin LL, Herten L, Rengan R, Teo BK: Effect of body mass index on magnitude of setup errors in patients treated with adjuvant radiotherapy for endometrial cancer with daily image guidance. *Int J Radiat Oncol Biol Phys* 2012; **83**: 670-5. doi: 10.1016/j.ijrobp.2011.07.026
- Lai YL, Yu CY, Liang JA, Chen SW. Impact of the body-mass factors on set-up displacement in patients treated with pelvic irradiation for gynecological cancer with daily on-line image guidance. *Therapeut Radiol Oncol* 2014; **21**: 21-30.
- American Joint Committee on Cancer. *AJCC Cancer Staging Manual*. 7th edition. New York: Springer Verlag; 2010.
- Melancon AD, Kudchadker RJ, Amos R, Johnson JL, Zhang Y, Yu ZH. Patient-specific and generic immobilization devices for prostate radiotherapy. *Int J Med Phys Clin Engin Radiat Oncol* 2013; **2**: 125-32. doi: 10.4236/ijmp-cero.2013.24017
- Benedict SH, Yenice KM, Followill D, Galvin JM, Hinson W, Kavanagh B. Stereotactic body radiation therapy: the report of AAPM Task Group 101. *Med Phys* 2010; **37**: 4078-101. doi: 10.1118/1.3438081
- Waxman A; World Health Assembly. WHO global strategy on diet, physical activity and health. *Food Nutr Bull* 2004; **25**: 292-302. doi: 10.1177/156482650402500310
- Lai YL, Yang SN, Liang JA, Wang YC, Yu CY, Su CH, et al. Impact of body-mass factors on setup displacement in patients with head and neck cancer treated with radiotherapy using daily on-line image guidance. *Radiat Oncol* 2014; **9**: 19. doi: 10.1186/1748-717X-9-19
- Stroom JC, Heijman BJ. Geometrical uncertainties, radiotherapy planning margins, and the ICRU-62 report. *Radiother Oncol* 2002; **64**: 75-83. doi: 10.1016/S0167-8140(02)00140-8
- Remeijer P, Geerlof E, Ploeger L, Gilhuijs K, van Herk M, Lebesque JV. 3-D portal image analysis in clinical practice: An evaluation of 2-D and 3-D analysis techniques as applied to 30 prostate cancer patients. *Int J Radiat Oncol Biol Phys* 2000; **46**: 1281-90. doi: 10.1016/S0360-3016(99)00468-X
- van Herk M, Remeijer P, Rasch C, Lebesque JV. The probability of correct target dosage: Dose-population histograms for deriving treatment margins in radiotherapy. *Int J Radiat Oncol Biol Phys* 2000; **47**: 1121-35. doi: 10.1016/j.ijrobp.2011.09.010
- Van Herk M. Errors and margins in radiotherapy. *Semin Radiat Oncol* 2004; **14**: 52-64. doi: 10.1053/j.semradonc.2003.10.003
- Laaksomaa M, Kapanen M, Tulijoki T, Peltola S, Hyödynmaa S, Kellokumpu-Lehtinen PL. Evaluation of overall setup accuracy and adequate setup margins in pelvic image-guided radiotherapy: comparison of the male and female patients. *Med Dosim* 2014; **39**: 74-8. doi: 10.1016/j.meddos.2013.09.009
- Dieperink KB¹, Hansen S, Wagner L, Johansen C, Andersen KK, Hansen O. Living alone, obesity and smoking: important factors for quality of life after radiotherapy and androgen deprivation therapy for prostate cancer. *Acta Oncol*. 2012; **51**: 722-9. doi: 10.3109/0284186X.2012.682627.
- Ko GT, Tang JS, Chan JC. Worsening trend of central obesity despite stable or declining body mass index in Hong Kong Chinese between 1996 and 2005. *Eur J Clin Nutr* 2010; **64**: 549-52. doi:10.1038/ejcn.2010.49

Radiol Oncol 2019; 53(2): 131-147.
doi: 10.2478/raon-2019-0024

Biologija in klinična uporabnost cirkulirajočih tumorskih celic

Ložar T, Geršak K, Čemažar M, Grašič Kuhar C, Jesenko T

Izhodišča. Tumorske celice se v procesu zasevanja sprostijo iz primarnega tumorja v krvni obtok, v katerem nato potujejo do oddaljenega mesta. Te celice imenujemo cirkulirajoče tumorske celice (CTC). Sposobnost CTC, da kolonizirajo oddaljena tkiva in organe, predstavlja glavni način, kako tumorske celice zasevajo. Njihove biološke lastnosti in interakcije z drugimi celicami so zapletene in regulirane s številnimi signalnimi molekulami, vključno z različnimi citokini in kemokini. Spremljanje CTC v krvi bolnikov postaja vedno bolj klinično zanimivo, saj vzorec pridobimo z enostavnim odvzemom krvi. Tak odvzem krvi imenujemo tekočinska biopsija, s katero lahko poleg samih CTC določujemo tudi njihove produkte; prosto cirkulirajočo DNA ali RNA (cfDNA/cfRNA), mikro RNA (miRNA) in eksosome.

Zaključki. Z napredkom tekočinske biopsije postaja področje CTC tudi vedno bolj klinično zanimivo. Spremljanje CTC lahko uporabljamo za iskanje prisotnosti raka (presejanje) ter kot dejavnik za napoved poteka bolezni in napoved za odgovor na zdravljenje pri bolnikih z rakom. S hitrim tehnološkim napredkom v metodah za izolacijo CTC lahko v prihodnje pričakujemo še večjo klinično uporabnost spremljanja CTC v krvi bolnikov. Prav tako pa bo večje razumevanje biologije CTC in njihovih interakcij z drugimi vrstami celic pripomoglo k razvoju novih možnosti za zdravljenje metastatske bolezni.

Radiol Oncol 2019; 53(2): 148-158.
doi: 10.2478/raon-2019-0018

Cisplatin in mnogo več. Molekularni mehanizmi delovanja in razvoja rezistence pri kemoterapiji

Makovec T

Izhodišča. Spojine s platino so ene najpogosteje uporabljenih protirakavih učinkovin. Njihova glavna pomanjkljivost je razvoj odpornosti proti zdravlilu in njihova toksičnost. Zato je pomembno razumeti kemične lastnosti, prenos in metabolične poti ter mehanizem delovanja teh spojin. Poznamo širok nabor dokazov, da terapevtski in toksični učinki zdravil s platino ne temeljijo le na tvorbi kompleksov platine z DNA, temveč tudi z RNA in mnogimi proteini. Ti procesi določajo tudi mehanizme, na katerih temelji odpornost proti tem zdravilom ter njihova toksičnost. Povečano izražanje različnih transportnih proteinov ter encimov, ki popravljajo s platino povzročene poškodbe na DNA, so glavni mehanizmi pri razvoju odpornosti. Poleg transportnih sistemov ima pomembno vlogo pri predvidevanju bolnikovega odgovora na zdravlila s platino tudi funkcionalna genomika. Tako so pomembni genetski polimorfizmi, ki so lahko osnova individualiziranega pristopa k zdravljenju raka s temi zdravili.

Zaključki. Cisplatin uvrščamo med najpomembnejša kemoterapevtska zdravila. Klinično je preizkušen za zdravljenje različnih vrst karcinomov in sarkomov.

Radiol Oncol 2019; 53(2): 159-170.
doi: 10.2478/raon-2019-0021

Multiparametrična magnetna resonanca. Določanje stadija raka prostate

Caglič I, Kovač V, Barrett T

Izhodišča. Natančna ocena lokalne razširjenosti bolezni je bistvena za načrtovanje zdravljenja in napoved poteka bolezni pri bolnikih z rakom prostate. Predvsem želimo ugotoviti, ali je bolezen omejena na organ ali pa je lokalno napredovala in je zato napoved poteka bolezni slabša. Slikanje z multiparametrično magnetno resonanco (MR) je metoda izbora za oceno lokalne razširjenosti raka prostate in ima dodano vrednost pri opredelitvi medeničnih bezgavk in skeleta medenice. V primerjavi s tradicionalnimi metodami, ki temeljijo na kliničnih nomogramih, dodatno poda informacijo o lokaciji in stopnji razširjenosti bolezni. MR ima visoko specifičnost pri diagnozi ekstrakapsularne razširjenosti, invaziji v seminalne vezikle in pri zasevkih v bezgavkah, vendar senzitivnost ostaja slaba. Zato je še vedno zlati standard pri določitvi stadija bezgavk razširjena limfadenektomija pelvičnih bezgavk, v zadnjem času pa je bil tudi dosežen napredek v razvoju naprednih slikovnih tehnik, ki določijo celotni stadij.

Zaključki. T2-obteženo slikanje je osnovna sekvenca pri določanju lokalne razširjenosti raka prostate. Natančnost lahko zviša slikanje z magnetnoresonančnim aparatom 3T ter vključitev difuzijsko obteženega in dinamično kontrastno ojačanega slikanja. Tako imenovana naslednja generacija slikovne diagnostike, ki vključuje MR celotnega telesa in PET-MR z uporabo specifičnega membranskega antigena prostate (^{68}Ga -PSMA), je pokazala vzpodbudne rezultate pri odkrivanju zasevkov v bezgavke in kosti v primerjavi z običajnimi protokoli.

Radiol Oncol 2019; 53(2): 171-177.
doi: 10.2478/raon-2019-0023

Vrednotenje natančnosti preiskave MR po primarni sistemski terapiji pri bolnicah z rakom dojke glede na biologijo tumorja

Bouzón A, Iglesias A, Acea B, Mosquera C, Santiago P, Mosquera J

Izhodišča. Analizirali smo natančnost magnetno resonančne preiskave dojk po primarni sistemski terapiji glede na tumorski podtip.

Bolniki in metode. Analizirali smo 204 bolnic z rakom dojke, ki smo jih zdravili s primarno sistemsko terapijo. Primerjali smo izsledke preiskave MR po primarni sistemski terapiji s patološkimi ugotovitvami in jih primerjali glede na tumorski podtip.

Rezultati. Od 204 bolnic z rakom dojke jih je 84 (41,2 %) imelo popoln odgovor na terapijo. Natančnost preiskave MR za napovedovanje popolnega odgovora na terapijo je bilo najvišje pri trojno negativnem in HER-2 pozitivnem (neluminalnem) tipu raka dojke (83,9 in 80,9 %). Najmanjša diskrepanca povprečne velikosti, ki smo jo merili z MR, in velikostjo rezidualnega tumorja je bila pri trojno negativnem raku dojke in največja pri luminalnem B-podobnem (HER2-negativnem) raku dojke (0,45 cm proti 0,98 cm; $p = 0,003$). Po ohranitveni operaciji dojke, smo ugotovili manjšo mero pozitivnih varnostnih robov pri trojno negativnem raku dojke ter višjo pri luminalnem B-podobnem (HER2-negativnem) raku dojke (2,4 % proti 23,6 %).

Zaključki. Pri ocenjevanju odgovora tumorja na primarno sistemsko terapijo s preiskavo MR moramo pri načrtovanju ohranitvene operacije dojke upoštevati podtip tumorja. Natančnost preiskave MR je največja pri trojno negativnem raku dojke.

Radiol Oncol 2019; 53(2): 178-186.
doi: 10.2478/raon-2019-0027

Diagnostična točnost standardizirane ultrazvočne metode za zaznavo zgodnjih sprememb hemofilčne artropatije (HEAD-US). Primerjava z magnetno resonančnim slikanjem

Plut D, Faganel Kotnik B, Preložnik Zupan I, Ključevšek D, Vidmar G, Snoj Ž, Martinoli C, Salapura V

Izhodišča. Ponavljajoče krvavitve v sklep prizadenejo okoli 90 % bolnikov s hudo hemofilijo in vodijo v kronično okvaro sklepov z invalidnostjo. Slikovna diagnostika omogoča zaznavo tudi klinično nemih sprememb hemofilčne artropatije in lahko vpliva na potek profilaktičnega zdravljenja. Slikanje z magnetno resonanco (MR) predstavlja zlati standard za natančno oceno sklepnih sprememb, vendar pri rednem sledenju bolnikov s hemofilijo ni enostavno izvedljivo. Uvedba standardizirane ultrazvočne metode za zaznavo zgodnjih sprememb hemofilčne artropatije (HEAD-US) je odprla nove možnosti za uporabo ultrazvoka (UZ) pri sledenju teh bolnikov. Protokol omogoča hitro oceno šestih najpogosteje prizadetih sklepov hkrati. Cilj prospektivne raziskave je bil ugotoviti diagnostično točnost HEAD-US za zaznavanje in oceno stopnje prizadetosti sklepov pri hemofilčni artropatiji v primerjavi z MR.

Bolniki in metode. V raziskavo smo vključili 30 bolnikov s hudo obliko hemofilije. Pri vseh preiskovancih smo ocenili komolce, gležnje in kolena (skupaj 168 sklepov) s preiskavo UZ po protokolu HEAD-US. Rezultate preiskav UZ smo primerjali z rezultati pri slikanju MR ovrednotenimi z lestvico IPSPG MR.

Rezultati. Rezultati so pokazali visoko stopnjo ujemanja med skupno vrednostjo HEAD-US in lestvic IPSPG MR ($r = 0.92$). Stopnja ujemanja je bila zelo visoka za ocenjevanje komolčnih in kolenskih sklepov ($r \approx 0.95$) ter nekoliko nižja za oceno gleženjskih sklepov ($r \approx 0.85$).

Zaključki. HEAD-US protokol je hitra, zanesljiva in točna metoda za zaznavo in oceno stopnje prizadetosti sklepov pri hemofilčni artropatiji.

Radiol Oncol 2019; 53(2): 187-193.
doi: 10.2478/raon-2019-0026

Učinkovitost in dolgoročna uspešnost zdravljenja zdrsa medvretenčne ploščice z radioopačnim etanolom v gelu

Kuhelj D, Dobrovolec A, Kocijančič IJ

Izhodošča. Želeli smo preveriti učinkovitost in dolgoročno uspešnost perkutanega zdravljenja zdrsa medvretenčne ploščice (*hernia disci*) z radioopačnim etanolom v gelu v obdobju 36 mesecev.

Bolniki in metode. Med majem 2014 in decembrom 2015 smo s to metodo zdravili 83 bolnikov (47 moških, 36 žensk, starih od 18–79 let, srednja starost 48,9 let). 16 bolnikov je imelo omejen zdrs v predelu vratne hrbtenice in 67 bolnikov v predelu lumbalne hrbtenice. Bolečino smo ocenili s pomočjo vizualne analogne lestvice (VAS), zanimala nas je tudi fizična aktivnost, uporaba analgetikov, zadovoljstvo bolnikov z zdravljenjem in njihova pripravljenost, da bi se ponovno zdravili na tak način.

Rezultati. 59 bolnikov je odgovorilo na vprašalnik, pri 89,8 % smo zabeležili statistično značilno nižjo vrednost bolečine po VAS-u mesec po posegu ($p < 0,001$). Izboljšanje smo ugotovili pri 76,9 % bolnikov s težavami v vratnem delu in pri 93,5 % bolnikov s težavami v lumbalnem delu. Pri bolnikih s težavami v predelu vratu je bilo stanje stabilno po 36 mesecih, pri bolnikih s težavami v lumbalnem predelu se je vrednost VAS dodatno pomembno znižala ($p = 0,012$). Le en bolnik je bil po posegu operiran. Zmerna in resna fizična omejenost (96,6 %) je bila 12 mesecev po posegu prisotna le pri 30 % bolnikov, večina delovno aktivnih se je vrnila na staro delovno mesto (71,1 %) in potrebovala manj analgetikov (78 %). Le 5,1 % bolnikov ni bilo zadovoljnih z izidi zdravljenja in 10,2 % jih ne bi ponovilo zdravljenja.

Zaključki. Perkutano zdravljenje zdrsa medvretenčne ploščice z vbrizganjem radioopačnega etanola v gelu se je izkazalo za varno, uspešno ter dolgoročno učinkovito tako v vratnem kot v lumbalnem področju, zato bi lahko postalo prva metoda zdravljenja pri izbranih bolnikih.

Radiol Oncol 2019; 53(2): 194-205.

doi: 10.2478/raon-2019-0025

Uporaba visokofrekvenčnih bipolarnih pulzov pri zdravljenju z elektrokemoterapijo

Scuderi M, Reberšek M, Miklavčič D, Dermol-Černe J

Izhodišča. Elektrokemoterapija znatno znižuje preživetje malignih celic. Pri zdravljenju tumorjev na ta način kemoterapevtike najprej injiciramo intratumorsko ali intravenozno, nato pa dovedemo 100 μ s dolge monopolarne pulze. Le-ti pa povzročajo bolnikom bolečine zaradi krčenja mišic, zato z uporabo mišičnih relaksantov izvajamo obsežnejše postopke tudi v splošni anesteziji. Dovajanje pulzov pa je potrebno tudi sinhronizirati s srčnim ritmom bolnika, zaradi česar je postopek še zahtevnejši in zamudnejši. V zadnjem času je bilo v literaturi omenjeno zdravljenje tumorjev s kratkimi visokofrekvenčnimi bipolarnimi pulzi, kjer je bilo krčenje mišic zanemarljivo. Namen raziskave je bil preveriti, ali je mogoče doseči povišan vnos kemoterapevtikov v celice tudi s kratkimi visokofrekvenčnimi bipolarnimi pulzi.

Materiali in metode. Poskuse smo izvedli na celični liniji mišjega melanoma B16-F1. V prvem poskusu smo celicam dodali cisplatin in klasične 100 μ s dolge monopolarne pulze, v drugem pa visokofrekvenčne kratke bipolarne pulze.

Rezultati. V obeh primerih je bila kombinacija cisplatina in električnih pulzov učinkovitejša pri zniževanju preživetja celic, kot če bi uporabili samo kemoterapevtik ali samo električne pulze. Ko pa smo hoteli doseči primerljive rezultate z dovajanjem enih ali drugih pulzov, se je izkazalo, da je potrebno pri visokofrekvenčnih kratkih bipolarnih pulzih dovesti dvainpolkrat višje električno polje (3 kV/cm), pri klasičnih dolgih monopolarnih pulzih pa nižje, le 1,2 kV/cm.

Zaključki. Ugotovili smo, da je mogoče pri elektrokemoterapiji uporabljati tudi kratke bipolarne pulze, ki povzročajo manj zapletov, to pa na račun dovajanja višjih električnih polj kot pri klasičnih dolgih monopolarnih pulzih. Dobljeni rezultati tako utirajo pot uporabi visokofrekvenčnih kratkih pulzov tudi v elektrokemoterapiji.

Radiol Oncol 2019; 53(2): 206-212.

doi: 10.2478/raon-2019-0016

Genetska variabilnost mehanizmov popravljanja DNK in tveganje za nastanek malignega mezotelioma

Levpušček K, Goričar K, Kovač V, Dolžan V, Franko A

Izhodišče. Maligni mezoteliom je redek in agresiven tumor seroznih površin, ki nastane zaradi izpostavljenosti azbestu. Domnevamo, da genetska variabilnost proteinov, ki sodelujejo pri popravljanju poškodb DNK, vpliva na tveganje za nastanek malignega mezotelioma. Namen raziskave je bil preučiti vpliv funkcionalnih polimorfizmov v genih *ERCC1* in *XRCC1*, interakcije med polimorfizmi teh genov ter interakcije med navedenimi polimorfizmi in izpostavljenostjo azbestu na tveganje za razvoj malignega mezotelioma.

Bolniki in metode. V raziskavo smo vključili 237 bolnikov z malignim mezoteliomom ter 193 kontrolnih subjektov, ki niso zboleli za nobeno poklicno boleznijo, povezano z izpostavljenostjo azbestu. Za določanje polimorfizmov *ERCC1* in *XRCC1* smo uporabili metode, ki temeljijo na reakciji PCR v realnem času.

Rezultati. Polimorfizem *ERCC1* rs3212986 je bil statistično značilno povezan z zmanjšanim tveganjem za razvoj malignega mezotelioma (razmerje obetov [RO] = 0,61; 95 % interval zaupanja [IZ] = 0,41–0,91; $p = 0,014$). Ostali preučevani polimorfizmi niso imeli statistično značilnega vpliva na tveganje za pojav bolezni. Nosilci polimorfnih alelov *ERCC1* rs11615, ki so bili izpostavljeni nizkim odmerkom azbesta, so imeli statistično značilno zmanjšano tveganje za pojav malignega mezotelioma (OR = 0,40; 95 % IZ = 0,19–0,84; $p = 0,016$). Če pa je bila pri njih izpostavljenost srednja ali visoka, se je tveganje za maligni mezoteliom statistično značilno povečalo (OR = 7,58; 95 % IZ = 3,53–16,31; $p = < 0,001$). Interakcije med preostalimi polimorfizmi in izpostavljenostjo azbestu niso statistično značilno vplivale na tveganje za maligni mezoteliom.

Zaključki. Rezultati raziskave nakazujejo, da bi genetska variabilnost proteinov, ki sodelujejo pri popravljanju poškodb DNA, lahko vplivala na tveganje za razvoj malignega mezotelioma.

Radiol Oncol 2019; 53(2): 213-218.
doi: 10.2478/raon-2019-0014

Radiološke in klinične značilnosti mieloidnega sarkoma

Meyer HJ, Beimler M, Borte G, Pönisch W, Surov A

Izhodišča. Mieloidni sarkom, znan tudi kot granulocitni sarkom ali klorom, je soliden tumor ekstramedularne lokalizacije, sestavljen iz malignih primitivnih mieloidnih celic. Namen raziskave je bil ugotoviti klinične in slikovne značilnosti v velikem vzorcu bolnikov.

Bolniki in metode. V raziskavo smo vključili 71 bolnikov s histopatološko potrjenim mieloidnim sarkomom, 34 žensk (47,9 %) in 37 moških (52,1 %) s srednjo starostjo 56 let (± 16). Ugotavljali smo osnovno hematološko bolezen, pojavnost, lokalizacije in klinične simptome ter slikovne značilnosti vidne na računalniški tomografiji in slikanju z magnetno resonanco.

Rezultati. V 4 primerih (5,63 %) se je mieloidni sarkom pojavil s srednjim časom $3,8 \pm 2,1$ meseca pred sistemsko hematološko boleznijo. V 13 primerih se je prva predstavitev mieloidnega sarkoma pojavila sočasno z začetno diagnozo levkemije, 51 bolnikov pa je imelo mieloidni sarkom po začetni diagnozi osnovne maligne bolezni s povprečno latentnostjo $39,8 \pm 44,9$ mesecev. V 26 primerih so bila prizadeta visceralna mehka tkiva, v 21 primerih pa sta bila prizadeta koža in/ali podkožje. Nadaljnje lokalizacije bolezni so bile kosti ($n = 13$), osrednji živčni sistem ($n = 9$), bezgavke ($n = 4$) in visceralni organi ($n = 9$).

Zaključki. Mieloidni sarkom je redko spremlja več hematoloških malignomov, predvsem akutne mieloične levkemije in lahko prizadene vsak del telesa. V večini primerov se pojavi po diagnozi osnovnega malignoma in pogosto prizadene kožo in podkožje.

Radiol Oncol 2019; 53(2): 219-224.
doi: 10.2478/raon-2019-0020

Novo orodje za napovedovanje preživetja bolnic z možganskimi metastazami raka dojke, ki smo ga razvili pri enovito zdravljeni skupini

Janssen S, Hansen HC, Dziggel L, Schild SE, Rades D

Izhodišča. Dosedanje podatke o preživetju bolnic, ki so imele rak dojke z možganskimi metastazami, so pridobili na skupinah bolnic, ki so prejemale različna zdravljenja, kar lahko vodi v pristranskost. Predstavili smo novo orodje za točkovanje WBRT-30-BC, ki smo ga razvili pri skupini 170 bolnic, ki so prejemale samo radioterapijo celotnih možganov s 30 Gy v 10 frakcijah.

Bolniki in metode. V točkovalnik WBRT-30-BC smo vključili tisti značilnosti bolnic, pri katerih smo z multivariatno analizo ugotovili statistično značilno povezanost s celokupnim preživetjem ($p < 0,05$) ali pa so kazale takšno težnjo ($p < 0,08$). Za vsako od značilnosti smo določili število točk, tako da je bila stopnja 6-mesečnega celokupnega preživetja deljena z 10. Točke smo nato določili za vsako bolnico. Točkovanje z WBRT-30-BC smo primerjali z diagnostično klasifikacijo stopnje napovedne ocene (DS-GPA) in z oceno točkovanja po Radesu pri bolnicah z rakom dojke. Glede na pozitivno napovedno vrednost, smo prepoznali bolnice, ki umrejo zaradi raka dojke v prvih 6 mesecih in tiste, ki 6-mesečno obdobje po radioterapiji celotnih možganov preživijo.

Rezultati. Multivariatna analiza je pokazala, da je bil statistično pomemben Karnofskyjev indeks stanja splošne zmogljivosti (KPS) (razmerje tveganja [RR]: 2,45, $p < 0,001$). Analiza je tudi pokazala trend vpliva na celokupno preživetje zaradi zasevkov izven možganov (RR: 1,52, $p = 0,071$) in zaradi časa med diagnozo raka dojke in radioterapijo celotnih možganov (RR: 1,37, $p = 0,070$). Na podlagi teh treh značilnosti so bile bolnice razdeljene v štiri napovedne skupine. 6-mesečno celokupno preživetje je bilo pri 7–9 točkah 8 %, pri 10–12 točkah 41 %, pri 13–15 točkah 68 % in pri 16 točkah 100 % ($p < 0,001$). Pozitivna napovedna vrednost bolnic, ki so umrle v 6 mesecih, je bila pri točkovanju WBRT-30-BC 92 %, pri DS-GPA 84 % in pri točkovanju po Radesu 92 %, medtem ko je bila pozitivna napovedna vrednost za bolnice, ki so preživele 6 mesecev po radioterapiji celotnih možganov pri točkovanju WBRT-30-BC 100 %, pri DS-GPA 74 % in pri točkovanju po Radesu 68 %.

Zaključki. Točkovalnik WBRT-30-BC je bil zelo natančen pri napovedovanju smrti bolnic z rakom dojke, ki so prejele radioterapijo celotnih možganov in so preživele ≤ 6 mesecev oz. tistih, ki so preživele ≥ 6 mesecev. Napovedna vrednost preživetja ≥ 6 mesecev je bil boljša od dosedanjih točkovalnikov, ki nam služijo za napoved poteka bolezni.

Radiol Oncol 2019; 53(2): 225-230.
doi: 10.2478/raon-2019-0028

Motnje požiranja po zdravljenju raka glave in vratu

Pezdirec M, Strojjan P, Hočevar Boltežar I

Izhodišča. Motnje požiranja so pogosta posledica zdravljenja raka glave in vratu. Namen raziskave je bil oceniti prevalenco disfagije v skupini bolnikov, ki so se zdravili zaradi raka glave in vratu v Sloveniji, in identificirati dejavnike, ki prispevajo k razvoju disfagije.

Bolniki in metode. V raziskavo smo vključili 109 zaporednih bolnikov, ki smo jih zdravili zaradi raka glave in vratu v dveh terciarnih centrih. Bolniki so izpolnili vprašalnika EORTC QLQ-H & N35 in „Motnje požiranja zaradi raka glave in vratu“. Primerjali smo bolnike, ki so imeli disfagijo s tistimi brez motenj požiranja.

Rezultati. Težave s požiranjem smo ugotovili pri 41,3 % bolnikov. Disfagija je vplivala na njihovo družbeno življenje (v 75,6 %), še posebej na prehranjevanje v javnosti (v 80 %). Najpogosteje smo ugotovili disfagijo pri bolnikih z rakom ustne votline in/ali rakom ustnega žrela (57,6 %) ter pri tistih, ki so bili zdravljeni pred manj kot 2 leti ($p = 0,014$). Pri univariatni analizi rezultatov vprašalnikov smo ugotovili statistično pomembno povezavo med pojavom motenj požiranja in nekaterimi posledicami zdravljenja raka (omejeno odpiranje ust, lepljiva slina, izguba voha, zmanjšana sposobnost okušanja, bolečine v ustih in žrelu, perzistentni kašelj in hripavost), radioterapijo ($p = 0,003$) ter simptomi gastroezofagealnega refluksa ($p = 0,027$). Po uporabi modela multiple regresije je le perzistentni kašelj še vedno ostal povezan z disfagijo ($p = 0,023$).

Zaključki. Da bi izboljšali sposobnost požiranja in posledično kakovost življenja bolnikov z rakom glave in vratu bi bilo primerno poskrbeti za sistematično rehabilitacijo požiranja. Poseben poudarek je potrebno posvetiti zdravljenju gastroezofagealnega refluksa pred, med in po zdravljenju raka glave in vratu.

Radiol Oncol 2019; 53(2): 231-237.
doi: 10.2478/raon-2019-0015

Z zdravjem povezana kakovost življenja pri slovenskih bolnikih z rakom debelega črevesa in danke

Grosek J, Novak J, Kitek K, Bajrić A, Majdič A, Košir JA, Tomažič A

Izhodišča. Rak debelega črevesa in danke je pomemben vzrok smrtnosti in zmanjšane kakovosti življenja. Edina možnost ozdravitve je radikalna kirurška resekcija tumorja. Z raziskavo smo želeli ovrednotiti z zdravjem povezano kakovost življenja pri bolnikih z rakom debelega črevesa in danke ter jo primerjati z zdravjem povezano kakovostjo življenja splošne slovenske populacije.

Bolniki in metode. Uporabili smo dva standardizirana in validirana vprašalnika EORTC QLQ-C30 verzija 3 in EORTC QLQ-CR29. Vprašalnika smo poslali 413 še živim bolnikom z rakom debelega črevesa in danke, ki so bili operirani v obdobju od 1. 1. 2016 do 31. 12. 2017. Pri statistični obdelavi smo uporabili enovzorčni t-test za primerjavo povprečja naših bolnikov in splošne populacije Republike Slovenije ter Mann-Whitneyev U test za primerjavo po spolu in starosti.

Rezultati. 197 bolnikov je odgovorilo na vprašalnik. Ko smo primerjali bolnike z rakom debelega črevesa in danke s splošno populacijo Republike Slovenije smo z enovzorčnim t testom dokazali nižjo kakovost življenja bolnikov na področju fizičnega funkcioniranja ($p < 0,001$), opravljanja funkcij ($p = 0,002$), kognitivnega ($p = 0,021$) in socialnega funkcioniranja ($p < 0,001$). V primerjavi s splošno populacijo imajo bolniki več težav z zaprtostjo ($p < 0,001$), drisko ($p < 0,001$) in finančnimi težavami ($p < 0,001$). Z Mann-Whitneyevim U testom smo pri primerjavi bolnikov po spolu dokazali slabše kognitivno ($p = 0,034$) in čustveno funkcioniranje ($p = 0,008$), pogostejšo napihnenost ($p = 0,049$) in izgubo las ($p = 0,010$) pri ženskah v primerjavi z moškimi. Z Mann-Whitneyevim U testom smo dokazali slabše fizično funkcioniranje med starejšo skupino bolnikov ($p < 0,001$), prav tako pogostejšo frekvenco uriniranja ($p = 0,007$), inkontinenco urina ($p = 0,007$), bolečine v zadnjici ($p = 0,007$) in skrb zaradi telesne teže ($p = 0,031$) v primerjavi z mlajšo skupino bolnikov.

Zaključki. Splošna kakovost življenja bolnikov po operaciji zaradi raka debelega črevesa in danke je primerljiva s kakovostjo življenja splošne populacije. Statistično značilno nižja je kakovost na posameznih področjih življenja. Med bolnicami sta kognitivno in socialno funkcioniranje statistično značilno slabše ocenjena kot med bolniki, prav tako je med bolnicami več napihnenosti in izgube las kot med bolniki. Med starejšimi bolniki je ocena fizičnega funkcioniranja nižja, pojavnost določenih simptomov pa višja kot med mlajšimi bolniki.

Radiol Oncol 2019; 53(2): 238-244.
doi: 10.2478/raon-2019-0022

Dolgotrajno preživetje 200 bolnikov z napredovalim stadijem kolorektalnega raka in sladkorno boleznijo. Izkušnje posamične ustanove

Bešič N, Kerin Povšič M

Izhodišča. Sladkorna bolezen in zapleti sladkorne bolezni lahko povzročijo težave med specifičnim onkološkim zdravljenjem in lahko vplivajo na zdravljenje raka in izid poteka bolezni. Cilj raziskave je bil ugotoviti, ali pri bolnikih z napredovalim kolorektalnim rakom obstaja povezava med prisotnostjo sladkorne bolezni in preživetjem, specifičnim za raka ali celokupnim preživetjem.

Bolniki in metode. V raziskavo smo vključili 200 zaporednih bolnikov (131 moških, 69 žensk, povprečna starost 63 let), ki smo jih na Onkološkem inštitutu Ljubljana zdravili z elektivnim kirurškim posegom zaradi kolorektalnega raka. Sladkorna bolezen smo ugotovili pri 39 (19,5 %) bolnikih. Kar 64 % bolnikov je imelo raka v stadiju 3 ali 4, zato je bilo 59 % bolnikov zdravljenih z neoadjuvantno kemoterapijo in/ali radioterapijo. Podatke o spolu, starosti, indeksu telesne mase (ITM), prisotnosti sladkorne bolezni, stopnji ogroženosti bolnika po klasifikaciji Ameriškega društva za anesteziologijo (ASA), stadiju bolezni in pooperativnih zapletih smo zbrali prospektivno. S testom *log-rank* smo primerjali preživetje, specifično za raka in celokupno preživetje.

Rezultati. Bolniki s sladkorno boleznijo so imeli višjo stopnjo ASA, ITM, stadij bolezni, delež masivnih krvavitev in so dobili večjo količino transfuzije krvi in imeli daljše bivanje v bolnišnici kot tisti brez sladkorne bolezni. Povprečno obdobje spremljanja je bilo 4,75 let. Med bolnikih s sladkorno boleznijo je umrlo 23 % bolnikov, med bolniki brez sladkorne bolezni pa 27 % bolnikov. Triletno preživetje, specifično za raka je bilo med bolniki s sladkorno boleznijo 85 %, med bolniki brez sladkorne bolezni pa 89 % ($p = 0,68$). Triletno celokupno preživetje bolnikov s sladkorno boleznijo je bilo 82 %, bolnikov brez sladkorne bolezni pa 84 % ($p = 0,63$).

Zaključki. Prisotnost sladkorne bolezni ni bila povezana s stadijem bolezni, preživetjem, specifičnim za raka ali s celokupnim preživetjem bolnikov z napredovalim kolorektalnim rakom.

Radiol Oncol 2019; 53(2): 245-255.

doi: 10.2478/raon-2019-0019

Vpliv perioperativnega zdravljenja na preživetje bolnikov z operabilnim rakom želodca po limfadenektomiji D2. Analiza z metodo usklajevanja uteži v posamičnem evropskem centru

Jagrič T, Ilijevec B, Velenik V, Ocvirk J, Potrč S

Izhodišča. Da bi ugotovili učinke perioperativnega zdravljenja bolnikov z rakom želodca, smo izvedli analizo skupin bolnikov z metodo usklajevanja uteži (*propensity score matching*) z namenom ugotoviti vlogo perioperativne kemoterapije pri bolnikih po limfadenektomiji D2.

Bolniki in metode. Iz naše baze podatkov 1563 bolnikov smo izbrali 482 bolnikov z metodo usklajevanja uteži in jih razdelili v dve uravnoteženi skupini. V prvo skupino smo razvrstili 241 bolnikov, ki smo jih samo operirali in v drugo 241 bolnikov, ki so prejeli perioperativno terapijo. Med skupinama smo primerjali dolgoročne rezultate zdravljenja.

Rezultati. Večina vključenih bolnikov je prejela radio-kemoterapijo s kapecitabinom ($n = 111$; 46 %) in perioperativno kemoterapijo z epirubicinom, oksaliplatinom in kapecitabinom ($n = 91$; 37,7 %). Pri 92,9 % bolnikov je bila narejena limfadenektomija D2. Perioperativna obolevnost je bila podobna med samo kirurško (18,3 %) in perioperativno skupino (20,7 %) ($p = 0,537$). Perioperativno zdravljenje ni vplivalo na perioperativno smrtnost. Patološki odziv smo opazovali pri 12,5 % bolnikov. Skupno 5-letno in srednje preživetje sta bili pomembno višji v perioperativni skupini (50,5 %; 51,7 mesecev) v primerjavi s samo kirurško skupino (41,8 %; 34,9 mesecev; $p = 0,038$). Analiza podskupin je razkrila pomembno korist per operativnega zdravljenja samo pri bolnikih s TNM stadiji T3 ($p = 0,028$), N2 ($p = 0,009$), N3b ($p = 0,043$) ter UICC stadiji IIIb ($p = 0,003$) in IIIc ($p = 0,03$).

Zaključki. Perioperativno zdravljenje pri bolnikih z radikalno resekcijo raka želodca in limfadenektomiji D2 je bilo koristno v stadijih IIIb in IIIc. Neučinkovitost perioperativnega zdravljenja v nižjih stadijih bolezni si lahko razlagamo z učinkovitostjo radikalne kirurgije v teh stadijih, v višjih stadijih pa z biologijo bolezni.

Radiol Oncol 2019; 53(2): 256-264.
doi: 10.2478/raon-2019-0017

Vpliv dejavnikov telesne mase na nastavitveno napako med obsevanjem medenice pri bolnikih z rakom spodnjega abdomna

Wu WC, Chang YR, Ali YL, Shiau AC, Liang JA, Chien CR, Kuo YC, Chen SW

Izhodišča. Namen raziskave je bil proučiti vpliv dejavnikov telesne mase na nastavitveno napako med obsevanjem medenice pri bolnikih z raki spodnjega abdomna.

Bolniki in metode. Analizirali smo klinične podatke kohorte 60 bolnikov z raki rodil, danke ali prostate in podatke o dnevni poravnavi pri slikovno vodeni radioterapiji. Nastavitvene napake smo ocenili s sistemsko napako in naključno napako v smereh superiorno-inferiorno (SI), anteriorno-posteriorno (AP) in medialno-lateralno (ML). Več dejavnikov telesne mase in od bolnikov odvisne dejavnike smo analizirali z binarno logistično regresijo in krivuljami ROC. Uporabili smo točkovni sistem za prepoznavo bolnikov z večjim odstopanjem lege med vsakodnevnim zdravljenjem. Rezultate smo potrdili v drugi kohorti.

Rezultati. Velik lateralni premer kolka je sovpadal z večjo SI in AP sistemsko napako, medtem ko je velik umbilikalni premer AP sovpadal z večjo ML sistemsko napako in ML naključno napako. Večja SI naključna napaka je bila združena z velikim obsegom kolka. Pozitivni napovedovalci nastavitvene negotovosti so bili izbrani z namenom razvrstiti bolnike v skupini z visokim in nizkim tveganjem za odstopanje lege. Glede na točkovni sistem so bili ustrezni terapevtski robovi za smer SI v skupinama z visokim in nizkim tveganjem 5,4 in 3,8 mm, medtem ko so bili robovi za smer ML 8,2 in 4,2 mm. V potrditveni kohorti je bil trend podoben.

Zaključki. Veliki dejavniki telesne mase, tj. lateralni premer kolka, obseg kolka in umbilikalni premer AP, so bili združeni z večjo nastavitveno negotovostjo. Glede na točkovni sistem bi pri bolnikih z dejavniki visokega tveganja lahko prilagodil postopek slikovno vodenega obsevanja ali zahtevane terapevtske robove.



FUNDACIJA "DOCENT DR. J. CHOLEWA"
JE NEPROFITNO, NEINSTITUCIONALNO IN NESTRANKARSKO
ZDRUŽENJE POSAMEZNIKOV, USTANOV IN ORGANIZACIJ, KI ŽELIJO
MATERIALNO SPODBUJATI IN POGLABLJATI RAZISKOVALNO
DEJAVNOST V ONKOLOGIJI.

DUNAJSKA 106
1000 LJUBLJANA

IBAN: SI56 0203 3001 7879 431



Activity of "Dr. J. Cholewa" Foundation for Cancer Research and Education - a report for the second quarter of 2019

Doc. Dr. Josip Cholewa Foundation for cancer research and education continues with its planned activities in the second quarter of 2019. Its primary focus remains the provision of grants and scholarships and other forms of financial assistance for basic, clinical and public health research in the field of oncology. In parallel, it also makes efforts to provide financial and other support for the organisation of congresses, symposia and other forms of meetings to spread the knowledge about prevention and treatment of cancer, and finally about rehabilitation for cancer patients. In Foundation's strategy, the spread of knowledge should not be restricted only to the professionals that treat cancer patients, but also to the patients themselves and to the general public.

The Foundation continues to provide support for »Radiology and Oncology«, a quarterly scientific magazine with a respectable impact factor that publishes research and review articles about all aspects of cancer. The magazine is edited and published in Ljubljana, Slovenia. »Radiology and Oncology« is an open access journal available to everyone free of charge. Its long tradition represents a guarantee for the continuity of international exchange of ideas and research results in the field of oncology for all in Slovenia that are interested and involved in helping people affected by many different aspects of cancer.

The Foundation will continue with its activities in the future, especially since the problems associated with cancer affect more and more people in Slovenia and elsewhere. Ever more treatment that is successful reflects in results with longer survival in many patients with previously incurable cancer conditions. Thus adding many new dimensions in life of cancer survivors and their families.

Viljem Kovač M.D., Ph.D.
Borut Štabuc, M.D., Ph.D.
Tomaž Benulič, M.D.
Andrej Plesničar, M.D., M.Sc.

TANTUM VERDE®

benzidaminijev klorid

Za lajšanje bolečine in oteklin v ustni votlini in žrelu, ki so posledica radiomukozitisa



Bistvene informacije iz Povzetka glavnih značilnosti zdravila

Tantum Verde 1,5 mg/ml oralno pršilo, raztopina

Tantum Verde 3 mg/ml oralno pršilo, raztopina

Sestava 1,5 mg/ml: 1 ml raztopine vsebuje 1,5 mg benzidaminijevega klorida, kar ustreza 1,34 mg benzidamina. V enem razpršku je 0,17 ml raztopine. En razpršek vsebuje 0,255 mg benzidaminijevega klorida, kar ustreza 0,2278 mg benzidamina. **Sestava 3 mg/ml:** 1 ml raztopine vsebuje 3 mg benzidaminijevega klorida, kar ustreza 2,68 mg benzidamina. V enem razpršku je 0,17 ml raztopine. En razpršek vsebuje 0,51 mg benzidaminijevega klorida, kar ustreza 0,4556 mg benzidamina.

Terapevtske indikacije: Samozdravljenje; Lajšanje bolečine in oteklin pri vnetju v ustni votlini in žrelu, ki so lahko posledica okužb in stanj po operaciji. **Po nasvetu in navodilu zdravnika:** Lajšanje bolečine in oteklin v ustni votlini in žrelu, ki so posledica radiomukozitisa. **Odmerjanje in način uporabe:** **Odmerjanje 1,5 mg/ml:** Odrasli: 4 do 8 razprškov 2- do 6-krat na dan (vsake 1,5 do 3 ure). **Pediatrična populacija:** Mladostniki, stari od 12 do 18 let: 4-8 razprškov 2- do 6-krat na dan. Otroci od 6 do 12 let: 4 razprški 2- do 6-krat na dan. Otroci, mlajši od 6 let: 1 razpršek na 4 kg telesne mase; do največ 4 razprške 2- do 6-krat na dan. **Odmerjanje 3 mg/ml:** Uporaba 2- do 6-krat na dan (vsake 1,5 do 3 ure). Odrasli: 2 do 4 razprški 2- do 6-krat na dan. **Pediatrična populacija:** Mladostniki, stari od 12 do 18 let: 2 do 4 razprški 2- do 6-krat na dan. Otroci od 6 do 12 let: 2 razprška 2- do 6-krat na dan. Otroci, mlajši od 6 let: 1 razpršek na 8 kg telesne mase; do največ 2 razprška 2- do 6-krat na dan.

Starejši bolniki, bolniki z jetrno okvaro in bolniki z ledvično okvaro: Uporabo oralnega pršila z benzidaminijevim kloridom se svetuje pod nadzorom zdravnika. **Način uporabe:** Za orofaringealno uporabo. Zdravilo se razprši v usta in žrelo. **Kontraindikacije:** Preobčutljivost na učinkovino ali katero koli pomožno snov. **Posebna opozorila in previdnostni ukrepi:** Če se simptomi v treh dneh ne izboljšajo, se mora bolnik posvetovati z zdravnikom ali zobozdravnikom, kot je primerno. Benzidamin ni priporočljiv za bolnike s preobčutljivostjo na salicilno kislino ali druga nesteroidna protivnetna zdravila. Pri bolnikih, ki imajo ali so imeli bronhialno astmo, lahko pride do bronhospazma, zato je potrebna previdnost. To zdravilo vsebuje majhne količine etanola (alkohola), in sicer manj kot 100 mg na odmerek. To zdravilo vsebuje metilparahidroksibenzoat (E218). Lahko povzroči alergijske reakcije (lahko zapoznele). Zdravilo z jakostjo 3 mg/ml vsebuje makrogolglicerol hidrosistearat 40. Lahko povzroči želodčne težave in drisko. **Medsebojno delovanje z drugimi zdravili in druge oblike interakcij:** Študij medsebojnega delovanja niso izvedli. **Nosečnost in dojenje:** O uporabi benzidamina pri nosečnicah in doječih ženskah ni zadostnih podatkov. Uporaba zdravila med nosečnostjo in dojenjem ni priporočljiva. **Vpliv na sposobnost vožnje in upravljanja strojev:** Zdravilo v priporočenem odmerku nima vpliva na sposobnost vožnje in upravljanja strojev. **Neželeni učinki:** Neznana pogostnost (ni mogoče oceniti iz razpoložljivih podatkov): anafilaktične reakcije, preobčutljivostne reakcije, odrevenelost, laringospazem, suha usta, navzea in bruhanje, angioedem, fotosenzitivnost, pekoč občutek v ustih. Neposredno po uporabi se lahko pojavi občutek odrevenelosti v ustih in v žrelu. Ta učinek se pojavi zaradi načina delovanja zdravila in po kratkem času izgine. **Način in režim izdaje zdravila:** BRp-Izdaja zdravila je brez recepta v lekarnah in specializiranih prodajalnah. **Imetnik dovoljenja za promet:** Angelini Pharma Österreich GmbH, Brigittenauer Lände 50-54, 1200 Dunaj, Avstrija. **Predstavnik imetnika dovoljenja za promet:** Angelini Pharma d.o.o., Koprška ulica 108A, 1000 Ljubljana.

Datum zadnje revizije besedila: za 1,5 mg/ml: 24.05.2017, za 3 mg/ml: 23.08.2018

Pred svetovanjem ali izdajo preberite celoten Povzetek glavnih značilnosti zdravila.

Samo za strokovno javnost.

Datum priprave informacije: maj 2019

Podaljšajmo, kar lahko.



Dokazano podaljša celokupno preživetje (OS) na več kot 1 leto (12,6 mesecev VARGATEF® + docetaksel pri primerjavi z 10,3 mesecev placebo + docetaksel; HR: 0,83 [95% CI 0,70 – 0,99]; P = 0,0359) pri bolnikih, ki ga prejemajo v kombinaciji z docetakselom, z lokalno napredovalim, metastatskim ali lokalno ponovljivim nedrobnoceličnim pljučnim rakom (non-small cell lung cancer – NSCLC) s histologijo adenokarcinoma po kemoterapiji prve izbire.^{1,2}

Vargatef 100 mg mehke kapsule, Vargatef 150 mg mehke kapsule

➤ Za to zdravilo se izvaja dodatno spremljanje varnosti. **Sestava:** ena kapsula vsebuje 100 mg nintedaniba oz. 150 mg nintedaniba (v obliki esilata). Vsebuje sojin lecitin. **Terapevtske indikacije:** indicirano v kombinaciji z docetakselom za zdravljenje odraslih bolnikov z lokalno napredovalim, metastatskim ali lokalno ponovljivim nedrobnoceličnim pljučnim rakom (NSCLC) s histologijo adenokarcinoma po kemoterapiji prve izbire. **Odmerjanje in način uporabe:** zdravljenje mora uvesti in nadzirati zdravnik, ki ima izkušnje z uporabo onkoloških zdravil. Priporočeni odmerek nintedaniba je 200 mg 2x/dan, ki ga je treba jemati v približno 12-urnem razmiku, od 2. do 21. dne standardnega 21-dnevnega cikla zdravljenja z docetakselom. Bolnik ne sme vzeti Vargatefa istega dne, ko prejme kemoterapijo z docetakselom (to je 1. dne). Če bolnik pozabi vzeti priporočeni odmerek nintedaniba, naj ga začne ponovno jemati ob naslednjem načrtovanem času. Posameznih dnevnih priporočenih odmerkov nintedaniba ni dovoljeno povečati, zato da bi nadomestili pozabljene odmerke. Ne smete prekoračiti niti največjega priporočenega dnevnega odmerka 400 mg. Bolniki lahko z zdravljenjem z nintedanibom nadaljujejo po prekinitvi docetaksela, dokler so vidne klinične koristi ali do pojavnosti nesprejemljive toksičnosti. **Prilaganje odmerka:** začetni ukrep za obravnavo neželenih učinkov je začasna prekinitve zdravljenja z nintedanibom, dokler specifični neželeni učinek ne bo izvenel do ravni, ki omogoča nadaljevanje zdravljenja (do 1. stopnje ali izhodiščnega stanja). Zdravljenje lahko nadaljujete z zmanjšanim odmerkom; priporočljivo je postopno prilaganje odmerka po 100 mg na dan (to je zmanjšanje za 50 mg na odmerek) na podlagi individualne varnosti in prenašanja. Kadar neželeni učinki ne izginejo, tj. če bolnik ne prenaša odmerka po 100 mg 2x/dan, je treba zdravljenje trajno ukiniti. V primeru specifičnih povišanih vrednosti AST/ALT na > 3 x ULN v povezavi s povečanjem celokupnega bilirubina na ≥ 2 x ULN in ALKP < 2 x ULN je treba zdravljenje prekiniti. Če ni ugotovljen drug razlog, je treba zdravljenje trajno ukiniti. **Posebne skupine bolnikov:** varnost in učinkovitost pri otrocih, starih 0 do 18 let, še nista dokazani. Pri starejših bolnikih (≥ 65 let) pa na splošno niso opazili razlike. Začetnega odmerka ni treba prilagajati bolnikovi starosti. Podatki o varnosti za črnce in Afroameričane so omejeni. Bolnikom z blago do zmerno ledvično okvaro ali z blago jetno okvaro začetnega odmerka ni treba prilagajati. Začetnega odmerka pri bolnikih z blago jetno okvaro (Child Pugh A) na podlagi kliničnih podatkov ni treba prilagajati. Zdravljenje bolnikov z zmerno (Child Pugh B) in hudo (Child Pugh C) jetno okvaro z Vargatefom ni priporočeno. Kapsule Vargatefa je treba zaužiti cele z vodo, najbolje s hrano; ne sme se jih žvečiti ali drobiti. **Kontraindikacije:** preobčutljivost za nintedanib, arašide ali sojo ali katerokoli pomožno snov. **Previdnostni ukrepi in opozorila:** boleznih prebavil (driska, ki tesno sovpadajo z dajanjem docetaksela; resni primeri driske s posledično dehidracijo in elektrolitskimi motnjami, navzea in bruhanje; zdravljenje je zato včasih treba prekiniti, zmanjšati odmerek ali trajno ukiniti), nevtropenija in sepsa (potrebno je spremljati krvno sliko), delovanje jeter (večja izpostavljenost pri Child Pugh A, zdravljenje pri Child Pugh B ali C pa ni priporočeno, opažene poškodbe jeter (vključno s hudo poškodbo jeter s smrtnim izidom), tveganje za povečanje ravnih jetrnih encimov), delovanje ledvic (pozornost ob ledvični okvari/odpovedi), krvavitev (blaga do zmerna epistaksa, večina usodnih krvavitev je bila povezanih s tumorjem). Poročali so o resnih in neresnih krvavitvah (tudi smrtni izid), ki vključujejo prebavila, dihala in organe osrednjega živčnega sistema, najbolj pogoste pa so krvavitve v dihalih. V primeru krvavitve je treba razmisliti o prilagoditvi odmerka, prekinutvi ali trajni ukinitvi zdravljenja na podlagi klinične ocene), terapevtska antikoagulacija, metastaza v možganih (stabilne in aktivne metastaze v možganih), venska tromboembolija (povečano tveganje za vensko tromboembolijo, vključno z globoko vensko trombozo), arterijski tromboembolični dogodki (pri bolnikih z IPF, z večjim srčnožilnim tveganjem, vključno z znano koronarno arterijsko boleznijo), predrtje prebavil, zapleti s celjenjem ran, vpliv na interval QT, alergijska reakcija (alergija na sojo in arašidove beljakovine), posebne populacije (izpostavljenost se večja z bolnikovo starostjo in obratno korelira s telesno maso, večja pri bolnikih azijske rase). **Interakcije:** močni zaviralci P-gp (ketokonazolom, eritromicin), močni induktorji P-gp (rifampicin, karbamazepin, fenitoin in šentjanževka), encimi citokroma (CYP), sočasno dajanje z drugimi zdravili (sočasno dajanje nintedaniba z docetakselom ni spremenilo farmakokinetike nobenega od zdravil v pomembnem obsegu). **Neželeni učinki: Zelo pogosti:** nevtropenija (vključno s febrilno nevtropenijo), zmanjšan apetit, neravnovesje elektrolitov, periferna nevropatija, krvavitev, driska, bruhanje, navzea, trebušna bolečina, povečana vrednost ALT, AST in ALKP, mukoziti (vključno s stomatitisom) in izpuščaj. **Pogosti:** febrilna nevtropenija, abscesi, sepsa, trombocitopenija, dehidracija, zmanjšanje telesne mase, venska tromboembolija, hipertenzija, hiperbilirubinemija, povečana vrednost GGT in pruritusa. **Občasni:** miokardni infarkt, perforacija, pankreatitis, z zdravilom povzročena poškodba jeter in ledvična odpoved. **Imetnik dovoljenja za promet:** Boehringer Ingelheim International GmbH, Binger Str. 173, D-55216 Ingelheim am Rhein, Nemčija. **Način in režim izdaje:** Rp. **Za podrobnejše informacije glejte SPC, z dne 07/2018.**

Literatura: 1. VARGATEF® Povzetek glavnih značilnosti zdravila 2. Reck M et al. Lancet Oncol. 2014;15:143-55.

V kolikor imate medicinsko vprašanje v povezavi z zdravilom podjetja Boehringer Ingelheim, Podružnica Ljubljana, Vas prosimo, da pokličete na telefonsko številko 01/5864-000 ali pošljete vaše vprašanje na elektronski nastav: medinfo@boehringer-ingelheim.com.

Our collection of VWR Brands

solutions for science



Zdravilo za predhodno že zdravljene bolnike z mKRR

Več časa za trenutke, ki štejejo




Lonsurf®
trifluridin/tipiracil

Spremeni zgodbo predhodno že zdravljenih bolnikov z mKRR

LONsurf® (trifluridin/tipiracil) je indiciran za zdravljenje odraslih bolnikov z metastatskim kolorektalnim rakom (mKRR), ki so bili predhodno že zdravljeni ali niso primerni za zdravljenja, ki so na voljo. Ta vključujejo kemoterapijo na osnovi fluoropirimidina, oksaliplatina in irinotekana, zdravljenje z zaviralci žilnega endotelijskega rastnega dejavnika (VEGF) in zaviralci receptorjev za epidermalni rastni dejavnik (EGFR).

mKRR = metastatski kolorektalni rak

Družba Servier ima licenco družbe Taiho za zdravilo Lonsurf®. Pri globalnem razvoju zdravila sodelujeta obe družbi in ga tržiša na svojih določenih področjih.



TAIHO PHARMACEUTICAL CO., LTD.



Skrajšan povzetek glavnih značilnosti zdravila: Lonsurf 15 mg/6,14 mg filmsko obložene tablete in Lonsurf 20 mg/8,19 mg filmsko obložene tablete

▼ Za to zdravilo se izvaja dodatno spremljanje varnosti. **SESTAVA:** Lonsurf 15 mg/6,14 mg: Ena filmsko obložena tableta vsebuje 15 mg trifluridina in 6,14 mg tipiracila (v obliki klorida). Lonsurf 20 mg/8,19 mg: Ena filmsko obložena tableta vsebuje 20 mg trifluridina in 8,19 mg tipiracila (v obliki klorida). **TERAPEVTSKE INDIKACIJE:** Zdravilo Lonsurf je indicirano za zdravljenje odraslih bolnikov z metastatskim kolorektalnim rakom, ki so bili predhodno že zdravljeni ali niso primerni za zdravljenja, ki so na voljo. Ta vključujejo kemoterapijo na osnovi fluoropirimidina, oksaliplatina in irinotekana, zdravljenje z zaviralci žilnega endotelijskega rastnega dejavnika (VEGF - Vascular Endothelial Growth Factor) in zaviralci receptorjev za epidermalni rastni dejavnik (EGFR - Epidermal Growth Factor Receptor). **ODMERJANJE IN NAČIN UPORABE:** Priporočeni začetni odmerek zdravila Lonsurf pri odraslih je 35 mg/m²/odmerek peroralno dvakrat dnevno na 1. do 5. dan in 8. do 12. dan vsakega 28-dnevnega cikla zdravljenja, najpozneje 1 uro po zaključku jutranjega in večernega obroka. Odmernjevanje, izračunano glede na telesno površino, ne sme presegati 80 mg/odmerek. Možne prilagoditve odmerka glede na varnost in prenašanje zdravila: dovoljena so največ 3 zmanjšanja odmerka na najmanjši odmerek 20 mg/m² dvakrat dnevno. Potem ko je bil odmerek zmanjšan, povečanje ni dovoljeno. **KONTRAINDIKACIJE:** Preobčutljivost na zdravilni učinkovini ali katero koli pomožno snov. **OPAZORILA IN PREVIDNOSTI UKREPI:** Supresija kostnega mozga: Pred uvedbo zdravljenja, pred vsakim ciklom zdravljenja in po potrebi je treba pregledati celotno krvno sliko. Zdravljenja ne sme začeti, če je absolutno število levkocitov < 1,5 x 10⁹/l, če je število trombocitov < 75 x 10⁹/l ali če se je pri bolniku zaradi predhodnih zdravljenj pojavila klinično pomembna nehematološka toksičnost 3. ali 4. stopnje, ki še traja. Bolnike je treba skrbno spremljati zaradi morebitnih okužb, uvesti je treba ustrezne ukrepe, kot je klinično indicirano. **Toksičnosti za prebavila:** Potrebna je uporaba antiemetikov, antidiaroičkov ter drugih ukrepov, kot je klinično indicirano. Če je potrebno, prilagodite odmerke. **Ledvična okvara:** Zdravilo Lonsurf ni primerno za uporabo pri bolnikih s hudo ledvično okvaro ali končno stopnjo ledvične okvare. Bolnike z zmerno ledvično okvaro je treba zaradi hematološke toksičnosti bolj pogosto spremljati. **Jetrna okvara:** Uporaba zdravila Lonsurf pri bolnikih z obstoječo zmerno ali hudo jetrno okvaro ni priporočljiva. **Proteinurija:** Pred začetkom zdravljenja in med njim je priporočljivo spremljanje proteinurije z urinskimi testnimi lističi. **Pomožne snovi:** Zdravilo vsebuje laktozo. **INTERAKCIJE:** Zdravila, ki medsebojno delujejo z nukleozidnimi prenašalci CNT1, ENT1 in ENT2, zaviralci OCT2 ali MATE1, substrati humane timidin-kinaze (npr. zidovudinom), hormonskimi kontraceptivi. **PLODNOST, NOSEČNOST IN DOJEJENJE:** Ni priporočljivo. **KONTRACEPCIJA:** Zenske in moški morajo uporabljati učinkovito metodo kontracepcije med zdravljenjem in do 6 mesecev po zaključku zdravljenja. **VPLIV NA SPOSOBNOST VOZNIJE IN UPRAVLJANJA S STROJI:** Med zdravljenjem se lahko pojavijo utrujenost, omotica ali splošno slabo počutje. **NEŽELENI UČINKI:** **Zelo pogosti:** nevropenija, levkopenija, anemija, trombocitopenija, zmanjšan apetit, diareja, navzea, bruhanje, utrujenost. **Pogosti:** okužba spodnjih dihal, okužba zgornjih dihal, febrilna nevropenija, limfopenija, monocitoza, hipalbuminemija, nespečnost, disgevgzija, periferna nevropatija, omotica, glavobol, vročinski oblivi, dispneja, kašelj, bolečina v trebuhu, zaprtje, stomatitis, boleži ustne votline, hiperbilirubinemija, sindrom palmarne plantarne eritrodiseestezijske, izpuščaj, alopecija, pruritus, suha koža, proteinurija, pireksija, edem, vnetje sluznice, splošno slabo počutje, zvišanje jetrnih encimov, zvišanje alkalne fosfataze v krvi, zmanjšanje telesne mase. **Občasni:** septični šok, infektivni enteritis, pljučnica, okužba žolčevoda, gripa, okužba sečil, vnetje dlesni, herpes zoster, tinea pedis, kandidiaza, bakterijska okužba, okužba, bolečina zaradi raka, pancitopenija, granulocitopenija, monocitopenija, eritropenija, levkocitoza, dehidracija, hiperglikemija, hiperkalemija, hipokaliemija, hipofosfatemija, hipernatriemija, hiponatriemija, hipokalcemija, protin, anksioznost, neurotoksičnost, disestezijska, hiperestezijska, hipoestezijska, sinkopa, parestezijska, pekoč občutek, letargija, zmanjšana ostrina vida, zamogeljen vid, diplopija, katarakta, konjunktivitis, suho oko, vrtoglavica, neugodje v ušesu, angina pectoris, aritmija, palpitacije, embolija, hipertenzija, hipotenzija, pljučna embolija, plevralni izliv, izcedek iz nosu, disonija, orofaringea bolečina, epistaksa, hemoragični enterokolitis, krvavitve v prebavilih, akutni pankreatitis, ascites, ileus, subileus, kolitis, gastritis, reflukсни gastritis, ezofagitis, moteno praznjenje želodca, abdominalna distenzija, analno vnetje, razjede v ustih, dispepsija, gastroezofagealna refleksna bolezen, proktalgija, bukalni polip, krvavitve dlesni, glositis, parodontalna bolezen, bolezen zob, siljenje na bruhanje, flatulenca, slab zadah, hepatotoksičnost, razširitev žolčnih vodov, luščenje kože, urtikarija, preobčutljivostne reakcije na svetlobo, eritem, akne, hiperhidroza, žulj, boleži nohtov, otekanje sklepov, artralgijska, bolečina v kosteh, migalgijska, mišično-skeletna bolečina, mišična oslabelost, mišični krči, bolečina v okončinah, občutek teže, ledvična odpoved, neinfektivni cistitis, motnje mikcije, hematURIJA, levkociturija, motnje menstruacije, poslabšanje splošnega zdravstvenega stanja, bolečina, občutek spremembe telesne temperature, kseroza, zvišanje kreatinina v krvi, podaljšanje intervala QT na elektrokardiogramu, povečanje mednarodnega umerjenega razmerja (INR), podaljšanje parcialega aktiviranega trombolastinskega časa (aPTC), zvišanje sečnine v krvi, zvišanje laktatne dehidrogenaze v krvi, znižanje celokupnih proteinov, zvišanje C-reaktivnega proteina, zmanjšan hematokrit. **Post-marketingne izkušnje:** pri bolnikih, zdravljenih z zdravilom Lonsurf na Japonskem, so poročali o primerih intersticijske bolezni pljuč. **PREVELIKO ODMERJANJE:** Neželeni učinki, o katerih so poročali v povezavi s prevelikim odmerjanjem, so bili v skladu z uveljavljenim varnostnim profilom. Glavni pricakovani zaplet prevelikega odmerjanja je supresija kostnega mozga. **FARMAKODINAMIČNE LASTNOSTI:** **Farmakoterapevtska skupina:** zdravila z delovanjem na novotvorbo, antimetaboliti, oznaka ATC: L01BC59. Zdravilo Lonsurf sestavljata antineoplastični timidinski nukleozidni analog, trifluridin, in zaviralec timidin-fosforilaze (TPaze), tipiraciljev klorid. Po prizemu v rakuve celice timidin-kinaza fosforilira trifluridin. Ta se v celicah nato presnovi v substrat deoksiribonukleinske kisline (DNA), ki se vgradi neposredno v DNA ter tako preprečuje celično proliferacijo. TPaza hitro razgradi trifluridin in njegova presnova po peroralni uporabi je hitra zaradi učinka prvega prehoda, zato je v zdravilo vključen zaviralec TPaze, tipiraciljev klorid. **PAKIRANJE:** 20 filmsko obloženih tablet, 15 mg/6,14 mg, EU/1/16/1096/004 (Lonsurf 20 mg/8,19 mg). **Datum zadnje revizije besedila:** avgust 2017. * Pred predpisovanjem preberite celoten povzetek glavnih značilnosti zdravila. Celoten povzetek glavnih značilnosti zdravila in podrobnejše informacije so na voljo pri: Servier Pharma d.o.o., Podmilščakova ulica 24, 1000 Ljubljana, tel.: 01 563 48 11, www.servier.si.

NOVO
pri HR+/
HER2- mBC

Verzenios™
abemaciclib

EDINI zaviralec CDK4 & 6, ki se jemlje NEPREKINJENO VSAK DAN.^{1, 2, 3}

SKRAJŠAN POVZETEK GLAVNIH ZNAČILNOSTI ZDRAVILA

▼ Za to zdravilo se izvaja dodatno spremljanje varnosti. Tako bodo hitreje na voljo nove informacije o njegovi varnosti. Zdravstvene delavce naprošamo, da poročajo o katerem koli domnevem neželenem učinku zdravila.

IME ZDRAVILA Verzenios 50 mg/100 mg/150 mg filmsko obložene tablete **KAKOVOSTNA IN KOLIČINSKA SESTAVA** Ena filmsko obložena tableta vsebuje 50 mg/100 mg/150 mg abemacicliba. Ena filmsko obložena tableta vsebuje 14 mg/28 mg/42 mg laktoze (v obliki monohidrata). **Terapevtske indikacije** Zdravilo Verzenios je indicirano za zdravljenje žensk z lokalno napredovalim ali metastatskim, na hormonske receptorje (HR – *Hormone Receptor*) pozitivnim in na receptorje humanega epidermalnega rastnega faktorja 2 (HER2 – *Human Epidermal Growth Factor Receptor 2*) negativnim rakom dojk v kombinaciji z zaviralcem aromataze ali s fulvestrantom kot začetnim endokrinim zdravljenjem ali pri ženskah, ki so prejele predhodno endokrinno zdravljenje. Pri ženskah v pred- in perimenopavzi je treba endokrinno zdravljenje kombinirati z agonistom gonadoliberina (LHRH – *Luteinizing Hormone-Releasing Hormone*). **Odmerjanje in način uporabe** Zdravljenje z zdravilom Verzenios mora uvesti in nadzorovati zdravnik, ki ima izkušnje z uporabo zdravil za zdravljenje rakavih bolezni. **Zdravilo Verzenios v kombinaciji z endokrinim zdravljenjem** Priporočeni odmerek abemacicliba je 150 mg dvakrat na dan, kadar se uporablja v kombinaciji z endokrinim zdravljenjem. Zdravilo Verzenios je treba jemati, dokler ima bolnica od zdravljenja klinično korist ali dokler se ne pojavi nesprejemljiva toksičnost. Če bolnica bruha ali izpusti odmerek zdravila Verzenios, ji je treba naročiti, da naj naslednji odmerek vzame ob predvidenem času; dodatnega odmerka ne sme vzeti. Obvladovanje nekaterih neželenih učinkov lahko zahteva prekinitve in/ali zmanjšanje odmerka. Sočasni uporabi močnih zaviralcev CYP3A4 se je treba izogibati. Če se uporabi močnih zaviralcev CYP3A4 ni mogoče izogniti, je treba odmerek abemacicliba zmanjšati na 100 mg dvakrat na dan. Pri bolnicah, pri katerih je bil odmerek zmanjšán na 100 mg abemacicliba dvakrat na dan in pri katerih se sočasnemu dajanju močnega zaviralca CYP3A4 ni mogoče izogniti, je treba odmerek abemacicliba zmanjšati na 50 mg dvakrat na dan. Pri bolnicah, pri katerih je bil odmerek zmanjšán na 50 mg abemacicliba dvakrat na dan in pri katerih se sočasnemu dajanju močnega zaviralca CYP3A4 ni mogoče izogniti, je mogoče z odmerkom abemacicliba nadaljevati ob natančnem spremljanju znakov toksičnosti. Alternativno je mogoče odmerek abemacicliba zmanjšati na 50 mg enkrat na dan ali prekiniti dajanje abemacicliba. Če je uporaba zaviralca CYP3A4 prekinjena, je treba odmerek abemacicliba povečati na odmerek, kakršen je bil pred uvedbo zaviralca CYP3A4 (po 3–5 razpolovnih časih zaviralca CYP3A4). Prilagajanje odmerka glede na starost in pri bolnicah z blago ali zmerno ledvično okvaro ter z blago (Child Pugh A) ali zmerno (Child Pugh B) jetrno okvaro ni potrebno. Pri dajanju abemacicliba bolnicam s hudo ledvično okvaro sta potrebna previdnost in skrbno spremljanje glede znakov toksičnosti. Način uporabe Zdravilo Verzenios je namenjeno za peroralno uporabo. Odmerek se lahko vzame s hrano ali brez nje. Zdravilo se ne sme jemati z grenivko ali grenivkinim sokom. Bolnice naj odmerke vzamejo vsak dan ob približno istem času. Tableto je treba zaužiti celo (bolnice je pred zaužitjem ne smejo gristi, drobiti ali deliti). **Kontraindikacije** Preobčutljivost na učinkovino ali katero koli pomožno snov. **Posebna opozorila in previdnostni ukrepi** Pri bolnicah, ki so prejemale abemaciclib, so poročali o nevtropeniji, o večji pogostosti okužb kot pri bolnicah, zdravljenih s placebom in endokrinim zdravljenjem, o povečanih vrednostih ALT in AST. Pri bolnicah, pri katerih se pojavi nevtropenija stopnje 3 ali 4, je priporočljivo prilagoditi odmerek. Bolnice je treba spremljati za znake in simptome globoke venske tromboze in pljučne embolije ter jih zdraviti, kot je medicinsko utemeljeno. Glede na povečanje vrednosti ALT ali AST je mogoče potrebna prilagoditev odmerka. Driska je najpogostejši neželeni učinek. Bolnice je treba ob prvem znaku tekočega blata začeti zdraviti z antiidiaroiiki, kot je loperamid, povečati vnos peroralnih tekočin in obvestiti zdravnika. Sočasni uporabi močnih induktorjev CYP3A4 se je treba izogibati zaradi tveganja za zmanjšano učinkovitost abemacicliba. Bolnice z redkimi dednimi motnjami, kot so intoleranca za galaktozo, popolno pomanjkanje laktaze ali malabsorpcija glukoze/galaktoze, tega zdravila ne smejo jemati. **Medsebojno delovanje z drugimi zdravili in druge oblike interakcij** Abemaciclib se primarno presnavlja s CYP3A4. Sočasna uporaba abemacicliba in zaviralcev CYP3A4 lahko poveča plazemsko koncentracijo abemacicliba. Uporabi močnih zaviralcev CYP3A4 sočasno z abemaciclibom se je treba izogibati. Če je treba uporabiti zaviralce CYP3A4, je treba dati sočasno, je treba odmerek abemacicliba zmanjšati, nato pa bolnico skrbno spremljati glede toksičnosti. Pri bolnicah, zdravljenih z zmernimi ali šibkimi zaviralci CYP3A4, ni potrebno prilagajanje odmerka, vendar jih je treba skrbno spremljati za znake toksičnosti. Sočasni uporabi močnih induktorjev CYP3A4 (vključno, vendar ne omejeno na: karbamazepin, fenitoin, rifampicin in šentjanževko) se je treba izogibati zaradi tveganja za zmanjšano učinkovitost abemacicliba. Abemaciclib in njegovi glavni aktivni presnovki zavirajo prenašalce v ledvicah, in sicer kationski organski prenašalec 2 (OCT2) ter prenašalca MATE1. *In vivo* lahko pride do medsebojnega delovanja abemacicliba in klinično pomembnih substratov teh prenašalcev, kot je dofetilid ali kreatinin. Trenutno ni znano, ali lahko abemaciclib zmanjša učinkovitost sistemskih hormonskih kontraceptivov, zato se ženskam, ki uporabljajo sistemske hormonske kontraceptive, svetuje, da hkrati uporabljajo tudi mehansko metodo. **Neželeni učinki** Najpogostejši neželeni učinki so driska, okužbe, nevtropenija, anemija, utrujenost, navzea, bruhanje in zmanjšanje apetita. **Zelo pogosti:** okužbe, nevtropenija, levkopenija, anemija, trombocitopenija, driska, bruhanje, navzea, zmanjšanje apetita, disgevizija, omotica, alopecija, pruritus, izpuščaji, utrujenost, piroksija, povečana vrednost alanin-aminotransferaze, povečana vrednost aspartat-aminotransferaze **Pogosti:** limfopenija, povečano solzenje, venska tromboembolija, suha koža, mišična šibkost **Občasni:** febrilna nevtropenija **Imetnik dovoljenja za promet z zdravilom:** Eli Lilly, Nederland B.V., Papendorpseweg 83, 3528BJ, Utrecht, Nizozemska. Datum prve odobritve dovoljenja za promet: 27. september 2018 Datum zadnje revizije besedila: 2.11.2018 **Režim izdaje:** Rp/Spec - Predpisovanje in izdaja zdravila je le na recept zdravnika specialista ustreznega področja medicine ali od njega pooblaščenega zdravnika.

Reference

1. Povzetek glavnih značilnosti zdravila Verzenios. Datum zadnje revizije besedila: 2.11.2018. **2.** Povzetek glavnih značilnosti zdravila Ibrance. Dostop preverjen 22.11.2018. **3.** Povzetek glavnih značilnosti zdravila Kisqali. Dostop preverjen 22.11.2018.

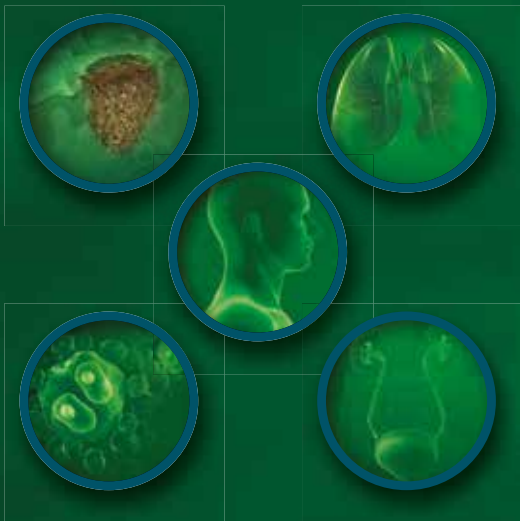
Pomembno obvestilo

Pričujoče gradivo je namenjeno samo za strokovno javnost. Predpisovanje in izdaja zdravila Verzenios je le na recept zdravnika specialista ustreznega področja medicine ali od njega pooblaščenega zdravnika. Pred predpisovanjem zdravila Verzenios vas vlijudno prosimo, da preberete celotni Povzetek glavnih značilnosti zdravila. Podrobnejše informacije o zdravilu Verzenios in o zadnji reviziji besedila Povzetka glavnih značilnosti zdravila so na voljo na sedežu podjetja Eli Lilly (naslov podjetja in kontaktni podatki spodaj) in na spletni strani European Medicines Agency (EMA); www.ema.europa.eu in na spletni strani European Commission <http://ec.europa.eu/health/documents/community-register/html/alfregister.htm>.

Eli Lilly farmacevtska družba, d.o.o., Dunajska cesta 167, 1000 Ljubljana, telefon 01 / 580 00 10, faks 01 / 569 17 05

PP-AL-SI-0001, 23.11.2018, Samo za strokovno javnost.

Lilly



- Melanom¹
- Nedrobnocelični pljučni rak¹
- Urotelijski karcinom¹
- Hodgkinov limfom¹
- Ploščatocelični karcinom glave in vratu¹

References: 1. Keytruda EU SmPC

SKRAJŠAN POVZETEK GLAVNIH ZNAČILNOSTI ZDRAVILA

Pred predpisovanjem, prosimo, preberite celoten Povzetek glavnih značilnosti zdravila!

▼ Za to zdravilo se izvaja dodatno spremljanje varnosti.

Ime zdravila: KEYTRUDA 25 mg/ml koncentrat za raztopino za infundiranje vsebuje pembrolizumab.

Terapevtske indikacije: Zdravilo KEYTRUDA je kot samostojno zdravljenje indicirano za zdravljenje: napredovalega (neoperabilnega ali metastatskega) melanoma pri odraslih; za adjuvantno zdravljenje odraslih s melanomom v stadiju III, ki se je razširil na bezgavke, po popolni kirurški odstranitvi; metastatskega nedrobnoceličnega pljučnega raka (NSCLC) v prvi liniji zdravljenja pri odraslih, ki imajo tumorje z $\geq 50\%$ izraženostjo PD-L1 (TPS) in brez pozitivnih tumorskih mutacij EGFR ali ALK; lokalno napredovalega ali metastatskega NSCLC pri odraslih, ki imajo tumorje z $\geq 1\%$ izraženostjo PD-L1 (TPS) in so bili predhodno zdravljeni z vsaj eno shemo kemoterapije. Bolniki s pozitivnimi tumorskimi mutacijami EGFR ali ALK so pred prejemom zdravila KEYTRUDA morali prejeti tudi tarčno zdravljenje; odraslih bolnikov s ponovljenim ali neodzivnim klasičnim Hodgkinovim limfomom (cHL), pri katerih avtologna presaditev matičnih celic (ASCT) in zdravljenje z brentuksimabom vedotinom (BV) nista bila uspešna, in odraslih bolnikov, ki za presaditev niso primerni, zdravljenje z BV pa pri njih ni bilo uspešno; lokalno napredovalega ali metastatskega urotelijskega karcinoma pri odraslih, predhodno zdravljenih s kemoterapijo, ki je vključevala platino; lokalno napredovalega ali metastatskega urotelijskega karcinoma pri odraslih, ki niso primerni za zdravljenje s kemoterapijo, ki vsebuje cisplatin in imajo tumorje z izraženostjo PD-L1 ≥ 10 , ocenjeno s kombinirano pozitivno oceno (CPS); ponovljenega ali metastatskega ploščatoceličnega karcinoma glave in vratu (HNSCC) pri odraslih, ki imajo tumorje z $\geq 50\%$ izraženostjo PD-L1 (TPS), in pri katerih je bolezen napredovala med zdravljenjem ali po zdravljenju s kemoterapijo, ki je vključevala platino; Zdravilo KEYTRUDA je v kombinaciji s pemetreksedom in kemoterapijo na osnovi platine indicirano za prvo linijo zdravljenja metastatskega neploščatoceličnega NSCLC pri odraslih, pri katerih tumorji nimajo pozitivnih mutacij EGFR ali ALK; v kombinaciji s karboplatinom in bodisi paklitakselom bodisi nab-paklitakselom indicirano za prvo linijo zdravljenja metastatskega ploščatoceličnega NSCLC pri odraslih.

Odmerjanje in način uporabe: Testiranje PD-L1 pri bolnikih z NSCLC, urotelijskim karcinomom ali HNSCC: Pri bolnikih z NSCLC je priporočljivo opraviti testiranje izraženosti PD-L1 tumorja z validirano preiskavo. Bolnike s predhodno nezdravljenim urotelijskim karcinomom ali HNSCC je treba za zdravljenje izbrati na podlagi izraženosti PD-L1, potrjene z validirano preiskavo.

Odmerjanje: Priporočeni odmerek zdravila KEYTRUDA za samostojno zdravljenje je bodisi 200 mg na 3 tedne ali 400 mg na 6 tednov, apliciran z intravensko infuzijo v 30 minutah. Priporočeni odmerek za kombinirano zdravljenje je 200 mg na 3 tedne, apliciran z intravensko infuzijo v 30 minutah. Če se uporablja kot del kombiniranega zdravljenja skupaj s kemoterapijo, je treba zdravilo KEYTRUDA aplicirati prvo. Bolnike je treba zdraviti do napredovanja bolezni ali nesprejemljivih toksičnih učinkov. Pri adjuvantnem zdravljenju melanoma je treba zdravilo uporabljati do ponovitve bolezni, pojava nesprejemljivih toksičnih učinkov oziroma mora zdravljenje trajati do enega leta. Pri bolnikih starih ≥ 65 let, bolnikih z blago do zmerno okvaro ledvic, bolnikih z blago okvaro jeter prilagoditev odmerka ni potrebna. Odložitev odmerka ali ukinitve zdravljenja: Za primere, kjer je treba zdravljenje zadržati, dokler se neželeni učinki ne zmanjšajo na stopnjo 0-1 in kadar je treba zdravilo KEYTRUDA trajno ukiniti, prosimo, glejte celoten Povzetek glavnih značilnosti zdravila. Kontraindikacije: Preobčutljivost na učinkovino ali katero koli pomožno snov.

Povzetek posebnih opozoril, previdnostnih ukrepov, interakcij in neželenih učinkov Imunsko pogojeni neželeni učinki (pnevmonitis, kolitis, hepatitis, nefritis, endokrinopatije, neželeni učinki na kožo in drugi): Pri bolnikih, ki so

prejemali pembrolizumab, so se pojavili imunsko pogojeni neželeni učinki, vključno s hudimi in smrtnimi primeri. Večina imunsko pogojenih neželenih učinkov, ki so se pojavili med zdravljenjem s pembrolizumabom, je bila reverzibilnih in so jih obvladali s prekinitvami uporabe pembrolizumaba, uporabo kortikosteroidov in/ali podporno oskrbo. Pojavijo se lahko tudi po zadnjem odmerku pembrolizumaba in hkrati prizadanejo več organskih sistemov. V primeru suma na imunsko pogojene neželeno učinke je treba poskrbeti za ustrezno oceno za potrditev etiologije oziroma izključitev drugih vzrokov. Glede na izrazitost neželenega učinka je treba zadržati uporabo pembrolizumaba in uporabiti kortikosteroide – za natančna navodila prosim pogledajte Povzetek glavnih značilnosti zdravila Keytruda. Zdravljenje s pembrolizumabom lahko poveča tveganje za zavrnitev pri prejemnikih presadkov čvrstih organov. Pri bolnikih, ki so prejemali pembrolizumab, so poročali o hudih z infuzijo povezanih reakcijah, vključno s preobčutljivostjo in anafilaksijo. Pembrolizumab se iz obtoka odstrani s katabolizmom, zato presnovnih medsebojnih delovanj zdravil ni pričakovati. Uporabi sistemskih kortikosteroidov ali imunosupresivov pred uvedbo pembrolizumaba se je treba izogibati, ker lahko vplivajo na farmakodinamično aktivnost in učinkovitost pembrolizumaba. Vendar pa je kortikosteroide ali druge imunosupresive mogoče uporabiti za zdravljenje imunsko pogojenih neželenih učinkov. Ženske v rodni dobi morajo med zdravljenjem s pembrolizumabom in vsaj še 4 mesece po zadnjem odmerku pembrolizumaba uporabljati učinkovito kontracepcijo, med nosečnostjo in dojenjem se ga ne sme uporabljati. Varnost pembrolizumaba pri samostojnem zdravljenju so v kliničnih študijah ocenili pri 4.948 bolnikih z napredovalim melanomom, kirurško odstranjenim melanomom v stadiju III (adjuvantno zdravljenje), NSCLC, cHL, urotelijskim karcinomom ali HNSCC s štirimi odmerki (2 mg/kg na 3 tedne, 200 mg na 3 tedne in 10 mg/kg na 2 ali 3 tedne). V tej populaciji bolnikov je mediani čas opazovanja znašal 7,3 mesece (v razponu od 1 dneva do 31 mesecev), najpogostejši neželeni učinki zdravljenja s pembrolizumabom so bili utrujenost (34,1 %), izpuščaj (22,7 %), navzea (21,7 %), diareja (21,5 %) in pruritus (20,2 %). Večina poročanih neželenih učinkov pri samostojnem zdravljenju je bila po izrazitosti 1. ali 2. stopnje. Najresnejši neželeni učinki so bili imunsko pogojeni neželeni učinki in hude z infuzijo povezane reakcije. Varnost pembrolizumaba pri kombiniranem zdravljenju s kemoterapijo so ocenili pri 791 bolnikih NSCLC, ki so v kliničnih študijah prejeli pembrolizumab v odmerkih 200 mg, 2 mg/kg ali 10 mg/kg na vsake 3 tedne. V tej populaciji bolnikov so bili najpogostejši neželeni učinki naslednji: navzea (49 %), anemija (48 %), utrujenost (38 %), zaprtost (34%), diareja (31%), nevropenija (29 %), in zmanjšanje apetita (28 %). Pri kombiniranem zdravljenju s pembrolizumabom je pojavnost neželenih učinkov 3. do 5. stopnje znašala 67 %, pri zdravljenju samo s kemoterapijo pa 66 %. Za celoten seznam neželenih učinkov prosimo, glejte celoten Povzetek glavnih značilnosti zdravila.

Način in režim izdaje zdravila: H – Predpisovanje in izdaja zdravila je samo na recept, zdravilo se uporablja samo v bolnišnicah.

Imetnik dovoljenja za promet z zdravilom: Merck Sharp & Dohme B.V., Waarderweg 39, 2031 BN Haarlem, Nizozemska

Datum zadnje revizije besedila: 28. marec 2019



Merck Sharp & Dohme inovativna zdravila d.o.o.,
Šmartinska cesta 140, 1000 Ljubljana,
tel: +386 1/520 42 01, fax: +386 1/520 43 50
Pripravljen v Sloveniji, marec 2019; SI-KEY-00002 EXP: 03/2021

Samo za strokovno javnost.

H - Predpisovanje in izdaja zdravila je le na recept, zdravilo pa se uporablja samo v bolnišnicah. Pred predpisovanjem, prosimo, preberite celoten Povzetek glavnih značilnosti zdravila Keytruda, ki je na voljo pri naših strokovnih sodelavcih ali na lokalnem sedežu družbe.

Instructions for authors

The editorial policy

Radiology and Oncology is a multidisciplinary journal devoted to the publishing original and high quality scientific papers and review articles, pertinent to diagnostic and interventional radiology, computerized tomography, magnetic resonance, ultrasound, nuclear medicine, radiotherapy, clinical and experimental oncology, radiobiology, radiophysics and radiation protection. Therefore, the scope of the journal is to cover beside radiology the diagnostic and therapeutic aspects in oncology, which distinguishes it from other journals in the field.

The Editorial Board requires that the paper has not been published or submitted for publication elsewhere; the authors are responsible for all statements in their papers. Accepted articles become the property of the journal and, therefore cannot be published elsewhere without the written permission of the editors.

Submission of the manuscript

The manuscript written in English should be submitted to the journal via online submission system Editorial Manager available for this journal at: www.radioloncol.com.

In case of problems, please contact Sašo Trupej at saso.trupej@computing.si or the Editor of this journal at gsera@onko-i.si

All articles are subjected to the editorial review and when the articles are appropriated they are reviewed by independent referees. In the cover letter, which must accompany the article, the authors are requested to suggest 3-4 researchers, competent to review their manuscript. However, please note that this will be treated only as a suggestion; the final selection of reviewers is exclusively the Editor's decision. The authors' names are revealed to the referees, but not vice versa.

Manuscripts which do not comply with the technical requirements stated herein will be returned to the authors for the correction before peer-review. The editorial board reserves the right to ask authors to make appropriate changes of the contents as well as grammatical and stylistic corrections when necessary. Page charges will be charged for manuscripts exceeding the recommended length, as well as additional editorial work and requests for printed reprints.

Articles are published printed and on-line as the open access (<https://content.sciendo.com/raon>).

All articles are subject to 700 EUR + VAT publication fee. Exceptionally, waiver of payment may be negotiated with editorial office, upon lack of funds.

Manuscripts submitted under multiple authorship are reviewed on the assumption that all listed authors concur in the submission and are responsible for its content; they must have agreed to its publication and have given the corresponding author the authority to act on their behalf in all matters pertaining to publication. The corresponding author is responsible for informing the coauthors of the manuscript status throughout the submission, review, and production process.

Preparation of manuscripts

Radiology and Oncology will consider manuscripts prepared according to the Uniform Requirements for Manuscripts Submitted to Biomedical Journals by International Committee of Medical Journal Editors (www.icmje.org). The manuscript should be written in grammatically and stylistically correct language. Abbreviations should be avoided. If their use is necessary, they should be explained at the first time mentioned. The technical data should conform to the SI system. The manuscript, excluding the references, tables, figures and figure legends, must not exceed 5000 words, and the number of figures and tables is limited to 8. Organize the text so that it includes: Introduction, Materials and methods, Results and Discussion. Exceptionally, the results and discussion can be combined in a single section. Start each section on a new page, and number each page consecutively with Arabic numerals.

The Title page should include a concise and informative title, followed by the full name(s) of the author(s); the institutional affiliation of each author; the name and address of the corresponding author (including telephone, fax and E-mail), and an abbreviated title (not exceeding 60 characters). This should be followed by the abstract page, summarizing in less than 250 words the reasons for the study, experimental approach, the major findings (with specific data if possible), and the principal conclusions, and providing 3-6 key words for indexing purposes. Structured abstracts are required. Slovene authors are requested to provide title and the abstract in Slovene language in a separate file. The text of the research article should then proceed as follows:

Introduction should summarize the rationale for the study or observation, citing only the essential references and stating the aim of the study.

Materials and methods should provide enough information to enable experiments to be repeated. New methods should be described in details.

Results should be presented clearly and concisely without repeating the data in the figures and tables. Emphasis should be on clear and precise presentation of results and their significance in relation to the aim of the investigation.

Discussion should explain the results rather than simply repeating them and interpret their significance and draw conclusions. It should discuss the results of the study in the light of previously published work.

Charts, Illustrations, Images and Tables

Charts, Illustrations, Images and Tables must be numbered and referred to in the text, with the appropriate location indicated. Charts, Illustrations and Images, provided electronically, should be of appropriate quality for good reproduction. Illustrations and charts must be vector image, created in CMYK color space, preferred font "Century Gothic", and saved as .AI, .EPS or .PDF format. Color charts, illustrations and Images are encouraged, and are published without additional charge. Image size must be 2.000 pixels on the longer side and saved as .JPG (maximum quality) format. In Images, mask the identities of the patients. Tables should be typed double-spaced, with a descriptive title and, if appropriate, units of numerical measurements included in the column heading. The files with the figures and tables can be uploaded as separate files.

References

References must be numbered in the order in which they appear in the text and their corresponding numbers quoted in the text. Authors are responsible for the accuracy of their references. References to the Abstracts and Letters to the Editor must be identified as such. Citation of papers in preparation or submitted for publication, unpublished observations, and personal communications should not be included in the reference list. If essential, such material may be incorporated in the appropriate place in the text. References follow the style of Index Medicus, DOI number (if exists) should be included.

All authors should be listed when their number does not exceed six; when there are seven or more authors, the first six listed are followed by "et al.". The following are some examples of references from articles, books and book chapters:

Dent RAG, Cole P. In vitro maturation of monocytes in squamous carcinoma of the lung. *Br J Cancer* 1981; **43**: 486-95. doi: 10.1038/bjc.1981.71

Chapman S, Nakielny R. *A guide to radiological procedures*. London: Bailliere Tindall; 1986.

Evans R, Alexander P. Mechanisms of extracellular killing of nucleated mammalian cells by macrophages. In: Nelson DS, editor. *Immunobiology of macrophage*. New York: Academic Press; 1976. p. 45-74.

Authorization for the use of human subjects or experimental animals

When reporting experiments on human subjects, authors should state whether the procedures followed the Helsinki Declaration. Patients have the right to privacy; therefore the identifying information (patient's names, hospital unit numbers) should not be published unless it is essential. In such cases the patient's informed consent for publication is needed, and should appear as an appropriate statement in the article. Institutional approval and Clinical Trial registration number is required. Retrospective clinical studies must be approved by the accredited Institutional Review Board/Committee for Medical Ethics or other equivalent body. These statements should appear in the Materials and methods section.

The research using animal subjects should be conducted according to the EU Directive 2010/63/EU and following the Guidelines for the welfare and use of animals in cancer research (*Br J Cancer* 2010; 102: 1555 – 77). Authors must state the committee approving the experiments, and must confirm that all experiments were performed in accordance with relevant regulations.

These statements should appear in the Materials and methods section (or for contributions without this section, within the main text or in the captions of relevant figures or tables).

Transfer of copyright agreement

For the publication of accepted articles, authors are required to send the License to Publish to the publisher on the address of the editorial office. A properly completed License to Publish, signed by the Corresponding Author on behalf of all the authors, must be provided for each submitted manuscript.

The non-commercial use of each article will be governed by the Creative Commons Attribution-NonCommercial-NoDerivs license.

Conflict of interest

When the manuscript is submitted for publication, the authors are expected to disclose any relationship that might pose real, apparent or potential conflict of interest with respect to the results reported in that manuscript. Potential conflicts of interest include not only financial relationships but also other, non-financial relationships. In the Acknowledgement section the source of funding support should be mentioned. The Editors will make effort to ensure that conflicts of interest will not compromise the evaluation process of the submitted manuscripts; potential editors and reviewers will exempt themselves from review process when such conflict of interest exists. The statement of disclosure must be in the Cover letter accompanying the manuscript or submitted on the form available on www.icmje.org/coi_disclosure.pdf

Page proofs

Page proofs will be sent by E-mail to the corresponding author. It is their responsibility to check the proofs carefully and return a list of essential corrections to the editorial office within three days of receipt. Only grammatical corrections are acceptable at that time.

Open access

Papers are published electronically as open access on <https://content.sciendo.com/raon>, also papers accepted for publication as E-ahead of print.



XALKORI® – 1. linija zdravljenja napredovalega, ALK pozitivnega nedrobnočeličnega pljučnega raka¹

ALK = anaplastična limfomska kinaza

BISTVENI PODATKI IZ POVZETKA GLAVNIH ZNAČILNOSTI ZDRAVILA

XALKORI 200 mg, 250 mg trde kapsule

Sestava in oblika zdravila: Ena kapsula vsebuje 200 mg ali 250 mg krizotiniba. **Indikacije:** Monoterapija za: - prvo linijo zdravljenja odraslih bolnikov z napredovalim nedrobnočeličnim pljučnim rakom (NSCLC – *Non-Small Cell Lung Cancer*), ki je ALK (anaplastična limfomska kinaza) pozitiven; - zdravljenje odraslih bolnikov s predhodno zdravljenim, napredovalim NSCLC, ki je ALK pozitiven; - zdravljenje odraslih bolnikov z napredovalim NSCLC, ki je ROS1 pozitiven. **Odmerjanje in način uporabe:** Zdravljenje mora uvesti in nadzorovati zdravnik z izkušnjami z uporabo zdravil za zdravljenje rakavih bolezni. **Preverjanje prisotnosti ALK in ROS1:** Pri izbiri bolnikov za zdravljenje je treba pred zdravljenjem opraviti točno in validirano preverjanje prisotnosti ALK ali ROS1. **Odmerjanje:** Priporočeni odmerek je 250 mg dvakrat na dan (500 mg na dan), bolniki pa morajo zdravilo jemati brez prekinitev. Če bolnik pozabi vzeti odmerek, ga mora vzeti takoj, ko se spomni, razen če do naslednjega odmerka manjka manj kot 6 ur. V tem primeru bolnik pozabljenega odmerka ne sme vzeti. **Prilagajanja odmerkov:** Glede na varnost uporabe zdravila pri posameznem bolniku in kako bolnik zdravljenje prenaša, utegne biti potrebna prekinitev in/ali zmanjšanje odmerka pri bolnikih, ki se zdravijo s krizotinibom 250 mg peroralno dvakrat na dan (za režim zmanjševanja odmerka glejte poglavje 4.2 v povzetku glavnih značilnosti zdravila). Za prilagajanje odmerkov pri hematološki in nehematološki toksičnosti (povečanje vrednosti AST, ALT, bilirubina; ILD/pnevmonitis; podaljšanje intervala QTc, bradikardija, boleznji oči) glejte preglednici 1 in 2 v poglavju 4.2 povzetka glavnih značilnosti zdravila. **Okvara jeter:** Pri zdravljenju pri bolnikih z okvaro jeter je potrebna previdnost. Pri blagi okvari jeter prilagajanje začetnega odmerka ni priporočeno, pri zmerni okvari jeter je priporočeni začetni odmerek 200 mg dvakrat na dan, pri hudi okvari jeter pa 250 mg enkrat na dan (za merila glede klasifikacije okvare jeter glejte poglavje 4.2 v povzetku glavnih značilnosti zdravila). **Okvara ledvic:** Pri blagi in zmerni okvari prilagajanje začetnega odmerka ni priporočeno. Pri hudi okvari ledvic (ki ne zahteva peritonealne dialize ali hemodialize) je začetni odmerek 250 mg peroralno enkrat na dan; po vsaj 4 tednih zdravljenja se lahko poveča na 200 mg dvakrat na dan. **Starejši bolniki (≥ 65 let):** Prilagajanje začetnega odmerka ni potrebno. **Pediatrična populacija:** Varnost in učinkovitost nista bili dokazani. **Način uporabe:** Kapsule je treba pogoltniti cele, z nekaj vode, s hrano ali brez nje. Ne sme se jih zdrobiti, raztopiti ali odpreti. Izogibati se je treba uživanju grenivk, grenivkinega soka ter uporabi šentjanževke. **Kontraindikacije:** Preobčutljivost na krizotinib ali katerokoli pomožno snov. **Posebna opozorila in previdnostni ukrepi:** **Določanje statusa ALK in ROS1:** Pomembno je izbrati dobro validirano in robustno metodologijo, da se izognemo lažno negativnim ali lažno pozitivnim rezultatom. **Hepatotoksičnost:** V kliničnih študijah so poročali o hepatotoksičnosti, ki jo je povzročilo zdravilo (vključno s primeri s smrtnim izidom). Delovanje jeter, vključno z ALT, AST in skupnim bilirubinom, je treba preveriti enkrat na teden v prvih 2 mesecih zdravljenja, nato pa enkrat na mesec in kot je klinično indicirano. Ponovite preverjanj morajo biti pogostejši pri povečanih vrednosti stopnje 2, 3 ali 4. **Interistijska bolezen pljuč (ILD)/pnevmonitis:** Lahko se pojavi huda, življenjsko nevarna ali smrtna ILD/pnevmonitis. Bolnike s simptomi ILD/pnevmonitisa je treba spremljati, zdravljenje pa prekiniti ob sumu na ILD/pnevmonitis.

Podaljšanje intervala QT: Opažali so podaljšanje intervala QTc. Pri bolnikih z obstoječo bradikardijo, podaljšanjem intervala QTc v anamnezi ali predispozicijo zanj, pri bolnikih, ki jemljejo antiaritmike ali druga zdravila, ki podaljšujejo interval QT, ter pri bolnikih s pomembno obstoječo srčno boleznijo in/ali motnjami elektrolitov je treba krizotinib uporabljati previdno; potrebno je redno spremljanje EKG, elektrolitov in delovanja ledvic; preiskavi EKG in elektrolitov je treba opraviti čim bližje uporabi prvega odmerka, potem se priporoča redno spremljanje. Če se interval QTc podaljša za 60 ms ali več, je treba zdravljenje s krizotinibom začasno prekiniti in se posvetovati s kardiologom. **Bradikardija:** Lahko se pojavi simptomatska bradikardija (lahko se razvije več tednov po začetku zdravljenja); izogibati se je treba uporabi krizotiniba v kombinaciji z drugimi zdravili, ki povzročajo bradikardijo; pri simptomatski bradikardiji je treba prilagoditi odmerek. **Srčno popuščanje:** Poročali so o hudih, življenjsko nevarnih ali smrtnih neželenih učinkih srčnega popuščanja. Bolnike je treba spremljati glede pojavov znakov in simptomov srčnega popuščanja in ob pojavu simptomov zmanjšati odmerjanje ali prekiniti zdravljenje. **Nevtropenija in levkopenija:** V kliničnih študijah so poročali o neutropeniji, levkopeniji in febrilni neutropeniji; spremljati je treba popolno krvno sliko (pogostejše preiskave, če se opazijo abnormalnosti stopnje 3 ali 4 ali če se pojavi povišana telesna temperatura ali okužba). **Perforacija v prebavilih:** V kliničnih študijah so poročali o perforacijah v prebavilih, v obdobju trženja pa o smrtnih primerih perforacij v prebavilih. Krizotinib je treba pri bolnikih s tveganjem za nastanek perforacije v prebavilih uporabljati previdno; bolniki, pri katerih se razvije perforacija v prebavilih, se morajo prenehati zdraviti s krizotinibom; bolnike je treba poučiti o prvih znakih perforacije in jim svetovati, naj se nemudoma posvetujejo z zdravnikom. **Vplivi na ledvice:** V kliničnih študijah so opazili zvišanje ravnih kreatinina v krvi in zmanjšanje očistka kreatinina. V kliničnih študijah in v obdobju trženja so poročali tudi o odpovedi ledvic, akutni odpovedi ledvic, primerih s smrtnim izidom, primerih, ki so zahtevali hemodializo in hiperkaliemiji stopnje 4. **Vplivi na vid:** V kliničnih študijah so poročali o izpadu vidnega polja stopnje 4 z izgubo vida. Če se na novo pojavi huda izguba vida, je treba zdravljenje prekiniti in opraviti oftalmološki pregled. Če so motnje vida trdovratne ali se poslabšajo, je priporočilj oftalmološki pregled. **Histološka preiskava, ki ne nakazuje adenokarcinoma:** Na voljo so le omejeni podatki pri NSCLC, ki je ALK in ROS1 pozitiven in ima histološke značilnosti, ki ne nakazujejo adenokarcinoma, vključno s ploščatoceličnim karcinomom (SCC). **Medsebojno delovanje z drugimi zdravili in druge oblike interakcij:** Izogibati se je treba sočasni uporabi z močnimi zaviralci CYP3A4, npr. atazanavir, ritonavir, kobicistat, itrakonazol, ketokonazol, posakonazol, vorikonazol, klaritromicin, telitromicin in eritromicin (razen če morebitna korist za bolnika odtehta tveganje, v tem primeru je treba bolnike skrbno spremljati glede neželenih učinkov krizotiniba), ter grenivko i n grenivkinim sokom, saj lahko povečajo koncentracije krizotiniba v plazmi. Izogibati se je treba sočasni uporabi z močnimi induktorji CYP3A4, npr. karbamazepin, fenobarbital, fenitoin, rifampicin in šentjanževka, saj lahko zmanjšajo koncentracije krizotiniba v plazmi. Učinek zmernih induktorjev CYP3A4, npr. efavirenz in rifabutin, še ni jasen, zato se je treba sočasni uporabi s krizotinibom izogibati. Zdravila, katerih koncentracije v plazmi lahko krizotinib spremeni (midazolam, alfentanil, cisaprid, ciklosporin, derivati etrog alkoholdov, fentanyl, pimizid, kinidin, sirolimus, takrolimus, digoksin, dabigatran, kolhicin, pravastatin; sočasni uporabi s temi zdravili se

XALKORI
KRIZOTINIB

je treba izogibati oziroma izvajati skrben klinični nadzor; bupropion, efavirenz, peroralni kontraceptivi, raltegravir, i ritonekani, morfin, nalokson, metformin, prokainamid). Zdravila, ki podaljšujejo interval QT ali ki lahko povzročijo Torsades de pointes (antiaritmiki skupine IA (kinidin, disopiramid), antiaritmiki skupine III (amiodaron, sotalol, dofetilid, ibutilid), metadon, cisaprid, moksifloksacin, antipsihotiki) – v primeru sočasne uporabe je potreben skrben nadzor intervala QT. Zdravila, ki povzročajo bradikardijo (nedihidropiridinski zaviralci kalcijevih kanalčkov (verapamil, diltiazem), antagonist adrenergičnih receptorjev beta, klonidin, gvanfacin, digoksin, melforkin, antiholinesteraze, pilokarpin) – krizotinib je treba uporabljati previdno. **Plodnost, nosečnost in dojenje:** Ženske v rodni dobi se morajo izogibati zanositvi. Med zdravljenjem in najmanj 90 dni po njem je treba uporabljati ustrezno kontracepcijo (velja tudi za moške). Zdravilo lahko škoduje plodu in se ga med nosečnostjo ne sme uporabljati, razen če klinično stanje matere ne zahteva takega zdravljenja. Matere naj se med jemanjem zdravila dojenju izogibajo. Zdravilo lahko zmanjša plodnost moških in žensk. **Vpliv na sposobnost vožnje in upravljanja strojev:** Lahko se pojavijo simptomatska bradikardija (npr. sinkopa, omotica, hipotenzija), motnje vida ali utrujenost; potrebna je previdnost. **Neželeni učinki:** Najresnejši neželeni učinki so bili hepatotoksičnost, ILD/pnevmonitis, neutropenija in podaljšanje intervala QT. Najpogostejši neželeni učinki (≥ 25 %) so bili motnje vida, navzea, diareja, bruhanje, edem, zaprtje, povečane vrednosti transaminaz, utrujenost, pomanjkanje apetita, omotica in nevropatija. Ostali zelo pogosti (≥ 1/10 bolnikov) neželeni učinki so: neutropenija, anemija, levkopenija, disgevizija, bradikardija, bolečina v trebuhu in izpuščaji. **Način in režim izdaje:** Predpisovanje in izdaja zdravila je le na recept, zdravilo pa se uporablja samo v bolnišnicah. Izjemoma se lahko uporablja pri nadaljevanju zdravljenja na domu ob odpustu iz bolnišnice in nadaljnjem zdravljenju. **Imetni dovoljenja za promet:** Pfizer Europe MA EEEG, Boulevard de la Plaine 17, 1050 Bruxelles, Belgija. **Datum zadnje revizije besedila:** 28.02.2019

Pred predpisovanjem se seznanite s celotnim povzetkom glavnih značilnosti zdravila.

Vir 1: Povzetek glavnih značilnosti zdravila Xalkori, 28.02.2019



